UNIVERSIDAD NACIONAL AUTÓNOMA DE MÉXICO
PROGRAMA DE MAESTRÍA Y DOCTORADO EN INGENIERÍA
INGENIERÍA ELÉCTRICA – CONTROL

STABILITY ANALYSIS OF NONLINEAR SYSTEMS AND DESIGN OF CONTINUOUS HIGHER-ORDER SLIDING-MODE CONTROLLERS FROM A HOMOGENEOUS POINT OF VIEW

TESIS
QUE PARA OPTAR POR EL GRADO DE:
DOCTOR EN INGENIERÍA

PRESENTA:
JESÚS MENDOZA AVILA

TUTORES PRINCIPALES
DR. LEONID FRIDMAN, FACULTAD DE INGENIERÍA, UNAM
DR. JAIME A. MORENO PÉREZ, INSTITUTO DE INGENIERÍA, UNAM

COMITE TUTOR
DR. LUIS A. ALVAREZ ICAZA LONGORIA, INSTITUTO DE INGENIERÍA, UNAM
DR. MARCO A. ARTEAGA PÉREZ, FACULTAD DE INGENIERÍA, UNAM

CIUDAD DE MÉXICO, AGOSTO 2021

JURADO ASIGNADO:

Presidente: Dr. Álvarez-Icaza Longoria Luis Agustín

Secretario: Dr. Arteaga Pérez Marco Antonio

1 er. Vocal: Dr. Fridman Leonid

2 do. Vocal: Dr. Moreno Pérez Jaime Alberto

3 er. Vocal: Dr. Castaños Luna Fernando

Lugar o lugares donde se realizó la tesis: Facultad de ingeniería, UNAM

TUTORES DE TESIS:

DR. JAIME A. MORENO PÉREZ

DR. LEONID FRIDMAN

_____ FIRMA

_____ FIRMA

A mi papá Vicente con todo mi amor,
siempre estarás en mi corazón.
¡Gracias por todo!

Abstract

This thesis is devoted to the study of the stability of homogeneous systems and the design of homogeneous controllers based on Continuous Higher-Order Sliding Mode. The homogeneity properties of a class of discontinuous systems are exploited to extend classical results on the design of Lyapunov functions, and a numerical method to design Lyapunov functions for this class of systems is developed. Moreover, an analysis of the stability of homogeneous systems affected by parasitic dynamics is performed in the framework of Lyapunov methods. In the general case of homogeneous systems, these results allows to conclude that the classical concept of motion separation of singularly perturbed systems works only when the involved dynamics have the same homogeneity degree. When the parasitic dynamics has a smaller homogeneity degree than the main dynamics, this concept of motion separation is valid locally in a vicinity of the origin, while for the contrary case such a concept works only outside of a neighborhood of the origin. So, these results can be seen as a generalization of the concept of motion separation for a wider class of homogeneous singularly perturbed systems. Later, three schemes of control: state feedback, output feedback, and adaptive, based on Continuous Twisting Algorithm of Third Order are proposed, where the stability analysis and gain design are realized based on homogeneous Lyapunov functions. Additionally, experimental results of the implementation of these controllers in electromechanical setups are provided. Finally, sub-optimal designs of a continuous sliding mode controller in the PID form and a homogeneous controller in the PD-form are presented, based on frequency methods. Two sets of gains for these controllers are suggested to minimize the amplitude of chattering caused by the presence of a critically-damped second-order fast-actuator in the control system or the energy needed to maintain the trajectories into a real sliding mode. In addition, finite-time stability at the origin for the ideal system (without an actuator) with the suggested design is proven by using homogeneous Lyapunov functions. Most of the results in this thesis address one of the main issues in the implementation of sliding mode controllers, the so-called chattering. They represent new directions in further research of analysis of chattering and design of sliding mode controllers with criteria for chattering minimization.

Keywords: Chattering analysis, Differential inclusions, Discontinuous control, Frequency domain methods, Homogeneity, Lyapunov methods, Nonlinear system, Robust control applications, Singular perturbations, Sliding Mode Control.

Resumen

Esta tesis aborda el estudio de la estabilidad de sistemas homogéneos y el diseño de controladores homogéneos basados en modos deslizantes de orden superior. Las propiedades de homogeneidad de cierta clase de sistemas discontinuos son utilizadas para ampliar resultados clásicos acerca del diseño de funciones de Lyapunov. Además, se desarrolla un método numérico para diseñar funciones de Lyapunov para la clase de sistemas bajo estudio. Por otro lado, se realiza un análisis de la estabilidad de sistemas homogéneos afectados por dinámicas parásitas en el marco de los métodos de Lyapunov. En el caso general de sistemas homogéneos, estos resultados concluyen que el concepto clásico de separación de dinámicas para sistemas singularmente perturbados funciona solo cuando los sistemas involucrados tienen el mismo grado de homogeneidad. Cuando la dinámica parásita tiene un grado de homogeneidad menor que la dinámica principal, dicho concepto de separación de dinámicas es válido localmente en una vecindad del origen, mientras que en el caso contrario, tal concepto funciona solo fuera de una vecindad del origen. Por lo tanto, estos resultados pueden verse como una generalización del concepto de separación de dinámicas para una clase más amplia de sistemas homogéneos singularmente perturbados. Posteriormente, se proponen tres esquemas de control: realimentación de estado, realimentación de salida y adaptable, basados en el algoritmo twisting continuo de tercer orden, donde el análisis de estabilidad y el diseño de ganancias se realizan basados en funciones de Lyapunov homogéneas. Además, se presentan resultados de la implementación de estos controladores en sistemas electromecánicos. Finalmente, se presentan diseños subóptimos de un controlador continuos por modos deslizantes en la forma de PID y un controlador homogéneo en la forma de PD mediante métodos de frecuencia. Se sugieren dos conjuntos de ganancias para minimizar la amplitud del chattering causado por la presencia de un actuador rápido de segundo orden críticamente amortiguado en el sistema de control, ó la energía necesaria para mantener las trayectorias en un modo deslizante real. Además, se prueba la estabilidad en tiempo finito del sistema ideal (sin un actuador) con el diseño sugerido mediante el uso de funciones de Lyapunov homogéneas. La mayoría de los resultados de esta tesis abordan uno de los principales problemas en la implementación de controladores por modos deslizantes, el llamado chattering, las cuales representan nuevas direcciones de investigación acerca del análisis de chattering y el diseño de controladores por modos deslizantes con criterios para minimizar el chattering.

Palabras clave: Análisis de chattering, Inclusiones diferenciales, Control discontinuo, Métodos en el dominio de la frecuencia, Homogeneidad, Métodos de Lyapunov, Sistema no lineales, Aplicaciones de control robusto, Perturbaciones singulares, Control por modos deslizantes.

Acknowledgment

To my family for their love and unconditional support. Thanks very much!

To Dr. Leonid Fridman for guide my path in science, and overall for the friendship provided.

To Dr. Jaime A. Moreno for all the knowledge shared, the trust provided, and the invaluable contributions to my work.

To Dr. Denis Efimov for having contributed enormously to the development of my research.

To the members of the committee: Dr. Marco A. Arteaga and Dr. Luis A. Álvarez-Icaza for their valuable comments on my work.

To the colleagues of the group of Sliding Mode Control UNAM for the shared time and knowledge.

To the Programa de Maestría y Doctorado en Ingeniería of UNAM; to the Consejo Nacional de Ciencia y Tecnología (CONACYT): projects 241171, 282013 and CVU 711867; to the Programa de Apoyo a Proyectos de Investigación e Innovación Tecnológica (PAPIIT-UNAM) IN 115419, IN 110719, IN113216, and IN 113617; to the Programa DGAPA PASPA, Fondo de Colaboracón del II-FI UNAM IISGBAS-100-2015; and to Homogeneity Tools for Sliding Mode Control and Estimation (HoTSMoCE) INRIA associate team program; for the funding granted for my master's and doctoral studies.

Agradecimientos

A mi familia por todo su cariño y apoyo incondicional. ¡Gracias por todo!

Al Dr. Leonid Fridman por haber guiado mi camino en la ciencia y sobretodo por la amistad brindada.

Al Dr. Jaime A. Moreno por todos los conocimientos compartidos, la confianza brindada, y los invaluables aportes hacia mi trabajo.

Al Dr. Denis Efimov por haber contribuido enormemente en el desarrollo de mi investigación.

A los miembros el comité tutor: Dr. Marco A. Arteaga y Dr. Luis A. Álvarez-Icaza por sus valiosos comentarios hacia mi trabajo.

A los compañeros del grupo de Control por Modos Deslizantes de la UNAM por el tiempo y los conocimientos compartidos.

Al Programa de Maestría y Doctorado en Ingeniería de la UNAM; al Consejo Nacional de Ciencia y Tecnología (CONACYT): proyectos 241171, 282013 y CVU 711867; al Programa de Apoyo a Proyectos de Investigación e Innovación Tecnológica (PAPIIT-UNAM) IN 115419, IN 110719, IN113216, y IN 113617; al Programa DGAPA PASPA, Fondo de Colaboracón del II-FI UNAM IISGBAS-100-2015; y a Homogeneity Tools for Sliding Mode Control and Estimation (HoTSMoCE) INRIA associate team program; por el financiamiento otorgado para mis estudios de maestría y doctorado.

Contents

Abbreviations

3-ACTA	Adaptive Continuous Twisting Algorithm of Third-Order
3-CTA	Continuous Twisting Algorithm of Third-Order
3-OFCTA	Output Feedback Continuous Twisting Algorithm of Third-Order
3-RED	Robust and Exact Differentiator of Third-Order
ACTA	Adaptive Continuous Twisting Algorithm
BL	Boundary layer
CHOSM	Continuous Higher-Order Sliding Mode
CTA	Continuous Twisting Algorithm
DF	Describing function
DIC	Discontinuous Integral Controller
Etcetera	Etc.
FD	Fast dynamics
Fig.	Figure
FOSMC	First-Order Sliding Mode Controllers
GAS	Global asymptotic stability, or Globally asymptotically stable
GF	Generalized form
HB	Harmonic balance
HD	Homogeneity degree
HOSM	Higher-Order Sliding Mode
ISS	Input-to-state stability
ISpS	Input-to-state practical stability
IWP	Inertial wheel pendulum
LF	Lyapunov function
LMI	Linear matrix inequality
MD	Main dynamics
MLS	Magnetic levitation system
n-CTA	Continuous Twisting Algorithm of Arbitrary Order
OAS	Orbitally asymptotically stable or Orbital asymptotic stability

OFCTA	Output Feedback Continuous Twisting Algorithm
PD	Proportional Derivative or Parasitic dynamics (Skipping ambiguity)
PD-HC	Homogeneous Controller in the PD form
PI	Proportional Integral
PID	Proportional Integral Derivative
PID-CSMC	Continuous Sliding Mode Controller in the PID form
RED	Robust and Exact Differentiator
ROD	Reduced-order dynamics
SD	Slow dynamics
SISO	Single-input-single-output
SMC	Sliding Mode Control
SOS	sum of squares
SPP	Singular perturbation parameter
STA	Super-Twisting Algorithm
w.r.t.	with respect to

List of Figures

List of Tables

Chapter 1

Introduction

The *homogeneity* [Zubov, 1964, Bacciotti and Rosier, 2005, Polyakov, 2020] is a kind of symmetry of a function with respect to a dilation of its arguments. One of the first notions of homogeneity appeared in the eighteenth century, when Leonhard Euler focused in the study of homogeneous polynomials. A generalization of this concept was introduced by [Zubov, 1964] and independently by [Hermes, 1986, Hermes, 1991] with the so-called *weighted homogeneity*.

Homogeneous systems constitute a subclass of nonlinear dynamics admitting special properties like scalability of solutions, global expansion of local behaviors, robustness, and different rates of convergence: rational, exponential and finite-time. Moreover, homogeneous systems have many properties similar to linear ones. All these features have been found advantageous in analysis and design of nonlinear control systems [Zubov, 1964, Bacciotti and Rosier, 2005, Polyakov, 2020]. Remarkably, nonlinear systems can be approximated by homogeneous maps for local analysis, when linearization is non-informative or simply impossible [Hermes, 1991, Polyakov, 2020].

The Lyapunov function (LF) method is one of the main approaches to analyze the stability of dynamical systems [Bacciotti and Rosier, 2005, Khalil, 2002, Zubov, 1964]. Particularly, for linear systems the design of LF's has been widely studied [Khalil, 2002, Bacciotti and Rosier, 2005]. Many of these results can be extended to nonlinear homogeneous systems, e.g., if a homogeneous system is asymptotically stable at the origin, then there exists a homogeneous proper LF [Zubov, 1964, Rosier, 1992, Efimov et al., 2018]. However, most of those results are restricted to homogeneous systems with continuous vector fields.

Commonly, systems with discontinuous right-hand side are represented by differential inclusions [Filippov, 1988]. For this class of systems, the homogeneity concepts have been generalized by [Bernuau et al., 2013a, Levant et al., 2016]. The design of homogeneous LF's for homogeneous systems with discontinuous right-hand side has been widely studied, see for example the works of [Nakamura et al., 2002, Tuna and Teel, 2006, Sánchez and Moreno, 2016, Sanchez and Moreno, 2019]. Furthermore, a more general framework is proposed in [Mendoza-Avila et al., 2021], where explicit formulas of Lipschitz-continuous and homogeneous LF's are provided with a posterior construction through a numerical methodology. These results can be seen as a generalization of the classical results

of [Persidskii, 1937, Massera, 1949, Yoshizawa et al., 1955] and [Kurzweil, 1963] for discontinuous homogeneous system of negative degree.

Other concepts of stability have been also extended to the class of homogeneous system. For instance, input-to-stability and some other related notions for homogeneous system are subject of the papers [Ryan, 1995, Hong, 2001, Bernuau et al., 2013b], homogeneous approximations have been reported by [Hermes, 1991, Andrieu et al., 2008], and the relationship between homogeneity properties and finite-time convergence is studied by [Bhat and Bernstein, 2005]. Furthermore, the paper [Mendoza-Avila et al., 2020a] presents an analysis of the stability of singularly perturbed systems in the framework of homogeneity notions. Three types of stability were discovered by depending on the relation between the Homogeneity Degrees (HD) of the Fast Dynamics (FD) and the Slow Dynamics (SD): global asymptotic stability (GAS) when both dynamics have the same HD and the Singular Perturbation Parameter (SPP) is sufficiently small, practical GAS when the FD has a greater HD than the SD, and local asymptotic stability when the FD has a smaller HD than the SD. In the last two cases, we show that both the final bound of the trajectories and the domain of attraction depends on the SPP.

Many examples of homogeneous systems with discontinuous right-hand side can be found in the family of sliding-mode algorithms [Levant, 2005a, Bernuau et al., 2014, Levant and Livne, 2016]. Sliding Mode Control [Utkin, 1992, Shtessel et al., 2014] is one of the most efficient techniques to deal with systems under uncertainty conditions. In theory, this kind of controllers are able to provide an exact compensation of bounded and matched disturbances, and finite-time convergence of the system trajectories to the sliding set by means of a discontinuous control signal.

Higher Order Sliding Mode (HOSM) controllers were developed in order to ensure, for a chain of integrators of order n, finite-time convergence to the $n-th$ order sliding mode, i.e., to nullify the output $\sigma(t)$ and its $(n-1)$ derivatives ($\sigma(t) = \dot{\sigma}(t) = \ldots = \sigma^{(n-1)}(t) = 0$), even in presence of bounded, non-vanishing and matched disturbances or uncertainties [Levant, 2001, Levant, 2003a, Levant, 2005b] .

Continuous Higher Order Sliding Mode (CHOSM) controllers were recently introduced in order to obtain a *continuous control signal*, which leads to a significantly reduction the level of chattering, see [Zamora et al., 2013, Fridman et al., 2015, Levant, 1993, Kamal et al., 2016, Moreno, 2016, Torres-González et al., 2017, Mendoza-Avila et al., 2017, Moreno, 2018, Mendoza-Avila et al., 2020b, Laghrouche et al., 2017, Mercado-Uribe and Moreno, 2020]. Such controllers provide finite-time convergence to the $(n+1)-th$ order sliding set for the trajectories of a chain of integrators of order n with non-vanishing Lipschitz-continuous and matched disturbances by means of a continuous control signal and using only information of the output and its derivatives up to the order $(n-1)$.

Particularly, [Mendoza-Avila et al., 2020b] presents the design of a Third-Order Continuous Twisting Algorithm (3-CTA). This controller is able to provide, in theory, finite-time convergence to zero for the trajectories of a third-order chain of integrators, and an exact compensation of Lipschitz-continuous and matched disturbances. In addition, an output feedback 3-CTA (3-OFCTA) was introduced by using a third-order Robust and Exact Differentiator to estimate the states from the measurable output. Separation principle for 3-OFCTA was proven which allows the design of the gains for controller and observer, independently. Moreover, [Mendoza-Avila et al., 2018] provides an adaptive version of the 3-CTA (3-ACTA), where the adaptive gain is automatically adjusted until the stability

is ensured for all future time. The main advantages of the 3-ACTA are the rejection of Lipschitz-continuous and matched disturbances with an unknown Lipschitz constant, and a proper tunning of the gains reducing the amplitude of the chattering.

In practice, the presence of parasitic dynamics in the control system (e.g., delays, actuators, sensors, hysteresis, etc.) deteriorates the performance CHOSM controllers, such that, the chattering arise despite the continuous control signal [Boiko and Fridman, 2005, Pérez-Ventura and Fridman, 2019]. So, a proper design of these controllers is needed to optimize the the response of the closed-loop system. For instance, engineers are accustomed to work with PID control structures where the gains are chosen from several criteria depending on the parasitic dynamics which are not considered in the model, see for example [Ziegler and Nichols, 1942, Aström and Hägglund, 2005, Boiko et al., 2006, Boiko, 2014a, Pilloni et al., 2012a, Pilloni et al., 2012b]. Hence, [Pérez-Ventura et al., 2021] proposes a sub-optimal design of the Continuous Sliding Mode Controller in the PID form (PID-CSMC) (originally introduced by [Zamora et al., 2013]) based on frequency domain methods. This controller has only three gains directly related to the error signal in proportional, integral and derivative ways, which implies a synergistic relation between with the conventional PID. The proposed design considers a critically damped second-order actuator to parameterize the effects of fast-parasitic dynamics and uses the describing function approach to predict the parameters of the main harmonic approximation of chattering [Atherton, 1975, Gelb and Vander Velde, 1968, Boiko, 2009, Boiko, 2018, Utkin, 2016].

This thesis is devoted to the study of stability of homogeneous systems and the design of homogeneous controllers based on Continuous Higher-Order Sliding Mode (CHOSM). Here, the most of the results obtained through my doctoral research are collected in a detailed and extended way. Briefly, the homogeneity properties of some nonlinear systems are exploited to extend classical results on the design of LF's, and on stability analysis of singularly perturbed systems. Moreover, three schemes of control: state feedback, output feedback and adaptive, based on Continuous Twisting Algorithm of third Order (3-CTA) are proposed, where stability analysis and design of gains are realized based on homogeneous LF's. Finally, it is presented a sub-optimal design of the PID-CSMC based on frequency domain methods and homogeneous LF's. The contributions and the outline of the thesis are summarized in the following.

Chapter 3 presents two converse Lyapunov theorems for a class of discontinuous and homogeneous systems of negative degree. This results can be seen as a generalization of classical results about LF design to the considered class of systems. Moreover, a numerical methodology to construct LF is proposed, which consists of two steps: first point-wise calculation of values of the the LF provided by the converse theorems; second, interpolation of this points on the unit sphere. Both together, the converse theorem and the numerical methodology, constitute a new framework for the numerical design of homogeneous and Lipschitz-continuous LF for a wide class of discontinuous Higher-Order Sliding Mode algorithms.

Later, chapter 4 studies the effect of Parasitic Dynamics (PD) on the stability of a homogeneous control system, assuming just continuity of the considered vector fields. Three types of stability for such an interconnection were discovered depending on the relation between the HD's of the PD and the Main Dynamics (MD): GAS when both dynamics have the same HD and the SPP is sufficiently small, practical GAS when the PD has a greater HD than the MD, and local asymptotic stability when the PD

has a smaller HD than the MD. In the last two cases, both the final bound of the trajectories and the domain of attraction depends on the SPP. In the general case of homogeneous systems, these results allows to conclude that the classical concept of motion separation of singularly perturbed systems works only when the involved dynamics have the same homogeneity degree. When the parasitic dynamics has a smaller homogeneity degree than the main dynamics, this concept of motion separation is valid locally in a vicinity of the origin, while for the contrary case such a concept works only outside of a neighborhood of the origin. So, these results can be seen as a generalization of the concept of motion separation for a wider class of homogeneous singularly perturbed systems. Moreover, a LF-based approach for analysis of the chattering generated by finite-time convergent controllers due to the presence of fast actuators is introduced. Under the assumption that chattering arises in the steady state of the system trajectories, this result allows to show the relationship between the amplitude of chattering, the SPP, and the HD of the finite-time convergent controller.

In Chapter 5, the design of a Third-Order Continuous Twisting Algorithm (3-CTA) is presented. This controller is able to provide, in theory, finite-time convergence to zero for the trajectories of a third-order chain of integrators, exact compensation of Lipschitz-continuous and matched disturbances, and steady-state precision of fourth order w.r.t. sampling step for the system's output. Moreover, an adaptive version of the 3-CTA (3-ACTA) is provided, where the adaptive gain adjusts its value automatically until the stability of the closed-loop system is assured for all future time. The main advantages of the 3-ACTA are the rejection of Lipschitz-continuous and matched disturbances with an unknown Lipschitz constant, and a proper adjustment of the gains reducing the amplitude of the chattering in the states. In addition, it is introduced an output feedback 3-CTA (3-OFCTA) using a third-order Robust and Exact Differentiator to estimates the states from the measurable output. The 3-OFCTA preserves, in theory, all features of robustness, convergence, and precision of the 3-CTA while requiring only information from the measurable output. Separation principle for 3-OFCTA is proven which allows the design of the gains for controller and observer, independently. Finally, both controllers 3-ACTA and 3-OFCTA were implemented in a reaction wheel pendulum and a magnetic levitation system, respectively, with satisfactory results.

Further, Charter 6 addresses with a sub-optimal design of the PID-CSMC and a homogeneous controller in the PD-form (PD-HC) based on frequency methods. Two sets of gains for the PID-CSMC and two more for the PD-HC are suggested in order to minimize the amplitude of chattering caused by the presence of a critically damped second-order actuator in the control system or the energy needed to maintain the trajectories into a real sliding mode. The proposed design uses the describing function approach to predict the parameters of the main harmonic approximation of chattering. Then, it is proven that the suggested gins ensure finite-time stability at the origin for the ideal system (without an actuator) by means of a homogeneous LF.

Finally, Chapter 7 summarizes and makes conclusion of the results presented in this thesis.

Chapter 2

Preliminaries

This chapter presents some notation and a brief review of concepts of homogeneity and stability that will be use along this thesis. Most of these results are taken from the works in [Zubov, 1964, Filippov, 1988, Bacciotti and Rosier, 2005, Polyakov, 2012, Bernuau et al., 2013a, Levant et al., 2016, Bernuau et al., 2014, Levant, 2005a, Polyakov, 2020]

2.1 Notation

- $\mathbb{N}$, $\mathbb{Q}$ and $\mathbb{R}$ are the sets of natural, rational and real numbers, respectively. Moreover, $\mathbb{R}_+$ represents the set of non-negative real numbers, i.e., $\mathbb{R}_+ = \{x \in \mathbb{R} : x \geq 0\}$ and in a similar way for the sets $\mathbb{N}$ and $\mathbb{Q}$.
- $|\cdot|$ denotes the absolute value in $\mathbb{R}$, $\|\cdot\|$ denotes the Euclidean norm in $\mathbb{R}^n$.
- $diag(a_i)$ denotes the diagonal matrix with elements $a_1, a_2, \ldots, a_n \in \mathbb{R}$.
- For any matrix $A \in \mathbb{R}^{n\times n}$, $s(A)$ represents its eigenvalues. Also, $s_{\min}(A)$ and $s_{\max}(A)$ depict the minimum and the maximum eigenvalue of A, respectively.
- The closed convex hull of a set $D \subset \mathbb{R}^n$ (the minimal closed convex set containing D) is denoted by $\bar{C}O(D)$.
- The boundary of a set $D \subset \mathbb{R}^n$ is denoted by $\partial(D)$.
- $\mathbb{S}(x_0, \rho) = \{x \in \mathbb{R}^n : \|x - x_0\| = \rho\}$ represents the sphere in $\mathbb{R}^n$ of radius ρ with center at x_0. Also, $\mathbb{B}(x_0, \rho) = \{x \in \mathbb{R}^n : \|x - x_0\| \leq \rho\}$ represents the closed ball in $\mathbb{R}^n$ of radius ρ with center at x_0. If $x_0 = 0$ then $\mathbb{S}(\rho)$ and $\mathbb{B}(\rho)$ denotes the sphere and the ball centered at the origin, respectively.

- The *sign* function can be defined as a set-valued function given by

$$\lceil x \rfloor^0 = \begin{cases} 1; & x > 0, \\ [-1, 1]; & x = 0, \\ -1; & x < 0, \end{cases}$$

  On the other hand, it can also be defined as a single-valued function denoted by

$$\text{sign(x)} = \begin{cases} 1; & x > 0, \\ a; & x = 0, \\ -1; & x < 0, \end{cases}$$

  for some $a \in [-1, 1] \subset \mathbb{R}$.

- For $x \in \mathbb{R}$ and $\gamma \in \mathbb{R}$, define $\lceil x \rfloor^\gamma := |x|^\gamma \text{sign(x)}$, i.e., the signed power γ of x. Accordingly, $\lceil x \rfloor^0 = \text{sign(x)}$. Note that if γ is an even number then $\lceil x \rfloor^\gamma = |x|^\gamma \text{sign(x)} \neq x^\gamma$, e.g., $\lceil x \rfloor^{\frac{1}{2}} = |x|^{\frac{1}{2}} \text{sign(x)} \neq x^{\frac{1}{2}}$ or $\lceil x \rfloor^4 = |x|^4 \text{sign(x)} \neq x^4$. Otherwise, if γ is an odd number then $\lceil x \rfloor^\gamma = |x|^\gamma \text{sign(x)} = x^\gamma$, e.g., $\lceil x \rfloor^{\frac{1}{3}} = |x|^{\frac{1}{3}} \text{sign(x)} = x^{\frac{1}{3}}$ or $\lceil x \rfloor^1 = |x|^1 \text{sign(x)} = x$. Moreover, $\lceil x \rfloor^{\gamma_1} \lceil x \rfloor^{\gamma_2} = |x|^{\gamma_1 + \gamma_2}$, $\lceil x \rfloor^\gamma \lceil x \rfloor^0 = |x|^\gamma$, $|x|^\gamma \lceil x \rfloor^0 = \lceil x \rfloor^\gamma$, $\frac{d}{dx} \lceil x \rfloor^\gamma = \gamma |x|^{\gamma - 1}$, and $\frac{d}{dx} |x|^\gamma = \gamma \lceil x \rfloor^{\gamma - 1}$.

- A continuous function $\alpha : \mathbb{R}_+ \to \mathbb{R}_+$ belongs to the class $\mathcal{K}$ if $\alpha(0) = 0$ and it is strictly increasing. The function $\alpha : \mathbb{R}_+ \to \mathbb{R}_+$ belongs to the class $\mathcal{K}_\infty$ if $\alpha \in \mathcal{K}$ and it increases to infinity. A continuous function $\beta : \mathbb{R}_+ \times \mathbb{R}_+ \to \mathbb{R}_+$ belongs to the class $\mathcal{KL}$ if $\beta(\cdot, t) \in \mathcal{K}_\infty$ for each fixed $t \in \mathbb{R}_+$ and $\lim_{t \to \infty} \beta(s, t) = 0$ for each fixed $s \in \mathbb{R}_+$.

- For a Lebesgue measurable function $u : \mathbb{R}_+ \to \mathbb{R}^m$ define the norm

$$\|u\|_{(t_0, t_1)} = ess \sup_{t \in (t_0, t_1)} |u(t)|,$$

  then $\|u\|_\infty = \|u\|_{(0, +\infty)}$. The space $\mathcal{L}_\infty^m$ is defined as the set of measurable essentially bounded functions $u : \mathbb{R}_+ \to \mathbb{R}^m$, such that, $\|u\|_{\mathcal{L}_\infty} = \|u\|_\infty < \infty$.

- For a $V : \mathbb{R} \to \mathbb{R}_+$ denote the upper Dini derivative:

$$\dot{V}^+(t) = \limsup_{h \to 0^+} \frac{V(t + h) - V(t)}{h}, \ \forall t \in \mathbb{R}_+.$$

  If V is locally Lipschitz continuous then $\dot{V}^+$ is finite, and if V is differentiable then $\dot{V}^+$ is the usual derivative of V. For $V : \mathbb{R}^n \to \mathbb{R}_+$ the generalized directional derivative at $x \in \mathbb{R}^n$ in the direction $d \in \mathbb{R}^n$ is defined by

$$D^+ V(x) d = \limsup_{y \to x \ \ h \to 0^+} \frac{V(y + hd) - V(y)}{h}.$$

- C_k is the set of continuous functions with continuous derivatives at least up to the order k, where $k \in \mathbb{N}_+$. Particularly, C^0 is the set of continuous functions, C_1 is the set of continuous differentiable functions and C^∞ is the set of differentiable functions, also called smooth functions.

2.2 Stability definitions

The concept of stability introduced by Lyapunov at the end of the 19th century refers to the fact that some nominal motion of a dynamical system are stable if other motions with initial conditions nearby remains close to the nominal one. Without lost of generality, we can consider the zero solution (equivalently, the origin) of a dynamical system as the nominal motion since we can translate any other solution to the origin through a change of coordinates. Most of the following results are taken from [Khalil, 2002, Bacciotti and Rosier, 2005, Polyakov, 2020].

Consider the differential equation

$$\dot{x} = f(x), \tag{2.1}$$

where $x \in \mathbb{R}^n$ is the state and the vector field $f : \mathbb{R}^n \to \mathbb{R}^n$ ensures forward existence and uniqueness of the system solutions at least locally in time. Moreover, the origin is the only equilibrium motion, e.i., $f(0) = 0$ and $f(x) \neq 0 \quad \forall \quad x \neq 0$. Many dynamical systems are modeled by the differential equation (2.1).

A more general model is given by the differential inclusion

$$\dot{x} \in F(x) \tag{2.2}$$

where x is the state and $F : \mathbb{R} \rightrightarrows \mathbb{R}^n$ is a set-valued map, with an unique equilibrium motion at the origin, e.i., $0 \in F(0)$ and $0 \notin F(x) \quad \forall \quad x \neq 0$. Under some restrictions on F, the system (2.2) has unique solution in forward time. The differential inclusion (2.2) allows to represent a wider class of system like discontinuous right-hand side ones. It is clear that the differential equation (2.1) is a particular case of the differential inclusion (2.2) with $F(x) = \{f(x)\}$.

The solutions of the system (2.2) are denoted by $\chi(t, x_0)$ where $x_0 \in \mathbb{R}^n$ is the initial condition, such that, $\chi(0, x_0) = x_0$.

Definition 2.1. For the system (2.2) possessing uniqueness of solutions in forward time for any $x_0 \in \Omega \subseteq \mathbb{R}^n$, the origin is said to be

- *Locally (globally) Lyapunov stable* if for any $x_0 \in \Omega$ ($x_0 \in \mathbb{R}^n$, respectively) the solution $\chi(t, x_0)$ is defined for all $t \geq 0$ and for any $\epsilon > 0$ there exists $\delta > 0$, such that, for any $x_0 \in \Omega$ ($x_0 \in \mathbb{R}^n$) if $\|x_0\| < \delta$ then $\|\chi(t, x_0)\| < \epsilon$ for all $t \geq 0$. It is unstable in any other case.

- *Locally (globally) asymptotically stable* if it is locally (globally) Lyapunov stable and locally (globally) asymptotically attractive. The latter means that there exists a set Ω ($\Omega = \mathbb{R}^n$), such that, $\lim_{t \to +\infty} \|\chi(t, x_0)\| = 0$ for any $x_0 \in \Omega$ ($x_0 \in \mathbb{R}^n$). The set Ω is called the *domain of attraction*.

- *Locally (globally) exponentially stable* if it is locally (globally) asymptotically stable with a domain of attraction Ω ($\Omega = \mathbb{R}^n$) and there exist $C > 0$ and $r > 0$, such that, $\|\chi(t, x_0)\| \leq C\|x_0\|e^{-rt}$ for all $t > 0$ and any $x_0 \in \Omega$ ($x_0 \in \mathbb{R}^n$).
- *Locally (globally) finite-time stable* if it is locally (globally) Lyapunov stable and locally (globally) finite-time attractive with a domain of attraction Ω ($\Omega = \mathbb{R}^n$). The latter means that there exists $T_s : \mathbb{R}^n \to \mathbb{R}_+$, such that, $\|\chi(t, x_0)\| = 0$ for all $t \geq T_s(x_0)$ and all $x_0 \in \Omega$ ($x_0 \in \mathbb{R}^n$). The function $T_s : \mathbb{R}^n \to \mathbb{R}_+$ is called the settling time function.
- *Locally (globally) fixed-time stable* if it is locally (globally) finite-time stable and the settling time function $T(x_0)$ is bounded for all $x_0 \in \Omega$ ($x_0 \in \mathbb{R}^n$), i.e., there exists $T_{max} > 0$ such that $T(x_0) \leq T_{max}$ for all $x_0 \in \Omega$ ($x_0 \in \mathbb{R}^n$).

The stability definition for the trajectories of the system (2.2) can be also formulated in the framework of the *comparisson functions* (see [Hahn, 1967]).

Proposition 2.1. *[Bacciotti and Rosier, 2005]. The following statements are equivalent:*

1. *The origin of* (2.2) *is globally asymptotically stable (GAS);*
2. *there exist a function $\beta : \mathbb{R}_+ \times \mathbb{R}_+ \to \mathbb{R}_+$ which is of class $\mathcal{KL}$ such that*
$$||\chi(t, x_0)|| \leq \beta(||x_0||, t) \tag{2.3}$$
for each $x_0 \in \mathbb{R}^n$ and all $t \geq 0$.

Recall that a function V satisfying that $V(0) = 0$ and $V(x) > 0$ ($V(x) \geq 0$) for all $x \neq 0$ is said to be *positive definite (semidefinite)*. A function V is said to be *negative definite (semidefinite)* if $-V$ is positive definite (semidefinite).

The Lyapunov function method offers a simple and effective tool for stability analysis of dynamical systems. This method consists in select a positive definite function and investigate its behavior along the system's trajectories, such that, if it is decreasing then it is called a *Lyapunov function*.

Theorem 2.1. *The origin of the system* (2.2) *is locally (globally) Lyapunov stable if and only if there exist a positive definite function $V : \Omega \subseteq \mathbb{R}^n \to \mathbb{R}_+$ and some functions $\alpha_1, \alpha_2 \in \mathcal{K}$ ($\alpha_1, \alpha_2 \in \mathcal{K}_\infty$, respectively) such that the inequalities*
$$\alpha_1(\|x\|) \leq V(x) \leq \alpha_2(\|x\|), \tag{2.4}$$
and
$$\sup_{d \in F(x)} D^+V(x)d \leq 0, \tag{2.5}$$
hold for any $x \in \Omega \setminus \{0\}$ where Ω is a neighborhood of the origin ($\Omega = \mathbb{R}^n$, respectively). In addition, if there exists a function $\alpha_3 \in \mathcal{K}$ such that the inequality (2.5) *is replaced by*
$$\sup_{d \in F(x)} D^+V(x)d \leq \alpha_3(\|x\|), \tag{2.6}$$
then the origin of the system (2.2) *is locally (globally) asymptotically stable.*

Proofs of the previous theorem can be found in [Bacciotti and Rosier, 2005, Polyakov, 2020].

2.3 Homogeneity

The symmetry of a function w.r.t. an uniform dilation of its arguments is called *homogeneity*. The linear functions are a subset of homogeneous ones w.r.t. the uniform dilation. Then, homogeneous nonlinear mappings keep some features of linear ones, and these have been found advantageous for analysis and design of control systems.

2.3.1 Standard homogeneity

In the eighteenth century, Leonhard Euler introduced the concept of standard homogeneity (homogeneity w.r.t. the uniform dilations) in the context of homogeneous polynomials. In control theory, this concept was introduced by Lasalle and Hahn in the 1940's.

Definition 2.2. A function $f : \mathbb{R}^n \to \mathbb{R}^m$ is said to be *homogeneous* (in the standard sense) if there exists a number $\kappa \in \mathbb{R}$ such that

$$f(\lambda x) = \lambda^\kappa f(x) \qquad \forall \lambda > 0, \qquad \forall x \in \mathbb{R}^n.$$

The number κ is called the *homogeneity degree* of the function f.

Another necessary and sufficient condition for homogeneity is given by the Euler's theorem on homogeneous function as presented below.

Theorem 2.2. *A continuously differentiable function $f : \mathbb{R}^n \to \mathbb{R}^m$ is homogeneous of a degree κ if and only if for all $i \in \{1, \ldots, m\}$*

$$\sum_{j_1}^{n} x_j \frac{\partial f_i}{\partial x_j}(x) = \kappa f_i(x), \qquad x \in \mathbb{R}^n.$$

It is clear that any linear function is homogeneous of degree $\kappa = 1$, i.e., if $f(x) = Ax$, $0 \neq A \in \mathbb{R}^{m \times n}$, then $f(\lambda x) = \lambda A x = \lambda f(x)$. Another example of these functions are homogeneous polynomials, e.g., a quadratic function $f(x) = x_1^2 + x_1 x_2 + x_2^2$ is homogeneous of degree $\kappa = 2$:

$$f(\lambda x) = (\lambda x_1)^2 + \lambda x_1 \lambda x_2 + (\lambda x_2)^2 = \lambda^2 f(x).$$

Moreover, the sign function is homogeneous of degree $\kappa = 0$, i.e., $\mathrm{sign}(\lambda \mathrm{x}) = \mathrm{sign}(\mathrm{x})$.

Note that products and quotients of homogeneous functions are also homogeneous besides the sum of homogeneous function of the same degree inherits the property. Moreover, from the Euler's homogeneous function theorem we can conclude that the derivative of a homogeneous function is also homogeneous.

For example, the function

$$f(x) = \frac{x_1^3 + x_2^3}{x_1^2 + x_2^2}$$

is homogeneous of degree $\kappa = 1$ but it is not linear. Whereas the function

$$f(x) = \frac{x_1 + x_2}{|x_1| + |x_2|}$$

is homogeneous of degree $\kappa = 0$ and it is discontinuous at $x = 0$.

Some necessary conditions that relate the regularity of a homogeneous mapping $f : \mathbb{R}^n \to \mathbb{R}$ to its homogeneity degree κ are:

- if $\kappa \leq 0$ then f is discontinuous at $x = 0$,
- if $0 < \kappa < 1$ then f is not Lipschitz continuous at the origin.

2.3.2 Weighted homogeneity

The standard homogeneity has been introduced by means of a uniform dilation $x \to \lambda x$, $\lambda > 0$. Nevertheless, this definition of homogeneity has a quite restrictive field of use. So, [Zubov, 1964] proposed a generalization of the standard concept of homogeneity by performing a weighted dilation of the variable $x = (x_1, x_2, \ldots, x_n)^\top \in \mathbb{R}^n$. This generalization is called *wighted homogeneity* and it has permitted to deal with a broader class of mathematical objects.

For strictly positive real numbers $r_i \quad (i = 1, \ldots, n)$ called weights define the vector $r = [r_1, \ldots, r_n]^\top$, where $r_{\max} = \max_{1 \leq j \leq n} r_j$ and $r_{\min} = \min_{1 \leq j \leq n} r_j$, and the dilation matrix $\Lambda_r(\lambda) = \operatorname{diag}(\lambda^{r_i})_{i=1}^n$ where $\lambda > 0$, such that,

$$\Lambda_r(\lambda)x = (\lambda^{r_1}x_1, \ldots, \lambda^{r_i}x_i, \ldots, \lambda^{r_n}x_n)^T .$$

The wighted homogeneity is also called r-homogeneity. Note that if $r_1 = r_2 = \ldots = r_n = 1$ then the standard definition of homogeneity is recovered. So, the homogeneity properties of a function in the weighted sense can be identified analogously to the standard case.

Definition 2.3. A function $g : \mathbb{R}^n \to \mathbb{R}$ is said to be *r-homogeneous of degree $\mu \in \mathbb{R}$* if for all $\lambda > 0$ and all $x \in \mathbb{R}^n$,

$$g(\Lambda_r(\lambda)x) = \lambda^\mu g(x).$$

A vector field $f : \mathbb{R}^n \to \mathbb{R}^n$ is said to be *r-homogeneous of degree $\nu \in \mathbb{R}$* ($\nu \geq -r_{\min}$) if $\forall x \in \mathbb{R}^n$ and $\forall \lambda > 0$,

$$f(\Lambda_r(\lambda)x) = \lambda^\nu \Lambda_r(\lambda) f(x),$$

which is equivalent to the i-th component of f being a r-homogeneous function of degree $r_i + \nu$.

Under this definition of a r-homogeneous vector field, the condition of the Euler's theorem on homogeneous functions becomes:

Proposition 2.2. *[Zubov, 1964]. A continuously differentiable vector field $f : \mathbb{R}^n \to \mathbb{R}^n$ is r-homogeneous of degree ν if and only if for all $i \in \{1, \ldots, n\}$*

$$\sum_{j_1}^{n} r_j x_j \frac{\partial f_i}{\partial x_j}(x) = (\nu + r_i) f_i(x), \qquad x \in \mathbb{R}^n.$$

Remark 2.1. The degree and the weights of a r-homogeneous function (vector field) are not unique. So that, if the function $g : \mathbb{R}^n \to \mathbb{R}$ (the vector field $f : \mathbb{R}^n \to \mathbb{R}^n$) is r-homogeneous of degree μ (ν) with wights $r = [r_1, \dots, r_n]^\top$, then it is also $\tilde{r}$-homogeneous for with a degree $\tilde{\mu} = p\mu$ ($\tilde{\nu} = p\nu$) with weights $\tilde{r} = [pr_1, \dots, pr_n]^\top$ for all $p > 0$.

Let's see some examples of r-homogeneous functions.

- the function $g = \operatorname{sign}(\mathrm{x}_1 + \lceil \mathrm{x}_2 \rfloor^2)$ is r-homogeneous of degree $\mu = 0$ with weights $r = [2, 1]$.
- the function $g = |x_1|^3 + x_1 \lceil x_2 \rfloor^4 + x_2^6$ is r-homogeneous of degree $\mu = 6$ with weights $r = [2, 1]$. Also, it is $\tilde{r}$-homogeneous of degree $\mu = 3$ with weights $\tilde{r} = [1, \frac{1}{2}]$.
- the vector field
$$f = \begin{bmatrix} x_2 \\ -\lceil x_1 \rfloor^{\frac{1}{3}} - 2\lceil x_2 \rfloor^{\frac{1}{2}} \end{bmatrix}$$
is r-homogeneous of degree $\nu = -\frac{1}{2}$ with weights $r = [\frac{3}{2}, 1]^\top$. Also, it is r-homogeneous of degree $\tilde{nu} = -1$ with weights $r = [3, 2]$.

Note that these functions are not homogeneous in the standard sense but they are homogeneous in the wighted one.

In addition, products, quotients, sums (for the same degree) and derivatives of r-homogeneous functions inherit the property. On the other hand, the relation between the continuity and the homogeneity degree of a homogeneous function is kept in the weighted sense. Furthermore, for a r-homogeneous vector field f of degree ν we have that fixing $r_{\min} = 1$:

- f is discontinuous on every axis of the states space if $\nu = -1$, and
- f does not satisfy the Lipschitz condition if $-1 < \nu < 0$.

Definition 2.4. Given a vector of weights $r = [r_1, \dots, r_n]^\top$. For any $\rho \geq 1$, a r-homogeneous norm is given by
$$\|x\|_r = \left(\sum_{i=1}^{n} |x_i|^{\frac{\rho}{r_i}} \right)^{\frac{1}{\rho}}, \qquad \forall x \in \mathbb{R}^n.$$
Additionally, the sphere and the ball of radius $s > 0$ are defined in terms of the r-homogeneous norm as $S_r(s) = \{x \in \mathbb{R}^n : \|x\|_r = s\}$ and $B_r(s) = \{x \in \mathbb{R}^n : \|x\|_r \leq s\}$, respectively.

Note that the *r-homogeneous norm* does not satisfy the triangle inequality hence it is not a norm in the usual sense. By its definition , the function $x \mapsto \|x\|_r$ is a r-homogeneous of degree 1. Moreover, there exists $\underline{\sigma}, \bar{\sigma} \in \mathcal{K}_\infty$ such that
$$\underline{\sigma}(\|x\|_r) \leq \|x\| \leq \bar{\sigma}(\|x\|_r) \qquad \forall x \in \mathbb{R}^n, \tag{2.7}$$
i.e. there is a relation between the norms $\|\cdot\|$ and $\|\cdot\|_r$ [Efimov et al., 2018].

Corollary 2.1. *[Efimov et al., 2018]. Let $r_{max} \leq 1$ and $\rho \geq 1$, then $\|\cdot\|_r$ is locally Lipschitz continuous.*

According to Remark 2.1, the conditions $r_{max} \leq 1$ and $\rho \geq 1$ can be always assumed, such that, the Lipschitz continuity of the r-homogeneous norm $\|\cdot\|_r$ is guaranteed. .

Definition 2.5. The system (2.1) is said to be r-homogeneous of degree ν if the vector field f is r-homogeneous of degree ν.

Following theorem establishes that the solution of a r-homogeneous differential equation is endowed with a kind of symmetry.

Theorem 2.3. *[Zubov, 1964, Bernuau et al., 2013a]. Assume that the system (2.1) is r-homogeneous of degree ν and admits a unique solution $\chi(t, x_0)$ in forward time for each initial condition $x_0 \in \mathbb{R}^n$. Then*

$$\Lambda_r(\lambda)\chi(\lambda^\nu t, x_0) = \chi(t, \Lambda_r(\lambda)x_0), \tag{2.8}$$

for all $\lambda > 0$ and all $t \geq 0$ where solutions are defined.

Note that similar to linear systems, the origin $x = 0$ is always an equilibrium point of a r-homogeneous systems. Moreover, from Theorem 2.3 we can see that any local property, like local stability or the existence of solutions for small initial conditions, can always be extended globally.

Now, let us recall some results about the homogeneity of differential inclusion, see for example [Levant, 2005a, Bernuau et al., 2014].

Definition 2.6. [Levant, 2005a]. A set-valued map $F : \mathbb{R} \rightrightarrows \mathbb{R}^n$ is r-homogeneous of degree $\nu \in \mathbb{R}$ if for all $x \in \mathbb{R}^n$ and for all $\lambda > 0$ we have

$$F(\Lambda_r(\lambda)x) = \lambda^\nu \Lambda_r(\lambda)F(x).$$

Furthermore, the differential inclusion (2.2) is r-homogeneous of degree ν if the set-valued map F is so.

Proposition 2.3. *[Levant, 2005a, Bernuau et al., 2013a]. Let a set-valued vector field $F : \mathbb{R} \rightrightarrows \mathbb{R}^n$ be r-homogeneous of degree ν. Then for all $x_0 \in \mathbb{R}^n$ and any solution $\chi(t, x_0)$ of the system (2.2) with initial condition x_0, and all $\lambda > 0$, the absolutely continuous curve $t \mapsto \Lambda_r(\lambda)\chi(\lambda^\nu t, x_0)$ is also a solution of the system (2.2) with initial condition $\Lambda_r(\lambda)x_0$, i.e.,*

$$\Lambda_r(\lambda)\chi(\lambda^\nu t, x_0) = \chi(t, \Lambda_r(\lambda)x_0), \tag{2.9}$$

for all $\lambda > 0$ and all $t \geq 0$ where solutions are defined.

Similarly to the previous cases, several properties of set-valued r-homogeneous maps can be extended from the sphere $S_r(s)$ to almost everywhere $x\mathbb{R}^n \setminus \{0\}$.

Proposition 2.4. *[Bernuau et al., 2013a]. Let a set-valued vector field $F : \mathbb{R}^{\rightrightarrows}\mathbb{R}^n$ be r-homogeneous of degree ν. Then $F(x)$ is compact for all $x\mathbb{R}^n \setminus \{0\}$ if and only if $F(x)$ is compact for all $x \in S_r(1)$. The same property hold for convexity or upper semi-continuity.*

The following proposition establishes the relationship between the homogeneity properties of a discontinuous vector field f and its Filippov regularization (see [Filippov, 1988]) given by a set-valued map F.

Proposition 2.5. *[Bernuau et al., 2013a]. Let f be a discontinuous vector field and F be the associated set-valued map. If f is r-homogeneous of degree ν, then F is also r-homogeneous of degree ν.*

The homogeneity properties of nonlinear functions have been found advantageous in the analysis and design of control systems.

2.4 Stability of homogeneous systems

The homogeneity properties of some nonlinear dynamical system have been found useful for a generalization of classical results on stability analysis.

Theorem 2.4. *[Zubov, 1964, Hahn, 1967]. If the origin of a locally attractive equilibrium point of a r-homogeneous system, then the origin is globally asymptotically stable.*

So, we have that the homogeneity simplifies global expansion of any local stability property (asymptotic, finite-time, etc.) [Bacciotti and Rosier, 2005, Polyakov, 2020].

The Lyapunov theorem has been also generalized form continuous r-homogeneous systems.

Theorem 2.5. *[Zubov, 1964]. Consider the system (2.1) where the vector field f is continuous and r-homogeneous of degree ν. Then the origin is globally asymptotically stable if and only if there exist a r-homogeneous and continuous function V, of class C^1 on $\mathbb{R}^n \setminus \{0\}$, such that, V and $-\dot{V}$ are positive definite.*

Recall that if a linear system is asymptotically stable at the origin then it has a Lyapunov function in the family of quadratic forms. Similarly, it turns out that if the origin of a r-homogeneous system is asymptotically stable then it admits a r-homogeneous Lyapunov function. Several converse Lyapunov theorems have been reported in the literature, however, the following generalized all its predecessors.

Theorem 2.6. *[Rosier, 1992]. Consider the system (2.1) where the vector field f is continuous and r-homogeneous of degree ν. If the origin is an asymptotically stable equilibrium point, then for any $p \in \mathbb{N}$ and any $\nu > p \cdot \max_i\{r_i\}$ there exists a class C^p and r-homogeneous Lyapunov function V of degree μ for the system (2.1).*

The counterpart of this theorem for r-homogeneous differential inclusions is presented in the following result. We say that a set-valued map F satisfies the standard assumptions if it is upper semi-continuous, and for all $x \in \mathbb{R}^n$, it is not empty, compact and convex.

Theorem 2.7. *[Bernuau et al., 2013a]. Let F be a r-homogeneous set-valued map of degree ν, satisfying the standard assumptions. Then the following statements are equivalent:*

- *The system (2.2) is strongly globally asymptotically stable.*
- *For all $\mu > \max(-\nu, 0)$, there exists a pair (V, W) of continuous functions, such that:*
  1. *V is of class C^∞ in $\mathbb{R}^n$, positive definite and r-homogeneous of degree μ;*
  2. *W is of class C^∞ in $\mathbb{R}^n \setminus \{0\}$, strictly positive outside of the origin and r-homogeneous of degree $\mu + \nu$;*
  3. *$\sup_{d \in F(x)} D^+V(x)d \leq -W(x)$ for all $x \neq 0$.*

In the previous theorem, the ward strongly means that the asymptotic stability holds for all solutions of the differential inclusion starting at he same initial condition, for the case of non-uniqueness of solutions. Therefore, from the previous we can conclude that if the system (2.2) is r-homogeneous of degree ν and asymptotically stable at origin, then there exists a smooth, r-homogeneous, Lyapunov function $V : \mathbb{R}^n \to \mathbb{R}_+$ of degree $\mu > \max\{0, -\nu\}$, which satisfies

$$\begin{aligned} a\|x\|_r^\mu \leq V(x) \leq b\|x\|_r^\mu, \quad \forall x \in \mathbb{R}^n, \\ \sup_{d \in F(x)} D^+V(x)d \leq -cV^{1+\frac{\nu}{\mu}}(x), \quad \forall x \in \mathbb{R}^n, \end{aligned}$$

for some $0 < a \leq b$ and $c > 0$ [Zubov, 1964, Rosier, 1992, Bernuau et al., 2013a].

Recall Proposition 2.1, for the case of an r-homogeneous systems of degree ν there is a generic parametrization of the $\mathcal{KL}$-function β in inequality (2.3) given by

$$\beta(s,t) = \begin{cases} \dfrac{\left(\frac{b}{a}\right)^{\frac{1}{\mu}} s}{\left(1 + a^{\frac{\nu}{\mu}} \frac{\nu}{\mu} c s^\nu t\right)^{\frac{1}{\nu}}} & \nu > 0, \\ \begin{cases} \left(\left(\frac{b}{a}\right)^{-\frac{\nu}{\mu}} s^{-\nu} + \frac{\nu}{\mu} c a^{\frac{\nu}{\mu}} t\right)^{-\frac{1}{\nu}} & t < -\dfrac{b^{-\frac{\nu}{\mu}} s^{-\nu}}{\frac{\nu}{\mu} c} \\ 0 & t \geq -\dfrac{b^{-\frac{\nu}{\mu}} s^{-\nu}}{\frac{\nu}{\mu} c} \end{cases} & \nu < 0, \\ \left(\frac{b}{a}\right)^{\frac{1}{\mu}} e^{\frac{-ct}{\mu}} s & \nu = 0. \end{cases} \tag{2.10}$$

for all $t \geq 0$ [Efimov et al., 2018].

One important feature of r-homogeneous systems is that their rate of convergence is related to their homogeneity degree. For instance, [Hong et al., 1999, Rosier, 1992, Bhat and Bernstein, 1997, Bhat and Bernstein, 2005] study this property for the case of a ordinary differential equation (2.1) with a continuous vector field f. On the other hand, the works of [Nakamura et al., 2002, Levant, 2005a, Bernuau et al., 2013a] extend that results for a differential inclusion (2.2) with a set-valued map F. The following theorem was taken from [Nakamura et al., 2002] and it can be seen as a generalization of all other results.

Theorem 2.8. *[Nakamura et al., 2002]. Assume that the differential inclusion (2.2) is r-homogeneous of degree ν and strongly asymptotically stable at origin. Then it is*

- *globally finite-time stable at the origin if $\nu < 0$*
- *globally exponentially stable at the origin if $\nu = 0$*
- *globally fixed-time stable w.r.t. a unit ball $B_r(1)$ if $\nu > 0$.*

The finite-time convergence is associated with the lack of Lipschitz continuity of r-homogeneous vector fields of negative degree in the origin.

Corollary 2.2. *[Bhat and Bernstein, 1997]. Let $f_1, \ldots, f_p$ be continuous r-homogeneous vector fields with degree $\nu_1 < \nu_2 < \ldots < \nu_p$ and denote $f = f_1 + f_2 + \ldots + f_p$. Moreover, assume that $f(0) = 0$. If the origin is globally asymptotically stable under f_1 then the origin is locally asymptotically stable under f. Moreover, if the origin is globally finite-time stable under f_1 then the origin is locally finite-time stable under f.*

Roughly speaking, the last results implies that dynamics with a smaller homogeneity degree dominate near to the origin.

2.5 Sliding mode control

Sliding Mode Control (SMC) technique is one of the main tools to robust control design. In theory, this kind of controllers are able to ensure finite-time convergence for system's trajectories to zero even in the presence of non-vanishing, bounded and matched disturbances [Utkin, 1992, Shtessel et al., 2014].

Consider the second order system

$$\begin{aligned} \dot{x}_1 &= x_2\,, \\ \dot{x}_2 &= \phi(t) + u\,, \end{aligned} \tag{2.11}$$

where x_1 and x_2 are the states, u is the control input and ϕ is a bounded disturbance, i.e., $|\phi(t)| \leq L$ with a known upper-bound $L > 0$.

Basically, the idea of SMC design consists in introduced a nominal dynamics for the system (2.11), for example a linear time-invariant differential equation

$$\dot{x}_1 + cx_1 = 0, \qquad c > 0. \tag{2.12}$$

It can be readily seen that the nominal dynamics (2.12) is exponentially stable at the origin. Let's introduce the variable

$$\sigma = x_2 + cx_1, \qquad c > 0, \tag{2.13}$$

in the state space of the system (2.11), such that, if we drive the variable σ to zero in finite-time then the system (2.11) collapses to the nominal dynamics (2.12) and exponential stability of the states x_1

and x_2 is guaranteed even in presence of the perturbation ϕ. For this task we can design a suitable control law like the sign function:

$$\bar{u} = -K\text{sign}(\sigma), \qquad K > 0. \tag{2.14}$$

Let us proof the stability of the system (2.11) in closed loop with the proposed control scheme. First, from (2.11) and (2.13), the dynamics of σ is given by

$$\dot{\sigma} = cx_2 + \phi(t) + u.$$

Now, considering $\bar{u} = -cx_2 + \bar{u} = -cx_2 - K\text{sign}(\sigma)$ we obtain

$$\dot{\sigma} = -K\text{sign}(\sigma) + \phi(t).$$

The last differential equation can be associated with the differential inclusion

$$\dot{\sigma} \in -\left[-K, K\right] + \left[-L, L\right].$$

Clearly, this differential inclusion is asymptotically stable at the origin for $K > L$, and r-homogeneous of degree $\nu = -1$ with weight $r = 1$. Thus, from Theorem 2.8, finite-time convergence of the variable σ to zero is guaranteed despite the perturbation term ϕ (see [Shtessel et al., 2014] for more details about SMC design).

Definition 2.7. [Shtessel et al., 2014]. The variable (2.13) is called a *sliding variable*.

Definition 2.8. [Shtessel et al., 2014]. Equations (2.12) and (2.13) rewritten in a form

$$\sigma = x_2 + cx_1 = 0, \qquad c > 0,$$

correspond to a straight line in the state space of the system (2.11) and it is referred to as a *sliding surface*.

Definition 2.9. [Shtessel et al., 2014]. The control u that drives the system's states to a sliding surface in a finite-time T_s, and keeps them on the surface thereafter in the presence of bounded disturbances, is called a *sliding mode controller*. The behavior of the system's trajectories in the interval of time $[0, T_s)$ is called the *reaching phase* and an *ideal sliding mode* is said to be taking place in the system's trajectories for all $t > T_s$.

Note that the previous case correspond to the so-called first-order sliding mode, where the sliding variable has a relative degree one. Likely, all these definition can be extended to sliding variable of higher relative degree through the concept of *Higher-Order Sliding Mode* (HOSM) [Levant, 1993, Levant, 2003b, Shtessel et al., 2014, Fridman et al., 2015, Fridman and Levant., 2002].

From [Fridman et al., 2015], the sliding mode controller can be sorted out in five generations as it is briefly described as follows:

First generation: Conventional Sliding Modes

First-order sliding mode controllers (FOSMC) was introduced by [Utkin, 1992] (the first version in English). There, a two-step procedure for FOSMC design was establish: I) sliding surface design; II) selection of a discontinuous (relay or unit) controller ensuring the sliding mode.

In theory, this controllers are able to provide an exact compensation (insensitivity) of bounded matched disturbances, and finite-time convergence of the system trajectories to a sliding surface.

However, the FOSMC has some disadvantages like the generation of a discontinuous control signal which causes the undesired effect of *chattering* (high frequency oscillation in the steady state of the system's trajectories), the sliding surface converges to zero in finite-time but the states variables do so asymptotically, and the sliding surface is restricted to have relative degree one w.r.t. the control input, hence, high-order derivatives of the state variables are required for the sliding surface design.

Second generation: Second-Order Sliding Modes

The controllers of this generation ensure finite-time convergence to second-order sliding modes, that is, for systems with relative degree two the output and its first derivative are nullified in finite-time in spite of the presence of bounded disturbances [Levant, 1993].

These controllers achieve quadratic and linear precision of convergence w.r.t. the sampling step for the sliding output and its first time-derivative, respectively, [Levant, 1993]. In addition, in the presence of fast actuator in control systems, quadratic precision for the sliding output and linear precision for the sliding output's derivative are ensured w.r.t. the actuator's time-constant [Boiko et al., 2007, Levant and Fridman, 2010].

The Twisting Algorithm [Emel'Yanov et al., 1986] and the Terminal Algorithm [Wu et al., 1998, Feng et al., 2002] belong to this generation of sliding mode controllers.

However, the control action is still discontinuous and the undesired *chattering* arise.

Third generation: the Super-Twisting algorithm

The Super-Twisting (STA) controller [Levant, 1993]:

$$u = -k_1 \lceil \sigma \rfloor^{\frac{1}{2}} + z, \qquad \dot{z} = -k_2 \lceil \sigma \rfloor^{0},$$

where σ is a sliding output of relative degree one w.r.t the control input, is able to provide finite-time convergence to second-order sliding modes despite the presence of perturbations with a bounded first derivative, e.i., $\sigma = \dot{\sigma} = 0$ for all $t \geq T_s$ without the usage of $\dot{\sigma}$.

The main advantages of this algorithm are the theoretically exact compensation of disturbances with a bounded first derivative (but they do not need to be bounded), and the generation of a continuous control signal, which offers a substantially chattering attenuation (but not its complete removal [Boiko and Fridman, 2005]).

Another interesting feature of the STA is that it can be used to construct a "robust exact" sliding mode differentiator [Levant, 1998] in the form

$$\dot{\hat{x}}_1 = -k_1 \lceil \hat{x} - f \rfloor^{\frac{1}{2}} + \hat{x}_2, \qquad \dot{\hat{x}}_2 = -k_2 \lceil \hat{x} - f \rfloor^{0},$$

where f is the signal to be differentiated and it is assumed that $|\ddot{f}| \leq L$ for some known constant L. For an appropriated selection of the gains k_1 and k_2, the convergence properties of the STA ensure that $f - \hat{x}_1 = \dot{f} - \hat{x}_2 = 0$ after a finite-time. Thus, $\hat{x}_2$ is an exact estimation of the derivative $\dot{f}$ in the absence of noise and sampling, and the best possible approximation under uncertainty conditions [Levant, 1993].

The disadvantages of this controller include that: for systems with relative degree higher than one, the design of a sliding surface is still needed. Hence, the sliding variable is nullified in finite-time but the states converge to the origin asymptotically.

Forth generation: Arbitrary Order Sliding Mode Controllers

For dynamical systems affected by bounded Lebesgue measurable perturbations and with an output of arbitrary relative degree r w.r.t. the control input, the HOSM controllers are able to provide finite-time convergence to zero of the output σ and its derivatives up to order $r-1$, e.i., $\sigma = \dot{\sigma} = \ldots = \sigma^{(r-1)} = 0$. This controllers warranty precision of $r - th$ order w.r.t sampling step and fast parasitic dynamics [Levant, 2003a, Levant and Fridman, 2010]. In addition, the sliding surface design is no longer needed.

The Nested HOSM Algorithm [Levant, 2001] was the first controller belonging to this generation. This controller uses information from $\sigma, \dot{\sigma}, \ldots, \sigma^{(r-1)}$ and it is constructed by combining the relay controller with hierarchical terminal sliding modes [Wu et al., 1998] in a recursive way, generalizing the last one for higher-order systems.

However, this algorithm produces discontinuous control signal and the effect of chattering is still arising. Another example of an algorithm of this generation is the so-called Quasi-continuous HOSM controller [Levant, 2005b], which is continuous everywhere except at the sliding set $\sigma = \dot{\sigma} = \ldots = \sigma^{(r-1)} = 0$. In practice, the last condition is rarely achieve due to the non-idealities (noise, delays, discretization, etc.) in the control system hence the control law remains continuous. Thus, this allows a substantially reduction of the chattering.

Moreover, an arbitrary order differentiator based on HOSM was introduced by [Levant, 2003a, Levant, 2005a] to estimate the $k-1$ consecutive derivatives of a signal f, exactly and in finite-time, under ideal conditions. Whereas, in presence of measurement noise or discretization, this differentiator provides the best possible asymptotic accuracy for the estimations [Levant, 1993]. In both cases, with the unique information of the upper-bound L for $|f^{(k)}|$.

Fifth generation: Continuous Arbitrary Order Sliding Mode Controllers

For dynamical systems affected by non-vanishing perturbations with a bounded first derivative, the continuous HOSM controllers are able to provide finite-time convergence to $(r+1) - th$ sliding set $\Pi_r = \{\sigma = \dot{\sigma} = \ldots = \sigma^{(r)} = 0\}$, i.e., the output σ, of arbitrary relative degree r w.r.t. the control input, and its derivatives up to order r are nullified in finite-time.

There are reported in the literature many continuous HOSM controllers, which can be seen as generalizations of the Super-Twisting Algorithm for higher-order systems. Four types of such controllers

can be distinguished:

- Continuous Terminal Sliding Mode Controllers introduced by [Kamal et al., 2016] (see also [Fridman et al., 2015]). For arbitrary order systems, these controllers are performed by the first-order Super-Twisting with a terminal sliding surface. This surface is given by a r-homogeneous polynomial of the states with an appropriated degree and weights to provide finite-time convergence.

- Higher Order Super-Twisting presented by [Laghrouche et al., 2017]. For a perturbed chain of n-integrators, this controller is based on a nominal homogeneous controller and its associated Lyapunov function (LF). The integral action depends on all plant's states, and it is of quasi-continuous type.

- Discontinuous Integral Control given by [Zamora et al., 2013, Moreno, 2016, Moreno, 2018] for second-order systems, and [Mercado-Uribe and Moreno, 2020] for arbitrary order systems. This algorithm is performed by a memoryless, homogeneous and nonlinear state feedback, with the addition of a discontinuous integral term, which is a sign function of the output variable or of a homogeneous polynomial of the state variables.

- Continuous Twisting Algorithm introduced by [Torres-González et al., 2017] for second-order system, and by [Mendoza-Avila et al., 2020b] for third-order systems. This algorithms can be seen as a memoryless, homogeneous, nonlinear state feedback plus a discontinuous integral extension consisting of a linear combination of sign functions of all system coordinates. For the case of second-order, this term contains the sign of the output plus sign of its derivative similar to the Twisting Algorithm.

The HOSM controllers produce a continuous control signal which attenuates the chattering, substantially. Moreover, they achieve precision of $(r+1)-th$ order w.r.t sampling step and fast parasitic dynamics. In addition, the sliding surface design is not longer needed.

Chapter 3

Converse theorems and numerical construction of Lyapunov functions for a class of Sliding-Mode algorithms

The Lyapunov function (LF) method is one of the main approaches to analyze the stability of dynamical systems [Bacciotti and Rosier, 2005, Zubov, 1964]. For linear systems, the design of LF has already been widely studied [Bacciotti and Rosier, 2005]. In the case of nonlinear systems, a general methodology to design LF is still an open problem. However, several converse Lyapunov theorems have been developed to demonstrate the existence of a LF for certain classes of nonlinear stable systems [Kurzweil, 1963, Massera, 1949, Persidskii, 1937, Yoshizawa et al., 1955].

On the other hand, [Clarke et al., 1998] presents the construction of a smooth LF for Filippov differential inclusions generalizing the results of [Kurzweil, 1963], which is an extension of the results of [Massera, 1949] for the case of smooth vector fields. A remarkable fact in [Clarke et al., 1998] is that only the upper semi-continuous behavior of the Filippov inclusion is required for the existence of a smooth LF for. Moreover, [Rosier, 1999] presents other inverse Lyapunov theorem for discontinuous systems, where a smooth LF is provided and Lyapunov and Lagrange stabilities are studied. The counterpart of the work in [Clarke et al., 1998] for discrete-time systems was developed by [Kellett and Teel, 2004], where the existence of smooth LF for robust globally asymptotically stable difference inclusions was proven.

The homogeneity has been found advantageous for the design of LF [Zubov, 1964, Rosier, 1992]. For homogeneous systems of positive degree, in [Efimov et al., 2018] several explicit formulas of homogeneous LF are provided based on the converse theorems of [Massera, 1949] and [Persidskii, 1937]. Moreover, they give a methodology for numerical construction of such functions. With a different approach, [Sanchez and Moreno, 2019, Sánchez and Moreno, 2016] use generalized homogeneous polynomials as LF for a class of homogeneous systems including negative homogeneity degree and discontinuous ones. On the other hand, [Nakamura et al., 2002] unifies the converse theorems presented by [Clarke et al., 1998] and [Rosier, 1999] into a simple and elegant framework with posterior con-

struction of a homogeneous LF associated with a homogeneous differential inclusion. Such a converse theorem was generalized by [Tuna and Teel, 2006] for homogeneous hybrid systems covering the discrete-time case as well.

Many examples of homogeneous and discontinuous systems are found in the family of Higher-Order Sliding Mode (HOSM) algorithms [Shtessel et al., 2014], and several approaches of LF design have been developed for particular cases of them. For instance, generalized polynomial LF for homogeneous HOSM algorithms are presented by [Sanchez and Moreno, 2019, Sánchez and Moreno, 2016]. On the other hand, [Moreno and Osorio, 2012] provide a family of strict LF for the Super-Twisting Algorithm by means of quadratic forms. Moreover, [Polyakov and Poznyak, 2009] introduced a LF for the Twisting Algorithm based on the method of Zubov. Furthermore, a unified LF for second order sliding mode control systems is presented by [Polyakov and Poznyak, 2012]. For a class of HOSM described by homogeneous and piecewise continuous vector fields, [Sánchez and Moreno, 2012] (see also [Sánchez and Moreno, 2014]) provided a constructive method to design homogeneous LF by integrating a positive definite function along the whole trajectories of the system. The latter method allows the design of a LF for Twisting and Terminal algorithms but its extension to a broader class of systems is complicated.

Despite the number of papers in the literature related to converse Lyapunov theorems for homogeneous and discontinuous systems, only the existence of the LF is proven in most of them under some restrictions. Contrarily, the present chapter provides two converse Lyapunov theorem with explicit formulas of homogeneous and Lipschitz continuous LF generalizing the results of [Kurzweil, 1963, Massera, 1949, Persidskii, 1937] and [Yoshizawa et al., 1955] for discontinuous homogeneous systems. Moreover, our results extend the methodology of [Efimov et al., 2018] of numerical construction of homogeneous LF to a class of discontinuous and homogeneous systems of negative degree. Both previous contribution establish a new framework to the numerical design of homogeneous and Lipschitz continuous LF for a wide class of HOSM. All the work presented here is already published in [Mendoza-Avila et al., 2021].

The rest of the chapter has the following structure. In Section 3.1, some useful definitions and preparatory results are presented. Section 3.2 contains the converse theorems and LF design for homogeneous discontinuous systems. Section 3.3 describes the methodology for a numerical construction of a LF for homogeneous discontinuous systems. In Section 3.4, the proposed methodology is applied to the numerical design of a LF for Twisting and Terminal algorithms. Finally, the conclusions are given in Section 3.5.

3.1 Preliminaries

Following [Filippov, 1988] (see also [Cortes, 2008]), a discontinuous vector field $f : \mathbb{R}^n \to \mathbb{R}^n$ is called piecewise continuous if there exist a finite number of disjoint, open and connected sets $D_i \subset \mathbb{R}^n;\ \ i = 1, \ldots, m$ whose closures $\bar{D}_i$ cover $\mathbb{R}^n$, i.e., $\mathbb{R}^n = \cup_{i=1}^{m} \bar{D}_i$, such that, for all $i = 1, \ldots, m$, the vector field is continuous on D_i.

Consider the system

$$\dot{x}(t) = f(x(t)), \quad t \in \mathbb{R}_+, \tag{3.1}$$

where $x(t) \in \mathbb{R}^n$ is the state and $f : \mathbb{R}^n \to \mathbb{R}^n$ is a piecewise continuous vector field with an equilibrium point at the origin, i.e., $f(0) = 0$. In the sequel, we will sometimes omit the time variable in $x(t)$ and just write x.

Let S be the set of points where f is discontinuous, such that S is equal to the union of the boundaries of the sets D_i, i.e., $S = \cup_{i=1}^{m} \partial(D_i)$. Note that S has measure zero.

For a piecewise continuous vector field $f : \mathbb{R}^n \to \mathbb{R}^n$, we can define a Filippov set-valued map

$$F(x) = \bar{\text{co}} \left\{ \lim_{i \to \infty} f(x_i) : x_i \to x, x_i \notin S \right\}, \qquad \forall x \in \mathbb{R}^n$$

where $\bar{\text{co}}$ denotes the convex closure of a set. By its definition, the set $F(x)$ is non-empty, compact and convex for all $x \in \mathbb{R}^n$ and the set-valued function F is upper semi-continuous [Filippov, 1988, Cortes, 2008].

For any initial condition $x_0 \in \mathbb{R}^n$ and $t \in [0, t_1] \subset \mathbb{R}_+$ with $t_1 > 0$, a Filippov solution of the piecewise continuous system (3.1) is an absolutely continuous functions $\chi : [0, t_1] \times \mathbb{R}^n \to \mathbb{R}^n$ satisfying the inclusion $\dot{\chi}(t, x_0) \in F(\chi(t, x_0))$ for almost all $t \in [0, t_1]$. A sufficient condition for uniqueness of solutions of a piecewise continuous system is given as follows

Proposition 3.1. *[Filippov, 1988]. Let $f : \mathbb{R}^n \to \mathbb{R}^n$ be a piecewise continuous vector field, with $\mathbb{R}^n = \bar{D}_1 \cup \bar{D}_2$ for some disjoint, open and connected sets $D_1, D_2 \subset \mathbb{R}^n$. Let $S = \partial(D_1) = \partial(D_2)$ be the set of points at which f is discontinuous and assume that S is a C^2-manifold. Moreover, assume that for $i = 1, 2$, the restriction of f to D_i admits a continuous extension to the closure $\bar{D}_i$ denoted by $f_{|\bar{D}_i}$, which is continuously differentiable on D_i and $f_{|\bar{D}_1} - f_{|\bar{D}_2}$ is continuously differentiable on S. If for each $x \in S$, either $f_{|\bar{D}_1}(x)$ points into D_2 or $f_{|\bar{D}_2}(x)$ points into D_1, then $\chi(t, x_0)$ is the unique Filippov solution of (3.1) starting from any initial condition $x_0 \in \mathbb{R}^n$.*

It is easy to check that the number of partitions $D_i \subset \mathbb{R}^n; \quad i = 1, \ldots, m$ can be extended to any arbitrary finite number $m \geq 2$. Roughly speaking, the uniqueness of solutions on each set D_i is guaranteed by the continuous differentiability of f on D_i while the assumption of continuous differentiability of $f_{|\bar{D}_i} - f_{|\bar{D}_j}$ along S, with $i \neq j$ and $i, j \in [1, m]$, guarantees that the uniqueness is not disrupted by the discontinuity [Cortes, 2008].

At the points belonging to S, the Filippov solution of the piecewise continuous system (3.1) can exhibit different behaviors. Suppose that $x \in S$ belongs to the boundary of just two sets, i.e., $x \in \partial(D_i) \cap \partial(D_j)$, for some $i, j \in [1, m]$, but $x \notin \partial(D_k)$, for all $k \in [1, m] \setminus \{i, j\}$. First, if all vectors belonging to $F(x)$ point into D_i (respectively, D_j), then a Filippov solution that reaches S at x continues its motion in D_i (respectively D_j). Second, if a vector in $F(x)$ is tangent to S, then either all Filippov solutions that start at x leave S immediately, or there exist Filippov solutions that reach the set S at x and slide on S afterwards, which is called *sliding motions* [Cortes, 2008].

Consider the following hypothesis about the system (3.1).

Assumption 3.1. Let the system (3.1) be r-homogeneous of degree $\nu < 0$ and be endowed with the property of uniqueness of Filippov solutions in $\mathbb{R}^n \setminus \{0\}$ with no sliding motion on $\mathbb{R}^n$ except at the origin. Furthermore, let f be discontinuous only on a set of measure zero $S \subseteq \bigcup_{i=1}^m \partial D_i$ for disjoint, open and connected sets $D_i \subset \mathbb{R}^n$, $i = 1, \dots, m$, where $m > 0$ is a finite integer, whose closures cover $\mathbb{R}^n$, i.e., $\mathbb{R}^n = \bigcup_{i=1}^m \bar{D}_i$. Moreover, on each $\bar{D}_i$ with $i = 1, \dots, m$, f admits a continuous projection $f_{|\bar{D}_i}$, which is locally Lipschitz continuous on D_i, and if $x \in \partial D_i \cap \partial D_j \subset S$ for $i \neq j \in \{1, \dots, m\}$, then either $f_{|\bar{D}_i}(x)$ points into D_j or $f_{|\bar{D}_j}(x)$ points into D_i.

Some examples of algorithms satisfying Assumption 3.1 are the twisting algorithm, the terminal algorithm (for a special selection of the controller gains $\beta^2 > 2\alpha$ the trajectories of this algorithm behave in twisting mode, hence, they exhibit sliding mode only at the origin), or the quasi-continuous controller, which belong to the family of HOSM [Shtessel et al., 2014].

Under Assumption 3.1, the solutions of the system (3.1) admit a local Lipschitz continuity property w.r.t. initial conditions on a bounded interval of time:

Lemma 3.1. *[Mendoza-Avila et al., 2021]. Let Assumption 3.1 be satisfied and the system (3.1) be globally finite-time stable, then for any $q > 1$ there is $L_{S_r(1),\bar{T}_q(1)} > 0$ such that for the solutions of (3.1)*

$$\|\chi(t, x_1) - \chi(t, x_2)\| \leq L_{S_r(1),\bar{T}_q(1)} \|x_1 - x_2\|$$

for any $x_1, x_2 \in S_r(1)$ and all $t \in [0, \bar{T}_q(1))$.

It can be seen that under Assumption 3.1 the continuous dependence of the trajectories w.r.t. the initial conditions follows from the existence of Lipschitz continuous projections $f_{|\bar{D}_i}$ of the vector field f, which cover the whole state space, and the absence of sliding motion outside the origin. The proof of Lemma 3.1 is provides in Section A.1 of Appendix A.

For a r-homogeneous system (3.1) of degree ν, if it is asymptotically stable at origin, then there exists a smooth and r-homogeneous LF $V : \mathbb{R}^n \to \mathbb{R}_+$ of degree $\mu > \max\{0, -\nu\}$ satisfying

$$a\|x\|_r^\mu \leq V(x) \leq b\|x\|_r^\mu, \quad \forall x \in \mathbb{R}^n, \tag{3.2}$$

$$\sup_{d \in F(x)} D^+V(x)d \leq -cV^{1+\frac{\nu}{\mu}}(x), \quad \forall x \in \mathbb{R}^n, \tag{3.3}$$

for some $0 < a \leq b$ and $c > 0$ [Zubov, 1964, Bernuau et al., 2013a]. Then, for any $x_0 \in \mathbb{R}^n$, the trajectories of the system (3.1) are bounded by

$$\|\chi(t, x_0)\|_r \leq \beta(\|x_0\|_r, t) \qquad \forall t \geq 0, \tag{3.4}$$

where

$$\beta(s,t) = \begin{cases} \left(\left(\frac{b}{a}\right)^{-\frac{\nu}{\mu}} s^{-\nu} + \frac{\nu c a^{\frac{\nu}{\mu}}}{\mu} t \right)^{-\frac{1}{\nu}} & t < \frac{-\mu b^{-\frac{\nu}{\mu}} s^{-\nu}}{\nu c} \\ 0 & t \geq \frac{-\mu b^{-\frac{\nu}{\mu}} s^{-\nu}}{\nu c} \end{cases} \qquad \nu < 0. \tag{3.5}$$

is a $\mathcal{KL}$-function, and it is a generic parametrization of the upper bound $\beta(\|x_0\|_r, t)$ in 3.4 for all $t \geq 0$ in homogeneous systems of negative degree [Efimov et al., 2018].

On the other hand, following the work in [Efimov et al., 2018] the speed of convergence of the trajectories of r-homogeneous systems can be quantified as follows:

Definition 3.1. Assume the system (3.1) is asymptotically stable. For $q > 1$, define the map $T_q : \mathbb{R}^n \to \mathbb{R}_+$ as the first time the norm of the solution becomes q times smaller than the norm of the initial condition:

$$\|\chi(T_q(x_0), x_0)\|_r = q^{-1}\|x_0\|_r.$$

From its definition, it is easily seen that T_q is r-homogeneous of degree $-\nu$:

$$T_q(\Lambda_r(\lambda)x_0) = \lambda^{-\nu}T_q(x_0), \quad \forall x_0 \in \mathbb{R}^n, \ \forall \lambda > 0.$$

Definition 3.2. Assume the system (3.1) is asymptotically stable. For $q > 1$, define a continuous function $\bar{T}_q : \mathbb{R}^n \to \mathbb{R}_+$ as the time from which the solution remains in the ball with a radius q times smaller than the norm of the initial condition:

$$\|\chi(t, x_0)\|_r \leq q^{-1}\|x_0\|_r, \quad \forall t \geq \bar{T}_q(x_0).$$

Moreover, define a continuous function $\bar{T}_q^{\max} : \mathbb{R}_+ \to \mathbb{R}_+$ as

$$\bar{T}_q^{\max}(\|x_0\|_r) = \sup_{x_0 \in S_r(s)} \bar{T}_q(x_0).$$

Note that $\bar{T}_q$ is also r-homogeneous of degree $-\nu$:

$$\bar{T}_q(\Lambda_r(\lambda)x_0) = \lambda^{-\nu}\bar{T}_q(x_0), \quad \forall x_0 \in \mathbb{R}^n, \ \forall \lambda > 0.$$

Moreover, $\bar{T}_q^{\max}$ is uniform on the sphere $S_r(s)$, and taking into account (3.5):

$$\bar{T}_q^{\max}(\|x_0\|_r) = \frac{\left(\frac{b}{a}\right)^{-\frac{\nu}{\mu}} - q^{\nu}}{-\frac{\nu}{\mu}ca^{\frac{\nu}{\mu}}}\|x_0\|_r^{-\nu}; \qquad \nu < 0. \tag{3.6}$$

3.2 Converse Theorems

The results of Massera [Massera, 1949] and Kurzweil [Kurzweil, 1963] provide the design of a LF as the integral of a $\mathcal{K}_\infty$ function depending on the system's trajectories, while Persidskii [Persidskii, 1937] and Yoshizawa [Yoshizawa et al., 1955] propose the design of LF based on the supremum of a $\mathcal{K}_\infty$ function of the system's solutions. In this section, these classical converse Lyapunov theorems are generalized for r-homogeneous discontinuous systems satisfying Assumption 3.1. Also, explicit formulas of r-homogeneous and Lipschitz continuous LF are provided.

3.2.1 Design based on the integral of the trajectories

Theorem 3.1. *Let the system (3.1) satisfy Assumption 3.1. Then the following is equivalent:*

(i) The discontinuous system (3.1) is globally finite-time stable at the origin.

(ii) For all $x \in \mathbb{R}^n$ and $\mu \geq 1$, there exists $q > 1$ such that the function

$$U(x) = \int_0^{T_q^{\max}(\|x\|_r)} \|\chi(t,x)\|_r^{\mu} dt, \tag{3.7}$$

where $T_q^{\max}(s) = \sup_{x \in S_r(s)} T_q(x)$ and T_q is given by Definition 3.1, is locally Lipschitz continuous on $\mathbb{R}^n \setminus \{0\}$, r-homogeneous of degree $\mu - \nu$, and satisfies

$$\begin{aligned} T_q^{\min} q^{-\mu} \|x\|_r^{\mu-\nu} \leq \quad & U(x) \quad \leq T_q^{\max}(1) \frac{b}{a} \|x\|_r^{\mu-\nu}, \ \forall x \in \mathbb{R}^n, \\ & D^+U(x)F(x) \quad < 0, \quad \text{for a.a. } x \in \mathbb{R}^n \setminus \{0\}, \end{aligned}$$

where $T_q^{\min} = \inf_{x \in S_r(1)} T_q(x)$.

The proof of Theorem 3.1 is presented in Section A.2 of Appendix A.

Remark 3.1. Note that when $q \to \infty$ the time $T_q(x)$ becomes the convergence time, and the LF (3.7) proposed by Theorem 3.1 corresponds to the case of [Massera, 1949], where the trajectory is integrated for all the time until it reaches the origin.

3.2.2 Design based on the supremum of the trajectories

First, let $\varrho > 0$ be a real parameter satisfying $|\varrho\nu| > 1$. Define a function $k : \mathbb{R}_+ \times \mathbb{R}^n \to \mathbb{R}_+$ by

$$k(t,x) = \frac{\|\chi(t,x)\|_r^{\varrho\nu} t^{\varrho} + \kappa_1}{\|\chi(t,x)\|_r^{\varrho\nu} t^{\varrho} + \kappa_2}, \tag{3.8}$$

for given parameters $0 < \kappa_1 < \kappa_2 < +\infty$.

Theorem 3.2. *Let the system (3.1) satisfy Assumption 3.1. Then, the following claims are equivalent:*

(i) The discontinuous system (3.1) is globally finite-time stable at the origin.

(ii) For all $x \in \mathbb{R}^n$, there exists $q > 1$ such that

$$V(x) = \sup_{t \in [0, T_q(x)]} \{\|\chi(t,x)\|_r \, k(t,x)\}, \tag{3.9}$$

where T_q is given in Definition 3.1, is a locally Lipschitz continuous on $\mathbb{R}^n \setminus \{0\}$ and $\mathbf{r}$–homogeneous function of degree 1 satisfying

$$\begin{aligned} \frac{\kappa_1}{\kappa_2} \|x\|_r \leq V(x) \leq \left(\frac{b}{a}\right)^{\frac{1}{\mu}} \|x\|_r \ \text{for all } x \in \mathbb{R}^n, \\ D^+V(x)f(x) < 0 \quad \text{for a.a. } x \in \mathbb{R}^n \setminus \{0\}. \end{aligned}$$

The proof of Theorem 3.2 is provided in Section A.3 of Appendix A.

Remark 3.2. Note that when $q \to \infty$ the time $T_q(x)$ becomes the convergence time, and the LF (3.9) proposed by Theorem 3.2 corresponds to the case of [Persidskii, 1937], where the supremum of the trajectories is looked for all the time until the origin is reached.

Both proposals of computing the LF (3.7) and (3.9) up to the times $T_q^{\max}(\|x\|_r)$ and $T_q(x)$, respectively, can be readily applied for systems with a positive homogeneity degree, which is studied by [Efimov et al., 2018] but using $\bar{T}_q(\|x\|_r)$. However, the time $T_q(x)$ (and $T_q^{\max}(\|x\|_r)$ defined as the supremum of $T_q(x)$ for all x in the same sphere) greatly simplifies the calculations because it is easier to identify when the trajectories $\chi(t,\, x)$ reach the sphere of radius $\frac{1}{q}\|x\|_r$ for the first time, in contrast to the time $\bar{T}_q(\|x\|_r)$ from which the trajectories $\chi(t,\, x)$ never left the ball of radius $\frac{1}{q}\|x\|_r$.

3.3 Numerical design

The LF provided by Theorems 3.1 and 3.2 can be numerically realized by following the methodology proposed by [Efimov et al., 2018].

First of all, due to homogeneity properties of the LF (3.7) and (3.9), for any $x \in \mathbb{R}^n$ there is a unique $y \in S_r(1)$ such that $x = \Lambda_r(\|x\|_r)y$ and $U(x) = \|x\|_r^{\rho_0} U(y)$, where ρ_0 is the homogeneity degree of the LF. Thus, it is enough to approximate the values of the LF on the unit sphere, and later recover its values globally applying the dilation $\Lambda_r(\|x\|_r)$.

The methodology of [Efimov et al., 2018], for numerical construction of r-homogeneous LF, consists of two steps:

1. Point-wise calculation of some values of the LF, uniformly distributed on the unit sphere $S_r(1)$, and
2. Interpolation of the LF for any $y \in S_r(1)$.

Although this methodology was developed by considering systems with positive homogeneity degree, an extension to the case of systems with negative homogeneity degree is straight forward because the LF provided by Theorems 3.1 and 3.2 satisfy the properties of homogeneity and Lipschitz continuity required by the proposal of [Efimov et al., 2018]. This extension is developed as follows.

Consider the explicit Euler method [Butcher, 2003]. Recall, from Assumptions 3.1, $\chi(t, x_0)$ is the unique solution of system (3.1) with initial condition x_0. So, for a given fixed sampling step $h > 0$, the discrete trajectory $\chi_h(t_i, x_0)$ denotes an approximation at instants $t_i = ih$, $i = 1, 2, 3, \ldots$ of the solution $\chi(t, x_0)$.

For $N > 0$, let the points $\xi_j \in S_r(1)$ (with $j = 1, \ldots, N$) form a uniform grid on the unit sphere. Then, considering the LF (3.7) based on the integral of the system's trajectories, define

$$U_j^h = h \sum_{i=1}^{J^{\max}} \|\chi_h(t_i, \xi_j)\|_r^{\mu}, \tag{3.10}$$

$$J^{\max} = \arg\inf_{i \geq 0} \sup_{1 \leq j \leq N} \|\chi_h(t_i, \xi_j)\|_r \leq q^{-1}.$$

Now, considering the LF (3.9) based on the supremum of the system's trajectories, define

$$V_j^h = \sup_{i\in[0,J]} \{\|\chi_h(t_i,\xi_j)\|_r \, k(t_i,\xi_j)\}, \tag{3.11}$$
$$J = \arg\inf_{i\geq 0} \|\chi_h(t_i,\xi_j)\|_r \leq q^{-1},$$

and

$$k_j(t_i,\xi_j) = \frac{\|\chi_h(t_i,\xi_j)\|_r^{\varrho\nu} t_i^{\varrho} + \kappa_1}{\|\chi_h(t_i,\xi_j)\|_r^{\varrho\nu} t_i^{\varrho} + \kappa_2},$$

where $\varrho > 0$ such that $|\varrho\nu| > 1$.

Remark 3.3. The parameter J in the proposal of [Efimov et al., 2018] is taken such that $\|\chi_h(t_i,\xi_j)\|_r \leq q^{-1}$ holds for all $1 \leq j \leq N$ and all $i \geq J$. However, in that case, it is not clear how to find J at least that the whole trajectory is computed until it converges to the origin. In contrast, our proposal simplifies the calculation of J because it is possible to determine the point when $\|\chi_h(t_i,\xi_j)\|_r \leq q^{-1}$ holds for the first time and take $J^{\max}$ as the largest J for the initial conditions $\xi_j \in S_r(1)$ (with $j = 1,\ldots,N$). Moreover, the definition of J presented here reduces the data load and make the numerical design of LF more efficient than the original approach of [Efimov et al., 2018]. Pleasantly, our proposal can be used for systems with positive homogeneity degree, as well.

Following proposition shows that homogeneous LF possess a kind of robustness w.r.t. small deformations under some restrictions.

Proposition 3.2. *(Efimov et al. [Efimov et al., 2018]). For a locally Lipschitz continuous and r-homogeneous function V of degree $\mu > -\nu$, assume that the estimates (3.2) and (3.3) are satisfied with constants $0 < a \leq b$ and $c > 0$. Let $\epsilon : \mathbb{R}^n \to \mathbb{R}$ be a locally Lipschitz continuous and r-homogeneous function of degree μ, such that, $-a < \underline{\epsilon}$ and $c > \bar{\epsilon}$, where $\underline{\epsilon} = \inf_{y\in S_r(1)} \epsilon(y)$ and $\bar{\epsilon} = \sup_{y\in S_r(1)} D^+\epsilon(y)f(y)$. Then $V'(x) = V(x) + \epsilon(x)$ is a locally Lipschitz continuous and r-homogeneous LF for the system (3.1).*

The following corollary shows that there exist some functions $\tilde{U}$ and $\tilde{V}$ which coincides in pointwise values with the discrete functions (3.10) and (3.11), respectively. Hence, under Proposition 3.2, they are also LF for the system (3.1).

Corollary 3.1. *Let Assumption 3.1 be satisfied by the system (3.1). Then there exist $q > 1$, $N > 0$ and $h > 0$, such that,*

$$U_j^h = \tilde{U}(\xi_j) \qquad \text{and} \qquad V_j^h = \tilde{V}(\xi_j),$$

for all $j = 1,\ldots,N$, where $\tilde{U} : \mathbb{R}^n \to \mathbb{R}_+$ and $\tilde{V} : \mathbb{R}^n \to \mathbb{R}_+$ are locally Lipschitz continuous and r-homogeneous LF of degree $\mu - \nu$ and 1, respectively, for the system (3.1).

Proof. Since all conditions of Theorems 3.1 and 3.2 are satisfied, for $q > 1$ sufficiently large a LF for the system (3.1) can be selected in the same form of U given by (3.7) or V given by (3.9). By the

properties of the (explicit) Euler method [Butcher, 2003], for a sufficiently large value of $N > 0$ and a small enough $h > 0$ the inequalities

$$|U_j^h - U(\xi_j)| < \epsilon_1, \qquad \text{and} \qquad |V_j^h - V(\xi_j)| < \epsilon_2,$$

hold for any $\epsilon_1, \epsilon_2 > 0$ and all $j = 1, \dots, N$. From Proposition 3.2, a r-homogeneous LF possesses certain robustness against small deformations. So, since the values of ϵ_1, ϵ_2 can be made arbitrarily small by increasing N and decreasing h, if U in (3.7) and V in (3.9) are LF for the system (3.1), then the same is true for a $\tilde{U}$ and $\tilde{V}$ described in Corollary 3.1. □

The next step is to make an interpolation of the points U_j^h and V_j^h in order to find the functions $\tilde{U}$ and $\tilde{V}$, respectively. This procedure is described in [Efimov et al., 2018] as follows.

First, note that a homogeneous norm is any positive definite, Lipschitz continuous and homogeneous function of degree 1, such that, $S_r(1) = \mathbb{S}^n = \{x \in \mathbb{R}^n : \|x\| = 1\}$ (e.g., an implicit definition of a canonical homogeneous norm from [Polyakov et al., 2016] can be used); then for any $x, y \in \mathbb{S}^n$, let $g(x, y) = \arccos(x^\top y)$ denotes the geodesic distance on the unit sphere $\mathbb{S}^n$.

Now, from the theory of radial basis function for interpolation on the sphere (see [Cheney, 1995, Hubbert, 2002]), a continuous function $p : [0, \pi] \to \mathbb{R}$ is (zonal) strictly positive definite on $\mathbb{S}^n$ if for all distinct points $\xi_j \in \mathbb{S}^n$ with $j = 1, \dots, N$ and for all $N > 0$, the matrix

$$\Pi_N = \{p(g(\xi_i, \xi_j))\}_{i,j=1}^N$$

is positive definite. Then selecting a zonal strictly positive definite function p (several examples are provided in [Cheney, 1995, Hubbert, 2002], e.g., $p(s) = e^{-as^2}$, $p(s) = s^3$, etc.):

- There exists always $\theta_U \in \mathbb{R}^N$ such that $U_j^h = \tilde{U}(\xi_j)$ for all $j = 1, \dots, N$ where

$$\tilde{U}(\xi) = \sum_{j=1}^N \theta_{U,j} p(g(\xi, \xi_j)). \tag{3.12}$$

  where the vector θ_U is the solution of the equation $\Gamma_N^U = \Pi_N \theta_U$, where $\Gamma_N^U = [U_1^h, \dots, U_N^h]^T \in \mathbb{R}^N$.

- There exists always $\theta_V \in \mathbb{R}^N$ such that $V_j^h = \tilde{V}(\xi_j)$ for all $j = 1, \dots, N$ where

$$\tilde{V}(\xi) = \sum_{j=1}^N \theta_{V,j} p(g(\xi, \xi_j)). \tag{3.13}$$

  where the vector θ_V is the solution of the equation $\Gamma_N^V = \Pi_N \theta_V$, where $\Gamma_N^V = [V_1^h, \dots, V_N^h]^T \in \mathbb{R}^N$.

The matrix Π_N is non-singular, symmetric and positive definite thanks to the properties of the function p. Some assumptions on p and Π_N are needed:

Assumption 3.2. The function $p(g(\xi,\xi_0))$ is locally Lipschitz continuous w.r.t. ξ for any $\xi,\xi_0\in\mathbb{S}^n$.

Assumption 3.3. There exist $\alpha>0$ and $\varrho>0$ such that for any $N>0$

$$\left\|\Pi_N^{-1}\right\|_2\leq\frac{\varrho}{N^{1+\alpha}}$$

where $\|\cdot\|_2$ is the induced matrix norm.

In [Efimov et al., 2018], it has been proven that a locally Lipschitz continuous and r-homogeneous LF for r-homogeneous systems with positive degree is given, on the unit sphere, in the form of (3.12) or (3.13). On the other hand, from the results of Corollary 3.1 and Theorems 3.1 and 3.2, the LF (3.7), (3.9), (3.12) and (3.13) have the properties of boundedness, homogeneity and Lipschitz continuity required by the proof of Theorem 3 in [Efimov et al., 2018]. Therefore, for a large enough $N>0$ (i.e., a sufficiently dense grid on the unit sphere) and a small enough sampling step $h>0$, (3.12) appropriately approximates the LF (3.7) on $S_r(1)$, whereas (3.13) appropriately approximates the LF (3.9) on $S_r(1)$, hence by the robustness of a homogeneous LF predicted by Proposition 3.2, it can be concluded that (3.12) and (3.13) are projections on $S_r(1)$ of LF for the system (3.1). Moreover, as it was mentioned before, for any $x\in\mathbb{R}^n$ there is a unique $\xi\in S_r(1)$ such that $x=\Lambda_r(\|x\|_r)\xi$ and $U(x)=\|x\|_r^{\rho_0}U(\xi)$, where ρ_0 is the homogeneity degree of the LF. Consequently, the following corollary is derived.

Corollary 3.2. *Let Assumptions 3.1, 3.2 and 3.3 be satisfied. Then there exist $q>1$, $N>0$ and $h>0$ such that for any $x\in\mathbb{R}^n$:*

- *A locally Lipschitz continuous and r-homogeneous of degree $\mu-\nu$ LF for the system (3.1) is given by*
$$\tilde{U}(x)=\|x\|_r^{\mu-\nu}\tilde{U}(\xi) \tag{3.14}$$
where $\tilde{U}$ is given by (3.12).

- *A locally Lipschitz continuous and r-homogeneous of degree 1 LF for the system (3.1) is given by*
$$\tilde{V}(x)=\|x\|_r\tilde{V}(\xi) \tag{3.15}$$
where $\tilde{V}$ is given by (3.13).

The main drawback of the present procedure of numerical design of LF is the selection of the parameters $q>1$, $N>0$ and $h>0$. There is no way to determine a priori their suitable values yet. Thus, the procedure should be repeated for different values of $q>1$, $N>0$, and $h>0$ till obtaining a desired LF.

Note that by construction, the functions (3.14) and (3.15) are positive definite, Lipschitz continuous and r-homogeneous of the corresponding degree. To confirm that the methodology was successfully realized, the negative definiteness of the derivative of those LF has to be tested. By homogeneity properties of the system (3.1) and the designed Lyaunov functions, the verification of the negative

definiteness of the derivatives can be performed on the unit sphere $S_r(1)$ only, that is, for any $x \in \mathbb{R}^n$ there exists an unique $y \in S_r(1)$ such that $x = \Lambda_r(\|x\|_r)y$, then considering V as a r-homogeneous and locally Lipschitz continuous LF:

$$D^+V(x)F(x) = \|x\|_r^{\rho_0} D^+V(y)F(y).$$

Thus, if $D^+V(y)F(y) < 0$ then we have obtained a LF.

Usually, the design of LF is employed to evaluate the stability of a system. If we consider a system satisfying Assumption 3.1 and the presented methodology returns a LF, then the asymptotic stability of that system is guaranteed.

3.4 Examples of numerical design of Lyapunov functions

As it has been mentioned before, many HOSM algorithms satisfy Assumption 3.1, hence a LF like (3.14) or (3.15) can be computed for them by following the methodology described in Section 3.3. In the following two examples are provided: the Twisting Algorithm for the design based on the integral of the trajectories and the (Nonsingular) Quasi-continuous Control Algorithm for the design based on the supremum of the trajectories. Both algorithms are described in detail in [Shtessel et al., 2014].

3.4.1 Design based on the integral of the trajectories

Consider the Twisting Algorithm given by

$$\begin{aligned} \dot{x}_1 &= x_2, \\ \dot{x}_2 &= -c_1 \lceil x_1 \rfloor^0 - c_2 \lceil x_2 \rfloor^0, \end{aligned} \tag{3.16}$$

where $x \in \mathbb{R}^2$ is the state and $c_1, c_2 \in \mathbb{R}_+$ have to satisfy $c_1 > c_2$ to guarantee stability at the origin. The system (3.16) is r-homogeneous of degree $\nu = -1$ and weights $r = [2, 1]$. From Corollary 3.2 and considering the parameters and expressions:

$$q = 10, \quad h = 0.01, \quad a = 50, \quad \mu = 3, \quad N = 50, \quad c_1 = 2, \quad c_2 = 1,$$
$$p(s) = e^{-as^2}, \qquad g(x, y) = \arccos(x^\top y),$$

a LF for the system (3.16) is given by

$$\tilde{U}(x) = \|x\|_r^{\mu-\nu} \sum_{j=1}^{N} \theta_j e^{-a \arccos^2(\xi^\top \xi_j)} \tag{3.17}$$

where $\xi \in S_r(1)$ such that $x = \Lambda_r(\|x\|_r)\xi$ and the points $\xi_j \in S_r(1)$, with $j = 1, \ldots, N$, form an uniform grid on the unique sphere. Moreover, the vector θ is the solution of the equation $\Gamma_N = \Pi_N \theta$, where $\Pi_N = \{e^{-a \arccos^2(\xi_i^\top \xi_j)}\}_{i,j=1}^N$ and $\Gamma_N = [U_1^h, \ldots, U_N^h]^T$ where U_j^h are given by (3.10) with

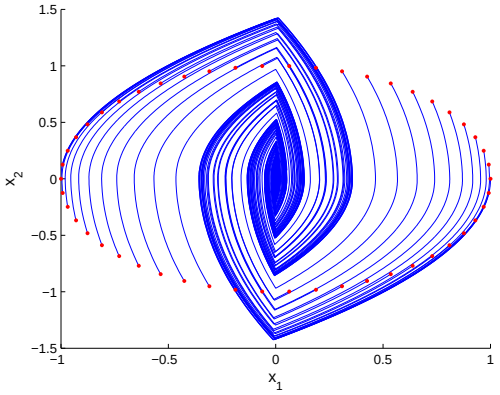

(a) Vector field.

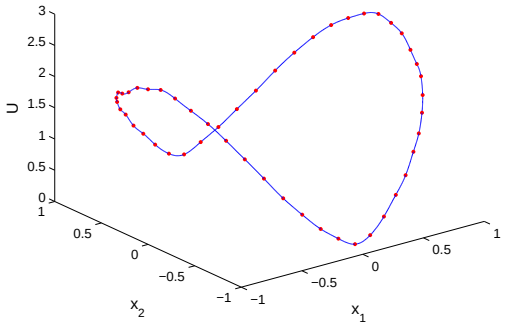

(b) LF on the unit sphere.

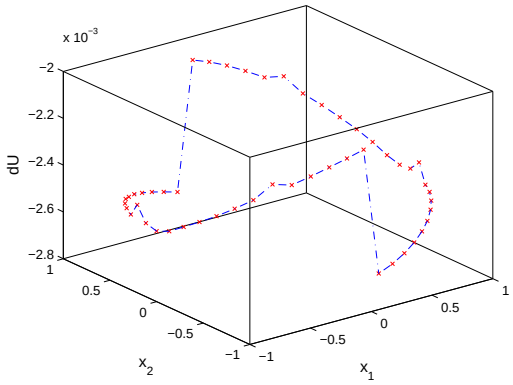

(c) Derivative of LF on the unit sphere.

Figure 3.1: Results of numerical design of a LF for the system (3.16).

$\mu = 3$. Furthermore, the system's trajectories $\chi_h(t_i, \xi_j)$, with $j = 1, \ldots, N$, are computed by using the Euler method [Butcher, 2003] with $h = 0.01$.

Fig. 3.1 presents the results of the numerical design of a LF for the system (3.16), Fig. 3.1(a) shows system's trajectories where the red points are the initial data. Note that there is not sliding motion on the interval of time where the trajectories were computed. Furthermore, Fig. 3.1(b) provides the values of the designed LF (3.17) on the unit sphere. The red points represents the components of the vector $\Gamma_N = [U_1^h, \ldots, U_N^h]^T$ and the blue line represents the interpolation. Finally, a point-wise calculation of the derivative of the LF is provided in Fig. (3.1(c)) depicted by the red marks and the dash-dot and blue line is just a reference to joint the points and highlight the plot.

3.4.2 Design based on the supremum of the trajectories

Consider the (nonsingular) Quasi-continuous Control Algorithm given by

$$\begin{aligned} \dot{x}_1 &= x_2, \\ \dot{x}_2 &= -k_1 \frac{k_2 x_1 + \lceil x_2 \rfloor^2}{k_2 |x_1| + |x_2|^2} \end{aligned} \tag{3.18}$$

where $x \in \mathbb{R}^2$ is the state and $k_1, k_2 > 0$ are tunning parameters. The system (3.18) is r-homogeneous of degree $\nu = -1$ and weights $r = [2, 1]$. From Corollary 3.2 and considering the parameters and expressions:

$$\begin{gathered} q = 3, \quad h = 0.01, \quad a = 50, \\ \varrho = 2, \quad \kappa_1 = 1, \quad \kappa_2 = 2, \\ N = 50, \quad k_1 = 3, \quad k_2 = 5, \\ p(s) = e^{-as^2}, \qquad g(x, y) = \arccos(x^\top y), \end{gathered}$$

a LF for the system (3.18) is given by

$$\tilde{V}(x) = \|x\|_r \sum_{j=1}^{N} \theta_j e^{-a \arccos^2(\xi^\top \xi_j)} \tag{3.19}$$

where $\xi \in S_r(1)$ such that $x = \Lambda_r(\|x\|_r)\xi$ and the points $\xi_j \in S_r(1)$, with $j = 1, \ldots, N$, form an uniform grid on the unique sphere. Moreover, the vector θ is the solution of the equation $\Gamma_N = \Pi_N \theta$, where $\Pi_N = \{e^{-a \arccos^2(\xi_i^\top \xi_j)}\}_{i,j=1}^N$ and $\Gamma_N = [V_1^h, \ldots, V_N^h]^T$ where V_j^h are given by (3.11) with $\varrho = 2$, $\kappa_1 = 1$ and $\kappa_2 = 2$. Furthermore, the system trajectories $\chi_h(t_i, \xi_j)$, with $j = 1, \ldots, N$, are computed by using the Euler method [Butcher, 2003] with $h = 0.01$.

The numerical design of a LF for the system (3.18) is shown by Fig. 3.2. The system's solutions are presented in Fig. 3.2(a) where the red points are the initial conditions, note that they do not exhibit sliding motion. Moreover, the values of the designed LF (3.19) on the unit sphere are depicted by Fig. 3.2(b), where the red points represents the components of the vector $\Gamma_N = [U_1^h, \ldots, U_N^h]^T$ and the blue line represents the interpolation. Finally, a point-wise calculation of the derivative of the LF is provided in Fig. (3.2(c)) highlighted by the red marks and the dash-dot and blue line is just a reference to joint the points.

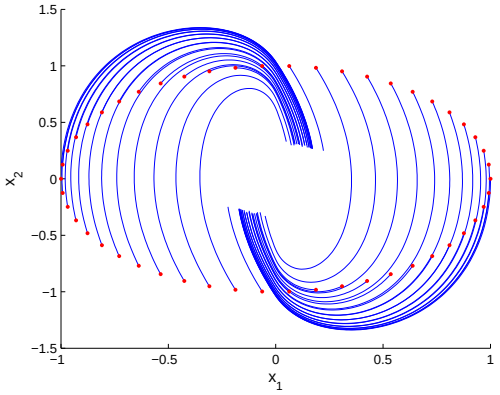

(a) Vector field.

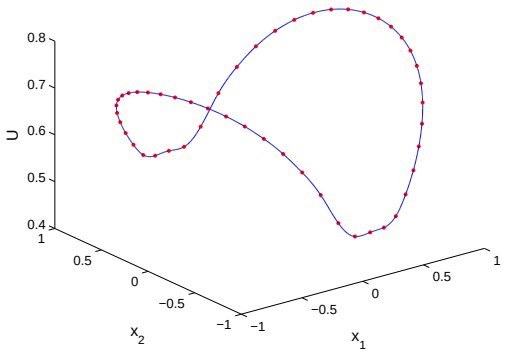

(b) LF on the unit sphere.

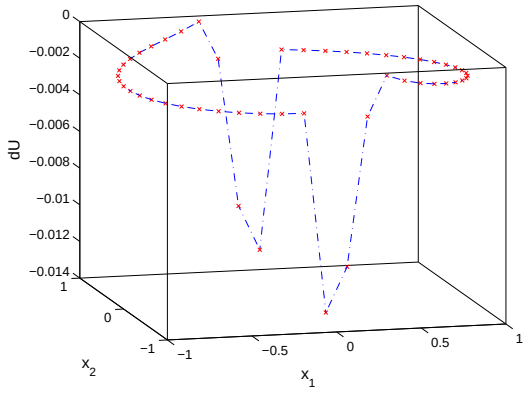

(c) Derivative of LF on the unit sphere.

Figure 3.2: Results of numerical design of a LF for the system (3.18).

3.5 Conclusion

This chapter presented two converse Lyapunov theorems for a class of discontinuous and homogeneous systems of negative degree, including some well-known HOSM algorithms. This results can be seen as a generalization of classical results about LF design (such as the approaches of Kurzweil, Massera, Persidskii, and Yoshizawa) to the considered class of systems. Moreover, explicit expressions of the homogeneous and Lipschitz continuous LF were provided. However, the realization of this LF requires the calculation of the system's trajectories, which is a very difficult task for nonlinear systems. Accordingly, a numerical methodology to construct LF is proposed under some technical assumptions, which consist of two steps: first pointwise calculation of values of the the LF provided by the converse theorems; second, interpolation of this points on the unit sphere. Both together, the converse theorem and the numerical methodology, constitute a new framework for the numerical design of homogeneous and Lipschitz continuous LF for a wide class of discontinuous HOSM algorithms as it is illustrated by the examples.

Chapter 4

Analysis of stability of homogeneous systems in presence of parasitic dynamics

Homogeneous controllers of negative degree posses an infinite gain near to the origin hence they are able to provide finite-time convergence of the system trajectories to zero [Bhat and Bernstein, 1997, Levant, 2005a, Boiko, 2020]. However, in presence of fast actuators this infinite gain produces the so-called chattering: a high frequency oscillatory behavior of the system trajectories in steady-state. Recently, the problems of reduction and analysis of chattering have attracted a lot of attention, see for example [Fridman, 1999, Fridman, 2002, Levant, 2010, Seeber and Horn, 2017, Rosales et al., 2018, Boiko, 2014b, Haimovich and De Battista, 2019, Banza et al., 2020].

Commonly, singularly perturbed models are used to justify the decomposition of interconnected systems in the Main Dynamics (MD) and the Parasitic Dynamics (PD) (see the list of reference in [Kokotovic et al., 1999]). Methods of stability analysis for smooth singularly perturbed systems are based on the results of [Klimushchev and Krasovskii, 1961], where asymptotic stability of the interconnection is concluded from uniform exponential stability of the linearized systems. Relaxing that assumption, [Saberi and Khalil, 1984] have addressed asymptotic and exponential stability by means of quadratic-type Lyapunov Functions (LF) and estimates the domain of attraction in terms of the upper bound of the Singular Perturbation Parameter (SPP). On the other hand, in the framework of *Input-to-State Stability* (ISS), [Christofides and Teel, 1996] has studied the properties of smooth singularly perturbed systems providing a kind of "total stability" under standard assumptions.

Despite the amount of publications on singular perturbations theory, those results do not cover the general case of homogeneous systems. The reasons for this include that the homogeneous systems can be non-smooth, the velocity of convergence of homogeneous systems is parametrized by their Homogeneity Degree (HD), the homogeneous systems of negative degree usually exhibit chattering in the presence of linear PD, and, the homogeneous systems of negative degree are faster around the origin than any exponentially converging dynamics but they are slower in the large.

In order to fill this gap, this chapter presents a study of the stability of the interconnection of a homogeneous MD and a homogeneous PD, with different HD's, by means of concepts of singular per-

turbations theory, Lyapunov methods, ISS properties and Small-Gain Theorem. This analysis requires just continuity of the MD and the PD. The obtained results allow to conclude three kinds of stability for the interconnection according to the HD:

- Global asymptotic stability (GAS) when the HD coincide and the SPP is sufficiently small.
- Practical GAS when the HD of the PD is greater than the HD of the MD (which also describes ROD). The final bound of the trajectories is a function of the SPP and its size decreases for a smaller SPP.
- Local asymptotic stability when the HD of the PD is smaller than the HD of the MD/ROD, where the domain of attraction is a function of the SPP and its size increases with decreasing the SPP.

Moreover, under the assumption that chattering arises in the steady state of the system trajectories, the previous results are used to develop a new approach based on Lyapunov methods for estimation of an upper-bound of chattering produced by finite-time convergent controllers in presence of a fast actuator, which has been commonly studied in frequency domain, e.g., by using: describing function, harmonic balance, equivalent gain, etc. [Boiko, 2009]. This new approach allows to show the relationship between the amplitude of chattering, the SPP ϵ, and the HD ν of the finite-time convergent algorithm.

The rest of the chapter has the following structure. In Section 4.1 some useful definitions and preliminaries results are presented. Section 4.2 contains the problem statement and the main result of this work. In Section 4.3, some examples are provided in order to illustrate the different cases of the main result. Furthermore, an study of chattering produced by finite-time convergent controllers in presence of a fast actuator is introduced in Section 4.4. Finally, the conclusions are presented in Section 4.5.

4.1 Preliminaries

4.1.1 Input-to-state stability

Consider the system

$$\dot{x} = f(x, u), \tag{4.1}$$

where $x \in \mathbb{R}^n$ is the state vector and $u \in \mathbb{R}^m$ is an input. In addition, $f : \mathbb{R}^{n+m} \to \mathbb{R}^n$ ensures forward existence and uniqueness of the system solutions at least locally in time, and $f(0, 0) = 0$. The next definitions and theorems were introduced by [Bernuau et al., 2013b, Dashkovskiy and Kosmykov, 2013, Jiang et al., 1996].

Definition 4.1. The system (4.1) is said to be input-to-state practically stable (ISpS), if there exist a class $\mathcal{KL}$ function β, a class $\mathcal{K}$ function γ and a constant $c \geq 0$, such that, for any $u \in \mathcal{L}_\infty$ and any $x_0 \in \mathbb{R}^n$, the solution $x(t)$ with initial condition $x(0) = x_0$ satisfies

$$\|x(t)\| \leq \max\{\beta(\|x_0\|, t), \gamma(\|u\|_{\mathcal{L}_\infty}), c\} \tag{4.2}$$

for all $t \geq 0$. The function γ is called nonlinear asymptotic gain. The system (4.1) is called ISS if $c = 0$.

If $u(t) = 0$ for all $t \geq 0$, then an ISpS system (4.1) is called practically GAS, and an ISS system (4.1) is called GAS; if the estimate (4.2) is satisfied just for a bounded set of initial conditions x_0, then such a system is called locally ISpS (locally ISS, respectively) [Bacciotti and Rosier, 2005].

Definition 4.2. A smooth function $V : \mathbb{R}^n \to \mathbb{R}$ is called the ISpS-LF for system (4.1) if there exist some $c \geq 0$, $\alpha_1, \alpha_2, \alpha_3 \in \mathcal{K}_\infty$ and $\chi \in \mathcal{K}$, such that, for all $x \in \mathbb{R}^n$ and $u \in \mathbb{R}^m$

$$\alpha_1(\|x\|) \leq V(x) \leq \alpha_2(\|x\|), \tag{4.3}$$

and

$$\|x\| \geq \chi(\max\{\|u\|, c\}) \implies \tfrac{\partial V}{\partial x} f(x, u) \leq -\alpha_3(\|x\|) \tag{4.4}$$

hold. Moreover, if $c = 0$ then V is called an ISS-LF for the system (4.1).

Remark 4.1. The function $\gamma(\cdot)$ in (4.2) can be computed from the functions $\alpha_1(\cdot)$, $\alpha_2(\cdot)$ and $\chi(\cdot)$. It is given by

$$\gamma(s) = \alpha_1^{-1} \circ \alpha_2 \circ \chi(s). \tag{4.5}$$

Theorem 4.1. *The system* (4.1) *is ISS (ISpS) if it admits an ISS (ISpS) LF.*

If the vector field f is locally Lipschitz continuous (at least outside the origin), then the existence of an ISS (ISpS) LF is also a necessary condition for the ISS (ISpS) stability of the system (4.1) [Lopez-Ramirez et al., 2020].

4.1.2 Input-to-state stability of interconnected systems

Consider the system

$$\dot{x} = f(x, y), \tag{4.6}$$
$$\dot{y} = g(x, y, u), \tag{4.7}$$

where $x \in \mathbb{R}^n$, $y \in \mathbb{R}^m$, $u \in \mathbb{R}^p$ and the origin $x = y = u = 0$ is an equilibrium point. The system (4.6)-(4.7) can be seen as two interconnected systems where y is an input to the system (4.6) and x, u are inputs to the system (4.7). Assume that both systems are ISpS w.r.t. their corresponding inputs. Therefore, from condition (4.2) for all $t \geq 0$:

$$\|x(t)\| \leq \max\{\beta_1(\|x_0\|, t), \gamma_1(\|y\|_{\mathcal{L}_\infty}), c_1\}$$
$$\|y(t)\| \leq \max\{\beta_2(\|y_0\|, t), \gamma_2(\|x\|_{\mathcal{L}_\infty}), \gamma_3(\|u\|_{\mathcal{L}_\infty}), c_2\}$$

where $x_0 \in \mathbb{R}^n$ and $y_0 \in \mathbb{R}^m$ are the initial conditions for each variable, $u \in \mathcal{L}_\infty$, $\beta_1, \beta_2 \in \mathcal{KL}$ and $\gamma_1, \gamma_2, \gamma_3 \in \mathcal{K}$ are some functions from the indicated classes.

Theorem 4.2. *[Dashkovskiy et al., 2010]. Let each system (4.6) and (4.7) be ISpS. If there exists some $c_0 \geq 0$, such that,*

$$\gamma_1 \circ \gamma_2(s) < s, \quad \text{for all} \quad s > c_0, \tag{4.8}$$

then the interconnected system (4.6)-(4.7) is ISpS. Furthermore, if $c_0 = c_1 = c_2 = 0$ then the system is ISS.

The inequality (4.8) is commonly refered as the *small-gain condition*. In particular, if the nominal system (4.6)-(4.7) is ISS then its solutions with $u = 0$ are GAS.

Roughly speaking, the Small-Gain Theorem establishes that the interconnected system (4.6)-(4.7) is ISS, if the composite function $\gamma_1 \circ \gamma_2(\cdot)$ is a simple contraction.

For the case of locally ISS systems, [Dashkovskiy and Rüffer, 2010] presents another version of Theorem 4.2, where the small-gain condition (4.8) is replaced by

$$\gamma_1 \circ \gamma_2(c_3) < c_3 \quad \text{and} \quad \gamma_1 \circ \gamma_2(s) < s, \tag{4.9}$$

for all $0 < s \leq c_3$, and some $c_3 > 0$. In this case, local ISS of the interconnected system (4.6)-(4.7) is concluded.

4.2 Problem statement and main result

Consider the singularly perturbed system

$$\dot{x} = f(x, y), \tag{4.10}$$
$$\epsilon \dot{y} = g(x, y), \tag{4.11}$$

where $x \in \mathbb{R}^n$ and $y \in \mathbb{R}^m$ are the state variables, $\epsilon > 0$ is a small parameter (also called the SPP), and $f : \mathbb{R}^{n+m} \to \mathbb{R}^n$ and $g : \mathbb{R}^{n+m} \to \mathbb{R}^m$ are continuous vector fields ensuring forward existence and uniqueness of the trajectories. In the sequel, the system (4.10) is called the MD and the system (4.11) is called the PD.

Moreover, for some vector of weights r and $\tilde{r}$ the vector fields f and g are $(r, \tilde{r})$-homogeneous of degree ν and μ, respectively, i.e.,

$$f(x, y) = \lambda^{-\nu} \Lambda_r^{-1}(\lambda) f(\Lambda_r(\lambda)x, \Lambda_{\tilde{r}}(\lambda)y) \tag{4.12}$$

and,

$$g(x, y) = \lambda^{-\mu} \Lambda_{\tilde{r}}^{-1}(\lambda) g(\Lambda_r(\lambda)x, \Lambda_{\tilde{r}}(\lambda)y). \tag{4.13}$$

In consequence, note that $f(0, 0) = 0$ and $g(0, 0) = 0$.

Now, consider the following assumption:

Assumption 4.1. Consider the system (4.10)-(4.11):

1. The equation $g(x,y)=0$ has an isolated and continuously differentiable solution $y=h(x)$ defining an invariant manifold of system (4.11).
2. The Reduced-Order Dynamics (ROD)
$$\dot{\bar{x}} = f(\bar{x}, h(\bar{x})), \tag{4.14}$$
is GAS at the origin.
3. Defining $z=y-h(x)$, the Boundary-Layer (BL)
$$\frac{dz}{d\tau} = g(x, z+h(x)); \;\; \tau = \frac{t}{\epsilon}, \tag{4.15}$$
is GAS at the origin, uniformly w.r.t. x. Moreover, there exists a smooth parametrized $(\tilde{r}, r)$-homogeneous LF $W(z,x)$ satisfying
$$W(\Lambda_{\tilde{r}}(\lambda)z, \Lambda_r(\lambda)x) = \lambda^{\iota} W(z,x), \tag{4.16}$$
$$\underline{a}_z \|z\|_{\tilde{r}}^{\iota} \leq W(z,x) \leq \bar{a}_z \|z\|_{\tilde{r}}^{\iota}, \tag{4.17}$$
$$\frac{\partial W(z,x)}{\partial z} g(x, z+h(x)) \leq -b_z \|z\|_{\tilde{r}}^{\mu+\iota}, \tag{4.18}$$
for all $z \in \mathbb{R}^m$, $x \in \mathbb{R}^n$ and for some $\underline{a}_z, \bar{a}_z, b_z > 0$, where $\iota > \max\{0, -\mu\}$ is the HD of W.

As a consequence of (4.13), the function h admits certain symmetry, i.e.,
$$h(\Lambda_r(\lambda)x) = \Lambda_{\tilde{r}}(\lambda) h(x),$$
and consequently, $h(0)=0$. This implies that the ROD (4.14) is r-homogeneous of a degree ν, i.e., the ROD inherits the homogeneity properties of the MD.

Moreover, by Assumption 4.1, the ROD (4.14) is GAS at the origin and r- homogeneous of degree ν, hence there exists a LF $V(x)$ which satisfies
$$V(x) = \lambda^{-\kappa} V(\Lambda_r(\lambda)x), \tag{4.19}$$
$$\underline{a}_x \|x\|_r^{\kappa} \leq V(x) \leq \bar{a}_x \|x\|_r^{\kappa}, \tag{4.20}$$
$$\frac{\partial V(x)}{\partial x} f(x, h(x)) \leq -b_x \|x\|_r^{\nu+\kappa}, \tag{4.21}$$
$$\sup_{\|x\|_r \leq 1} \| \frac{\partial V(x)}{\partial x} \| \leq c_x, \tag{4.22}$$
for all $x \in \mathbb{R}^n$ and for some $\underline{a}_x, \bar{a}_x, b_x, c_x > 0$, where $\kappa > \max\{0, -\nu\}$ is the HD of V. On the other hand, $W(z,x)$ is a $\tilde{r}$-homogeneous LF for the system (4.15), in consequence, the inequalities
$$\sup_{\substack{\|\zeta\|_{\tilde{r}} \leq 1 \\ \|\xi\|_r \leq 1}} \left\| \frac{\partial W(\zeta,\xi)}{\partial \zeta} \right\| \leq c_z, \tag{4.23}$$
$$\sup_{\substack{\|\zeta\|_{\tilde{r}} \leq 1 \\ \|\xi\|_r \leq 1}} \left\| \frac{\partial W(\zeta,\xi)}{\partial \xi} \right\| \leq d_z, \tag{4.24}$$

hold, for some $c_z, d_z > 0$.

Furthermore, by the continuity of $f(x,y)$ on the unit sphere, for any b_x, c_x and $0 < \theta < 1$, there exists δ, such that, if $\|\Lambda_{\tilde{r}}(\|x\|_r^{-1})z\|_{\tilde{r}} \leq \delta$, then

$$\|f(\xi, h(\xi) + \Lambda_{\tilde{r}}(\|x\|_r^{-1})z) - f(\xi, h(\xi))\| \leq \frac{\theta b_x}{c_x}, \tag{4.25}$$

for all $\xi \in S_r(1)$. On the other hand, there exists η such that

$$\eta = \frac{1}{b_z} \sup_{\substack{\xi \in B_r(1) \\ \zeta \in B_{\tilde{r}}(1)}} \left\{ \left(d_z + c_z \left\| \frac{\partial h(\xi)}{\partial \xi} \right\| \right) \|f(\xi, \zeta + h(\xi))\| \right\}. \tag{4.26}$$

Remark 4.2. Since $f(x,y)$ is r-homogeneous and due to equivalence of a homogeneous norm and the standard one, the r-homogeneous norm can be used to analyze the continuity of the functions. □

Remark 4.3. Note that the $\tilde{r}$-homogeneous norm $\|\cdot\|_{\tilde{r}}$ is $\tilde{r}$-homogeneous of degree 1, i.e., $\|\Lambda_{\tilde{r}}(\lambda)z\|_{\tilde{r}} = \lambda\|z\|_{\tilde{r}}$. Thus, if $\lambda = \|x\|_r^{-1}$ then $\|\Lambda_{\tilde{r}}(\|x\|_r^{-1})z\|_{\tilde{r}} = \|x\|_r^{-1}\|z\|_{\tilde{r}}$.

The following theorem contains the main result of this chapter, where the stability of the interconnected system (4.10)-(4.11) is studied in terms of the HD, besides estimations of the ultimate bound and the domain of attraction for the system trajectories are provided.

Theorem 4.3. *Let the system* (4.10)-(4.11) *satisfy Assumption 4.1. There exist constants* $\underline{a}_x, \bar{a}_x, \underline{a}_y, \bar{a}_y, b_x, c_x, b_y, c_y, \tilde{\theta}_1, \tilde{\theta}_2, \delta, \eta > 0$*, such that, the interconnected system* (4.10)-(4.11) *is*

- *GAS for* $\mu = \nu$ *and*

$$\epsilon < \min \left\{ \frac{\tilde{\theta}_1}{\eta}, \frac{\tilde{\theta}_2 \left(\delta \frac{\underline{a}_x \underline{a}_z}{\bar{a}_x \bar{a}_z} \right)^{\mu+\iota}}{\eta} \right\}. \tag{4.27}$$

- *Locally asymptotically stable for* $\mu < \nu$ *and all initial condition*

$$\|x_0\|_r < \left(\frac{\tilde{\theta}_2 \left(\delta \frac{\underline{a}_x \underline{a}_z}{\bar{a}_x \bar{a}_z} \right)^{\mu+\iota}}{\epsilon\eta} \right)^{\frac{1}{\nu-\mu}} \tag{4.28}$$

and

$$\|y_0 - h(x_0)\|_r < \min \left\{ \left(\frac{\tilde{\theta}_1}{\epsilon\eta} \right)^{\frac{1}{\nu-\mu}}, \left(\frac{\tilde{\theta}_2 \left(\frac{\underline{a}_z}{\bar{a}_z} \right)^{\mu+\iota}}{\epsilon\eta \left(\delta^{-1} \frac{\bar{a}_x}{\underline{a}_x} \right)^{\nu+\iota}} \right)^{\frac{1}{\nu-\mu}} \right\}. \tag{4.29}$$

- *Practically GAS for $\mu > \nu$, with final bounds*

$$\|x(t)\|_r < \left(\frac{\epsilon\eta}{\tilde{\theta}_2 \left(\delta \frac{\underline{a}_x \underline{a}_z}{\bar{a}_x \bar{a}_z} \right)^{\mu+\iota}} \right)^{\frac{1}{\mu-\nu}} \tag{4.30}$$

and

$$\|y(t) - h(x(t))\|_r \leq \max \left\{ \left(\frac{\epsilon\eta}{\tilde{\theta}_1} \right)^{\frac{1}{\mu-\nu}}, \left(\frac{\epsilon\eta \left(\delta^{-1} \frac{\bar{a}_x}{\underline{a}_x} \right)^{\nu+\iota}}{\tilde{\theta}_2 \left(\frac{\underline{a}_z}{\bar{a}_z} \right)^{\mu+\iota}} \right)^{\frac{1}{\mu-\nu}} \right\}. \tag{4.31}$$

for all $t > T$, with some $T > 0$, and all $x_0 \in \mathbb{R}^n$ and $y_0 \in \mathbb{R}^m$.

So, from Theorem 4.3 we have that for $\nu = \mu$ there exists a critical value ϵ^*, such that, GAS of the origin of the system (4.10)-(4.11) is ensured for $\epsilon < \epsilon^*$. Here, the value of ϵ determines how long the trajectories of the system (4.10)-(4.11) deviate from the trajectories of the ROD (4.14). Moreover, this case coincides with the concept of motion separation predicted by classical results on the stability of smooth (at least Lipschitz continuous) singularly perturbed systems (see [Kokotovic et al., 1999] and references therein), and it allows to ensure GAS.

For $\mu \neq \nu$, the system (4.10)-(4.11) always possesses some kind of stability (local or practical), and by decreasing the value of ϵ it is possible to enlarge the domain of attraction for $\mu < \nu$, or to decrease the size of the final bound of the solutions for $\mu > \nu$. Systems with a smaller HD are faster around the origin and slower in the large, and vice versa. Therefore, for $\nu > \mu$ the concept of motion separation given by the standard model of singularly perturbed systems is only valid near to the origin , hence, just local asymptotic stability of the origin of the system (4.10)-(4.11) can be concluded. On the other hand, for $\nu < \mu$ such a concept of motion separation is only valid outside of a neighborhood of the origin, in consequence, just practical stability of the trajectories of the system (4.10)-(4.11) can be predicted.

In the literature, the most of existing results about he stability of the system (4.10)-(4.11) require sufficient smoothness of the vector fields involved in the analysis. However, this condition is quite conservative for the general case of homogeneous systems. In contrast, our study request just continuity of the vector fields f, g of the system (4.10)-(4.11).

4.3 Illustrative Examples

The following examples have the purpose to illustrate the different kinds of stability predicted by Theorem 4.3. To this end, some simplifications are introduced in order to exhibit that results nicely.

4.3.1 Case $\nu < \mu$

Consider the system

$$\dot{x} = -\lceil y_1 \rfloor^{\frac{2}{3}} \tag{4.32}$$

$$\epsilon \dot{y}_1 = y_2, \quad \epsilon \dot{y}_2 = -y_1 - 2y_2 + \alpha^{\frac{3}{2}} x, \tag{4.33}$$

where x is the state of the MD (4.32), y_1, y_2 are the states of the PD (4.33), and ϵ is a small parameter. For $\epsilon = 0$, the solution $h(x)$ is given by $y_1 = \alpha^{\frac{3}{2}} x$ and $y_2 = 0$, such that, the ROD

$$\dot{x} = -\alpha \lceil x \rfloor^{\frac{2}{3}} \tag{4.34}$$

is continuous and r-homogeneous of degree $\nu = -\frac{1}{2}$ for the weight $r = \frac{3}{2}$. Also, for any $\alpha > 0$, it is finite-time stable at the origin. On the other hand, for $\epsilon \approx 0$ define $z_1 = y_1 - \alpha^{\frac{3}{2}} x$, $z_2 = y_2$ and $\tau = \epsilon^{-1} t$, such that, the BL

$$\frac{dz_1}{d\tau} = z_2, \quad \frac{dz_2}{d\tau} = -z_1 - 2z_2, \tag{4.35}$$

is continuous, $\tilde{r}$-homogeneous of degree $\mu = 0$ for the weights $\tilde{r} = [1, 1]$, and exponentially stable for any $\epsilon > 0$.

Then, $\nu < \mu$ and according to Theorem 4.3 the system (4.32)-(4.33) is practically GAS as it is depicted in Fig. 4.1.

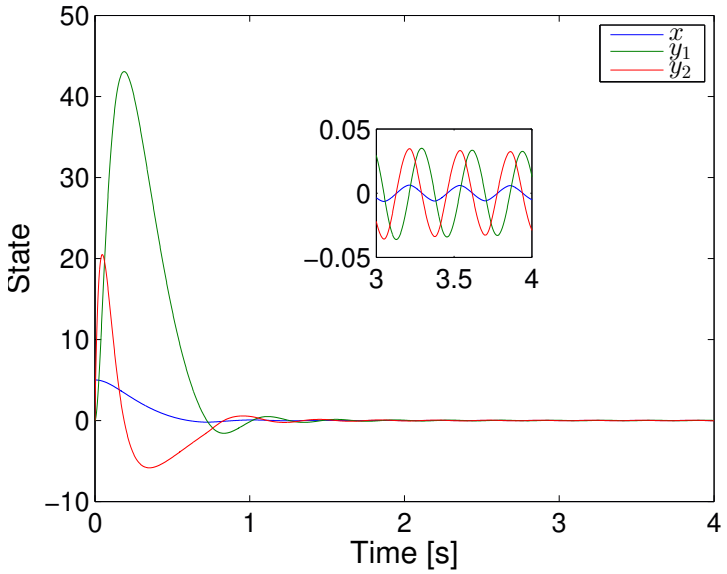

Figure 4.1: Simulation of the interconnected system (4.32)-(4.33) where $\alpha = 5$ and $\epsilon = 0.05$.

Note that the states of the system (4.32)-(4.33) exhibit oscillations in the steady state. To the intuition of the authors, this behavior is due to the PD is not fast enough to reach the quasi-stationary

state $h(x) = [\alpha^{\frac{3}{2}}x, 0]^\top$. According to Theorem 4.3, the amplitude of the oscillations depends on the parameter ϵ, and it is illustrated by Fig. 4.2.

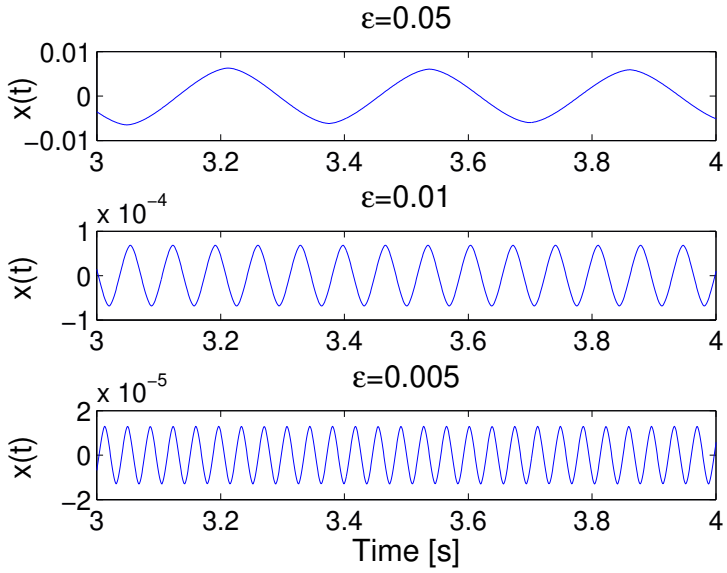

Figure 4.2: Chattering in the output of the closed-loop system (4.32)-(4.33) with $\alpha = 5$ and different values of ϵ.

Moreover, from Theorem 4.3 the region of practical stability is computed as follows. The stability of the ROD (4.34) can be proven by the LF $V(x) = \frac{1}{2}x^2$, which fulfills the inequalities (4.19)-(4.22) with the constants $\kappa = 2$, $\underline{a}_x = \bar{a}_x = 0.5$, $b_x = \alpha$ and $c_x = 1$. On the other hand, a LF for the BL (4.35) is given by $W(y) = \frac{1}{2}y^\top Py$, where $P = P^\top > 0$ is a solution of the equation $\bar{A}^\top P + P\bar{A} = -Q$ with $Q > 0$. Selecting

$$P = \begin{bmatrix} 3 & 0.5 \\ 0.5 & 3 \end{bmatrix}, Q = \begin{bmatrix} 1 & 1 \\ 1 & 11 \end{bmatrix},$$

the function $W(y)$ satisfies (4.16)-(4.18), (4.23) and (4.24) with $\iota = 2$, $\underline{a}_y = s_{\min}(P) = 2.5$, $\bar{a}_y = c_y = s_{\max}(P) = 3.5$, $b_y = s_{\min}(Q) \approx 0.9$ and $d_y = 0$. Furthermore, for the system (4.32)-(4.33), $\delta = 0.875\alpha^{\frac{3}{2}}$, $\eta = 5.13\alpha^{\frac{3}{2}}(\alpha^{\frac{3}{2}} + 1)^{\frac{2}{3}}$, $\theta = 0.75$ and $\tilde{\theta}_2 = 0.75$ satisfy (4.25) and (4.26). Finally, substituting all the parameters in equation (4.30), we have

$$\lim_{t\to\infty} \|x(t)\|_r \leq 39.53\epsilon^2.$$

The following table provides the estimation of chattering level for different values of ϵ. Note that the results presented by Fig. 4.2 satisfy the estimations provided by Table 4.1. Unfortunately, the final bound for the variable y is not computed in the example because it is strongly overestimated, as usual when estimations are obtained based on LF.

ϵ	$\lvert x\rvert$
0.05	0.0988
0.01	0.00395
0.005	0.000988

Table 4.1: Estimation of ultimate bounds for different values of ϵ.

4.3.2 Case $\nu = \mu$

Now, let us consider the following interconnection of two homogeneous systems of the same degree

$$\dot{x} = -\alpha\lceil y_1\rfloor^{\frac{2}{3}} \tag{4.36}$$

$$\epsilon\dot{y}_1 = y_2, \quad \epsilon\dot{y}_2 = -\lceil y_1 - x\rfloor^{\frac{1}{3}} - 2\lceil y_2\rfloor^{\frac{1}{2}}, \tag{4.37}$$

where x is the state of the system (4.36), y_1, y_2 are the states of the PD (4.37), and ϵ is a parameter. For $\epsilon = 0$, $y_1 = x$ and $y_2 = 0$ give the expression of $h(x)$, hence, the reduced order system (4.34) is recovered, which is continuous and r-homogeneous of degree $\nu = -\frac{1}{2}$ for the weight $r = \frac{3}{2}$, and for any $\alpha > 0$, finite-time stable at the origin. On the other hand, for $\epsilon \approx 0$ define $z_1 = y_1 - x$, $z_2 = y_2$ and $\tau = \epsilon^{-1}t$, such that, the BL

$$\frac{dz_1}{d\tau} = z_2, \quad \frac{dz_2}{d\tau} = -\lceil z_1\rfloor^{\frac{1}{3}} - 2\lceil z_2\rfloor^{\frac{1}{2}}, \tag{4.38}$$

is continuous, $\tilde{r}$-homogeneous of degree $\mu = -\frac{1}{2}$ for the weights $\tilde{r} = [\frac{3}{2}, 1]$, and finite-time stable at the origin, for any $\epsilon > 0$. In this case, $\nu = \mu$, hence by Theorem 4.3 the system (4.36)-(4.37) is expected to be globally finite-time stable as it is illustrated in Fig. 4.3.

A critical value ϵ^* is computed as follows. The stability of the ROD (4.34) can be proven by the LF $V(x) = \frac{1}{2}x^2$, which fulfills the inequalities (4.19)-(4.22) with the constants $\kappa = 2$, $\underline{a}_x = \bar{a}_x = 0.5$, $b_x = \alpha$ and $c_x = 1$. On the other hand, a LF for the BL (4.35) is given by $W(z, x) = 10.5|z_1|^{\frac{5}{3}} + 8.5|z_2|^{\frac{5}{2}} + 3.5z_1z_2$, which satisfies (4.16)-(4.18), (4.23) and (4.24) with $\iota = \frac{5}{2}$, $\underline{a}_y = 6.462$, $\bar{a}_y = 10.809$, $b_y = 2.654$, $c_y = 22.11$ and $d_y = 0$. Furthermore, solving (4.25) and (4.26) for the system (4.39)-(4.40), $\delta = 0.875$ and $\eta = 13.22\alpha$, where $\theta = 0.75$, $\tilde{\theta}_1 = 0.25$ and $\tilde{\theta}_2 = 0.75$ were used. Then, substituting all the parameter in (4.27) a critical value $\epsilon^* = 0.0129$ is obtained, hence, the stability of the interconnection (4.36)-(4.37) is guaranteed for any $\epsilon < 0.0129$. In this case the value of ϵ determines how the trajectories of (4.36)-(4.37) deviate from the trajectories of the reduced order dynamics (4.34) as it is shown in Fig. 4.4.

4.3.3 Case $\nu > \mu$

Finally, consider an interconnection given by

$$\dot{x} = -y_1, \tag{4.39}$$

$$\epsilon\dot{y}_1 = y_2, \quad \epsilon\dot{y}_2 = -\lceil y_1 - \alpha x\rfloor^{\frac{1}{3}} - 2\lceil y_2\rfloor^{\frac{1}{2}}, \tag{4.40}$$

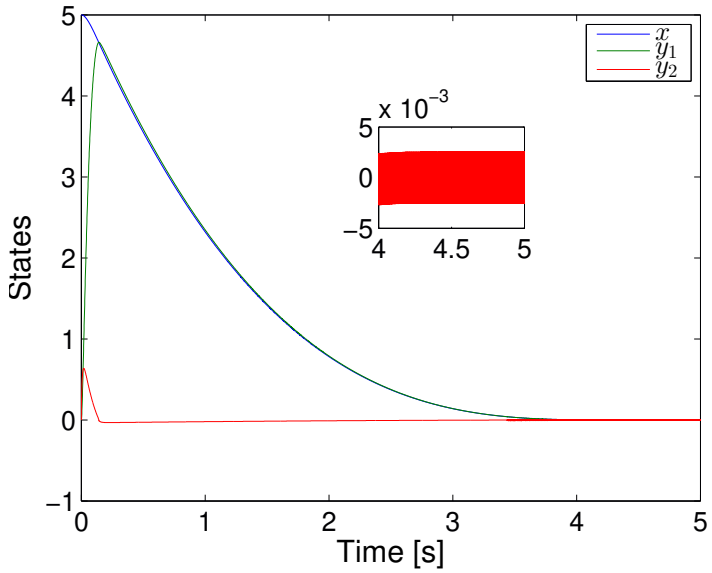

Figure 4.3: Simulation of the closed-loop system (4.36)-(4.37) where $\alpha = 1.2$ and $\epsilon = 0.01$.

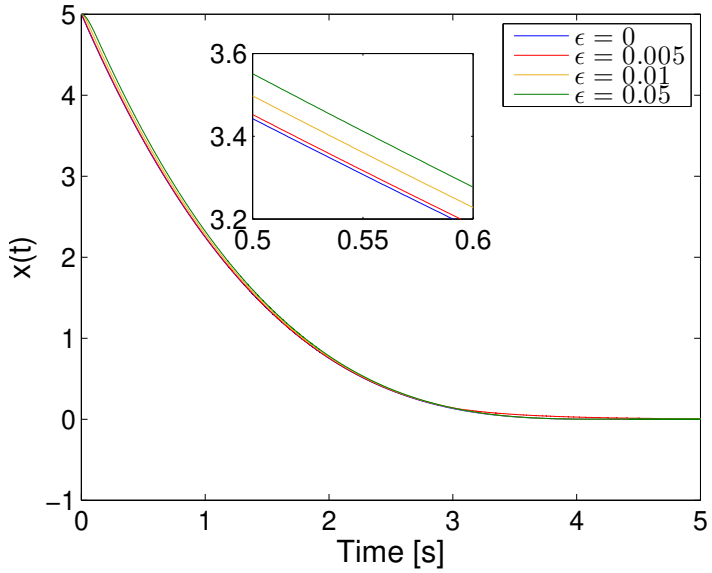

Figure 4.4: Response of the closed-loop system (4.36)-(4.37) for different values of ϵ.

where x is the state of the system (4.39), y_1, y_2 are the states of the PD (4.40), and ϵ is a small parameter. For $\epsilon = 0$, $y_1 = \alpha x$ and $y_2 = 0$, and the reduced order dynamics is given by

$$\dot{x} = -\alpha x, \tag{4.41}$$

which is a linear systems, r-homogeneous of degree $\nu = 0$ for the weight $r = 1$, and also, asymptotically stable at the origin for any $\alpha > 0$. On the other hand, for $\epsilon \approx 0$ define $z_1 = y_1 - \alpha x$, $z_2 = y_2$ and $\tau = \epsilon^{-1}t$, such that, the BL (4.38) is obtained again, which is continuous, $\tilde{r}$-homogeneous of degree $\mu = -\frac{1}{2}$ for the weights $\tilde{r} = [\frac{3}{2}, 1]$, and finite-time stable at the origin for any $\epsilon > 0$. In this case, the HD's of the subsystems (4.39) and(4.40) hold $\nu > \mu$, hence, it is locally asymptotically stable at the origin as it is predicted by Theorem 4.3 and confirmed in Fig. 4.5, where for an initial condition $x_0 = 3$ and $y_0 = [0, 0]$ the states converge to zero but for an initial condition $x_0 = 5$ and $y_0 = [0, 0]$ the stability cannot be ensured.

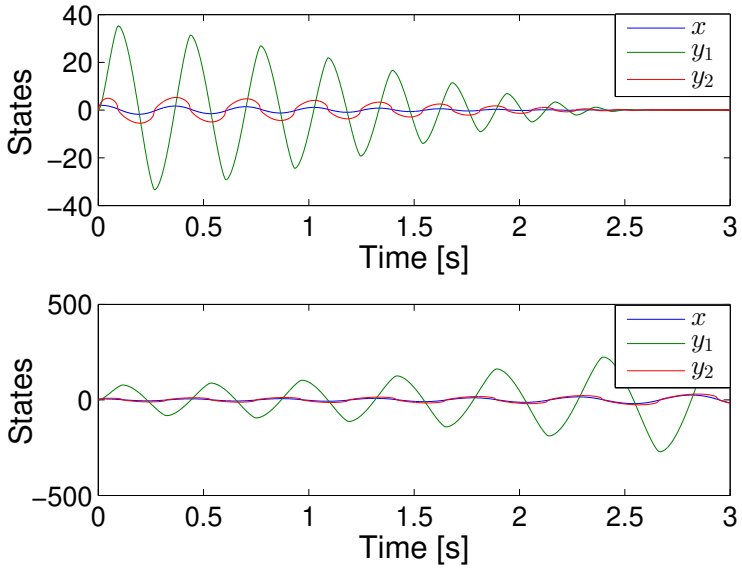

Figure 4.5: Simulation of the closed-loop systems (4.39)-(4.40) with $\alpha = 60$, $\epsilon = 0.01$, $x_0 = 2$ and $y_0 = [0, 0]$ (top), or $x_0 = 5$ and $y_0 = [0, 0]$ (bottom).

The domain of attraction for the trajectories of the system (4.39)-(4.40) is given by Theorem 4.3 as follows. The stability of the ROD (4.41) can be proven by the LF $V(x) = \frac{1}{2}x^2$, which fulfills the inequalities (4.19)-(4.22) with the constants $\kappa = 2$, $\underline{a}_x = \bar{a}_x = 0.5$, $b_x = \alpha$ and $c_x = 1$. On the other hand, a LF for the BL (4.38) is proposed as $W(z, x) = 10.5|z_1|^{\frac{5}{3}} + 8.5|z_2|^{\frac{5}{2}} + 3.5z_1z_2$, which satisfies (4.16)-(4.18), (4.23) and (4.24) with $\iota = \frac{5}{2}$, $\underline{a}_y = 6.462$, $\bar{a}_y = 10.809$, $b_y = 2.654$, $c_y = 22.11$ and $d_y = 0$. Furthermore, by solving (4.25) and (4.26) for the system (4.39)-(4.40), we obtain $\delta = 0.75\alpha$ and $\eta = 8.33\alpha(\alpha + 1)$, where $\theta = 0.75$ and $\tilde{\theta}_2 = 0.75$ were used.

So, substituting all the parameters in equation (4.28), $\|x_0\|_r \leq 0.000317\epsilon^{-2}$. Therefore, for $\epsilon = 0.01$, it is obtained $\|x_0\|_r \leq 3.17$ supporting the simulation results shown in Fig. 4.5. Now, if the value of the parameter ϵ decreases then the domain of attraction for trajectories $x(t)$ increases, such that, for $\epsilon = 0.005$ it turns out that $\|x_0\|_r \leq 12.68$. Accordingly, the stability of the interconnected system (4.39)-(4.40) is ensured for $x_0 = 5$ and $y_0 = [0, 0]$ as Fig. 4.6 shows. Similar to the first

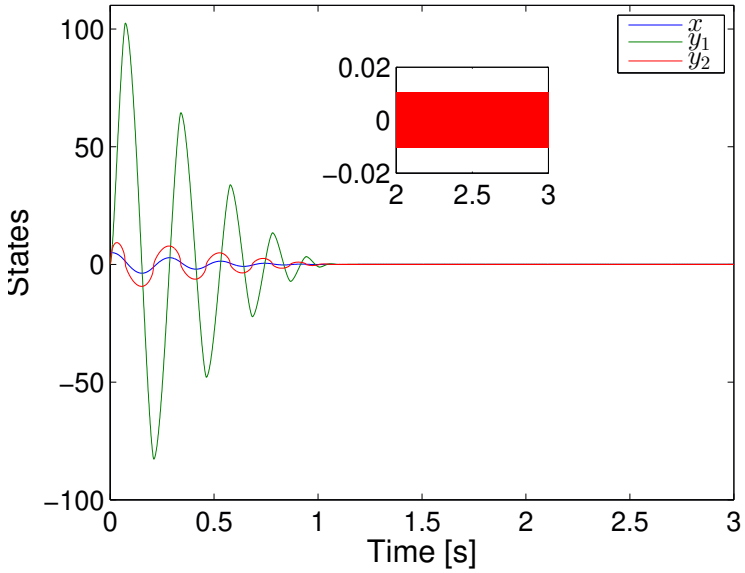

Figure 4.6: Simulation of the closed-loop systems (4.39)-(4.40) with $\alpha = 60$, $\epsilon = 0.005$, $x_0 = 5$ and $y_0 = [0, 0]$.

example, the domain of attraction for the variable y is not presented because the obtained estimation is not useful.

4.4 Finite-time convergent controllers in presence of a second-order fast actuator

A homogeneous controller of negative degree is able to provide finite-time convergence of the trajectories of the plant to zero [Bhat and Bernstein, 1997]. However, in practice the control signal is supplied to the plant by means of an actuator (see Fig. 4.7). Nevertheless, the presence of the actuator in the

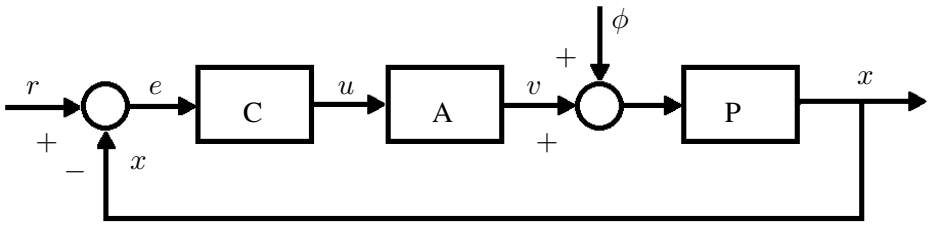

Figure 4.7: Control system with an actuator.

closed-loop deteriorates the performance of the controller.

4.4.1 Motivational example

For instance, consider the system

$$\dot{x} = v \tag{4.42}$$

where x is the state and v is an input. Selecting $v = u_h(x)$ where

$$u_h(x) = -\alpha \lceil x \rfloor^{\frac{1}{2}}, \tag{4.43}$$

the closed-loop system (4.42)-(4.43) is continuous and r-homogeneous of degree $\nu = -\frac{1}{2}$ and weight $r = 1$. Also, for any gain $\alpha > 0$, it is finite-time stable at the origin as it is shown by Fig. 4.8.

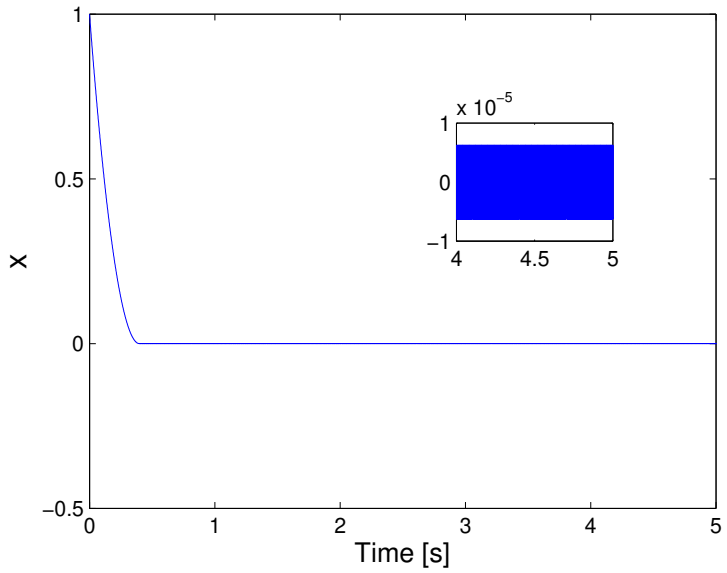

Figure 4.8: Nominal response of the closed-loop system (4.42)-(4.43).

Now, let the model of a linear fast actuator be

$$\begin{aligned} \epsilon \dot{y}_1 &= y_2, \\ \epsilon \dot{y}_2 &= -y_1 - 2y_2 + u_h(x), \\ v &= y_1, \end{aligned} \tag{4.44}$$

where y_1, y_2 are the states variables, ϵ parametrizes its time constant, v is an output of the system and the input $u_h(x)$ is given by (4.43). The behavior of the closed-loop system (4.42)-(4.43)-(4.44) is depicted in Fig. 4.9, where it can be seen that although the control law (4.43) is continuous the states of the plant exhibit oscillations in steady state. To the intuition of the authors, this behavior is due to

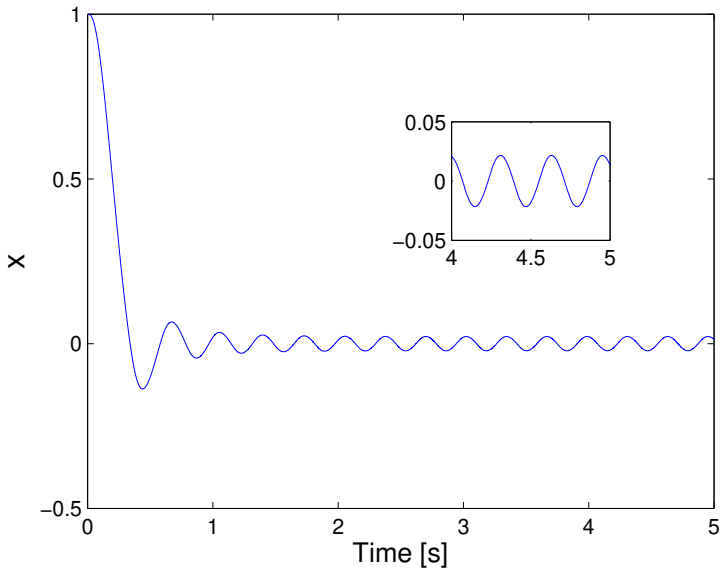

Figure 4.9: Response of the closed-loop system (4.42)-(4.43) in presence of the actuator (4.44) with $\epsilon = 0.05$ and $\alpha = 5$.

near to the origin the controller is faster than the PD hence it cannot be despised in the control system. Furthermore, the amplitude of the oscillations depends on the parameter ϵ and it is illustrated by Fig. 4.10.

4.4.2 Stability analysis and estimation of the final bound of the trajectories

Consider the system

$$\dot{x} = Ax + Bv \tag{4.45}$$

$$\begin{aligned} \epsilon\dot{y}_1 &= y_2, \\ \epsilon\dot{y}_2 &= -y_1 - 2y_2 + \psi(u(x)), \\ v &= \psi^{-1}(y_1), \end{aligned} \tag{4.46}$$

where $x \in \mathbb{R}^n$ is the state of the plant, $y = [y_1, y_2] \in \mathbb{R}^2$ are the states of the actuator, ϵ is a parameter, ψ is a smooth enough function, such that, $\psi(u(x))$ is Lipschitz continuous and $\psi(0) = 0$, $u(x)$ is a continuous control law designed to stabilize the plant and v is the connexion between the plant and the

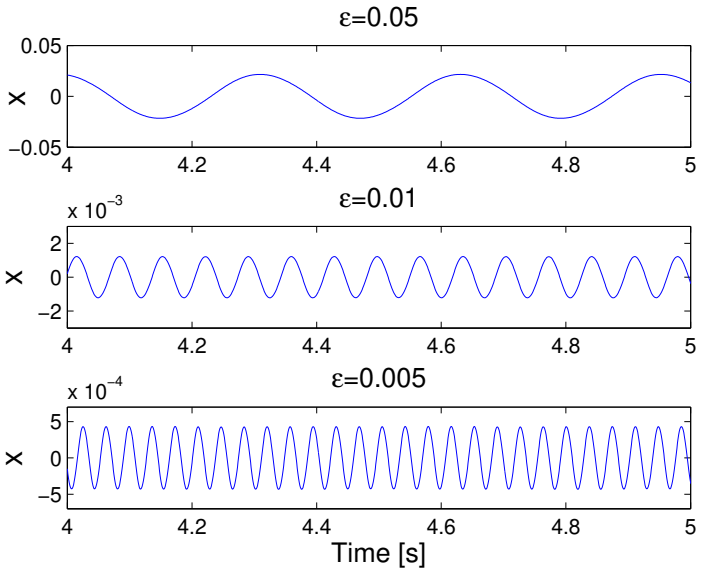

Figure 4.10: Chattering in the output of the closed-loop system (4.42)-(4.43) with $\alpha = 5$ due to presence of the actuator (4.44).

actuator. The matrices $A \in \mathbb{R}^{n\times n}$ and $B \in \mathbb{R}^n$ has the form

$$A = \begin{bmatrix} 0 & 1 & 0 & \dots & 0 \\ 0 & 0 & 1 & \dots & 0 \\ \vdots & \vdots & \vdots & \ddots & \vdots \\ 0 & 0 & 0 & \dots & 1 \\ 0 & 0 & 0 & \dots & 0 \end{bmatrix} \qquad B = \begin{bmatrix} 0 \\ 0 \\ \vdots \\ 0 \\ 1 \end{bmatrix} \tag{4.47}$$

such that, the subsystem (4.45) is a chain of integrators, which represents any nonlinear controllable system through feedback linearization. The mathematical models (4.45) and (4.46) describe the plant and the actuator of a control system like the depicted by Fig. 4.7.

Now, it can readily seen that $\epsilon = 0$ implies $y_1 = \psi(u(x))$, accordingly, the system (4.45)-(4.46) collapses to the reduced order dynamics

$$\dot{x} = Ax + Bu(x). \tag{4.48}$$

Assumption 4.2. The reduced order system (4.48) is r-homogeneous of degree $\nu < 0$ and finite-time stable at the origin.

By Assumption 4.2, there exists a r-homogeneous LF V of degree $\kappa > \max\{0, -\nu\}$, which satisfies inequalities (4.19)-(4.22) for all $x \in \mathbb{R}^n$ and for some $\underline{a}_x, \overline{a}_x, b_x, c_x > 0$. Additionally, by the

continuity of ψ and u on the unit sphere, for any b_x, c_x and $0 < \theta < 1$ there exist δ such that if

$$\frac{|z_1|}{\|x\|_r} \leq \delta \tag{4.49}$$

then

$$\|\psi^{-1}(\psi(u(\xi)) + \tfrac{z_1}{\|x\|_r}) - u(\xi)\| \leq \frac{\theta b_x}{c_x}, \tag{4.50}$$

for all $\|\xi\|_r = 1$.

On the other hand, from (4.46) the unforced actuator

$$\begin{bmatrix} \dot{y}_1 \\ \dot{y}_2 \end{bmatrix} = \tfrac{1}{\epsilon} \begin{bmatrix} 0 & 1 \\ -1 & -2 \end{bmatrix} \begin{bmatrix} y_1 \\ y_2 \end{bmatrix}$$

is a stable and linear system, which is $\tilde{r}$-homogeneous of degree $\mu = 0$ with weights $\tilde{r} = [1, 1]$. Hence, there exists a LF $W(y) = \frac{1}{2} y^\top P y$, where $P \in \mathbb{R}^2$ and $P = P^\top > 0$ is a solution of the equation

$$\begin{bmatrix} 0 & 1 \\ -1 & -2 \end{bmatrix}^\top P + P \begin{bmatrix} 0 & 1 \\ -1 & -2 \end{bmatrix} \leq -2Q \tag{4.51}$$

where $Q \in \mathbb{R}^2$ and $Q = Q^\top > 0$. Therefore, the LF W satisfies the inequalities (4.16)-(4.18), (4.23) and (4.24) with $\iota = 2$, $\underline{a}_y = s_{\min}(P)$, $\bar{a}_y = s_{\max}(P)$, $b_y = s_{\min}(Q)$, $c_y = s_{\max}(P)$ and $d_y = 0$.

Also, denote

$$\eta \geq \frac{s_{\max}(P)}{s_{\min}(Q)} \sup_{\|\xi\|_r \leq 1, \|\zeta\|_{\tilde{r}} \leq 1} \left\| \tfrac{\partial \psi(u(\xi))}{\partial \xi} \left[A\xi + B\psi^{-1}(\psi(u(\xi)) + \zeta_1) \right] \right\|. \tag{4.52}$$

According to Theorem 4.3, since the HD's of the systems (4.48) and (4.46) (with $x = 0$) satisfy $\nu < \mu$, then the interconnection is expected to be practically GAS at the origin. Note that the system (4.48)-(4.46) is a particular case of the system (4.10)-(4.11). In this case the PD is given by the subsystem (4.46). By its structure, it is GAS at the origin and $\tilde{r}$-homogeneous of degree 0, and the existence of an unique and Lipschitz continuous solution $y_1 = \psi(u(x))$ is guaranteed. Thus, Assumption 4.1 is reduced to Assumption 4.2 and the following corollary is readily derived from Theorem 4.3.

Corollary 4.1. *Let Assumption 4.2 be satisfied. Thus, the singularly perturbed system* (4.45)-(4.46) *is practically GAS at the origin. Moreover, there exist $T > 0$, such that, the trajectories of the system* (4.45) *are ultimate bounded by*

$$\|x(t)\|_r \leq \left(\tfrac{\eta\epsilon}{\tilde{\theta}} \left(\delta^{-1} \tfrac{\bar{a}_x s_{\max}(P)}{\underline{a}_x s_{\min}(P)} \right)^2 \right)^{-\frac{1}{\nu}}, \quad \forall t > T. \tag{4.53}$$

The result presented in Corollary 4.1 permits to ensure that the trajectories of the system (4.45)-(4.46) remains in a ball defined by (4.53) for all $t > T$ but it does not mean that the trajectories converge to a periodic solution like Fig. 4.9 depicts in the motivational example. However, under the assumption that such oscillations (chattering) arise in the steady state, an upper-bound of their amplitude is given by the inequality (4.53).

So, the result of Corollary 4.1 can be seen as an alternative based on Lyapunov methods for analysis of chattering produced finite-time convergent controllers, which has been usually performed in frequency domain, e.g., by using: describing function, harmonic balance, equivalent gain, etc. [Boiko, 2009]. This new approach allows to show the relationship between the amplitude of chattering, the SPP ϵ, and the HD ν of the system (4.48).

4.4.3 Motivational Example (Revisited)

Recall the example at the beginning of this section. Conditions of stability of the closed-loop system (4.42)-(4.43) in presence of the PD (4.44) are provided by Lemma 4.1, such that, the amplitude of the oscillations depicted in Fig. 4.10 can be predicted by inequality (4.53).

The stability of the nominal system $\dot{x} = -\alpha\lceil x \rfloor^{\frac{1}{2}}$ can be proven by the LF $V(x) = \frac{1}{2}x^2$, which fulfills the inequalities (4.19)-(4.20) with the constants $\kappa = 2$, $\underline{a}_x = \bar{a}_x = \frac{1}{2}$, $b_x = \alpha$ and $c_x = 1$. On the other hand, a LF for the unforced actuator dynamics (4.46) is given by $W(y) = \frac{1}{2}y^\top Py$, where

$$P = \begin{bmatrix} 2 & \frac{1}{2} \\ \frac{1}{2} & 2 \end{bmatrix}$$

is a solution of the equation (4.51) with

$$Q = \begin{bmatrix} 1 & 1 \\ 1 & 7 \end{bmatrix}.$$

Then, we have $s_{\min}(P) = \frac{3}{2}$, $s_{\max}(P) = \frac{5}{2}$, $s_{\min}(Q) \approx 0.84$, and $s_{\max}(Q) \approx 7.16$. Now, to compute the constant δ in (4.49), consider $\xi = \{-1, 1\}$, such that, the inequality

$$\left\| \lceil \alpha^2\xi + \tfrac{z_1}{\|x\|_r} \rfloor^{\frac{1}{2}} - \alpha\lceil \xi \rfloor^{\frac{1}{2}} \right\| \leq \frac{\alpha}{2},$$

is fulfilled by

$$\tfrac{|z_1|}{\|x\|_r} \leq \tfrac{3}{4}\alpha^2 = \delta.$$

On the other hand, the constant η in (4.52) is given by

$$\eta = \tfrac{1}{3}\alpha^2(\alpha^2 + 1)^{\frac{1}{2}}. \tag{4.54}$$

Then, substituting all the parameters in equation (4.53) it is obtained

$$\lim_{t\to\infty} \|x(t)\|_r \leq 28\epsilon^2. \tag{4.55}$$

Finally, the following table provides the estimation of the amplitude of chattering for different values of ϵ.

ϵ	$\lvert x \rvert$
0.05	0.03
0.01	0.0028
0.005	0.0007

Table 4.2: Estimation of chattering in the output of the closed-loop system (4.42)-(4.43) for different values of ϵ.

Note that the estimations provided by Table 4.2 are pretty similar to the results presented by Fig. 4.10. Nevertheless, the estimations obtained by using Lyapunov methods are usually overestimated.

4.5 Conclusion

This chapter presented a study of the effect of a stable homogeneous PD on the stability of a homogeneous MD, where the HD of every subsystem are possibly different. This analysis is based on ISS and Small-Gain Theorem by assuming only continuity of the considered vector fields. Three types of stability for such an interconnection were discovered depending on the relation between HDs of PD and MD:

- GAS when both dynamics have the same HD and the SPP is sufficiently small.
- Practical GAS, when the PD has a greater HD than the MD. The estimation of the final bound of the trajectories is provided and its size grows with the SPP. In this case, the chattering may appear if a finite-time convergent MD is considered.
- Local asymptotic stability with an estimation of the domain of attraction, when the PD has a smaller HD than the MD. The size of the domain of attraction decreases if the SPP is increased.

The first case can be interpreted as a generalization of the concept of motion separation predicted by classical results on smooth (at least Lipschitz continuous) singularly perturbed systems for a wider class of homogeneous systems. On the other hand, such a concept of motion separation is only valid outside of a neighborhood of the origin for the second case, and near to the origin for the third one, hence, just local and practical stability can be concluded, respectively.

Moreover, an analysis of the stability of finite-time convergent algorithms in presence of a fast actuator was performed. Under the assumption that chattering arises in the steady state of the system trajectories, this result allows to show the relationship between the amplitude of chattering, the SPP ϵ, and the HD ν of the finite-time convergent algorithm. Thus, this new approach can be seen as an alternative based on Lyapunov methods for analysis of chattering produced finite-time convergent controllers.

Chapter 5

Third-order Continuous Twisting Algorithm

The Continuous Twisting Algorithm (CTA) was introduced by [Torres-González et al., 2015] (see also [Torres-González et al., 2017]) to provide finite-time stability for the trajectories of a perturbed double integrator with Lipschitz-continuous non-vanishing and matched disturbances by means of a continuous control signal and using just information of the output and its first derivative. This controller consists of a r-homogeneous and nonlinear state feedback with an appropriated vector of weights r, such that, it is able to provide finite-time convergence for a nominal double integrator, and a discontinuous integral extension capable to reject Lipschitz-continuous non-vanishing and matched disturbances. This integral term contains a linear combination of the sign of the output plus the sign of its derivative similar to the Twisting Algorithm introduced by [Levant, 1993].

From [Torres-González et al., 2015, Torres-González et al., 2017], the stability analysis and the design of gains for the CTA consist of a two-step procedure based on the Generalized Form (GF) approach [Sánchez and Moreno, 2014, Sánchez and Moreno, 2016, Sanchez and Moreno, 2019]. First, an appropriated Lyapunov function (LF) candidate is selected in the class of GF. Second, parameters of the LF candidate and Gains of the CTA are computed, such that, the LF candidate is positive definite and its derivative along the trajectories of the controlled system is negative definite, which can be done by using Polya's theorem [Pólya, 1928] or Sum of Squares (SOS) methods [Parrilo, 2000].

Recently, the CTA has attracted a lot of attention in the community of Sliding Mode Control (SMC). For instance, [Moreno et al., 2016] proposes an adaptive version of the CTA (ACTA), where the controller gain is adjusted automatically, keeping all properties the original CTA in the case when the upper-bound of the perturbation's derivative is unknown. Further, [Sanchez et al., 2017b] presents two schemes of output feedback CTA (OFCTA) based on the first and second order Robust and Exact Differentiator (RED), and provides an analysis of robustness w.r.t. noise in the measurements of the output. Moreover, [Golkani et al., 2020] introduces a Lyapunov based saturated controller which incorporates the Twisting Algorithm and the CTA. On the other hand, the CTA has been proposed as a great solution to practical applications, for example, see the works of [Keshtkar et al., 2018,

Jin et al., 2019, Gutiérrez-Oribio et al., 2020, Rojas-Contreras et al., 2017, Pérez-Ventura et al., 2020, Franco et al., 2021].

The present chapter is devoted to the design of a CTA for third order systems (3-CTA). In theory, this controller is able to provide finite-time stability to the origin of a chain of integrators of third-order, with an exact compensation of Lipschitz-continuous non-vanishing and matched disturbances. This is achieved with a continuous control signal and using only information of the output and its derivatives of first and second order. Moreover, the proposed controller achieves sliding accuracy of orders 4, 3, 2 and 1, w.r.t. the sampling step, for the output and its derivatives up to third-order, respectively (see [Levant, 1993, Levant and Fridman, 2010] for details about sliding accuracy). The 3-CTA was firstly presented in [Mendoza-Avila et al., 2017] to illustrate a recursive procedure to select a proper LF candidate in the class of GF for the arbitrary order Continuous Twisting Algorithm (n-CTA).

Furthermore, an adaptive 3-CTA (3-ACTA) is provided for the case when the bound of perturbation's derivative is unknown. The controller gains are adjusted by an adaptation law until a level that allows to reject the perturbation and guarantees the finite-time convergence to zero for the system trajectories. In addition, this scheme avoids overestimation of gains which leads to reduction of chattering. The theoretical properties of this controller are validated by implementation in an Inertial Wheel Pendulum (IWP).

Moreover, for a chain of integrators of third order with an unique measurable output σ with relative degree three w.r.t. the control input, an output feedback 3-CTA (3-OFCTA) is introduced. This output feedback scheme consists of a 3-CTA complemented with an observer based on the Third-Order RED (3-RED), which allows to estimate two derivatives of the output, i.e., $\dot{\sigma}$, $\ddot{\sigma}$, robustly and in finite-time. A separation principle is established to design the controller and the observer independently. In the absence of noise, the 3-OFCTA preserves all features of robustness, finite time stability, homogeneity, and precision w.r.t. sampling step from the original 3-CTA, while requiring only information of a measurable output of the plant. Furthermore, experimental results for the implementation of the 3-OFCTA in a magnetic levitation system (MLS) are presented. This system is subjected to uncertainty conditions, and the plate position is the only measurable output with relative degree three w.r.t. the control input, hence the 3-OFCTA is a reasonable solution to control the MLS.

The rest of the chapter is structured as follows. Some definitions and preliminary results are given in Section 5.1. Section 5.2 presents the state feedback controller 3-CTA. In Section 5.3, we provide the adaptive controller 3-ACTA, besides a precision test to compare the 3-CTA vs the 3-ACTA, and experimental results of the implementation of the 3-ACTA in the IWP. An observer based on the 3-RED and the output feedback controller 3-OFCTA are presented in Section 5.4 with simulation and experimental results of its implementation in a MLS, and also precision tests for 3-CTA and 3-OFCTA are given. Finally, in Section 5.5 some conclusions are drawn.

5.1 Preliminaries: generalized forms

The concept of GF is introduced in [Sánchez and Moreno, 2014] as a generalization of (classical) forms. A form is a r-homogeneous polynomial function of degree $p \in \mathbb{N}$, where $r = [1, \ldots, 1]$

[Hardy et al., 1988]. The set of quadratic forms is a particular case of (classical) forms.

Definition 5.1. A function $g : \mathbb{R}^n \longrightarrow \mathbb{R}$ is a GF if it is r-homogeneous of degree $m \in \mathbb{R}$, and it consists of a linear combination of a finite number of homogeneous monomials, which are sums, products and sums of products of terms like:

$$a\lceil x \rfloor^p \quad \text{or} \quad b|x|^q, \quad \text{where} \quad a, b \in \mathbb{R}, \quad p, q \in \mathbb{R}_{>0}.$$

△

Note that a GF is not required to be continuous. Some examples of GF are:

$$\begin{aligned} g_1(x) &= \lceil x_1 \rfloor^{\frac{7}{2}} - 2x_1^2|x_2|^3 - 3\lceil x_1 \rfloor^{\frac{5}{2}}\lceil x_2 \rfloor^2 + 3|x_2|^7, \\ g_2(x) &= a|x_1|^{\frac{5}{3}} - \lceil x_1 \rfloor^{\frac{2}{3}}|x_2|^{\frac{3}{2}} - b\lceil x_1 \rfloor^0\lceil x_2 \rfloor^5 + c\lceil x_2 \rfloor^2 x_3 \end{aligned}$$

Moreover, GF have some important properties, e.g., partial derivatives of GF's are also GF's, or for the same r, sums or products of GF's are also GF's. Further, for $r \in \mathbb{Q}^n$ any GF can be represented by (classical) forms in each hyper-octant of the state space (see Example 5.1).

A set of forms that permits to represent a GF in the hold state space is called the set of associated forms. This associated forms are obtained by applying a suitable change of coordinates $x = d(z)$ in each hyper-octant of the state space, where every element of the variable $z \in \mathbb{R}^n$ is nonnegative. One option is

$$x_i = \begin{cases} z_i^{2r_i} & \text{for} \quad x_i \geq 0 \\ -z_i^{2r_i} & \text{for} \quad x_i < 0 \end{cases} \qquad i = 1, ..., n. \tag{5.1}$$

where $z_i > 0$ and r_i is the homogeneity weight of the corresponding variable x_i. With this transformation we obtain associated forms whose domains are restricted to the positive hyper-octant, i.e., $z_i > 0$, $i = 1, ..., n$, and all their exponents are even (see Example 5.1).

So, the problem of analyze the positive definiteness of a GF can be reduced to determine the positive definiteness of its associated forms, for which there are classical tools like Polya's theorem [Pólya, 1928] or SOS methods [Parrilo, 2000].

Example 5.1. Consider the GF

$$h(x) = x_1^2 - ax_1\lceil x_2 \rfloor^2 + bx_2^4, \tag{5.2}$$

which is r-homogeneous of degree 4 with weights $r = [2; 1]$. By applying the change of coordinates (5.1) to the GF (5.2) in each quadrant of the space state $\{x_1, x_2\}$, we obtain the following associated forms in $\{z_1 \geq 0, z_2 \geq 0\}$:

- for $\{x_1 \geq 0, x_2 \geq 0\}$ and $\{x_1 \leq 0, x_2 \leq 0\}$,

$$h_1(z) = z_1^8 - az_1^4z_2^4 + bz_2^8,$$

- for $\{x_1 \leq 0, x_2 \geq 0\}$ and $\{x_1 \geq 0, x_2 \leq 0\}$,

$$h_1(z) = z_1^8 + az_1^4 z_2^4 + bz_2^8.$$

Note that due to the GF (5.2) is symmetric w.r.t. the origin, it can be completely represented by only two associated forms. Moreover, if $a^2 = 4b$ for any $b > 0$, both associated forms $h_1(z)$ and $h_2(z)$ are positive definite, hence we can conclude that the GF (5.2) is also positive definite for any $b > 0$ and $a^2 = 4b$.

5.1.1 Sum of squares

A polynomial function $p(x_1, \ldots, x_n) = p(x)$ is a SOS if there exists some polynomials $h_1(x), \ldots, h_m(x)$ such that

$$p(x) = \sum_{i=1}^{m} h_i^2(x). \tag{5.3}$$

Note that if $p(x)$ is a SOS then it is positive semi-definite, i.e., $p(x) \geq 0$ for all $x \in \mathbb{R}^n$ [Parrilo, 2000].

The SOS condition (5.3) is equivalent to the existence of a positive semi-definite matrix Q such that

$$p(x) = Z^T(x) Q Z(x), \tag{5.4}$$

where the vector $Z(x)$ contains some properly chosen monomials [Choi et al., 1995]. This representation of a SOS polynomial permits to compute its coefficients through the solution of some matrix inequalities, which can be efficiently computed by means of semidefinite programming with available software. For instance, the Matlab toolbox SOSTOOLS with SEDUMI solver is able to determine the condition under which a polynomial is SOS [Prajna et al., 2002].

5.1.2 Generalized Forms approach for Lyapunov function design

The works in [Sánchez and Moreno, 2014, Sánchez and Moreno, 2016, Sanchez and Moreno, 2019] present a methodology for construction of LF for homogeneous HOSM algorithms based on GF's. It consists in propose a GF as a LF candidate and offers a systematic procedure to determine the coefficients of the GF that warranty its positive definiteness and the negative definiteness of its derivative. This procedure is summarized in the following steps:

1. Consider the system $\dot{x} = f(x)$, $x \in \mathbb{R}^n$, whose vector field f is described by GF. Obtain the homogeneity degree k and the vector of weights r of the system under study.

2. Select a GF $V : \mathbb{R}^n \to \mathbb{R}$ (with a homogeneity degree m and a vector of weights r) given by

$$V(x) = \sum_{i=1}^{n} \alpha_i |x_i|^{\frac{m}{r_i}} + P(\alpha_j, x); \quad j > n \tag{5.5}$$

where $P(\alpha_j, x)$ contains cross terms between the variables $x_i \in x;\ i = 1, ..., n$ with coefficients α_j.

3. Compute the negative of the derivative of V along the trajectories of the considered system, e.i., $W(x) = -\dot{V}(x) = -\frac{\partial V}{\partial x}\dot{x}$.

4. Apply an adequate change of coordinates from x to z (like (5.1)) to get the sets of associated forms $\{V_i(z)\}$ and $\{W_i(z)\}$ of the GF $V(x)$ and $W(x)$, respectively.

5. Find the parameters to guarantee that every form in the sets $\{V_i(z)\}$ and $\{W_i(z)\}$ is positive definite. For this we can use the SOS approach, where this parameters are calculated by means of the solution of some matrix inequalities, which can be efficiently done by using SOSTOOLS with SEDUMI solver.

5.2 A State feedback controller: 3-CTA

Consider a SISO system with a control input $u \in \mathbb{R}$ and an output $\sigma \in \mathbb{R}$ of relative degree 3, i.e. $\dddot{\sigma} = u + \phi(t)$. Introducing the state vector $x \in \mathbb{R}^3$ as $x_1 = \sigma$, $x_2 = \dot{\sigma}$, $x_3 = \ddot{\sigma}$, we obtain the third order model

$$\begin{array}{rcl} \dot{x}_1 & = & x_2, \\ \dot{x}_2 & = & x_3, \\ \dot{x}_3 & = & u + \phi(t)\,, \end{array} \tag{5.6}$$

where the disturbance $\phi(t)$ is given by a Lipschitz continuous function w.r.t. time, i.e., it satisfies $|\frac{d}{dt}\phi(t)| \leq \rho$. The control objective is to render the state x of the system (5.6) finite-time stable for every disturbance $\phi(t)$, with Lipschitz constant smaller than ρ, and such that the control law $u(t)$ is a continuous signal.

Assuming that all states of the system (5.6) are measurable, the 3-CTA (originally introduced in [Mendoza-Avila et al., 2017]) is given by

$$\begin{array}{rcl} u & = & -k_1 L^{\frac{3}{4}} \lceil x_1 \rfloor^{\frac{1}{4}} - k_2 L^{\frac{2}{3}} \lceil x_2 \rfloor^{\frac{1}{3}} - k_3 L^{\frac{1}{2}} \lceil x_3 \rfloor^{\frac{1}{2}} + \eta \\ \dot{\eta} & = & -k_4 L \mathrm{sign}(\mathrm{x}_1) - k_5 L \mathrm{sign}(\mathrm{x}_2) - k_6 L \mathrm{sign}(\mathrm{x}_3)\,, \end{array} \tag{5.7}$$

where k_i, $i = 1, ..., 6$, are (constant) gains to be designed for stability, and the constant $L > 0$ is a scaling factor to endow the controller of robustness. So, the 3-CTA (5.7) allows to achieve the control objective.

Moreover, in [Levant, 1993, Levant and Fridman, 2010] the accuracy of homogeneous HOSM controllers is defined as the supremum value of the states when the system's trajectories are in steady state. According to homogeneity weights of the states of the closed-loop systems (5.6)-(5.7), the accuracy of the states w.r.t. sampling time τ is given by

$$|x_1(t)| \leq \Delta_1 \tau^4, \quad |x_2(t)| \leq \Delta_2 \tau^3, \quad |x_3(t)| \leq \Delta_3 \tau^2, \quad |x_4(t)| \leq \Delta_4 \tau, \tag{5.8}$$

where $\Delta_1, \Delta_2, \Delta_3$ and Δ_4 are constants independent of τ. The value of Δ_i depends on several factors, e.g., the gains k_i and scaling factor L, etc. These parameters Δ_i can be seen as a measure of

	k_1	k_2	k_3	k_4	k_5	k_6	μ_c
D_1	1.3	2.2	3	0.009	0.004	0.002	0.001
D_2	1.3	2.2	3	0.008	0.003	0	0.0006
D_3	1.3	2.2	3	0.005	0	0.001	0.0003
D_4	1.3	2.2	3	0.004	0	0	0.0001

Table 5.1: Sets of gains for the 3-CTA.

chattering produced by the 3-CTA, and they can be estimated by means of frequency domain methods: describing function, harmonic balance equation, equivalent gain, etc., which has been studied by [Pérez-Ventura and Fridman, 2019] for different CHOSM algorithms.

Theorem 5.1. *Consider the disturbed system* (5.6)*, where* $|\frac{d}{dt}\phi(t)| \leq \rho$*, and the control law* (5.7)*. There exist gains* $k_1, k_2, k_3, k_4 \in \mathbb{R}_{>0}$*,* $k_5, k_6 \in \mathbb{R}$*, with* $k_4 > |k_5| + |k_6| + \rho$*, and a constant* $\mu_c \in \mathbb{R}_{>0}$*, such that, for any scaling factor* $L > \frac{\rho}{\mu_c}$ *the origin of the close-loop system* (5.6)-(5.7) *is globally finite-time stable.* △

The proof of Theorem 5.1 and gain design for controller (5.7) are presented in Section C.1 of Appendix C. Table 5.1 shows some examples of possible sets of gains for controller (5.7) and their level of tolerance μ_c. To implement the 3-CTA, the user only needs to select a set of gains of Table 5.1 and adjust the scaling factor L as $L > \frac{\rho}{\mu_c}$

Following the proof of Theorem 5.1 presented in Section C.1 of Appendix C, more sets of gains for the 3-CTA can be found. Moreover, note that there are three available configurations of the integrator η of the 3-CTA:

1. Three signs:
$$\dot{\eta} = -k_4 L\text{sign}(\text{x}_1) - k_5 L\text{sign}(\text{x}_2) - k_6 L\text{sign}(\text{x}_3),$$
with set D_1.

2. Twisting like:
$$\dot{\eta} = -k_4 L\text{sign}(\text{x}_1) - k_5 L\text{sign}(\text{x}_2),$$
with set D_2, or
$$\dot{\eta} = -k_4 L\text{sign}(\text{x}_1) - k_6 L\text{sign}(\text{x}_3),$$
with set D_3.

3. Integral discontinuous:
$$\dot{\eta} = -k_4 L\text{sign}(\text{x}_1),$$
with set D_4.

The differences between the configurations are related to the transient behavior of the 3-CTA.

Remark 5.1. The 3-CTA consists of two terms: (i) a memoryless continuous state feedback, depending on the gains k_1, k_2, k_3, that should stabilize the origin of the close-loop system (5.6)-(5.7) in finite time in the absence of the perturbation ϕ. This requires the gains k_1, k_2, k_3 to be positive. (ii) An integral controller, depending on the gains k_4, k_5, k_6, which should estimate and compensate the perturbation $\phi(t)$ in finite time, too. For this it is required that $k_4 > |k_5| + |k_6| + \rho$, so that the close-loop system (5.6)-(5.7) has a unique equilibrium point at the origin (see Section C.1 of Appendix C). Gains $k_5, k_6 \in \mathbb{R}$ are not required to be sign definite, and they can be used to improve the performance of controller (5.7).

5.3 Adaptive 3-CTA

The scaling factor L allows the 3-CTA (5.7) to deal with disturbances with any known bound of its first time derivative. However, the bound of perturbation's derivative is commonly unavailable making the tunning of the scaling factor L difficult. In order to solve this problem an adaptation law can be used to adjust automatically the scaling factor L to a proper value.

Following the proposal of [Moreno et al., 2016], the 3-CTA (5.7) with adaptive scaling factor $L(t)$ is proposed as

$$\begin{array}{rcl} u & = & -k_1 L^{\frac{3}{4}}(t)\lceil x_1 \rfloor^{\frac{1}{4}} - k_2 L^{\frac{2}{3}}(t)\lceil x_2 \rfloor^{\frac{1}{3}} - k_3 L^{\frac{1}{2}}(t)\lceil x_3 \rfloor^{\frac{1}{2}} + \eta \\ \dot{\eta} & = & -k_4 L(t)\mathrm{sign}(\mathrm{x}_1) - k_5 L(t)\mathrm{sign}(\mathrm{x}_2) - k_6 L(t)\mathrm{sign}(\mathrm{x}_3), \end{array} \tag{5.9}$$

where the adaptation law for the scaling factor $L(t)$ is given by

$$\dot{L}(t) = \begin{cases} \ell, & \text{if} \quad T_e(t) \neq 0 \quad \text{or} \quad ||\bar{x}(t)|| > 0 \\ 0, & \text{if} \quad T_e(t) = 0 \quad \text{and} \quad ||\bar{x}(t)|| = 0 \end{cases} \tag{5.10}$$

where $\bar{x} = (x_1, x_2, x_3)$ and ℓ is a positive constant. Function $T_e(t)$ represents a timer with behavior is given by

$$T_e(t) = \begin{cases} t_i + \tau_d - t, & \text{if} \quad t_i \leq t \leq t_i + \tau_d \\ 0, & \text{if} \quad t \geq t_i + \tau_d \end{cases} \tag{5.11}$$

where $\tau_d > 0$ is a constant *dwell time*. The time instants t_i are defined, such that, for $i = 0$, $t_0 = 0$, and for $i > 0$, they are the instants when $||\bar{x}(t)||$ changes from zero to a non zero value. The adaptation law lets the scaling factor $L(t)$ grows until $||\bar{x}(t)|| = 0$, for at least a period of time τ_d. If $\bar{x}$ deviates from zero due to an increasing of the disturbance size, then the gain grows for at least τ_d until it becomes zero again. This procedure is repeated a finite number of times until $||\bar{x}(t)||$ remains at zero for all future time. In practice the ideal condition $||\bar{x}|| = 0$ is replaced by a small neighborhood of zero, i.e., $||\bar{x}|| < \epsilon$. The constant ϵ depends on the precision of sensors and actuators, the integration step and the acceptable chattering level. However, a very small ϵ can generate a bug in the algorithm which can cause instability.

Theorem 5.2. *Consider system* (5.6) *where* $|\dot{\phi}(t)| < \rho$ *with* ρ *unknown, and controller* (5.9) *where scaling factor* $L(t)$ *is given by adaptation law* (5.10)*. If gains* $k_i; \quad i = 1 \ldots 6$ *satisfy Theorem 5.1,*

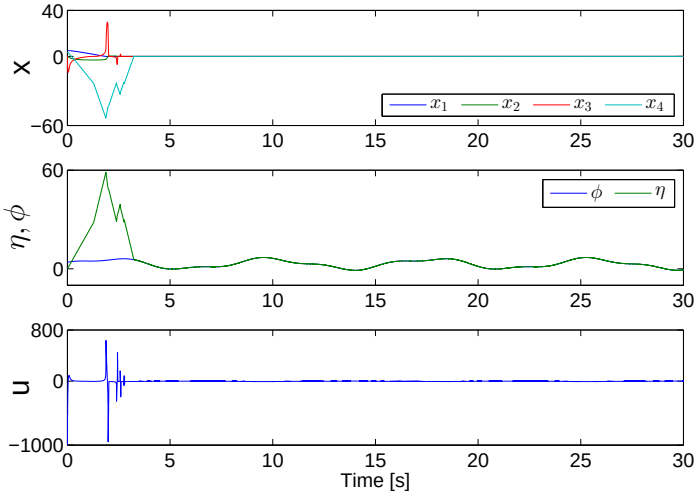

Figure 5.1: Simulation of the system (5.6) in closed-loop with controller (5.7) with set of gains D_1 and $L = 4500$.

then the trajectories of the closed-loop system (5.6)-(5.9) *converge to zero globally and in finite-time.* $\triangle$

The proof of Theorem 5.2 is presented in Section C.2 of Appendix C. Even in the case that the parameter ρ is known the 3-ACTA outmatches the 3-CTA because the parameter ρ can be overestimated making the scaling factor L of the 3-CTA bigger than needed. In contrast, the 3-ACTA includes the adaptation law (5.10) to find the correct value of the scaling factor $L(t)$, automatically. Nevertheless, the main disadvantage of the adaptation law (5.10) is that the scaling factor can grow up, only. Thus, if after certain time instant the perturbation decreases, there is no way to adjust the scaling factor $L(t)$ to more proper value.

Simulation results

The objective of simulations is to show the theoretical properties of the 3-CTA and the 3-ACTA. The simulations were performed in Matlab Simulink with sampling step $\tau = 0.00001[s]$ and the Euler integration method.

Stabilization by 3-CTA: Considering a perturbation $\phi(t) = 3\sin(0.8t) + \cos(2t) + 3$ and initial conditions $x_0 = [5, 0, 0]^T$, Fig. 5.1 shows the simulation of the system (5.6) in closed-loop with the controller (5.7), with the set of gains D_1 from Table 5.1. We can see that the states x_1, x_2, x_3 of system (5.6) converge to origin, while the integral term η compensate exactly perturbation ϕ, and the control signal u is continuous.

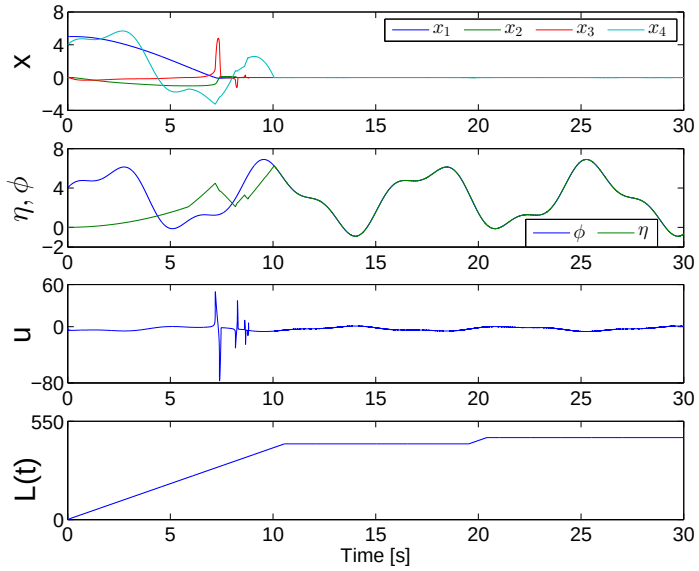

Figure 5.2: Simulation of the system (5.6) in close loop with controller (5.9) with set of gains D_1 and L given by adaptation law (5.10).

Stabilization by 3-ACTA: Considering a perturbation $\phi(t) = 3\sin(0.8t) + \cos(2t) + 3$ and initial conditions $x_0 = [5, 0, 0]^T$, Fig. 5.2 shows the simulation of the system (5.6) in closed-loop with the controller (5.9) with the set of gains D_1 from Table 5.1 and $L(t)$ given by adaptation law (5.10), where $\ell = 40$ and $\tau_d = 0.5$[s]. We can see that the states x_1, x_2, x_3 of system (5.6) converge to origin, while the integral extension η compensate exactly perturbation ϕ, and the control signal u is continuous.

Precision test: 3-CTA vs 3-ACTA

According to homogeneity weights of the states of the closed-loop systems (5.6)-(5.7) and (5.6)-(5.9), the accuracy of the states w.r.t. sampling time τ is given by (5.8). By the simulations shown in Fig. 5.1 and 5.2 with Euler method and $\tau = 0.00001[s]$, the constants Δ_i are determined in Fig. 5.3 as

$$\Delta_1 = 68000, \quad \Delta_2 = 44000, \quad \Delta_3 = 36600, \quad \Delta_4 = 1360,$$

and

$$\Delta_1 = 4180, \quad \Delta_2 = 2777, \quad \Delta_3 = 2544, \quad \Delta_4 = 612,$$

for for the 3-CTA nd the 3-ACTA, respectively. Such constants Δ_i can be confirmed by a simulation with a different sampling time, e.g., $\tau = 0.0001[s]$, as it is shown in Fig. 5.4.

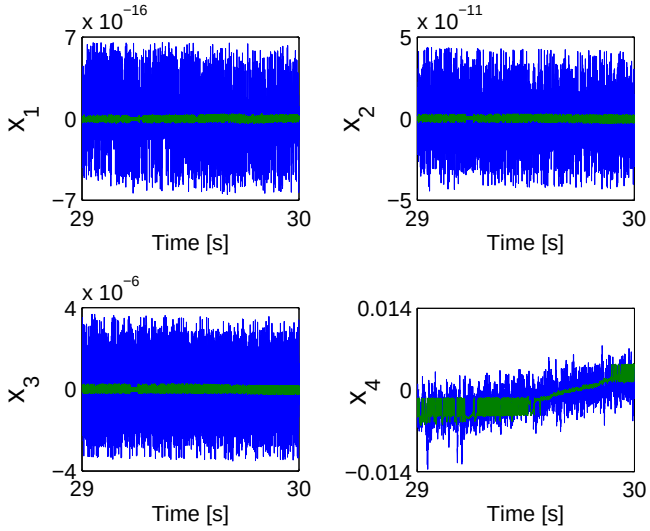

Figure 5.3: Accuracy provided by 3-CTA (——) and 3-ACTA (——) in closed-loop with a disturbed triple integrator, with sampling step $\tau = 0.00001$.

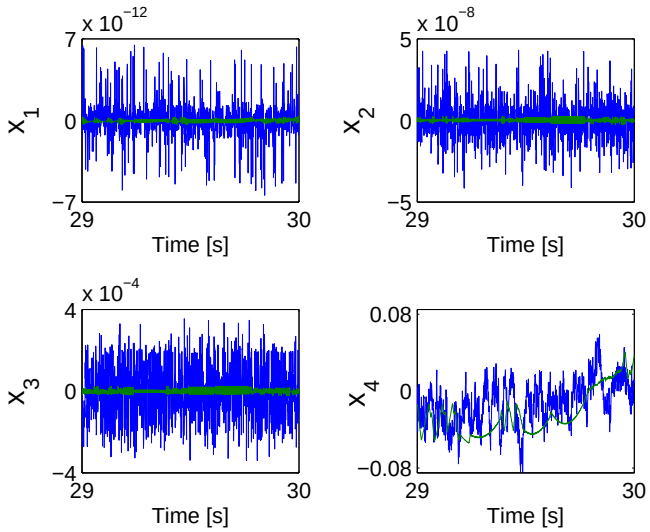

Figure 5.4: Simulation results, with sampling step $\tau = 0.0001$, of the accuracy provided by controller 3-CTA (——) and 3-ACTA (——) in closed-loop with a disturbed triple integrator.

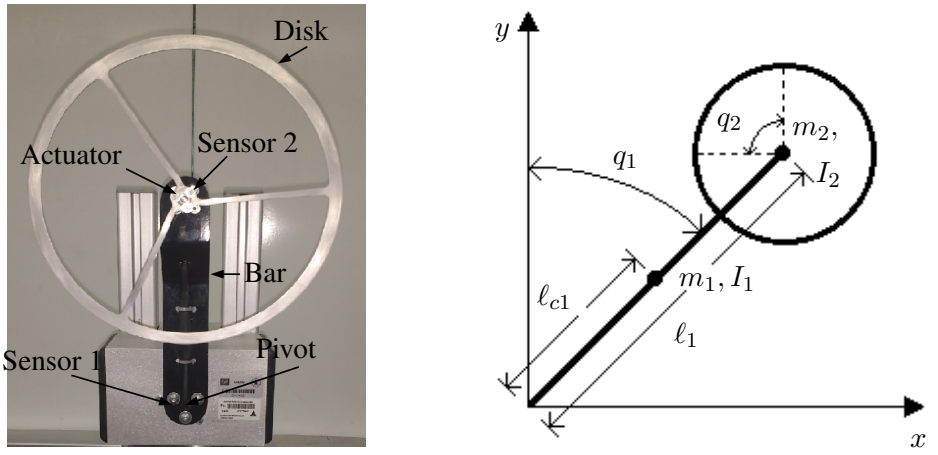

(a) Experimental setup

(b) q_1-pendulum angle and q_2-wheel angle.

Figure 5.5: Inertia wheel pendulum.

From Fig. 5.3 and 5.4, note that the accuracy provided by the 3-ACTA is higher than the accuracy of the 3-CTA. This is because the adaptation law (5.10) avoid the overestimation of the gains and it permits improve the performance of the 3-CTA and decrease chattering effects.

5.3.1 Implementation of the 3-ACTA in a reaction wheel pendulum

An IWP is an under-actuated mechanical system consisting in a bar suspended from a pivot with a rotating disk attached at the end. The disk is actuated by a 12 [v] DC-motor while the pendulum is unactuated, such that, the pendulum is drive by the inertia generated by the angular acceleration of the disk (see Fig. 5.5(a)).

The state vector is defined as $\bar{x}^T = [x_1 \quad x_2 \quad x_3] = [q_1 \quad \dot{q}_1 \quad \dot{q}_2]$, where q_1 is the pendulum angle, q_2 is the disk angle. Since the disk angular position is a cyclic variable, it can be ignored into a state space model. Then, a dynamical model of the IWP is given by

$$\begin{array}{rcl} \dot{x}_1 = & x_2, & \\ \dot{x}_2 = & -\frac{d_{22}}{D}\varphi(x_1) - \frac{d_{22}b_1}{D}x_2 + \frac{d_{12}b_2}{D}x_3 - \frac{d_{12}}{D}u & \\ \dot{x}_3 = & \frac{d_{21}}{D}\varphi(x_1) + \frac{d_{21}b_1}{D}x_2 - \frac{d_{11}b_2}{D}x_3 + \frac{d_{11}}{D}u & \end{array} \tag{5.12}$$

where u is the control input, b_1 is the friction term on the pendulum axis, b_2 the friction on the wheel axis and

$$\begin{array}{rcl} \varphi(x_1) & = & -\bar{m}g\sin(x_1), \\ \bar{m} & = & m_1\ell_{c1} + m_2\ell_1, \\ D & = & d_{11}d_{22} - d_{12}d_{21} > 0, \\ d_{11} & = & m_1\ell_{c1}^2 + m_2\ell_1^2 + I_1 + I_2, \\ d_{12} & = & d_{21} = d_{22} = I_2, \end{array} \tag{5.13}$$

are parameters, whose values are provided by Table 5.2 (see Fig. 5.5(b)).

Table 5.2: List of parameters of the Inertial Wheel Pendulum.

Parameters.	**Values.**	**Parameters.**	**Values.**
b_1	0.0173 $\frac{Ns}{m^2}$	b_2	0.0313 $\frac{Ns}{m^2}$
I_2	0.0027 kgm^2	d_{11}	0.0479 kgm^2
$\overline{m}$	0.2514 kg	g	9.81 $\frac{m}{s^2}$

The control objective is to stabilize the pendulum in the upper position from a different initial condition. Due to the uncertainties in the system (5.12), the 3-ACTA (5.9) is a great solution to this problem.

First, let's put the system (5.12) in a normal form. For this, define the diffeomorphism:

$$\begin{array}{rcl} \xi_1 & = & b_1 x_1 + d_{11} x_2 + d_{12} x_3, \\ \xi_2 & = & -\varphi(x_1), \\ \xi_3 & = & -\varphi'(x_1) x_2. \end{array} \tag{5.14}$$

Applying the transformation (5.14) to system (5.12), we obtain

$$\dot{\xi}_1 = \xi_2, \qquad \dot{\xi}_2 = \xi_3, \qquad \dot{\xi}_3 = f(x) + g(x)u. \tag{5.15}$$

where $g(x) = \frac{d_{12}}{D}\varphi'(x_1)$ and

$$f(x) = -\varphi''(x_1)x_2^2 + \varphi'(x_1)\left[\frac{d_{22}}{D}\varphi(x_1) + \frac{d_{22}b_1}{D}x_2 - \frac{d_{12}b_2}{D}x_3\right].$$

Remark 5.2. The system (5.15) is only valid in the upper part of pendulum workspace, i.e. $-\frac{\pi}{2} < \chi_1 < \frac{\pi}{2}$, around the origin.

Now, by an exact feedback linearization $u = \frac{1}{g(x)}\left(v - f(x)\right)$, the system (5.15) becomes

$$\dot{\xi}_1 = \xi_2, \qquad \dot{\xi}_2 = \xi_3, \qquad \dot{\xi}_3 = v + \phi(t), \tag{5.16}$$

where v is a new control input and $\phi(t)$ represents parametric uncertainties and disturbances which are assumed to be Lipschitz continuous functions.

For the experiments we use the dSPACE1103 and a sampling step of $1[ms]$. The IWP shown in Fig. 5.5(a) has a $12[v]$ DC-motor as actuator, also it has two encoders to measure the angular positions, one for the pendulum and the other for the disk, both velocities are computed by a RED of second-order (see [Levant, 2003a]) and we assume that the estimation errors vanish immediately, hence we can take all the states of the IWP are measurable. During the experiments two perturbations are executed, the first is a matched disturbance ϕ_1 at $t = 15$[s] and another unmatched ϕ_2 at $t = 22.5$[s]. Adaptive

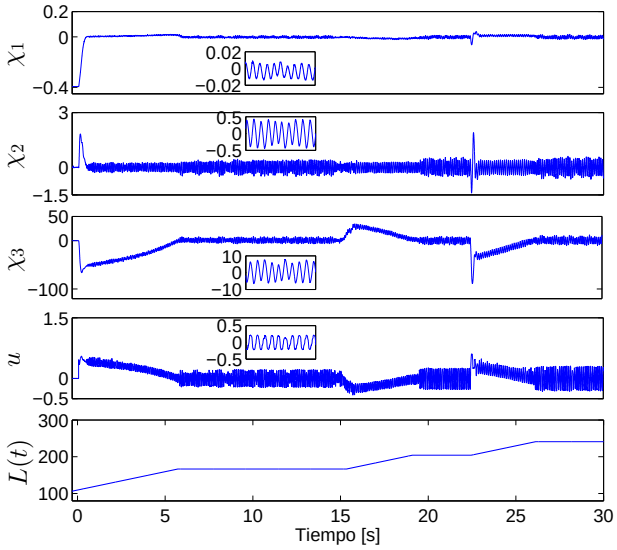

Figure 5.6: IWP driven by the 3-ACTA (5.9) with the set of gains D_1 of Table 5.1 and $L(t)$ given by the adaptation law (5.10).

gain $L(t)$ starts from an initial condition $L(0) = 107$ and it grows at the rate of $\ell = 40$ during at least $\tau_d = 0.5[s]$ or until $|\bar{x}_1| < 0.05$, $|\bar{x}_2| < 0.5$ and $|\bar{x}_3| < 12$ hold.

Fig. 5.6 shows the experimental results of the implementation of the 3-ACTA (5.9) on the IWP, with the set of gains D_1 of Table 5.1 and $L(t)$ given by the adaptation law (5.10). It can be looked at the states of the system (5.12) converge closely to origin from initial condition $\bar{x}_0 = [0.4, 0, 0]$, the control signal u is continuous and compensates the matched disturbance ϕ_1. On the other hand, the 3-ACTA is able to keep the IWP near to the upper position in spite of the unmatched disturbance ϕ_2. Furthermore, the adaptive gain $L(t)$ increases its value until the stability of IWP in the upper position is achieved.

5.4 Output feedback 3-CTA

Considering $\sigma = x_1$ as the only measurable output of system (5.6), the states x_2 and x_3 can be robustly estimated in finite time by the observer

$$\begin{aligned} \dot{\hat{x}}_1 &= -\lambda_1 H^{\frac{1}{4}} \lceil \hat{x}_1 - \sigma \rfloor^{\frac{3}{4}} + \hat{x}_2 \\ \dot{\hat{x}}_2 &= -\lambda_2 H^{\frac{2}{4}} \lceil \hat{x}_1 - \sigma \rfloor^{\frac{2}{4}} + \hat{x}_3 \\ \dot{\hat{x}}_3 &= -\lambda_3 H^{\frac{3}{4}} \lceil \hat{x}_1 - \sigma \rfloor^{\frac{1}{4}} + \zeta + u \\ \dot{\zeta} &= -\lambda_4 H \mathrm{sign}(\hat{x}_1 - \sigma), \end{aligned} \tag{5.17}$$

where $\lambda_i > 0$, $i = 1, \ldots, 4$, are gains and the constant $H > 0$ is a scaling factor. The observer (5.17) is a particular case (with $r = 3$ and $n_f = 0$) of the filtering observer presented in [Levant, 2018].

Theorem 5.3. *Consider the system* (5.6) *with an measurable output* $\sigma = x_1$ *and assume that* $|\frac{d}{dt}\phi(t)| \leq \rho$. *For any* $\rho \geq 0$, *there exist gains* $\lambda_i > 0$, $i = 1, \ldots, 4$, *and a constant* $H_{min} > 0$, *such that, for any scaling factor* $H > H_{min}$, *observer* (5.17) *estimates the states of the disturbed system* (5.6) *exactly and in finite-time.* △

The proof of Theorem 5.3 and a methodology for selection of gains for observer (5.17) are presented in Section C.3 of Appendix C.

An output feedback scheme 3-OFCTA is designed by combining the 3CTA (5.7) with the finite-time observer (5.17):

$$\begin{aligned} u &= -k_1 L^{\frac{3}{4}} \lceil \sigma \rfloor^{\frac{1}{4}} - k_2 L^{\frac{2}{3}} \lceil \hat{x}_2 \rfloor^{\frac{1}{3}} - k_3 L^{\frac{1}{2}} \lceil \hat{x}_3 \rfloor^{\frac{1}{2}} + \eta \\ \dot{\eta} &= -k_4 L \text{sign}(\sigma) - k_5 L \text{sign}(\hat{\text{x}}_2) - k_6 L \text{sign}(\hat{\text{x}}_3) \\ \dot{\hat{x}}_1 &= -\lambda_1 H^{\frac{1}{4}} \lceil \hat{x}_1 - \sigma \rfloor^{\frac{3}{4}} + \hat{x}_2 \\ \dot{\hat{x}}_2 &= -\lambda_2 H^{\frac{2}{4}} \lceil \hat{x}_1 - \sigma \rfloor^{\frac{2}{4}} + \hat{x}_3 \\ \dot{\hat{x}}_3 &= -\lambda_3 H^{\frac{3}{4}} \lceil \hat{x}_1 - \sigma \rfloor^{\frac{1}{4}} + \epsilon + u \\ \dot{\epsilon} &= -\lambda_4 H \text{sign}(\hat{\text{x}}_1 - \sigma). \end{aligned} \tag{5.18}$$

Theorem 5.4. *Consider the system* (5.6) *with* $|\frac{d}{dt}\phi(t)| \leq \rho$ *and a measurable output* $\sigma = x_1$. *If gains* k_i, $i = 1, \ldots, 6$, *and* L_{min} *satisfy Theorem 5.1 and gains* λ_j, $j = 1, \ldots, 4$, *and* H_{min} *satisfy Theorem 5.2, then for any* $L > L_{min}$ *and* $H > H_{min}$, *the trajectories of the closed-loop system* (5.6)-(5.18) *converge to zero globally and in finite-time.* △

The proof of Theorem 5.4 is presented in Section C.4 of Appendix C.

Remark 5.3. Note that the output feedback controller 3-OFCTA (5.18) is able to keep the same precision orders w.r.t. sampling step τ than the state feedback controller 3-CTA but with different coefficients Δ_i; $i = 1, ..., 4$.

5.4.1 Implementation of the 3-OFCTA in a magnetic levitator

The MLS (see Fig. 5.7) is a nonlinear, open loop unstable, time-varying, and dynamical system where a plate of magnetic material is suspended by means of the electromagnetic force produced by a coil.

Following [Khalil, 2002], a state space model of MLS is given by

$$\begin{aligned} \dot{x}_1 &= x_2, \\ \dot{x}_2 &= -\tfrac{k}{M} x_2 + \tfrac{aL_0}{2M} \tfrac{x_3^2}{(a+x_1)^2} - g, \\ \dot{x}_3 &= \tfrac{1}{L(x_1)} \left(-Rx_3 - aL_0 \tfrac{x_2 x_3}{(a+x_1)^2} + u \right), \end{aligned} \tag{5.19}$$

where x_1, x_2, x_3 represent the plate's position in $[m]$, velocity in $[\frac{m}{s}]$ and coil current in $[A]$, respectively, and u is the control input (voltage applied to coil). Furthermore, $M > 0$ is the mass of the

(a) This picture is taken from the ECP's website: http://www.ecpsystems.com/controls _maglevit.htm.

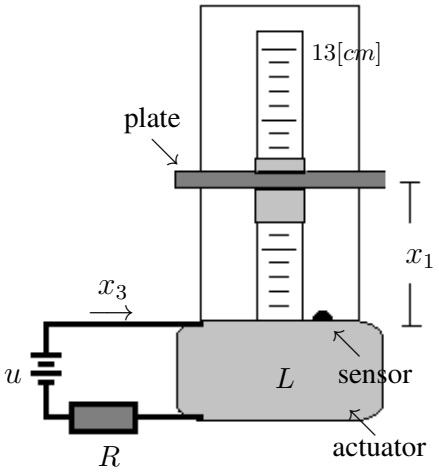

(b) x_1-plate position, x_2-plate velocity, and x_3-coil current

Figure 5.7: Magnetic Levitation System.

plate, $g > 0$ is the gravity acceleration, $k > 0$ is a viscous friction coefficient, $R > 0$ is the electric resistance, and $L(x_1) = L_1 + \frac{aL_0}{a+x_1}$ is the coil inductance, which is a function of the plate position, where a, L_0, L_1 are positive constants (see Fig. 5.7). The parameters values (obtained from the manufacturer) are presented in Table 5.3.

Parameter.	**Values.**	**Parameter.**	**Values.**
M	0.1203 $[kg]$	g	9.815 $[\frac{m}{s^2}]$
k	0.01 $[\frac{N\cdot}{s}m]$	L_1	0.1 $[H]$
L_0	0.245 $[H]$	a	0.0088 $[m]$
R	1.75 $[\Omega]$		

Table 5.3: List of parameters of the Magnetic Levitation System.

The physical setup contains an optical sensor to measure the plate position x_1. So, the control objective is that x_1 tracks the time-varying reference:

$$r(t) \quad = \quad 0.01 \sin(t) + 0.022[\text{m}]. \tag{5.20}$$

For $x_1 \geq 0$ and $x_3 \geq 0$, applying the diffeomorphism

$$\sigma_1 = x_1, \qquad \sigma_2 = x_2, \qquad \sigma_3 = -\frac{k}{M}x_2 + \frac{aL_0}{2M}\frac{x_3^2}{(a+x_1)^2} - g,$$

to the system (5.19) , we obtain

$$\dot{\sigma}_1 = \sigma_2, \qquad \dot{\sigma}_2 = \sigma_3, \qquad \dot{\sigma}_3 = f(\sigma) + g(\sigma)u, \tag{5.21}$$

where

$$f(\sigma) = \frac{k^2}{M^2}\sigma_2 + \frac{kg}{M} - 2\left(\frac{R}{L(\sigma_1)} + \frac{k}{2M} + \frac{\sigma_2}{a+\sigma_1} + \frac{aL_0\sigma_2}{L(\sigma_1)(a+\sigma_1)^2}\right) \times \left(\sigma_3 + \frac{k}{M}\sigma_2 + g\right),$$

and

$$g(\sigma) = \frac{\left(2aL_0\left(\sigma_3 + \frac{k}{M}\sigma_2 + g\right)\right)^{\frac{1}{2}}}{M^{\frac{1}{2}}L(\sigma_1)(a+\sigma_1)}.$$

Now, define the tracking errors $e_1 = \sigma_1 - r(t)$, $e_2 = \sigma_2 - \dot{r}(t)$, and $e_3 = \sigma_3 - \ddot{r}(t)$, whose dynamics is given by

$$\dot{e}_1 = e_2, \qquad \dot{e}_2 = e_3, \qquad \dot{e}_3 = f(\sigma) + g(\sigma)u - r^{(3)}(t)\,, \tag{5.22}$$

such that, by applying the feedback linearization

$$u = g(\sigma)^{-1}\left(v - f(\sigma)\right), \tag{5.23}$$

where v is the new control variable, we obtain

$$\dot{e}_1 = e_2, \qquad \dot{e}_2 = e_3, \qquad \dot{e}_3 = v + \phi(t)\,, \tag{5.24}$$

where $\phi(t)$ is a perturbation term, which includes external signals or model uncertainties. In our case, since $r^{(3)}(t)$ is not compensated, we have $\phi(t) = r^{(3)}(t) = -0.01\cos(t)$.

Simulation results

The objective of simulations is to show the theoretical properties of the 3-CTA and the 3-OFCTA to manage a MLS robustly and with high precision. The simulations were performed in Matlab Simulink with sampling step $\tau = 1[ms]$ for different numerical methods detailed below. The initial conditions are $x_0 = [0.01, 0, 0.58]^T$.

Tracking by 3-CTA: Fig. 5.8 shows the simulation results, using Dormand-Prince as integration method and $\tau = 1[ms]$, of a MLS in closed-loop with the 3-CTA. The gains were selected from the set D_1 in Table 5.1 and $L = 42$. We can see that the states x_1 and x_2 reach and keep the desired trajectory (5.20) in finite-time while x_3 remains bounded. Note that the control signal u is continuous and compensates the disturbance $r^{(3)}$.

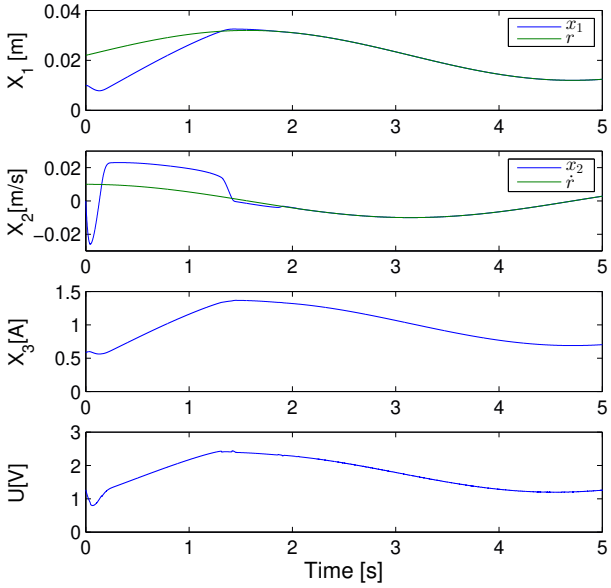

Figure 5.8: Simulation of tracking for MLS's plate position by means of 3-CTA.

Tracking by 3-OFCTA: Fig. 5.9 presents the simulation results, using Euler method and $\tau = 1[ms]$, of a MLS in closed-loop with the 3-OFCTA. The controller's gains were taken from the set D_1 in Table 5.1 and $L = 62$, while, for the observer the gains are

$$\lambda_1 = 4.5, \quad \lambda_2 = 2.4, \quad \lambda_3 = 0.8, \quad \lambda_4 = 0.1, \tag{5.25}$$

and $H = 1.5$. We can see that the states x_1 and x_2 follows the desired reference (5.20) while x_3 remains bounded. Note that the control signal u nullifies the tracking errors in finite-time by means of a continuous signal despite the presence of disturbance $r^{(3)}$. Moreover, the position error is the only information available to the controller while velocity and acceleration errors are estimated by the observer (5.17).

Precision test: 3-CTA vs 3-OFCTA

Fig. 5.10 presents the bound of the tracking errors in steady state when the MLS is driven by the 3-CTA. According to the sliding order of the closed-loop system (5.6)-(5.7), the accuracy provided by the 3-CTA is given by inequalities (5.8) where for a sampling time of $\tau = 1[ms]$ the constants Δ_i are:

$$\Delta_1 = 220, \qquad \Delta_2 = 105, \qquad \Delta_3 = 196$$

. Moreover, the independence of constants Δ_i w.r.t. sampling step τ is confirmed by the bound of the tracking errors (also presented in Fig. 5.10) when the simulation is performed with $\tau = 0.1[ms]$. On the other hand, Fig. 5.11 presents the bound of the tracking errors in steady state when the MLS

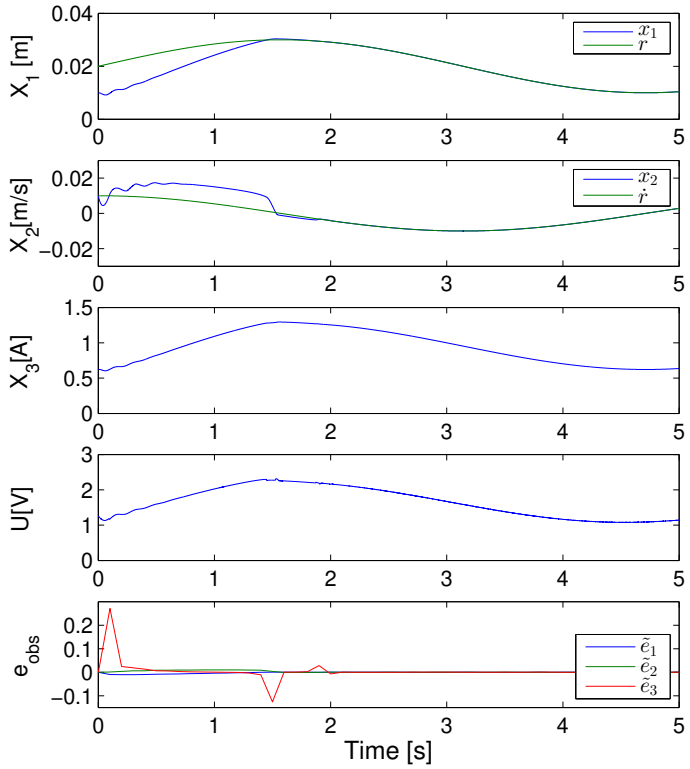

Figure 5.9: Simulation of tracking for MLS's plate position by means of 3-OFCTA.

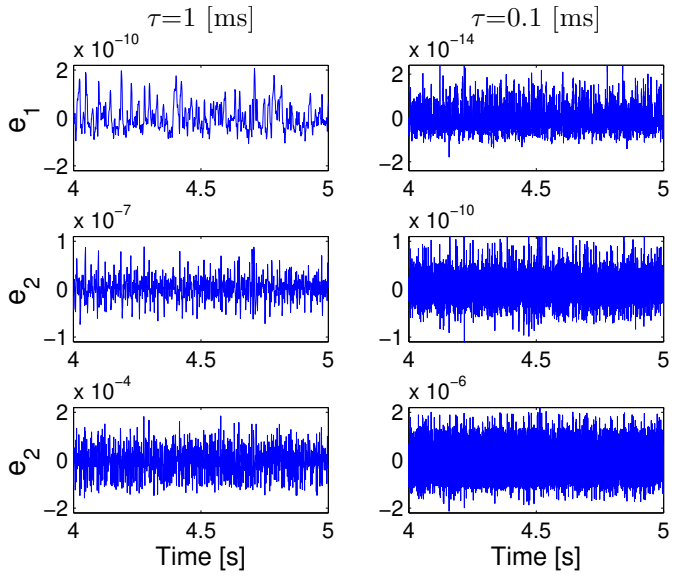

Figure 5.10: Precision test in tracking errors for 3-CTA.

is driven by the 3-OFCTA. According to the sliding order of closed-loop system (5.6)-(5.18), the accuracy provided by the 3-OFCTA is given by (5.8), and for a sampling time $\tau = 1[ms]$ the constants Δ_i are:

$$\Delta_1 = 510, \qquad \Delta_2 = 365, \qquad \Delta_3 = 350.$$

Moreover, when the simulation is performed with $\tau = 0.1[ms]$, the bound of the tracking errors (also presented in Fig. 5.11) confirmed the independence of constants Δ_i w.r.t. sampling step τ.

The theoretical accuracy (5.8) is validated for the 3-CTA and the 3-OFCTA by numerical simulations, where both differentiator and controller are discretized in the same computer chip with the same sampling step τ.

As we have said in Remark 5.3, the incorporation of the observer (5.17) in the control scheme does not change the accuracy orders of the trajectories of the closed-loop system. However, the constants Δ_i are a bigger for the case of the 3-OFCTA as it is expected for a more complex algorithm.

Experimental results: tracking via 3-OFCTA

Considering $\sigma = x_1$ (the plate position) as the only measurable output of the MLS, this experiment aims to show the effectiveness of the output feedback controller 3-OFCTA to make the plate position track the sinusoidal trajectory (5.20), robustly and with high precision .

The experimental setup consists of two parts:

- The magnetic levitation system (ECP model 730 depicted in Fig. 5.7), which includes laser sensors and a high magnetic flux coil .

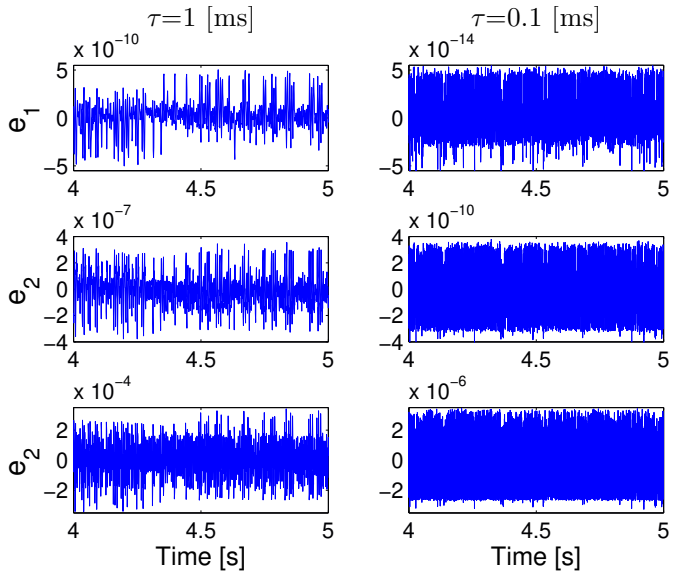

Figure 5.11: Precision test in tracking errors for 3-OFCTA.

- A PC with DSP board, ECP software and Simulink Matlab with the real-time toolbox.

A SISO version of the ECP model 730 is constructed with a single magnet managed by the repulsive force produced by the lower actuator. The measurable output of ECP model 730 is the plate position given by the lower laser sensor. Moreover, for discretization we use the Euler integration method with sampling step $\tau = 1[ms]$.

Fig. 5.12 shows the experimental results of the implementation of the 3-OFCTA in the MLS through the output feedback linearization (5.23). The nominal values of the parameters of the system ECP model 730 are given by the manufacturer (see Table 5.3). Moreover, the gains for the 3-OFCTA (5.18) are given by

$$\begin{aligned} k_1 &= 1.7, \quad k_2 = 3.2, \quad k_3 = 4.1, \quad k_4 = 0.9, \\ k_5 &= 0.4, \quad k_6 = 0.1, \quad L = 1150, \end{aligned} \tag{5.26}$$

for the controller (5.7), and the gains in (5.25) with H=1800, for the observer (5.17). Both sets of gains was adjusted experimentally in order to get a good performance.

We can see in Fig. 5.12 that the plate position x_1 tracks the sinusoidal trajectory with high precision, the plate velocity x_2 tracks the reference derivative, the coil current x_3 is bounded and control signal u is continuous despite of the presence of high-frequency oscillations. Furthermore, the actuator is protected by a saturation but the control signal does not exceed the saturation limits.

The smoothness of the measurements for the plate position x_1 and the coil current x_3 in Fig. 5.12 is a consequence of the high resolution of the optical sensor and the high magnetic flux actuator. Moreover, note in Fig. 5.13 that the plots of e_1, e_2 and e_3 present high-frequency oscillations due to they are estimated by means of the discontinuous observer (5.17).

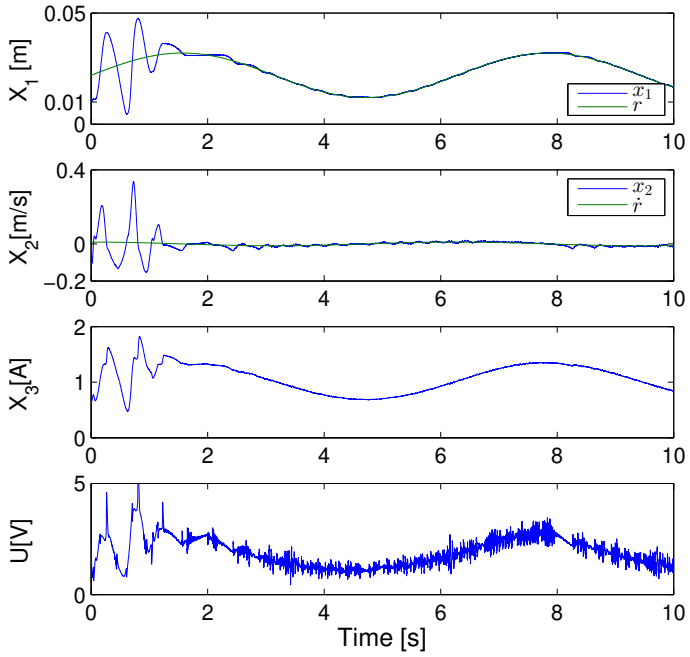

Figure 5.12: Tracking for plate position of a MLS via 3-OFCTA.

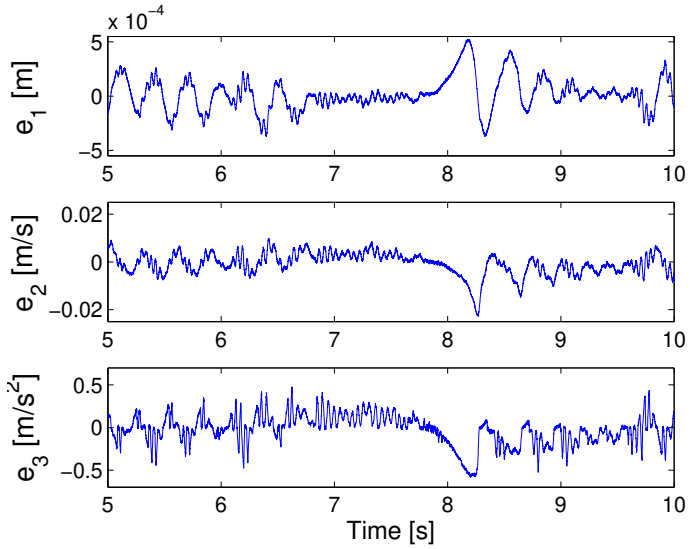

Figure 5.13: Tracking errors in steady state for position (e_1), velocity (e_2) and acceleration (e_3) of the MLS driven by 3-OFCTA.

Despite of the chattering caused by the discretization and the lack of finite-time convergence, we can observed the effectiveness of the 3-OFCTA to managed a physical system with robustness against perturbations and model uncertainties (as e.g. friction between the plate and the stab). In Fig. 5.13, we can appreciate the accuracy in steady state of the tracking for position, velocity and acceleration of the MLS. Note that the position error is more or less 5×10^{-4} [m], and this represents a deviation of 5% w.r.t. the reference, which varies 0.01 [m] around the point 0.022 [m].

5.5 Conclusion

For a third-order chain of integrators affected by Lipschitz-continuous non-vanishing and matched disturbances, three schemes of control were presented. The first one is a state feedback controller 3-CTA which is able to provide, in theory, finite-time convergence to zero, exact compensation of the considered perturbations, and precision in the steady state of fourth order w.r.t. sampling step for the system's output.

The second one an adaptive controller 3-ACTA where the adaptive gain adjusts its value automatically until the stability of the closed-loop system is assured for all future time despite the presence of perturbation in the considered class. The main advantages of the 3-ACTA are that the knowledge of the upper-bound of the perturbation's derivative is not required for gains design, and over-scaling of the gains is avoided, which reduce the amplitude of the chattering in the output. Moreover, experimental results of the implementation of 3-ACTA on an IWP were presented.

Finally, we introduced an output feedback controller 3-OFCTA which preserves, in theory, all features of robustness, convergence, and precision of the 3-CTA while requiring only information from the measurable output. Separation principle for 3-OFCTA is proven which allows the design of the gains for controller and observer, independently. Finally, experimental results of the implementation of 3-OFCTA in an MLS were presented where tracking of a sinusoidal trajectory for plate position is ensured.

Chapter 6

Design of a PID-like controller based on Discontinuous Integral Control

The classical Proportional-Integral–Derivative (PID) structure is the most employed controller in industrial processes. Some of the main advantages of the classical PID are their simplicity, suitable performance for "slow-dynamics" processes, and the availability of tuning rules like the methods of [Ziegler and Nichols, 1942] or [Aström and Hägglund, 2005]. The integral action provides the asymptotic rejection of constant disturbances, nullifying the steady–state error for constant set points. For first-order systems, the PI control place the closed-loop eigenvalues in desired positions of the complex plane, ensuring exponential stability and compensation of constant perturbations. For second-order systems, the PD enforces exponential stability to the origin, and due to the integral action the PID is endowed with this property plus robustness against constant perturbations. PI, PD and PID can also be used for systems of higher order rest in the framework of dominant pole approximation. However, these controllers may have weak performance in presence of nonlinear effects (i.e. friction, hysteresis, backlash) and/or fast time-varying set–points and perturbations.

Continuous Higher-Order Sliding Mode (CHOSM) controllers are structurally efficient to deal with systems affected by non-vanishing Lipschitz-continuous time-varying perturbations, see for example the works in [Levant, 1993, Moreno, 2016, Kamal et al., 2016, Torres-González et al., 2017, Laghrouche et al., 2017, Mendoza-Avila et al., 2020b, Mercado-Uribe and Moreno, 2020]. The well-known Super-Twisting Algorithm [Levant, 1993] belongs to the family of second-order CHOSM controllers and has a PI structure. This allows to establish tuning rules of its parameters in order to obtain pre–specified frequency and amplitude of the chattering generated by the presence of fast-actuators and delays in the control loop making the relative degree of the plant higher than one, for example see the proposals of [Boiko and Fridman, 2005, Pilloni et al., 2012a, Pilloni et al., 2012b]. A similar methodology was proposed by [Pérez-Ventura and Fridman, 2019], minimizing the amplitude of chattering and the average power needed to maintain the trajectories into real sliding-modes.

Continuous Terminal Algorithm [Fridman et al., 2015, Kamal et al., 2016], Discontinuous Integral Controller (DIC) [Moreno, 2016, Moreno, 2018], and Continuous Twisting Algorithm (CTA)

[Torres-González et al., 2017] were designed to drive the trajectories of disturbed second-order systems, in the form of a double integrator and affected by non-vanishing Lipschitz-continuous time-varying matched perturbations, to the origin in finite-time. They enforce a third-order sliding mode, i.e., the output and its first and second time-derivatives are nullified in finite-time, while the control signal convergences to the opposite value of perturbations in finite-time, as well. These CHOSM controllers provides, in the absence of measurement noises, sliding-accuracy proportional to cubic degree of the sampling step h for the output, proportional to quadratic degree of h for the output's first time-derivative, and proportional to h for the rejection of perturbations.

Stability proofs for the aforementioned CHOSM controllers are based on homogeneous polynomial Lyapunov function (LF) (see [Moreno, 2016, Torres-González et al., 2017, Moreno, 2018]). It results in the general case, the needing to solve bilinear inequalities that appeared when the coefficients of the LF and the controller gains are computed to guarantee the positive definiteness of the LF and the negative definiteness of its time-derivative. However, there is not any criteria of optimization for selecting that gains, besides Lyapunov-based designs leads to an overestimation of the gains, which affects the performance of the closed-loop system. All this reasons makes difficult the practical implementation of these CHOSM controllers.

Commonly, engineers are accustomed to work with PID control structures where the gains are chosen from several criteria depending on the parasitic dynamics which are neglected in the model like delays, actuators, sensors, hysteresis, etc. See for example [Ziegler and Nichols, 1942, Boiko, 2014b, Aström and Hägglund, 2005, Boiko et al., 2006, Pilloni et al., 2012a, Pilloni et al., 2012b]. In this chapter, the Continuous Sliding Mode Controller in the PID form (PID-CSMC) (originally introduced by [Zamora et al., 2013]) and a Homogeneous controller in the PD form (PD-HC), which coincides with the static part of the PID-CSMC, are considered. The first one has three gains to be selected, which are directly related to the error signal in proportional, integral and derivative ways, which implies a synergy relation with the conventional PID. Whereas, the second one has only two gains, which are related to nonlinear functions of the error signal and its first time-derivative, respectively, in a similar way than the classical PD. Indeed, the nonlinearities in the PID-CSMC and the PD-HC permit to overcome the features of the classical PID and PD, respectively, because finite-time stability and exact compensation of certain class of time-varying perturbations can be guaranteed, in theory. Nevertheless, despite the PID-CSMC and the PD-HC generate a continuous control signal, the chattering phenomena arise whenever applied to linear plants of relative greater than two [Pérez-Ventura and Fridman, 2019].

Considering a cascade connection of a perturbed second-order chain of integrators and a critically-damped second-order fast-actuator, we are proposing a frequency domain based criteria to design the PID-CSMC and the PD-HC gains in order to minimize the amplitude of chattering and the average power needed to maintain the trajectories in a real sliding mode. Additionally, for the perturbed second-order chain of integrators controlled by the PID-CSMC or the PD-HC with designed gains, stability at the origin is studied by means of homogeneous polynomial LF. On the other hand, in the presence of a critically-damped second-order fast-actuator , the Loeb's criterion allows to show that if the predicted oscillations arise, then the proposed design ensures their Orbital Asymptotic Stability (OAS).

The structure of this chapter is as follows: Section 6.1 presents some important definition and

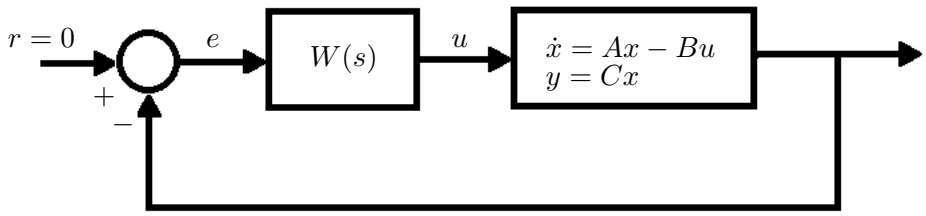

Figure 6.1: Block diagram of a system for DF analysis.

preliminaries results. The methodology to design the gains of the PID-CSMC in provided in Section 6.2. The PD-HC and is design are presented in Section 6.3. Finally, the conclusions are summarized in Section 6.4.

6.1 Preliminaries

6.1.1 Describing Function Approach

The Describing Function (DF) approach provides a simple and fairly precise method to find a possible periodic solution in nonlinear dynamical systems. This method is limited to system that can be separated in a static nonlinearity and a linear time-invariant differential equation, which are interconnected in a closed-loop (see Fig. 6.1). Moreover, the linear system must have low-pass filter characteristics such that the input to the nonlinearity can be well approximated by its main harmonics [Boiko, 2009].

The DF of the non-linearity $u(t)$ is defined as the first-harmonic of the Fourier's series of the periodic control $u(t)$ divided by the amplitude A of the possible oscillation [Boiko, 2009], i.e.,

$$N(A,\omega) = \frac{\omega}{\pi A}\left(\int_0^{\frac{2\pi}{\omega}} u(t)\sin(\omega t)\mathrm{d}t + j\int_0^{\frac{2\pi}{\omega}} u(t)\cos(\omega t)\mathrm{d}t\right). \tag{6.1}$$

Parameters of amplitude A and frequency ω of a possible periodic solution can be predicted by solving the Harmonic Balance (HB) equation

$$N(A,\omega)W(j\omega) = -1\,. \tag{6.2}$$

(see more details in [Atherton, 1975, Gelb and Vander Velde, 1968]). In other words, the parameter of a possible oscillation can be found in the intersection point of the Nyquist plot $W(j\omega)$ and the negative reciprocal of the DF $N(A,\omega)$ [Boiko, 2009].

Usually, the DF approach is used to predict the parameters of the main harmonic approximation of chattering caused by the presence of parasitic dynamics in non-smooth control systems [Atherton, 1975, Gelb and Vander Velde, 1968, Boiko, 2009, Boiko, 2018, Utkin, 2016].

6.1.2 Average Power

Consider a mechanical system, accordingly, $x_1(t)$ represents the position and $x_2(t)$ represents the velocity. Assume that the trajectories converge to an oscillatory behavior $x_1(t) = A\sin(\omega t)$ and $x_2(t) = A\omega\cos(\omega t)$. So, the (kinetic) energy of the oscillations is proportional to the square of the velocity, i.e., $e(t) \propto x_2^2(t)$. Thus, average power in a period $T = \frac{2\pi}{\omega}$ of the oscillation is given by

$$P = \frac{1}{T}\int_0^T e(t)dt = \frac{\omega}{2\pi}\int_0^{\frac{2\pi}{\omega}} \Big(A\omega\cos(\omega t)\Big)^2 dt = \frac{A^2\omega^2}{2}\,, \tag{6.3}$$

6.1.3 Loeb's stability criterion

The stability of an oscillatory state is presented in terms of quasi-static disturbances in amplitude and frequency of the predicted oscillations. So, a limit cycle is stable if it returns to its original equilibrium state, on the contrary, if its amplitude or frequency increases or decays then it is unstable [Gelb and Vander Velde, 1968].

The Loeb's stability criterion [Loeb, 1956] claims that if a system has periodic solution satisfying equation (6.2), then the following inequality should be satisfied for a stable oscillatory regime,

$$\frac{\partial U}{\partial A}\frac{\partial V}{\partial \omega} - \frac{\partial U}{\partial \omega}\frac{\partial V}{\partial A} > 0\,, \tag{6.4}$$

with

$$U(A,\omega) = \mathrm{Re}\{N(A,\omega) + W(j\omega)^{-1}\}\,,\quad V(A,\omega) = \mathrm{Im}\{N(A,\omega) + W(j\omega)^{-1}\}\,, \tag{6.5}$$

and it is unstable in any other case.

6.2 The Continuous Sliding-Mode Controller in PID form

Consider a process modeled by a perturbed double integrator:

$$\begin{array}{rcl} \dot{x}_1(t) &=& x_2(t)\,, \\ \dot{x}_2(t) &=& f(t) + u(t)\,, \end{array} \tag{6.6}$$

with $x_1(t)$ as the output and $u(t)$ as the control input. The disturbance term $f(t)$ is assumed Lipschitz-continuous, i.e., $|\dot{f}(t)| \leq L$ with a known upper-bound $L > 0$. Also, the measurements of the states $x_1(t)$ and $x_2(t)$ are available for all $t \geq 0$. For readability sake, the variable t will be omitted in the sequel.

The Continuous Sliding-Mode Controller in PID form (PID-CSMC),

$$\begin{array}{rcl} u &=& -k_1\lceil x_1\rfloor^{1/3} - k_2\lceil x_2\rfloor^{1/2} + v\,, \\ \dot{v} &=& -k_3\lceil x_1\rfloor^{0}\,, \end{array} \tag{6.7}$$

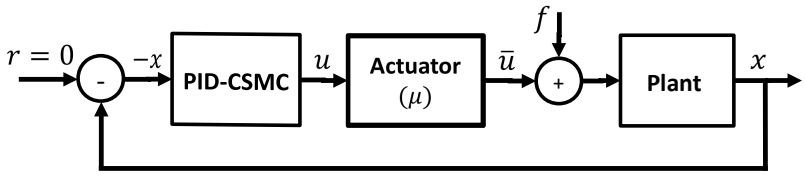

Figure 6.2: The PID-CSMC input is transferred to the plant through an actuator.

with properly designed gains $k_1, k_2, k_3 > 0$, ensures the finite-time stability to the origin of the closed-loop system

$$\begin{aligned} \dot{x}_1 &= x_2\,, \\ \dot{x}_2 &= -k_1\lceil x_1\rfloor^{1/3} - k_2\lceil x_2\rfloor^{1/2} + x_3\,, \\ \dot{x}_3 &= -k_3\lceil x_1\rfloor^{0} + \dot{f}\,. \end{aligned} \tag{6.8}$$

where $x_3 = f + v$ is an extended state due to the integral controller. Note that the PID-CSMC (6.7) is a simplified version of the CTA [Torres-González et al., 2017] and the DIC [Moreno, 2018]. From now on, the closed-loop system (6.8) will be called the ideal model due to the conditions established in the following theorem.

Theorem 6.1. *[Torres-González et al., 2017, Moreno, 2018] Consider the system (6.6) with a Lipschitz-continuous perturbation $f(t)$ with a Lipschitz constant L. Then, for an appropriated design of the gains k_1, k_2, k_3, the control law (6.7) stabilizes the origin of the ideal model (6.8) in finite-time.*

Remark 6.1. If the gains $k_1 = \lambda_1, k_2 = \lambda_2$ and $k_3 = \lambda_3$ with constants $\lambda_1, \lambda_2, \lambda_3 > 0$, ensure the finite-time stability of the ideal model (6.8), with a perturbation with a Lipschitz constant $L > 0$. Then, for an arbitrary $\Delta > 0$, the gains $k_1 = \lambda_1\Delta^{2/3}$, $k_2 = \lambda_2\Delta^{1/2}$ and $k_3 = \lambda_3\Delta$ ensure the finite-time stability of the ideal model (6.8), when it is affected by a perturbation with Lipschitz constant $L\Delta$.

There are reported in the literature several sets of gains for the PID-CSMC that ensure finite-time stabilization of the trajectories of the closed-loop system (6.8), see for example [Moreno, 2016, Torres-González et al., 2017, Moreno, 2018, Zamora et al., 2013]. However, there are not a criteria for selecting the gains from such sets other than guarantee the stability in the Lyapunov sense. However, it is a well known fact that methods of design based on LF leads to an overestimation of the gains, which can deteriorate the performance of the controller. Also, the Lyapunov-based design implies the solution of a larger set of matrix inequalities, where both the control gains and the coefficients of the LF must be found. These problems can be understood as bi-linear inequalities due to products of such gains and parameters appear in the time-derivative of the LF.

6.2.1 Real sliding modes

The presence of parasitic dynamics in the control system deteriorates the ideal properties of the PID-CSMC closed-loop (6.8), so that *chattering* may appear [Boiko, 2009, Utkin, 2016]. This behavior is

so-called *real* sliding mode [Fridman, 1999, Levant, 2010]. As shown in Fig. 6.2, the control signal is transferred to the plant (6.6) through an actuator, hence a more accurate model for this process is given by

$$\begin{aligned} \dot{x}_1 &= x_2\,, \\ \dot{x}_2 &= f + \bar{u}\,, \\ \mu\dot{z} &= g(z,u)\,, \quad \bar{u} = h(z)\,, \end{aligned} \tag{6.9}$$

where $z \in \mathbb{R}^m$ is the actuator state, $\bar{u} \in \mathbb{R}$ is the output of the actuator and $u \in \mathbb{R}$ is the control input defined by the PID-CSMC (6.7). The actuator dynamics is assumed stable, such that, for small values of the actuator's time-constant $\mu > 0$ the output $\bar{u}$ uniformly tends to the control input u. Any *stable* transfer function $G_a(s)$ with $G_a(0) = 1$ can be taken as a linearized model of the actuator dynamics in (6.9) [Levant, 2010].

Previous designs of PID-CSMC use reduced-order models of the plant which take into account only its main dynamics and neglect the parasitic ones. However, in real implementations the presence of unmodeled dynamics deteriorates the ideal properties of the closed-loop system (6.8). For instance, if the gains k_1, k_2 and k_3 of the PID-CSMC are designed to enforce an *ideal* sliding mode in the closed-loop (6.8), then, they are able to generate a *real* sliding mode in the presence of an actuator. In the latter case, the properties of finite-time convergence and insensibility w.r.t. disturbances are meaningless because the system trajectories exhibit *chattering* in steady state and a propagation of the low frequency disturbance (see [Boiko, 2009]), even when CHOSM controllers are used (see [Pérez-Ventura and Fridman, 2019, Boiko and Fridman, 2005, Pilloni et al., 2012a, Pilloni et al., 2012b, Utkin, 2016]).

6.2.2 Description of the system

The plant (6.6) can be expressed in a transfer function form as $G(s) = 1/s^2$. In addition, by following [Boiko and Fridman, 2005, Utkin, 2016, Pérez-Ventura and Fridman, 2019], let's consider a critically damped second-order actuator $G_a(s) = 1/(\mu s+1)^2$, where the small parameter $\mu > 0$ is the actuator's time-constant. Therefore, the actuator-plant cascade connection has the form

$$W(s) = G_a(s)G(s) = \frac{1}{s^2(\mu s + 1)^2}\,. \tag{6.10}$$

6.2.3 Sliding accuracy of the PID-CSMC

The sliding accuracy (level of chattering) is used to evaluate the performance of the closed-loop system (6.8) in steady state. For instance, in [Levant and Fridman, 2010] the sliding accuracy of n-th order discontinuous SMC w.r.t. the time-constant $\mu > 0$ was reported as $|x_1| < \gamma_1\mu^{r_1}$, $|x_2| < \gamma_2\mu^{r_2}, \ldots, |x_n| < \gamma_n\mu^{r_n}$ where $\gamma_i > 0$ are constants and r_i; $i = 1, \ldots, n$ are the homogeneity degree of the corresponding variable (see Chapter 2 for details about a homogeneity concepts). In the following, for the system (6.9) in closed-loop with the PID-CSMC (6.7) the coefficients $\gamma_i > 0$ of the real sliding mode are computed by using the DF approach.

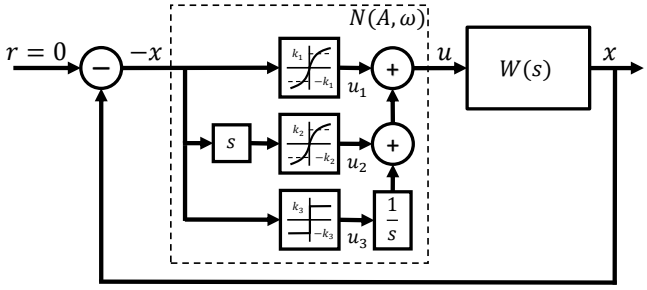

Figure 6.3: Diagram for DF of the PID-CSMC.

Proposition 6.1. *Let the actuator-plant model (6.10) have low-pass filter properties and the actuator time-constant $\mu > 0$ be small. The PID-CSMC (6.7) is able to provide sliding accuracy, w.r.t. the time-constant μ, of third and second order for the output x_1 and its time-derivative x_2, respectively, i.e.,*

$$|x_1| = \Delta \left(\frac{2\alpha_1 \lambda_1}{\pi \mathbb{K}^2 (1-\mathbb{K}^2)} \right)^{3/2} \mu^3 , \qquad |x_2| = \Delta \left(\frac{2\alpha_1 \lambda_1}{\pi \mathbb{K}^{\frac{4}{3}} (1-\mathbb{K}^2)} \right)^{3/2} \mu^2 , \tag{6.11}$$

where the parameter $\mathbb{K} \in (0,\, 1)$ is the solution of the non-linear equation,

$$2\mathbb{K}\lambda_1^{3/2} - (1-\mathbb{K}^2)^{3/4} \lambda_2 \lambda_1^{3/4} + (1-\mathbb{K}^2)^{3/2} \lambda_3 = 0 , \tag{6.12}$$

where $\lambda_1, \lambda_2, \lambda_3 > 0$ and $\Delta > 0$ are the parameters of the PID-CSMC, and $\alpha_1 \approx 1.821$ and $\alpha_2 \approx 1.748$ are the coefficients of the main-harmonic of the Fourier's series.

Proof. Recall that the actuator-plant dynamics (6.9) is assumed to have low-pass filter characteristics [Atherton, 1975, Gelb and Vander Velde, 1968], i.e., if $W(j\omega)$ is a linearized model of the actuator-plant dynamics (6.9), then $|W(j\omega)| >> |W(jn\omega)|$, for $n = 2, 3, ...$ where ω is the frequency of self-excited oscillations. Thus, a well approximation of the steady-state response of the closed-loop system (6.9)-(6.7) is given by its first-harmonic, i.e.,

$$\begin{array}{rcl} x_1(t) & \approx & A\sin(\omega t) \\ x_2(t) & \approx & A\omega\cos(\omega t) \end{array} \tag{6.13}$$

where A is the amplitude and ω the frequency. These parameters of the periodic motion (6.13) can be found by solving the HB equation (6.2).

Now, following the methodology of [Pérez-Ventura and Fridman, 2019] the DF of the PID-CSMC is given by

$$N(A,\omega) = \frac{2\alpha_1 k_1}{\pi A^{2/3}} + j\frac{2\alpha_2 k_2 \omega^{1/2}}{\pi A^{1/2}} + \left(\frac{4k_3}{\pi A}\right)\left(\frac{1}{j\omega}\right) , \tag{6.14}$$

where $\alpha_1 \approx 1.821$, $\alpha_2 \approx 1.748$ are the coefficients of the first-harmonic of the Fourier's series.

The HB equation (6.2) for the actuator-plant model (6.10) and the DF (6.14) can be rewritten as

$$\frac{2\alpha_1 k_1}{\pi A^{2/3}} + j\left(\frac{2\alpha_2 k_2 \omega^{1/2}}{\pi A^{1/2}} - \frac{4k_3}{\pi A\omega}\right) = \omega^2\left(1-\mu^2\,\omega^2\right) + j2\,\mu\,\omega^3\,. \tag{6.15}$$

If the amplitude A is cleared from the real part of (6.15) and substituted into the imaginary one, the following expression is obtained

$$\frac{\alpha_2 k_2}{\pi^{1/4}(2\alpha_1 k_1)^{3/4}}(1-\mu^2\omega^2)^{3/4} - \frac{2\pi^{1/2}k_3}{(2\alpha_1 k_1)^{3/2}}(1-\mu^2\omega^2)^{3/2} = \mu\omega\,. \tag{6.16}$$

Note that (6.16) can be rewritten as (6.12) using $k_1 = \lambda_1\Delta^{2/3}$, $k_2 = \lambda_2\Delta^{1/2}$, $k_3 = \lambda_3\Delta$ and $\mathbb{K} = \mu\omega$. Hence, from (6.15) the predicted chattering parameters are

$$A = \Delta\left(\frac{2\alpha_1\lambda_1}{\pi\mathbb{K}^2(1-\mathbb{K}^2)}\right)^{3/2}\mu^3\,, \tag{6.17}$$

$$\omega = \frac{\mathbb{K}}{\mu}\,. \tag{6.18}$$

Finally, substituting the parameters of amplitude (6.17) and frequency (6.18) into the main harmonic approximation (6.13), it is possible to derived the bounds (6.11). □

Note that similarly to [Levant and Fridman, 2010], Proposition 6.1 provides the sliding accuracy for the PID-CSMC trajectories in steady-state, where the level of chattering is proportional to the actuator time-constant powered by the homogeneity weight of the corresponding variable.

6.2.4 Stability of self-excited oscillations

Now, by means of the Loeb's criterion we are going to establish the conditions such that if the predicted oscillations (6.13) arise in the steady state response of the system (6.9) in closed-loop with the PID-CSMC (6.7), then they are going to be OAS.

Proposition 6.2. *Consider the actuator-plant model (6.10), with low-pass filter properties and a small actuator time-constant $\mu > 0$, in closed-loop with the PID-CSMC (6.7). For any $\Delta > 0$, the periodic solution (6.13) will be OAS if the inequality*

$$\lambda_1^{3/4} > \frac{3\mathbb{K}\left(1-\mathbb{K}^2\right)^{3/4}}{4\left(1+2\mathbb{K}^2\right)}\lambda_2\,, \tag{6.19}$$

holds, where $\mathbb{K} \in (0,\,1)$ is a solution of the non-linear equation (6.12), and $\lambda_1, \lambda_2, \lambda_3 \geq 0$ are the gains of the PID-CSMC.

Proof. Following the Loeb's criterion (see Section 6.1 for details), the real and imaginary parts of the HB equation (6.15) can be expressed as

$$U(A,\omega) = 2\alpha_1 k_1 A^{1/3}\omega + \pi A\omega^3(\mu^2\omega^2 - 1)\,,$$
$$V(A,\omega) = 2\alpha_2 k_2 A^{1/2}\omega^{3/2} - 4k_3 - 2\pi\mu A\omega^4\,,$$

and the partial derivatives w.r.t. A and ω are

$$\frac{\partial U}{\partial A} = \frac{2\alpha_1 k_1\omega}{3A^{2/3}} + \pi\omega^3(\mu^2\omega^2 - 1)\,, \qquad \frac{\partial U}{\partial \omega} = 2\alpha_1 k_1 A^{1/3} + \pi A\omega^2(5\mu^2\omega^2 - 3)\,,$$
$$\frac{\partial V}{\partial A} = \frac{\alpha_2 k_2\omega^{3/2}}{A^{1/2}} - 2\pi\mu\omega^4\,, \qquad \frac{\partial V}{\partial \omega} = 3\alpha_2 k_2 A^{1/2}\omega^{1/2} - 8\pi\mu A\omega^3\,.$$

Substituting this expressions in inequality (6.4), it is obtained

$$\pi A^{2/3}\omega^2(\mu^2\omega^2 + 1) - \alpha_2 k_2 A^{1/6}\omega^{3/2}\mu > \frac{2}{3}\alpha_1 k_1\,. \tag{6.20}$$

Finally, substituting the amplitude (6.17) and frequency (6.18) into (6.20), the condition (6.19) is derived and it must be fulfill to warranty an OAS periodic solution (6.13) in the steady state response of the system (6.9) in closed-loop with the PID-CSMC (6.7). □

6.2.5 Design of gains for the PID-CSMC

Here, the PID-CSMC gains are selected from a frequency domain approach, in a similar way as in the classical PID. So, we propose two criteria for selecting the PID-CSMC gains in order to minimize the upper-bounds (6.11), and this means to maximize the sliding accuracy provided by the controller.

Fig. 6.4 shows the amplitude of chattering (6.17) as a function of the PID-CSMC gains λ_1 and $\lambda_2 \in [1.5,\ 10]$, with a fixed gain $\lambda_3 = 1.1$. Note that the amplitude (6.17) can be minimized by a suitable selection of the PID-CSMC gains. For example, we can see in Fig. 6.4 (the plot on the right) that fixing the gain $\lambda_1 > 0$, there exist a gain $\lambda_2 > 0$ that minimize the function of amplitude of chattering (6.17).

Assuming that $\lambda_1 > 0$ and $\lambda_3 > 0$ are fixed, the term $\mathbb{K}^2\left(1 - \mathbb{K}^2\right)$, in the denominator of (6.17), has a maximum value if $\mathbb{K}^2 = 0.5$. Accordingly, it is a good idea to find the gain $\lambda_2 > 0$ in order to fix the solution of (6.12) as $\mathbb{K}^2 = 0.5$. Under this restriction, the equation (6.12) becomes

$$1.42\lambda_1^{3/2} - 0.595\lambda_2\lambda_1^{3/4} + 0.354\lambda_3 = 0\,, \tag{6.21}$$

from where it is derived

$$\lambda_2 = 2.387\frac{\lambda_1^{3/2} + 0.25\lambda_3}{\lambda_1^{3/4}}\,. \tag{6.22}$$

Moreover, the restriction (6.19) for $\mathbb{K}^2 = 0.5$ becomes

$$\lambda_1^{3/4} > 0.158\lambda_2\,, \tag{6.23}$$

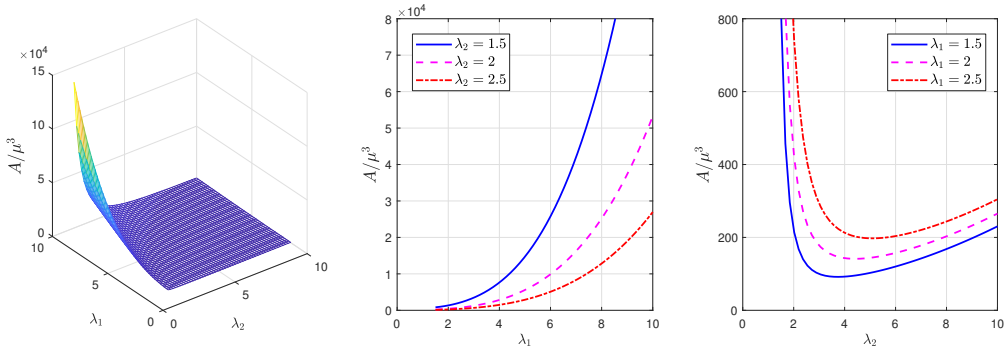

Figure 6.4: Amplitude of chattering in the steady-state response of the PID-CMSC closed-loop. **Left:** Amplitude behavior varying the gains λ_1 and λ_2. **Center:** Amplitude behavior varying the gain λ_1 and fixing λ_2 in different values. **Right:** Amplitude behavior varying the gain λ_2 and fixing λ_1 in different values. The gain $\lambda_3 = 1.1$ was chosen in all cases.

which must be satisfied in order to ensure an OAS periodic solution (6.13). From (6.22) and (6.23), it is derived

$$\lambda_1^{3/2} > 0.151\lambda_3. \tag{6.24}$$

Proposition 6.3. *Given the parameters $\lambda_1 > 0$ and $\lambda_3 > 0$ to fulfill (6.24), the value $\lambda_2 > 0$ minimizing the amplitude (6.17) is obtained from (6.22), such that, the triad λ_1, λ_2, λ_3 minimizes the amplitude (6.17) while ensures the stability of the predicted oscillations (6.13).*

On the other hand, we can select the gains of the PID-CSMC to minimize the (kinetic) energy needed to maintain the trajectories into a real sliding mode. Replacing the estimated parameters (6.17) and (6.18) in the average power (6.3), we obtain

$$P = \mu^4 \left(\frac{4(\alpha_1 k_1)^3}{\pi^3 \mathbb{K}^4 (1-\mathbb{K}^2)^3} \right) . \tag{6.25}$$

Note that the square root of (6.25) corresponds to the accuracy bound of $|x_2|$ in (6.11).

Similarly to the previous case, the average power (6.25) can be minimized by setting $\mathbb{K} \approx 0.6559$ such that $\mathbb{K}^4 \approx (1-\mathbb{K}^2)^3$. Substituting this value in equation (6.12), it is obtained

$$1.312\lambda_1^{3/2} - 0.656\lambda_2\lambda_1^{3/4} + 0.43\lambda_3 = 0\,, \tag{6.26}$$

from where it is derived

$$\lambda_2 = 2\frac{\lambda_1^{3/2} + 0.328\lambda_3}{\lambda_1^{3/4}}\,. \tag{6.27}$$

Moreover, the restriction (6.19) for $\mathbb{K} = 0.6559$ becomes

$$\lambda_1^{3/4} > 0.173\lambda_2\,, \tag{6.28}$$

which must be satisfied to ensure an OAS periodic solution (6.13). From (6.27) and (6.28), it is derived

$$\lambda_1^{3/2} > 0.174\lambda_3. \tag{6.29}$$

Proposition 6.4. *Given the parameters $\lambda_1 > 0$ and $\lambda_3 > 0$ to fulfill (6.29), the value $\lambda_2 > 0$ minimizing the average power (6.25) is obtained from (6.27), such that, the triad λ_1, λ_2, λ_3 minimizes the average power (6.25) while ensures the stability of predicted oscillations (6.13).*

Some examples of gains satisfying the statements of Propositions 6.3 and6.4 are provided by the sets D_1 and D_2 in Table 6.1, respectively.

6.2.6 Stability analysis of the ideal closed-loop

The sets of gains from Proposition 6.3 and 6.4 ensure an OAS periodic solution (6.13), while minimize the amplitude or the average power of chattering. However, such properties are verified only in the region where the approximation (6.13) of the steady-state response is valid. To ensure Global Asymptotic Stability (GAS) of the permanent oscillatory regime (6.13), it is sufficient to show that the ideal closed-loop system (6.8) possesses a kind of robustness against inputs (e.g., Input-to-State Stability (ISS) or $\mathbb{L}$-stability). To this end, the following lemma establishes the GAS of the origin of the closed-loop system (6.8).

Lemma 6.1. *Let the second-order system (6.6), with $|\dot{f}| < L$, in closed-loop with the PID-CSMC (6.7). For some gains λ_1, λ_2, λ_3 and $\Delta = 1$, there exist constants α_i; $i = 1, ..., 9$, such that,*

$$\begin{aligned} V(x) = \alpha_1|x_1|^{\frac{7}{3}} + \alpha_2|x_2|^{\frac{7}{2}} + \alpha_3|x_3|^7 + \alpha_4\lceil x_1\rfloor^{\frac{5}{3}}x_2 + \alpha_5|x_1|x_2^2 \\ + \alpha_6 x_1\lceil x_3\rfloor^4 + \alpha_7|x_1|^{\frac{5}{3}}x_3^2 + \alpha_8 x_2 x_3^5 + \alpha_9|x_2|^{\frac{3}{2}}x_3^4, \end{aligned} \tag{6.30}$$

is a LF for the closed-loop system (6.8).

The proof of Lemma 6.1 is presented in Section D.1 of Appendix D. So, the existence of a LF for the nominal system (6.8) ensures that it is asymptotically stable at the origin. Also, due to this system is r-homogeneous of negative degree $\nu = -1$, then it is endowed with a kind of ISS. Therefore, if Lemma 6.1 holds with a set of gains from Propositions 6.3 and6.4, then the proposed design works globally. Some examples of gains satisfying the statements of Lemma 6.1 are provided by the sets D_1 and D_2 in Table 6.1.

6.2.7 Summarizing the results

Since the gains in Table 6.1 satisfy Propositions 6.3 and 6.4, and Lemma 6.1, the following theorem is directly derived from these previous results.

Theorem 6.2. *Consider a second-order system in cascade connection with a critically damped actuator given by (6.9), with $|\dot{f}| < \bar{L}$ and a small time-constant $\mu > 0$. Given the parameters λ_1, λ_2, λ_3*

Set	λ_1	λ_2	λ_3
D_1	2.7	5.345	1.1
D_2	2.7	4.281	1.1

Table 6.1: Sets of gains for the PID-CSMC.

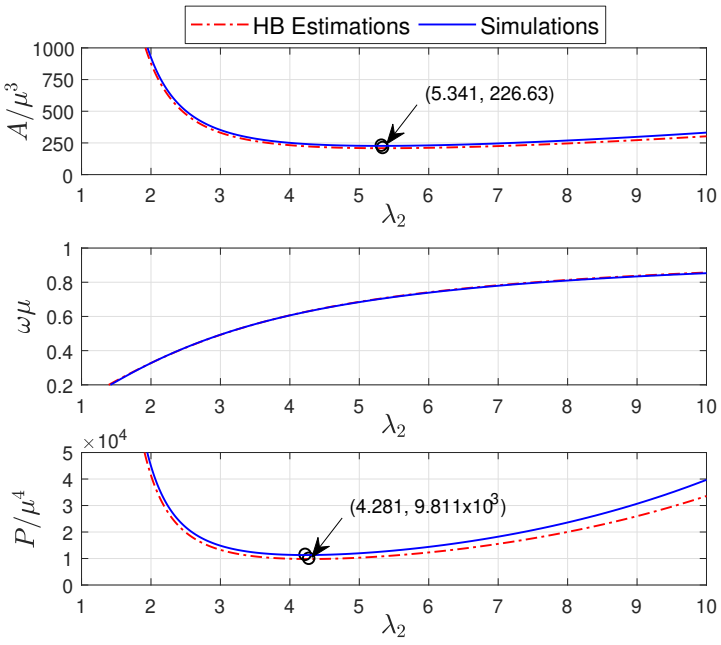

Figure 6.5: Normalized parameters: amplitude (6.17), frequency (6.18) and average power (6.25), for varying $k_2 \in [1\ \ 10]\Delta^{1/2}$ and fixing $k_1 = 2.7\Delta^{2/3}$, $k_3 = 1.1\Delta$, with $\Delta = 5$.

by the sets D_1 and D_2 in Table 6.1 and $\Delta > \frac{\bar{L}}{L}$ (for some $L > 0$), the PID-CSMC (6.7) is able to ensure that the system's trajectories converge to a permanent oscillatory regime, while minimize the amplitude (6.17) or the average power (6.25), respectively.

More suitable triads of the PID-CSMC gains λ_1, λ_2 and λ_3 that minimize the effects of chattering can be determined from Propositions 6.3 and 6.4. However, we need to check if the stability conditions of Lemma 6.1 hold, as well.

A numeric solution of the HB equation (6.15) for $\lambda_1 = 2.7$, $\lambda_3 = 1.1\Delta$ and several values of $\lambda_2 \in [1\ \ 10]$ is depicted by Fig. 6.5. It confirms that the suggested gains in Theorem 6.2 minimize the amplitude or the average power of chattering, respectively. Moreover, that result are supported by numerical simulation of the closed-loop system (6.9)-(6.7).

6.2.8 Numerical Tests

The simulations are performed in the following framework: the Euler's integration method with constant step $\tau = 10^{-4}$ is used to solve the closed-loop (6.9)-(6.7). Also, $\mu = 0.05$ is considered for the time-constant of the actuator dynamics in (6.10). Further, the upperbound $\Delta = 5$ is taken for simplicity.

Test 1: nominal behavior

Consider the unperturbed control system (6.9)-(6.7), with $f(t) = 0$. So, the steady-state response is only conformed by the oscillations caused by the parasitic dynamics in (6.10). Fig. 6.6 (on the left) shows the simulation of the system (6.9)-(6.7) with the gains $k_1 = 2.7\Delta^{2/3}$, $k_2 = 5.345\Delta^{1/2}$ and $k_3 = 1.1\Delta$, which are selected to minimize the amplitude of chattering according to Proposition 6.3. On the other hand, Fig. 6.6 (on the right) shows the simulation of the system (6.9)-(6.7) with the gains $k_1 = 2.7\Delta^{2/3}$, $k_2 = 4.281\Delta^{1/2}$ and $k_3 = 1.1\Delta$, which are chosen to minimize the energy needed to maintain the trajectories into a real sliding mode, according to Proposition 6.4. In both cases, we can see that increasing or decreasing the gain of k_2 from the critical value $k_{2_c} = 5.345\Delta^{1/2}$ or $k_{2_c} = 4.281\Delta^{1/2}$ lead to larger chattering amplitudes or energy needed to maintain the trajectories into a real sliding mode, respectively, validating the theoretical predictions.

Test 2: disturbed behavior

The disturbed response of the control system (6.9)-(6.7) contains a propagation of the perturbation term $f(t)$ due to the presence of an actuator [Gelb and Vander Velde, 1968, Boiko, 2009]. In general, we cannot expect for a periodic solution because it depends on the *shape* of the perturbations, e.g., slowly varying disturbances (w.r.t. the frequency of the oscillations generated by the actuator). A rigorous study of the perturbed case can be done via the so-called equivalent gains or dual-input DF's [Gelb and Vander Velde, 1968, West et al., 1956], but such analysis will be left as future work.

Just to illustrate this phenomenon, two perturbations are considered to show the sub-optimality of the proposed design of the PID-CSMC, a constant one $f(t) = 1$ and a sinusoidal one $f(t) = \sin(t)$. According to Proposition 6.3, the gains $k_1 = 2.7\Delta^{2/3}$, $k_2 = 5.345\Delta^{1/2}$ and $k_3 = 1.1\Delta$ minimize the amplitude of chattering. Fig. 6.7 (on the left) shows the simulation with a constant perturbation $f(t) = 1$ in the closed-loop (6.9)-(6.7) . Furthermore, Fig. 6.7 (on the right) shows simulations with a sinusoidal perturbation $f(t) = \sin(t)$ in the closed-loop (6.9)-(6.7). It can be seen that the fast-oscillations are mounted on slow-frequency components due to the propagation of the perturbation. In both cases, increasing or decreasing the value of k_2 from the critical one $k_{2_c} = 5.345\Delta^{1/2}$ lead to larger chattering amplitudes, validating the theoretical predictions, again.

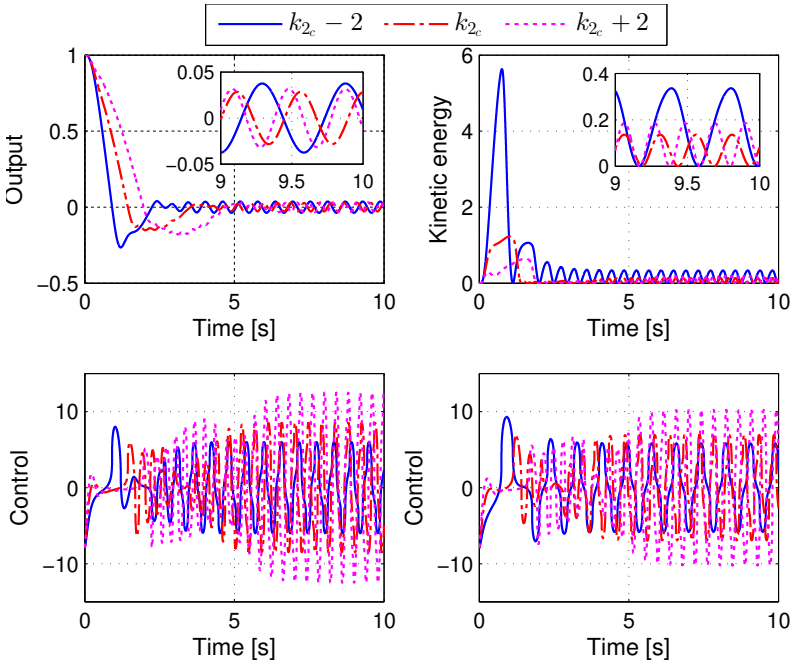

Figure 6.6: Response of the closed-loop system (6.9)-(6.7) for different values of k_2 around the critical gain k_{2_c}. Left: minimizing the chattering amplitude. Right: minimizing the energy needed to maintain the trajectories into a real sliding mode.

6.3 An homogeneous controller in PD form

Consider again the system (6.6). Now, let us introduce a homogeneous controller in PD form (PD-HC) given by

$$u = -k_1 \lceil x_1 \rfloor^{1/3} - k_2 \lceil x_2 \rfloor^{1/2}, \tag{6.31}$$

with gains $k_1, k_2, k_3 > 0$. In absence of perturbations, i.e., $f = 0$, this controller is able to provide finite-time stability to the origin of the closed-loop system

$$\begin{aligned} \dot{x}_1 &= x_2, \\ \dot{x}_2 &= -k_1 \lceil x_1 \rfloor^{1/3} - k_2 \lceil x_2 \rfloor^{1/2}. \end{aligned} \tag{6.32}$$

Remark 6.2. Note that the PD-HC lacks of any discontinuous term, so it is not able to enforce sliding mode to the trajectories of the closed-loop system (6.32). Nevertheless, this controller possesses an infinite gain near to the origin hence it is capable to provide finite-time convergence.

Remark 6.3. Similarly to the classical PD, the proposed controller if no able to reject perturbations. However, due to the homogeneity properties of the closed-loop system (6.32), it possesses a kind of ISS (see [Bernuau et al., 2013b]).

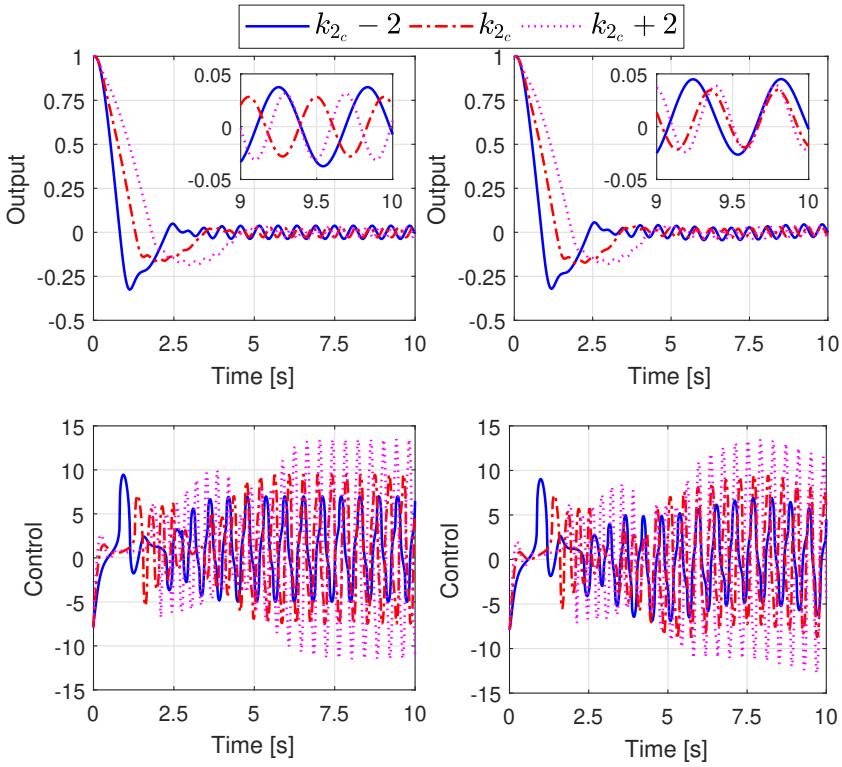

Figure 6.7: Response of the closed-loop system (6.9)-(6.7) in presence of perturbations for different values of k_2 around the critical gain $k_{2_c} = 5.345$. Left: a constant perturbation. Right: a sinusoidal perturbation.

Now, let's consider the system (6.9), which describes the control systems depicted by Fig. 6.2, where the control signal s supplied to the plant through an actuator. In this case, we cannot expect the finite-time convergence because the infinite gain of the PD-HC near to the origin cause the so-called chattering [Rosales et al., 2018] .

In the following, we aim to analyze the chattering generated by the PD-HC in the frequency domain, and propose a gain design to minimize the effect of this undesired phenomena in the control system.

6.3.1 Accuracy of the PD-HC

Recall that the actuator-plant dynamics (6.10) is assumed to have low-pass filter characteristics [Atherton, 1975, Gelb and Vander Velde, 1968]. Thus, the oscillatory regime (6.13) is a well approximation of the steady-state response of the closed-loop system (6.9)-(6.31).

Following the methodology of [Pérez-Ventura and Fridman, 2019] the DF of the PD-HC is given

by

$$N(A,\omega) = \frac{2\alpha_1 k_1}{\pi A^{2/3}} + j\frac{2\alpha_2 k_2 \omega^{1/2}}{\pi A^{1/2}}\,, \tag{6.33}$$

where $\alpha_1 \approx 1.821$, $\alpha_2 \approx 1.748$ are the coefficients of the first-harmonic of the Fourier's series.

The HB equation (6.2) for the actuator-plant model (6.10) and the DF (6.33) can be rewritten as

$$\frac{2\alpha_1 k_1}{\pi A^{2/3}} + j\frac{2\alpha_2 k_2 \omega^{1/2}}{\pi A^{1/2}} = \omega^2\,(1-\mu^2\,\omega^2) + j2\,\mu\,\omega^3\,. \tag{6.34}$$

If the amplitude A is cleared from the real part of (6.15) and substituted into the imaginary one, the following expression is obtained

$$\frac{\alpha_2 k_2}{\pi^{1/4}(2\alpha_1 k_1)^{3/4}}(1-\mu^2\omega^2)^{3/4} = \mu\omega\,. \tag{6.35}$$

Now, substituting $\alpha_1 \approx 1.821$, $\alpha_2 \approx 1.748$ $k_1 = \lambda_1\Delta^{2/3}$, $k_2 = \lambda_2\Delta^{1/2}$ and $\mathbb{K} = \mu\omega$ in (6.35), we obtain

$$2\mathbb{K}\lambda_1^{3/4} - \lambda_2(1-\mathbb{K}^2)^{3/4} = 0\,. \tag{6.36}$$

Note that due to the homogeneity properties of the closed-loop system (6.32), the change of variables $k_1 = \lambda_1\Delta^{2/3}$, $k_2 = \lambda_2\Delta^{1/2}$ preserves its qualitative behavior.

Finally, from the HB equation (6.34), the predicted chattering parameters are

$$A = \Delta\left(\frac{2\alpha_1\lambda_1}{\pi\mathbb{K}^2(1-\mathbb{K}^2)}\right)^{3/2}\mu^3\,, \tag{6.37}$$

$$\omega = \frac{\mathbb{K}}{\mu}\,. \tag{6.38}$$

where $\mathbb{K} \in (0,\,1)$ is a solution of equation (6.36). Finally, considering the parameters of amplitude (6.37) and frequency (6.38), and the main harmonic approximation (6.13), we obtain the bounds

$$|x_1| = \Delta\left(\frac{2\alpha_1\lambda_1}{\pi\mathbb{K}^2(1-\mathbb{K}^2)}\right)^{3/2}\mu^3\,, \qquad |x_2| = \Delta\left(\frac{2\alpha_1\lambda_1}{\pi\mathbb{K}^{\frac{4}{3}}(1-\mathbb{K}^2)}\right)^{3/2}\mu^2\,. \tag{6.39}$$

Proposition 6.5. *Let the actuator-plant model (6.10) have low-pass filter properties and the actuator time-constant $\mu > 0$ be small. The PD-HC (6.31) is able to provide accuracy, w.r.t. the time-constant μ, of third and second order for the output x_1 and its time-derivative x_2, respectively, i.e., the inequalities* (6.39) *hold.*

Remark 6.4. Note that the bounds of chattering for both the PID-CSMC and the PD-HC are the same. We can make two conclusion from this fact: first, the static part of the PID-CSMC establishes the convergence properties of the algorithm and it is the main source of chattering. Second, the discontinuity in the PID-CSMC is filtered by an integrator, hence its effect in the generation of chattering is mitigated.

6.3.2 Stability of the self-excited oscillations

Similarly to the case of the PID-CSMC, let us establish the conditions to keep the OAS of the predicted oscillations (6.13) in the steady state response of the system (6.9) in closed-loop with the PD-HC (6.31).

Following the Loeb's criterion (see Section 6.1 for details), the real and imaginary parts of the HB equation (6.34) can be expressed as

$$U(A,\omega) = 2\alpha_1 k_1 + \pi A^{2/3}\omega^2(\mu^2\omega^2 - 1)\,,$$
$$V(A,\omega) = 2\alpha_2 k_2 A^{1/6}\omega^{1/2} - 2\pi\mu A^{2/3}\omega^3\,.$$

So, their partial derivatives w.r.t. A and ω are given by

$$\frac{\partial U}{\partial A} = \frac{2\pi\omega^2(\mu^2\omega^2-1)}{3A^{1/3}}\,, \qquad \frac{\partial U}{\partial \omega} = 2\pi A^{2/3}\omega(2\mu^2\omega^2 - 1)\,,$$
$$\frac{\partial V}{\partial A} = \frac{2\alpha_2 k_2\omega^{1/2}}{6A^{5/6}} - \frac{4\pi\mu\omega^3}{3A^{1/3}}\,, \qquad \frac{\partial V}{\partial \omega} = \frac{\alpha_2 k_2 A^{1/6}}{\omega^{1/2}} - 6\pi\mu A^{2/3}\omega^2\,.$$

Substituting this expressions in inequality (6.4), we obtain

$$2\pi A^{1/2}\omega^{1/2}(\mu^2\omega^2 + 1) - \alpha_2 k_2\mu > 0\,. \tag{6.40}$$

Finally, considering $\alpha_1 \approx 1.821$, $\alpha_2 \approx 1.748$ $k_1 = \lambda_1\Delta^{2/3}$, $k_2 = \lambda_2\Delta^{1/2}$ and substituting the amplitude (6.37) and frequency (6.38) into (6.40), it becomes

$$\lambda_1^{3/4} > \frac{\mathbb{K}\left(1-\mathbb{K}^2\right)^{3/4}}{4\left(1+\mathbb{K}^2\right)}\lambda_2\,, \tag{6.41}$$

holds, where $\mathbb{K} \in (0,\,1)$ is a solution of the non-linear equation (6.36), and $\lambda_1, \lambda_2 \geq 0$ are the gains of the PD-HC.

Proposition 6.6. *Consider the actuator-plant model (6.10), with low-pass filter properties and a small actuator time-constant $\mu > 0$, in closed-loop with the PD-HC (6.31). For any $\Delta > 0$, the periodic solution (6.13) will be OAS if the inequality (6.41) is satisfied.*

6.3.3 Design of gains for the PD-HC

Here, the PD-HC gains are selected from a frequency domain approach, in a similar way as in the classical PD. So, we propose two criteria for selecting the PD-HC gains in order to minimize the upper-bounds of chattering (6.39).

Similarly to the design of the PID-CSMC, the term $\mathbb{K}^2\left(1-\mathbb{K}^2\right)$, in the denominator of (6.37), has a maximum value if $\mathbb{K}^2 = 0.5$. Accordingly, we should select the gains $\lambda_1 > 0$ and $\lambda_2 > 0$ in order to fix the solution of (6.36) in $\mathbb{K}^2 = 0.5$. Under this restriction, the equation (6.36) becomes obtain

$$\lambda_1^{3/4} = 0.421\lambda_2\,. \tag{6.42}$$

Moreover, the restriction (6.41) for $\mathbb{K}^2 = 0.5$ becomes

$$\lambda_1^{3/4} > 0.07\lambda_2\,. \tag{6.43}$$

It is clear that if the gains λ_1 and λ_2 satisfy the equation (6.42), then they also satisfy the inequality (6.43), such that, an OAS periodic solution (6.13) is ensured.

Proposition 6.7. *Given the parameter $\lambda_1 > 0$, if the value $\lambda_2 > 0$ is obtained from (6.42), then the amplitude (6.17) is minimized and the stability of the predicted oscillations (6.13) is guaranteed.*

Now, replacing the estimated parameters (6.37) and (6.38) in the average power (6.3), we obtain the estimation (6.25), again. So, it is minimized by setting $\mathbb{K} \approx 0.6559$ such that $\mathbb{K}^4 \approx (1-\mathbb{K}^2)^3$. Substituting this value in equation (6.36), it is obtained

$$\lambda_1^{3/4} = 0.5\lambda_2\,. \tag{6.44}$$

Furthermore, the restriction (6.41) for $\mathbb{K} = 0.6559$ becomes

$$\lambda_1^{3/4} > 0.075\lambda_2\,. \tag{6.45}$$

It can be readily seen that if the gains λ_1 and λ_2 satisfy the equation (6.44), then they also satisfy the inequality (6.45), ensuring an OAS periodic solution (6.13).

Proposition 6.8. *Given the parameter $\lambda_1 > 0$, if the value $\lambda_2 > 0$ is obtained from (6.44), then the amplitude (6.17) is minimized and the stability of the predicted oscillations (6.13) is guarantee.*

Some examples of gains satisfying the statements of Propositions 6.7 and 6.8 are provided by the sets D_1 and D_2 in Table 6.2, respectively.

6.3.4 Stability analysis of the ideal closed-loop

The following lemma establishes the conditions for GAS of the origin of the closed-loop system (6.32).

Lemma 6.2. *Let the second-order system (6.6), with $f = 0$, in closed-loop with the PD-HC (6.31). For some gains $\lambda_1,\ \lambda_2 > 0$ and $\Delta > 0$, there exist constants $\alpha_1,\ \alpha_2$, and α_3, such that,*

$$V(x) = \alpha_1|x_1|^3 + \alpha_2|x_2|^{\frac{9}{2}} + \alpha_3\lceil x_1\rfloor^{\frac{7}{3}}x_2. \tag{6.46}$$

is a LF for the closed-loop system (6.32).

The proof of Lemma 6.2 is presented in Section D.2 of Appendix D. So, the existence of a LF for the nominal system (6.32) ensures that it is asymptotically stable at the origin, and due to this system is r-homogeneous of negative degree $\nu = -1$, then it is endowed with a kind of ISS. Therefore, if Lemma 6.2 holds with a set of gains from Propositions 6.7 and6.8, then the proposed design works globally. Some examples of gains satisfying the statements of Lemma 6.2 are provided by the sets D_1 and D_2 in Table 6.2.

Set	λ_1	λ_2
D_1	1	2.375
D_2	1	2

Table 6.2: Sets of gains for the PD-HC.

6.3.5 Summarizing the results

Since the gains in Table 6.2 satisfy Propositions 6.7 and 6.8, and Lemma 6.2, the following theorem is directly derived from these previous results.

Theorem 6.3. *Consider a second-order system in cascade connection with a critically damped actuator given by (6.9), with $f = 0$ and a small time-constant $\mu > 0$. Given the parameters λ_1, λ_2, by the sets D_1 and D_2 in Table 6.2 and $\Delta > 0$, the PD-HC (6.31) is able to ensure that the system's trajectories converge to a permanent oscillatory regime (6.13), while minimize the amplitude (6.37) or the average power (6.25), respectively.*

More suitable pairs of gains λ_1, and λ_2 of the PD-HC minimizing the effects of chattering can be determined from Propositions 6.3 and 6.4. However, we need to check if they satisfy the conditions of Lemma 6.1, as well.

6.3.6 Numerical Tests

The simulations are performed in the following framework: the Euler's integration method with constant step $\tau = 10^{-4}$ is used to solve the closed-loop (6.9)-(6.31). Also, $\mu = 0.05$ is considered for the time-constant of the actuator dynamics in (6.10). Further, the upperbound $\Delta = 5$ is taken for simplicity.

Consider the unperturbed control system (6.9)-(6.31), with $f(t) = 0$. So, the steady-state response is only conformed by the oscillations caused by the parasitic dynamics in (6.10). Fig. 6.8 (on the left) shows the simulation of the system (6.9)-(6.7) with the gains $k_1 = 1\Delta^{2/3}$ and $k_2 = 2.375\Delta^{1/2}$, which are selected to minimize the amplitude of chattering according to Proposition 6.3. On the other hand, Fig. 6.8 (on the right) shows the simulation of the system (6.9)-(6.31) with the gains $k_1 = 1\Delta^{2/3}$ and $k_2 = 2\Delta^{1/2}$, which are chosen to minimize the energy needed to maintain the trajectories into a real sliding mode, according to Proposition 6.4. In both cases, we can see that increasing or decreasing the gain of k_2 from the critical value $k_{2_c} = 2.375\Delta^{1/2}$ or $k_{2_c} = 2\Delta^{1/2}$ lead to larger chattering amplitudes or energy needed to maintain the trajectories into a real sliding mode, respectively, validating the theoretical predictions.

Clearly, the controller (6.31) is not able to reject perturbations because it does not have an integral term. So, the simulations of the perturbed case are presented here.

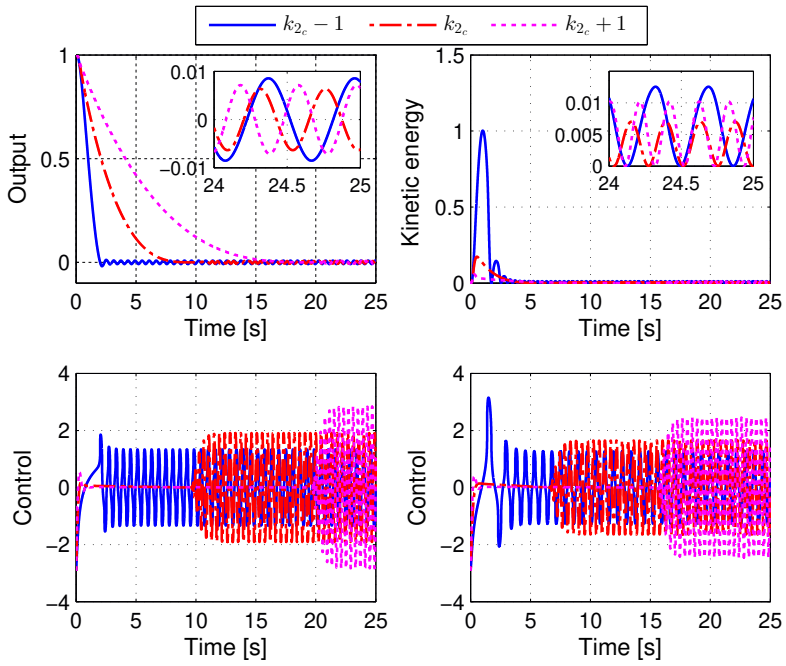

Figure 6.8: Response of the closed-loop system (6.9)-(6.31) for different values of k_2 around the critical gain k_{2_c}. Left: minimizing the chattering amplitude. Right: minimizing the energy needed to maintain the trajectories into a real sliding mode.

6.4 Conclusion

This charter presents a sub-optimal design of the PID-CSMC based on a frequency domain approach, similarly to the classical PID. Two sets of gains are suggested for the PID-CSMC in order to minimize the amplitude or the average power of the chattering caused by the presence of a critically damped second-order actuator in the control system. The DF approach and the HB equation have been used to predict an oscillatory behavior in the steady state of the trajectories (chattering), and calculate amplitude and frequency of this oscillations, as well. Moreover, we have proven by means of a homogeneous LF that the suggested gains ensure finite-time stability to the origin for the ideal system (without an actuator), and an exact compensation of Lipschitz-continuous matched perturbations. On the other hand, in the presence of fast-actuators the Loeb's criterion give the conditions on the gains of the PID-CSMC to generate an OAS oscillatory regime. The proposed design is validated by numerical simulations.

Furthermore, we have presented a sub-optimal design of the PD-HC, which is a nonlinear version of the classical PD. Through the DF approach and the HB equation, we have predicted chattering in the steady state of the trajectories caused by the presence of a critically damped second-order actuator

in the control system, with an estimation of its amplitude and frequency. Then, two sets of gains have been proposed in order to minimize the amplitude or the average power of the chattering. Additionally, we have proven that the suggested gains ensure finite-time stability to the origin for the ideal unperturbed system (without an actuator), by means of a LF. On the other hand, in the presence of fast-actuators the Loeb's criterion give the conditions on the gains of the PD-HC to generate an OAS oscillatory regime. The proposed design is validated by numerical simulations.

Moreover, our results have shown that the static part of the PID-CSMC, which coincides with the PD-HC, provides the convergence properties of the closed-loop system like the settling time or the rise time. On the other hand, the discontinuous integral term provides robustness against Lipschitz-continuous matched perturbations. This behavior is consistent with the classical PID, where the PD part molds the transitory behavior of the closed-loop system and the integral term nullify the steady state error. However, the nonlinearities in the PID-CSMC permit to overcome the features of the classical PID because finite-time stability and exact compensation of certain class of time-varying perturbations can be guaranteed, in theory. Also, the nonlinearities in the static part of the PID-CSMC (i.e., the PD-HC) are the main responsible of chattering because the discontinuity is filtered by an integrator and its contribution to the generation of this oscillations is mitigated.

Chapter 7

Conclusion

This thesis is devoted to the study of stability of homogeneous systems and the design of homogeneous controllers based on Continuous Higher-Order Sliding Mode (CHOSM). Briefly, the homogeneity properties of some nonlinear systems are exploited to extend classical results on the design of Lyapunov functions (LF), and on stability analysis of nonlinear systems affected by parasitic dynamics. Moreover, three schemes of control: state feedback, output feedback and adaptive, are proposed based on Continuous Twisting Algorithm of third Order (3-CTA), where stability analysis and design of gains are realized based on homogeneous LF's. Finally, it is presented a sub-optimal design of the CHOSM controller in PID form (PID-CSMC) based on frequency domain methods and homogeneous LF's.

Chapter 3 presented two converse Lyapunov theorems for a class of discontinuous and homogeneous systems of negative degree. This results can be seen as a generalization of classical results about LF design to the considered class of systems. Moreover, a numerical methodology to construct LF is proposed under some technical assumptions. It consists of two steps: first point-wise calculation of values of the the LF provided by the converse theorems; second, interpolation of this points on the unit sphere. Both together, the converse theorem and the numerical methodology, constitute a new framework for the numerical design of homogeneous and Lipschitz-continuous LF for a wide class of discontinuous Higher-Order Sliding Mode algorithms.

In Chapter 4, the effect of Parasitic Dynamics (PD) on the stability of a homogeneous control system is studied, assuming just continuity of the considered vector fields. Three types of stability for such an interconnection were discovered depending on the relation between the Homogeneity Degrees (HD) of the PD and the Main Dynamics (MD): Global Asymptotic stability (GAS) when both dynamics have the same HD and the Singular Perturbation Parameter (SPP) is sufficiently small, practical GAS when the PD has a greater HD than the MD, and local asymptotic stability when the PD has a smaller HD than the MD. In the last two cases, both the final bound of the trajectories and the domain of attraction depends on the SPP.

From these results, we can conclude that in the general case of nonlinear system the velocity of the different motions is not completely parametrized by the SPP. Particularly, for smooth systems this

parametrization works (at leas locally), and for homogeneous systems it is complemented with the homogeneity degree. Thus, when the involved dynamics have the same HD my results can be seen as a generalization of the concept of motion separation for a wider class of homogeneous singularly perturbed systems. When the PD has a smaller HD than the MD, this concept of motion separation is valid locally in a vicinity of the origin, and when the PD has a greater HD than the MD this concept of motion separation works only outside of a neighborhood of the origin. Therefore, in the last two cases just local or practical stability can be predicted.

Moreover, in Chapter 4 a LF-based approach for analysis of the chattering produced by finite-time convergent controllers in presence of a fast actuator is introduced. Under the assumption that chattering arises in the steady state of the system trajectories, this result allows to show the relationship between the amplitude of chattering, the SPP, and the HD of the finite-time convergent algorithm.

Chapter 5 presented the design of a Third-Order Continuous Twisting Algorithm (3-CTA). This controller is able to provide, in theory, finite-time convergence to zero for the trajectories of a third-order chain of integrators, exact compensation of Lipschitz-continuous and matched disturbances, and steady-state precision of fourth-order w.r.t. sampling step for the system's output. Moreover, an adaptive version of the 3-CTA (3-ACTA) is provided, where the adaptive gain is automatically tunned until the stability of the closed-loop system is assured for all future time. The main advantages of the 3-ACTA are the rejection of Lipschitz-continuous and matched disturbances with an unknown Lipschitz constant, and a proper adjustment of the gains reducing the amplitude of the chattering in the states. In addition, it is introduced an output feedback 3-CTA (3-OFCTA) by using a third-order Robust and Exact Differentiator to estimate the states from the measurable output. The 3-OFCTA preserves, in theory, all features of robustness, convergence, and precision of the 3-CTA while requiring only information from the measurable output. Separation principle for 3-OFCTA is proven which allows the design of the gains for controller and observer, independently. Finally, both controllers 3-ACTA and 3-OFCTA were implemented in a reaction wheel pendulum and a magnetic levitation system, respectively, with satisfactory results.

Finally, Charter 6 provided sub-optimal designs of the PID-CSMC and a homogeneous controller in the PD-form (PD-HC) based on frequency methods. Two sets of gains for the PID-CSMC and two more for the PD-HC are suggested in order to minimize the amplitude of chattering caused by the presence of a critically-damped second-order fast-actuator in the control system or the energy needed to maintain the trajectories into a real sliding mode. By means of a homogeneous LF, we have proven that the suggested designs ensure finite-time stability at the origin for the ideal system (without an actuator).

Moreover, these results have shown that the static part of the PID-CSMC, which coincides with the PD-HC, provides the convergence properties of the closed-loop system like the settling time or the rise time. On the other hand, the discontinuous integral term provides robustness against Lipschitz-continuous matched perturbations. This behavior is consistent with the classical PID, where the PD part molds the transitory behavior of the closed-loop system and the integral term nullify the steady state error. However, the nonlinearities in the PID-CSMC permit to overcome the features of the classical PID because finite-time stability and exact compensation of certain class of time-varying perturbations can be guaranteed, in theory. Also, the nonlinearities in the static part of the PID-CSMC

(i.e., the PD-HC) are the main responsible of chattering because the discontinuity is filtered by an integrator and its contribution to the generation of this oscillations is mitigated.

Most of the results in this thesis address to one of the main issues in implementation of CHOSM controller, the so-called chattering. Specifically, the results from Chapters 4 and 6 represent new directions in further research of analysis of chattering, and design of CHOSM algorithms with criteria for chattering minimization.

Appendix A

Converse theorems and numerical construction of Lyapunov functions for a class of Sliding-Mode algorithms: proofs

A.1 Proof of Lemma 3.1

Consider the interval $[0, \bar{T}_q(1))$ formed by a finite collection of subinterval $[t_k^{x_0}, t_{k+1}^{x_0})$, i.e.,

$$[0, \bar{T}_q(1)) = \bigcup_{k=0}^{N_{x_0}} [t_k^{x_0}, t_{k+1}^{x_0})$$

for some finite $N_{x_0} > 0$ and for any $x_0 \in \mathbb{R}^n$. Under Assumption 3.1, on each interval $(t_k^{x_0}, t_{k+1}^{x_0})$ the trajectory stays in a respective domain D_{i_k} with $i_k \in \{1, \dots, m\}$, such that, $\chi(t_k^{x_0}, x_0) \in S$ for all $k \in \{0, \dots, N_{x_0} + 1\}$ (except probably $t_0^{x_0}$ and $t_{N_{x_0}+1}^{x_0}$). Assume that the system (3.1) is stable and by the definition of $\bar{T}_q(1)$,

$$\chi(t, x_0) \in \mathcal{X} := \left\{ x \in \mathbb{R}^n : q'^{-1} \leq \|x\|_r \leq \left(\frac{b}{a}\right)^{\frac{1}{\mu}} \right\}$$

for all $t \in [0, \bar{T}_q(1))$ and $q' \in [q, +\infty)$, where a, b, μ are given in (3.5). Denote by $L_i > 0$ the corresponding Lipschitz constant of (3.1) on $D_i \cap \mathcal{X}$ with $i \in \{1, \dots, m\}$, and $L_{\max} = \max_{i=1,\dots,m} L_i$. In addition, there exist $\theta_{\mathcal{X}}, \Theta_{\mathcal{X}}, L_{\mathcal{X}} > 0$ such that

$$\theta_{\mathcal{X}} \leq \|f(x_1) - f(x_2)\| \leq L_{\mathcal{X}} \|x_1 - x_2\| + \Theta_{\mathcal{X}}, \qquad \forall x_1, x_2 \in \mathcal{X}.$$

Let us show the Lipschitz property of the solutions of the system(3.1) under Assumption 3.1 for any $x_1, x_2 \in S_r(1)$ on the interval $[0, \bar{T}_q(1))$. To this end, denote $\bar{N} = \sup_{x_0 \in S_r(1)} N_{x_0}$, which is a finite integer under hypotheses of the lemma.

Consider first the interval $[0, t')$, where $t' = \min\{t_1^{x_1}, t_1^{x_2}\}$ and $\chi(t, x_j) \in D_{i_j}$ for $j = 1, 2$ and $t \in (0, t')$. If $D_{i_1} = D_{i_2}$ then using Bellman-Gronwall lemma we obtain:

$$\begin{aligned}\|\chi(t,x_1) - \chi(t,x_2)\| &= \|x_1 - x_2 + \int_0^t f(\chi(s,x_1)) - f(\chi(s,x_2))ds\| \\ &\leq \|x_1 - x_2\| + \int_0^t \|f(\chi(s,x_1)) - f(\chi(s,x_2))\|ds \\ &\leq \|x_1 - x_2\| + L_{\max}\int_0^t \|\chi(s,x_1) - \chi(s,x_2)\|ds \\ &\leq e^{L_{\max}t}\|x_1 - x_2\|\end{aligned}$$

for all $t \in [0, t')$. If D_{i_1} and D_{i_2} are distinct sets, then

$$\begin{aligned}\|\chi(t,x_1) - \chi(t,x_2)\| &\leq \|x_1 - x_2\| + \int_0^t \|f(\chi(s,x_1)) - f(\chi(s,x_2))\|ds \\ &\leq \|x_1 - x_2\| + \int_0^t L_{\mathcal{X}}\|\chi(s,x_1) - \chi(s,x_2)\| + \Theta_{\mathcal{X}}ds \\ &\leq (1 + H_{\mathcal{X}}\bar{T}_q(1))\|x_1 - x_2\| + L_{\mathcal{X}}\int_0^t \|\chi(s,x_1) - \chi(s,x_2)\|ds \\ &\leq (1 + H_{\mathcal{X}}\bar{T}_q(1))e^{L_{\mathcal{X}}t}\|x_1 - x_2\|\end{aligned}$$

for all $t \in [0, t')$ provided that $\Theta_{\mathcal{X}} \leq H_{\mathcal{X}}\|x_1 - x_2\|$ for some $H_{\mathcal{X}} > 0$. Or alternatively,

$$\begin{aligned}\|\chi(t,x_1) - \chi(t,x_2)\| &\leq \|x_1 - x_2\| + \int_0^t L_{\mathcal{X}}\|\chi(s,x_1) - \chi(s,x_2)\| + \Theta_{\mathcal{X}}ds \\ &\leq \|x_1 - x_2\| + \Theta_{\mathcal{X}}t + L_{\mathcal{X}}\int_0^t \|\chi(s,x_1) - \chi(s,x_2)\|ds \\ &\leq (1 + K_{\mathcal{X}})e^{L_{\mathcal{X}}t}\|x_1 - x_2\|\end{aligned}$$

for all $t \in [0, t')$ provided that $\Theta_{\mathcal{X}}t \leq K_{\mathcal{X}}\|x_1 - x_2\|$ for some $K_{\mathcal{X}} > 0$. To complement these cases, it remains to consider the scenario with $\Theta_{\mathcal{X}} > H_{\mathcal{X}}\|x_1 - x_2\|$ and $\Theta_{\mathcal{X}}t > K_{\mathcal{X}}\|x_1 - x_2\|$, then for a sufficiently big value of $H_{\mathcal{X}}$, the initial conditions belong to a neighborhood of S (since $\|x_1 - x_2\| < \frac{\Theta_{\mathcal{X}}}{H_{\mathcal{X}}}$ and $x_1 \in D_{i_1}, x_2 \in D_{i_2}$). Recalling Assumption 3.1, in such a case either $\chi(t', x_1) \in D_{i_2}$ or $\chi(t', x_2) \in D_{i_1}$, hence, there is $S_{\mathcal{X}} > 0$ such that $t' \leq \frac{S_{\mathcal{X}}}{\theta_{\mathcal{X}}}\|x_1 - x_2\|$ and for $K_{\mathcal{X}} \geq S_{\mathcal{X}}\frac{\Theta_{\mathcal{X}}}{\theta_{\mathcal{X}}}$ we get a contradiction. Therefore,

$$\|\chi(t,x_1) - \chi(t,x_2)\| \leq \mathcal{L}\|x_1 - x_2\|$$

for all $t \in [0, t')$, where

$$\mathcal{L} = \max\{e^{L_{\max}\bar{T}_q(1)}, (1 + H_{\mathcal{X}}\bar{T}_q(1))e^{L_{\mathcal{X}}\bar{T}_q(1)}, (1 + K_{\mathcal{X}})e^{L_{\mathcal{X}}\bar{T}_q(1)}\}.$$

Now, consider $t \in [t', t'')$ for $t'' = \min\{\max\{t_1^{x_1}, t_1^{x_2}\}, \min\{t_2^{x_1}, t_2^{x_2}\}\}$, and applying the same argumentation as previously:

$$\|\chi(t, \chi(t', x_1)) - \chi(t, \chi(t', x_2))\| \leq \mathcal{L}\|\chi(t', x_1) - \chi(t', x_2)\| \leq \mathcal{L}^2\|x_1 - x_2\|$$

for all $t \in [t', t'')$, and we used continuity of the solutions for the time instant t'. Therefore,

$$\|\chi(t, x_1) - \chi(t, x_2)\| \leq \max\left\{\mathcal{L}, \mathcal{L}^2\right\}\|x_1 - x_2\|$$

for all $t \in [0, t'')$. The same consideration can be repeated for all other intervals of time in a similar way leading to the estimate:

$$\|\chi(t, x_1) - \chi(t, x_2)\| \leq \max_{j=0,\dots,2\bar{N}} \mathcal{L}^j\|x_1 - x_2\|$$

for all $t \in [0, \bar{T}_q(1))$, and the desired result follows for $L_{S_r(1),\bar{T}_q(1)} = \max\{\mathcal{L}, \mathcal{L}^{2\bar{N}}\}$.

A.2 Proof of Theorem 3.1

Under Assumption 3.1, the system (3.1) is r-homogeneous of negative homogeneity degree ν, hence, the existence of the LF (3.7) satisfying the statement of Theorem 3.1 is enough to conclude the finite-time stability of the origin of the discontinuous system (3.1). Conversely, assuming the first claim in Theorem 3.1, the existence of the LF (3.7) is proven as follows.

Assuming asymptotic stability for the system (3.1), by the definition of T_q and inequality (3.4), where the function β is given by (3.5), the solution $\chi(t, x_0)$ is bounded by

$$\|\chi(t, x_0)\|_r \in \left[\frac{1}{q'}, \left(\frac{b}{a}\right)^{\frac{1}{\mu}}\right], \tag{A.1}$$

where $q' > q > 1$, for all $t \in \left[0, T_q^{\max}(\|x\|_r)\right]$ and for any $x_0 \in S_r(1)$.

Now, for any $x_0 \in \mathbb{R}^n$ define

$$U(x_0) = \int_0^{T_q^{\max}(\|x_0\|_r)} \|\chi(t, x_0)\|_r^\mu dt, \tag{A.2}$$

where $T_q^{\max}(\|x_0\|_r)$ is defined in Theorem 3.1. The function (A.2) is r-homogeneous of degree $\mu - \nu$ since for all $x_0 \in \mathbb{R}^n$ and $\lambda > 0$

$$\begin{aligned} U(\Lambda_r(\lambda)x_0) &= \int_0^{T_q^{\max}(\|\Lambda_r(\lambda)x_0\|_r)} \|\chi(t, \Lambda_r(\lambda)x_0)\|_r^\mu dt \\ &= \int_0^{\lambda^{-\nu}T_q^{\max}(\|x_0\|_r)} \|\Lambda_r(\lambda)\chi(\lambda^\nu t, x_0)\|_r^\mu dt \\ &= \lambda^{\mu-\nu}\int_0^{T_q^{\max}(\|x_0\|_r)} \|\chi(\tau, x_0)\|_r^\mu d\tau = \lambda^{\mu-\nu}U(x_0), \end{aligned}$$

where the change of variables $\tau = \lambda^\nu t$ was used.

By construction $U(0) = 0$. Moreover, considering (A.1) and for any $x_0 \in S_r(1)$

$$U(x_0) = \int_0^{T_q^{\max}(1)} \|\chi(t, x_0)\|_r^\mu dt \geq \int_0^{T_q(x_0)} q^{-\mu} dt = T_q(x_0) q^{-\mu},$$

and

$$U(x_0) = \int_0^{T_q^{\max}(1)} \|\chi(t, x_0)\|_r^\mu dt \leq \int_0^{T_q^{\max}(1)} \frac{b}{a} dt = T_q^{\max}(1) \frac{b}{a}.$$

Hence, by homogeneity

$$T_q^{\min} q^{-\mu} \|x\|_r^{\mu-\nu} \leq U(x) \leq T_q^{\max}(1) \frac{b}{a} \|x\|_r^{\mu-\nu}, \tag{A.3}$$

for all $x \in \mathbb{R}^n$, where $T_q^{\min}$ and $T_q^{\max}(1)$ are defined in Theorem 3.1.

Now, in order to analyze the Lipschitz continuity of the function (A.2), consider two states $x_1, x_2 \in S_r(1)$ and

$$\begin{aligned} \left| U(x_1) - U(x_2) \right| &= \left| \int_0^{T_q^{\max}(\|x_1\|_r)} \|\chi(t, x_1)\|_r^\mu dt - \int_0^{T_q^{\max}(\|x_2\|_r)} \|\chi(t, x_2)\|_r^\mu dt \right| \\ &= \left| \int_0^{T_q^{\max}(1)} \|\chi(t, x_1)\|_r^\mu - \|\chi(t, x_2)\|_r^\mu dt \right| \\ &\leq \int_0^{T_q^{\max}(1)} \left| \|\chi(t, x_1)\|_r^\mu - \|\chi(t, x_2)\|_r^\mu \right| dt \,. \end{aligned} \tag{A.4}$$

Recall, from inequality (A.1) the solutions $\chi(t, x_0)$ are all bounded for any $x_0 \in S_r(1)$ and all $t \in [0, T_q^{\max}(1)]$. Under Assumption 3.1, the Lipschitz continuity of the trajectories $\chi(t, x_0)$ w.r.t. x_0 is predicted by Lemma 3.1 for all $t \in [0, \bar{T}_q(1)]$ (note that $T_q^{\max}(1) \leq \bar{T}_q(1)$), the Lipschitz continuity of the r-homogeneous norm is established by Corollary 2.1, and the power function $x \mapsto x^\mu$ is Lipschitz continuous for any $\mu > 1$ as well. As the composition of Lipschitz continuous functions inherits the property, then it is obtained

$$\left| \|\chi(t, x_1)\|_r^\mu - \|\chi(t, x_2)\|_r^\mu \right| \leq \bar{L} \|x_1 - x_2\|, \tag{A.5}$$

for all $t \in [0, T_q^{\max}(1)]$, all $x_1, x_2 \in S_r(1)$ and some $\bar{L} > 0$. Consequently, substituting (A.5) in (A.4)

$$\left| U(x_1) - U(x_2) \right| \leq \int_0^{T_q^{\max}(1)} \bar{L} \|x_1 - x_2\| dt \leq T_q^{\max} \bar{L} \|x_1 - x_2\|$$

for all $x_1, x_2 \in S_r(1)$, then the function U is locally Lipschitz continuous on the unit sphere, and by homogeneity, it is Lipschitz continuous in $\mathbb{R}^n \setminus \{0\}$ as needed.

Along a trajectory $\chi(t,x_0)$, the derivative of $U(\chi(t,x_0))$ at the point x_0 is given by

$$D^+U(x_0)F(x_0) = \limsup_{h\to 0^+} \frac{1}{h}\left[U(\chi(h,x_0)) - U(x_0)\right].$$

So, it is enough to show that the function (A.2) is decreasing along any trajectory of the system (3.1), i.e., $U(\chi(t,x_0)) < U(x_0)$, for any (small) $t \in \left(0, T_q^{\max}(\|x_0\|_r)\right)$, to conclude that $D^+U(x_0)F(x_0) < 0$ for almost all $x_0 \in \mathbb{R}^n \setminus \{0\}$.

From the semi-group property we have that $\|\chi(\tau,\chi(t,x_0))\|_r = \|\chi(\tau+t,x_0)\|_r$, for all $t,\tau \in \mathbb{R}_+$ and $x_0 \in \mathbb{R}^n$. Thus, for any $x_0 \in \mathbb{R}^n$ and all $t \in \mathbb{R}_+$,

$$\begin{aligned}
U(\chi(t,x_0)) &= \int_0^{T_q^{\max}(\|\chi(t,x_0)\|_r)} \|\chi(\tau,\chi(t,x_0))\|_r^\mu \, d\tau \\
&= \int_0^{T_q^{\max}(\|\chi(t,x_0)\|_r)} \|\chi(\tau+t,x_0)\|_r^\mu \, d\tau \\
&= \int_0^{t+T_q^{\max}(\|\chi(t,x_0)\|_r)} \|\chi(s,x_0)\|_r^\mu \, ds - \int_0^t \|\chi(s,x_0)\|_r^\mu \, ds \\
&= \int_{T_q^{\max}(\|x_0\|_r)}^{t+T_q^{\max}(\|\chi(t,x_0)\|_r)} \|\chi(s,x_0)\|_r^\mu \, ds - \int_0^t \|\chi(s,x_0)\|_r^\mu \, ds \\
&\qquad + \int_0^{T_q^{\max}(\|x_0\|_r)} \|\chi(s,x_0)\|_r^\mu \, ds.
\end{aligned}$$

with $q > 1$ and $\mu > 1$. The first term in the latter expression depends on q, the second one is negative and the third one corresponds to the LF (A.2). Let us show that growing q warranties the decreasing of the LF (A.2) along any trajectory $\chi(t,x_0)$. So, in the first integral

$$\|\chi(s,x_0)\|_r \le \beta\left(x_0, T_q^{\max}(\|x_0\|_r)\right) \qquad \forall s \ge T_q^{\max}(\|x_0\|_r),$$

where β is a $\mathcal{KL}$-function given by (3.5). Note that $T_q^{\max}(\|x_0\|_r)$ grows with q then $\beta\left(x_0, T_q^{\max}(\|x_0\|_r)\right)$ decreases to zero as q tends to infinity. For the second integral, since the function $\|\chi(t,x_0)\|_r^\mu$ is continuous w.r.t. t, for any $\epsilon > 0$ there exist $t_1 > 0$, such that, if $0 \le t < t_1$ then

$$\left| \|\chi(t_1,x_0)\|_r^\mu - \|\chi(0,x_0)\|_r^\mu \right| < \epsilon,$$

and

$$\|x_0\|_r - \epsilon < \|\chi(t,x_0)\|_r < \|x_0\|_r + \epsilon. \tag{A.6}$$

Thus, for $t \in [0,t_1)$, we obtain

$$\begin{aligned}
U(\chi(t,x_0)) - U(x_0) &\le \int_{T_q^{\max}(\|x_0\|_r)}^{t+T_q^{\max}(\|\chi(t,x_0)\|_r)} \beta^\mu\left(x_0, T_q^{\max}(\|x_0\|_r)\right) ds - \int_0^t \left(\|x_0\|_r - \epsilon\right)^\mu ds \\
&\le \beta^\mu\left(x_0, T_q^{\max}(\|x_0\|_r)\right)\left(t + T_q^{\max}(\|\chi(t,x_0)\|_r)\right. \\
&\qquad \left. - T_q^{\max}(\|x_0\|_r)\right) - \left(\|x_0\|_r - \epsilon\right)^\mu t.
\end{aligned}$$

By the homogeneity of $T_q^{\max}$:

$$T_q^{\max}\left(\|\chi(t,x_0)\|_r\right) = c(t) T_q^{\max}\left(\|x_0\|_r\right),$$

where $c(t) = \left(\frac{\|\chi(t,x_0)\|_r}{\|x_0\|_r}\right)^{-\nu}$. Let $t \in [0, t_1)$, then

$$\begin{aligned} U(\chi(t,x_0)) - U(x_0) &\leq \beta^\mu\left(x_0, T_q^{\max}(\|x_0\|_r)\right)\left(t + (c(t)-1)\, T_q^{\max}(\|x_0\|_r)\right) - (\|x_0\|_r - \epsilon)^\mu\, t \\ &\leq -\left((\|x_0\|_r - \epsilon)^\mu - \beta^\mu\left(x_0, T_q^{\max}(\|x_0\|_r)\right)\right) t \\ &\qquad + |c(t)-1|\, \beta^\mu\left(x_0, T_q^{\max}(\|x_0\|_r)\right) T_q^{\max}(\|x_0\|_r). \end{aligned}$$

It is enough for our purpose to study the behavior of U for $t \in [0, t_1]$ (where t_1 is a small positive constant) and $x_0 \in S_r(1)$. Since $-1 < \nu < 0$, if $\|\chi(t,x_0)\|_r > 1$ then $\|\chi(t,x_0)\|_r^{-\nu} < \|\chi(t,x_0)\|_r$, on the contrary, if $\|\chi(t,x_0)\|_r < 1$ then $\|\chi(t,x_0)\|_r^{-\nu} > \|\chi(t,x_0)\|_r$, hence, from both cases we can conclude that

$$\left|\|\chi(t,x_0)\|_r^{-\nu} - 1\right| \leq \left|\|\chi(t,x_0)\|_r - 1\right|,$$

and by homogeneity the property hold for all $x_0 \in \mathbb{R}^n$ and $t \in [0, t_1]$. So,

$$c(t) - 1 = \left(\frac{\|\chi(t,x_0)\|_r}{\|x_0\|_r}\right)^{-\nu} - 1 \leq \frac{\|\chi(t,x_0)\|_r}{\|x_0\|_r} - 1,$$

where the facts that $\nu \in [-1, 0)$ and $r_{\max} = 1$ were used for Lipschitz continuity of $\|\cdot\|_r$. Moreover, denote the respective Lipschitz constant by $L^{-\nu}_{\|\cdot\|_r, x_0} > 0$ for the set where the trajectories behave. Applying the last observation

$$c(t) - 1 \leq L^{-\nu}_{\|\cdot\|_r, x_0} \frac{\|\chi(t,x_0) - x_0\|}{\|x_0\|_r}.$$

Furthermore, since $\chi(t,\, x_0) = x_0 + \int_0^t f\left(\chi(\tau,\, x_0)\right) d\tau$ and f is bounded, we have

$$\|\chi(t,x_0) - x_0\| \leq \int_0^t \|f(\chi(s,x_0))\| ds \leq f_{\max,x_0} t,$$

where $f_{\max,x_0} = \sup_{t\geq 0} \|f(\chi(t,x_0))\|$, such that,

$$c(t) - 1 \leq L^{-\nu}_{\|\cdot\|_r, x_0} \frac{f_{\max,x_0}}{\|x_0\|_r} t.$$

Thus,

$$\begin{aligned} U(\chi(t,x_0)) - U(x_0) &\leq -\left((\|x_0\|_r - \epsilon)^\mu - \beta^\mu\left(x_0, T_q^{\max}(\|x_0\|_r)\right)\right) t \\ &\qquad + L_{\|\cdot\|_r, x_0} \frac{f_{\max,x_0}}{\|x_0\|_r} \beta^\mu\left(x_0, T_q^{\max}(\|x_0\|_r)\right) T_q^{\max}(\|x_0\|_r) t \\ &\leq -\left[(\|x_0\|_r - \epsilon)^\mu - \kappa_{x_0,q} \beta^\mu\left(x_0, T_q^{\max}(\|x_0\|_r)\right)\right] t \end{aligned}$$

for $t \in [0, t_1]$, where $\kappa_{x_0,q} = 1 + L_{\|\cdot\|_r,x_0} \frac{f_{\max,x_0}}{\|x_0\|_r} T_q^{\max}(\|x_0\|_r)$. Note that the first term in brackets of the right-hand side of the latter expression is negative if $\epsilon < \|x_0\|_r$ is selected, and the second one decreases monotonically to zero with growing q, and $\kappa_{x_0,q}$ stays bounded due to the system (3.1) is assumed finite-time stable and $T_q^{\max}(s) < T_s$ where T_s is the settling time function. This implies that there is a (finite) value q^* such that for $q > q^*$ the inequality $U(\chi(t, x)) - U(x) < 0$ holds. Due to homogeneity, it is sufficient to verify this only on the unit sphere $S_r(1)$ and since it is a compact set the existence of a constant value $q^* > 1$ is concluded. Consequently, U is decreasing along any trajectories of the system (3.1) for almost all $x_0 \in \mathbb{R}^n$. Finally, this completes the proof of Theorem 3.1.

A.3 Proof of Theorem 3.2

Under Assumption 3.1, the system (3.1) is r-homogeneous of negative homogeneity degree ν, hence, the existence of the LF (6.30) satisfying the statement of Theorem 3.2 is enough to conclude the finite-time stability of the origin of the discontinuous system (3.1). Conversely, assuming the first claim in Theorem 3.2, the existence of the LF (D.3) is proven as follows.

Consider $x_0 \in \mathbb{R}^n$, then

$$V(x_0) = \sup_{t \in [0, T_q(x_0)]} \{\|\chi(t, x_0)\|_r \, k(t, x_0)\}, \tag{A.7}$$

where $k : \mathbb{R}_+ \times \mathbb{R}^n \to \mathbb{R}_+$ is a continuous function, differentiable with respect to the first argument, given by

$$k(t, x_0) = \frac{\|\chi(t, x_0)\|_r^{\varrho\nu} t^{\varrho} + \kappa_1}{\|\chi(t, x_0)\|_r^{\varrho\nu} t^{\varrho} + \kappa_2}, \tag{A.8}$$

where $0 < \kappa_1 < \kappa_2 < +\infty$ and $\varrho > 0$ is a real parameter satisfying $|\varrho\nu| > 1$.

First, since the system (3.1) is assumed finite-time stable at the origin, then there exists a settling time T_{x_0} such that $\|\chi(t, x_0)\|_r = 0$ for all $t \geq T_{x_0}$. Thus, the supremum of the function $\|\chi(t, x_0)\|_r$ arises on the interval of time $t \in [0, T_{x_0}]$, i.e.,

$$\sup_{t \in [0, T_{x_0}]} \{\|\chi(\tau, x_0)\|_r\} = \sup_{t \geq 0} \{\|\chi(t, x_0)\|_r\}.$$

Note that function (A.8) is lower and upper bounded by $\frac{\kappa_1}{\kappa_2} \leq |k(t, \cdot)| < 1$, besides $V(x_0) = \frac{\kappa_1}{\kappa_2}\|x_0\|_r$ for $t = 0$, hence, $V(x_0) \geq \frac{\kappa_1}{\kappa_2}\|x_0\|_r$ for all $0 \leq t < T_{x_0}$. Recalling Definitions 4.1 and 3.2, there exists the time $\bar{T}_{\frac{\kappa_2}{\kappa_1}}(x_0)$, such that,

$$\|\chi(t, x_0)\|_r \leq \frac{\kappa_1}{\kappa_2}\|x_0\|_r, \quad \forall t \geq \bar{T}_{\frac{\kappa_2}{\kappa_1}}(x_0).$$

and for $q > 1$ sufficiently large, there exist also the time $T_q(x_0) \geq \bar{T}_{\frac{\kappa_2}{\kappa_1}}(x_0)$ when the trajectories $\chi(t, x_0)$ reach the sphere of radius $\frac{1}{q}\|x_0\|_r$ for the first time and they never leave the ball of radius

$\frac{\kappa_1}{\kappa_2}\|x_0\|_r$, thereafter. Consequently,

$$V(x_0) = \sup_{t\in[0,T_q(x_0)]}\{\|\chi(t,x_0)\|_r\, k(t,x_0)\} = \sup_{t\geq 0}\{\|\chi(t,x_0)\|_r\, k(t,x_0)\}, \tag{A.9}$$

for such a choice of q. In the sequel, both expressions for $V(x_0)$ will be used indistinctly.

So, considering equation (3.4) (see function β in (3.5)) and the facts $\chi(0,x_0) = x_0$ and $\frac{\kappa_1}{\kappa_2} \leq |k(t,\cdot)| < 1$, the function (A.9) satisfies $V(0) = 0$ (since $x = 0$ is an equilibrium point), and

$$\frac{\kappa_1}{\kappa_2}\|x_0\|_r \leq V(x_0) \leq \left(\frac{b}{a}\right)^{\frac{1}{\mu}} \|x_0\|_r \text{ for all } x_0 \in \mathbb{R}^n.$$

Now, since the system (3.1) is r-homogeneous of degree $\nu < 0$ and the norm $\|\cdot\|_r$ is r-homogeneous of degree 1 then

$$\|\chi(t,\Lambda_r(\lambda)x_0)\|_r = \|\Lambda_r(\lambda)\chi(\lambda^\nu t,x_0)\|_r = \lambda\|\chi(\lambda^\nu t,x_0)\|_r.$$

Also,

$$\begin{aligned} k\left(t,\Lambda_r(\lambda)x_0\right) &= \frac{\|\chi(t,\Lambda_r(\lambda)x_0)\|_r^{\varrho\nu}t^\varrho + \kappa_1}{\|\chi(t,\Lambda_r(\lambda)x_0)\|_r^{\varrho\nu}t^\varrho + \kappa_2} \\ &= \frac{\|\chi(\lambda^\nu t,x_0)\|_r^{\varrho\nu}\lambda^{\varrho\nu}t^\varrho + \kappa_1}{\|\chi(\lambda^\nu t,x_0)\|_r^{\varrho\nu}\lambda^{\varrho\nu}t^\varrho + \kappa_2} = k\left(\lambda^\nu t,x_0\right) \end{aligned}$$

for all $x_0 \in \mathbb{R}^n$, $t \in \mathbb{R}_+$. These properties imply that for all $x_0 \in \mathbb{R}^n$ and $\lambda > 0$:

$$\begin{aligned} V(\Lambda_r(\lambda)x_0) &= \sup_{t\geq 0}\{\|\chi(t,\Lambda_r(\lambda)x_0)\|_r\, k\left(t,\Lambda_r(\lambda)x_0\right)\} \\ &= \lambda \sup_{s\geq 0}\left\{\|\chi(s,x_0)\|_r\, k\left(s,x_0\right)\right\} = \lambda V(x_0), \end{aligned}$$

where the substitution $s = \lambda^\nu t$ was used, hence V is r-homogeneous of degree 1.

Now, let us prove the Lipschitz continuity of V. For this, consider $x_1, x_2 \in S_r(1)$ and $T_q^{\max}(1) = \sup_{x_0\in S_r(1)} T_q(x_0)$, such that,

$$|V(x_1) - V(x_2)| = \left|\sup_{t\in[0,T_q^{\max}(1)]}\{\|\chi(t,x_1)\|_r\, k(t,x_1)\} - \sup_{t\in[0,T_q^{\max}(1)]}\{\|\chi(t,x_2)\|_r\, k(t,x_2)\}\right|.$$

Adding a zero:

$$\sup_{t\in[0,T_q^{\max}(1)]}\{\|\chi(t,x_2)\|_r\, k(t,x_1)\} - \sup_{t\in[0,T_q^{\max}(1)]}\{\|\chi(t,x_2)\|_r\, k(t,x_1)\} = 0,$$

and applying the triangle inequality for the absolute value,

$$|V(x_1)-V(x_2)| \leq \left| \sup_{t\in[0,T_q^{\max}(1)]} \{\|\chi(t,x_1)\|_r\, k(t,x_1)\} - \sup_{t\in[0,T_q^{\max}(1)]} \{\|\chi(t,x_2)\|_r\, k(t,x_1)\} \right| + \left| \sup_{t\in[0,T_q^{\max}(1)]} \{\|\chi(t,x_2)\|_r\, k(t,x_2)\} - \sup_{t\in[0,T_q^{\max}(1)]} \{\|\chi(t,x_2)\|_r\, k(t,x_1)\} \right|,$$

and since the absolute value of difference of supremums is less than the supremum of absolute value of difference, then

$$\sup_{t\in[0,T_q^{\max}(1)]} \{|\|\chi(t,x_1)\|_r - \|\chi(t,x_2)\|_r|\; k(t,x_1)\} \geq \geq \left| \sup_{t\in[0,T_q^{\max}(1)]} \{\|\chi(t,x_1)\|_r\, k(t,x_1)\} - \sup_{t\in[0,T_q^{\max}(1)]} \{\|\chi(t,x_2)\|_r\, k(t,x_1)\} \right|,$$

and

$$\sup_{t\in[0,T_q^{\max}(1)]} \{\|\chi(t,x_2)\|_r\, |k(t,x_2)-k(t,x_1)|\} \geq \geq \left| \sup_{t\in[0,T_q^{\max}(1)]} \{\|\chi(t,x_2)\|_r\, k(t,x_2)\} - \sup_{t\in[0,T_q^{\max}(1)]} \{\|\chi(t,x_2)\|_r\, k(t,x_1)\} \right|,$$

hence it is obtained that

$$|V(x_1)-V(x_2)| \leq \sup_{t\in[0,T_q^{\max}(1)]} \{|\|\chi(t,x_1)\|_r - \|\chi(t,x_2)\|_r|\; k(t,x_1)\} + \sup_{t\in[0,T_q^{\max}(1)]} \{\|\chi(t,x_2)\|_r\, |k(t,x_2)-k(t,x_1)|\}.$$

From (A.8) it can be seen that $|k(t,x_0)|<1$, and from (3.5) $\|\chi(t,x_0)\|_r \leq \frac{b}{a}$, hence

$$|V(x_1)-V(x_2)| \leq \sup_{t\in[0,T_q^{\max}(1)]} |\|\chi(t,x_1)\|_r - \|\chi(t,x_2)\|_r| + \frac{b}{a} \sup_{t\in[0,T_q^{\max}(1)]} |k(t,x_2)-k(t,x_1)|.$$

Again, from (A.8)

$$|k(t,x_2)-k(t,x_1)| = \frac{|\|\chi(\tau,x_2)\|_r^{\varrho\nu} - \|\chi(\tau,x_1)\|_r^{\varrho\nu}|\,(\kappa_2-\kappa_1)t^{\varrho}}{(\|\chi(\tau,x_2)\|_r^{\varrho\nu}t^{\varrho}+\kappa_2)(\|\chi(\tau,x_1)\|_r^{\varrho\nu}t^{\varrho}+\kappa_2)},$$

besides for $|\varrho\nu| > 1$ the power function is locally Lipschitz continuous on $\mathbb{R}^n$ with the Lipschitz constant K in $B_r(\frac{b}{a}) \setminus \{0\}$, i.e.,

$$\left| \|\chi(\tau,x_2)\|_r^{\varrho\nu} - \|\chi(\tau,x_1)\|_r^{\varrho\nu} \right| \;\leq\; K \left| \|\chi(\tau,x_2)\|_r - \|\chi(\tau,x_1)\|_r \right|,$$

and there exists some constant M such that

$$\sup_{t\in[0,T_q^{\max}(1)]} \left\{ \frac{(\kappa_2-\kappa_1)t^\varrho}{(\|\chi(\tau,x_2)\|_r^{\varrho\nu} t^\varrho + \kappa_2)(\|\chi(\tau,x_1)\|_r^{\varrho\nu} t^\varrho + \kappa_2)} \right\} \leq M.$$

Therefore,

$$\begin{aligned} |V(x_1) - V(x_2)| \;\leq\; & \sup_{t\in[0,T_q^{\max}(1)]} \left| \|\chi(t,x_1)\|_r - \|\chi(t,x_2)\|_r \right| \\ & + \frac{b}{a} MK \sup_{t\in[0,T_q^{\max}(1)]} \left| \|\chi(t,x_1)\|_r - \|\chi(t,x_2)\|_r \right|. \end{aligned}$$

Moreover, under Assumption 3.1 and following Lemma 3.1, the trajectories $\chi(t,x_0)$ are locally Lipschitz continuous w.r.t. their initial conditions, and from Corollary 2.1 the r-homogeneous norm $\|\cdot\|_r$ is also locally Lipschitz continuous. Therefore,

$$|V(x_1) - V(x_2)| \leq L_2\|x_2 - x_1\| + \frac{b}{a} MKL_2\|x_2 - x_1\|.$$

and we conclude that the function (A.9) is locally Lipschitz continuous on $S_r(1)$ and by homogeneity it inherits this property for all $\mathbb{R}^n \setminus \{0\}$.

Now, using the semi-group property of the state transition map χ we obtain that $\|\chi(\tau,\chi(t,x_0))\|_r = \|\chi(\tau+t,x_0)\|_r$, for all $t,\tau \in \mathbb{R}_+$ and $x_0 \in \mathbb{R}^n$. In addition,

$$k\left(\tau,\chi(t,x_0)\right) = \frac{\|\chi(\tau,\chi(t,x_0))\|_r^{\varrho\nu}\tau^\varrho + \kappa_1}{\|\chi(\tau,\chi(t,x_0))\|_r^{\varrho\nu}\tau^\varrho + \kappa_2} = \frac{\|\chi(\tau+t,x_0))\|_r^{\varrho\nu}\tau^\varrho + \kappa_1}{\|\chi(\tau+t,x_0))\|_r^{\varrho\nu}\tau^\varrho + \kappa_2}$$

Then, for any $x_0 \in \mathbb{R}^n$, the function (A.9) satisfies

$$\begin{aligned} V(\chi(t,x_0)) &= \sup_{\tau\geq 0} \left\{ \|\chi(\tau,\chi(t,x_0))\|_r \, k\left(\tau,\chi(t,x_0)\right) \right\} \\ &= \sup_{\tau\geq 0} \left\{ \|\chi(\tau+t,x_0)\|_r \, \frac{\|\chi(\tau+t,x_0)\|_r^{\varrho\nu}\tau^\varrho + \kappa_1}{\|\chi(\tau+t,x_0)\|_r^{\varrho\nu}\tau^\varrho + \kappa_2} \right\} \\ &= \sup_{\tau\geq t} \left\{ \|\chi(\tau,x_0)\|_r \, \frac{\|\chi(\tau,x_0)\|_r^{\varrho\nu}(\tau-t)^\varrho + \kappa_1}{\|\chi(\tau,x_0)\|_r^{\varrho\nu}(\tau-t)^\varrho + \kappa_2} \right\} \\ &< \sup_{\tau\geq t} \left\{ \|\chi(\tau,x_0)\|_r \, \frac{\|\chi(\tau,x_0)\|_r^{\varrho\nu}\tau^\varrho + \kappa_1}{\|\chi(\tau,x_0)\|_r^{\varrho\nu}\tau^\varrho + \kappa_2} \right\} \\ &< \sup_{\tau\geq 0} \left\{ \|\chi(\tau,x_0)\|_r \, k(\tau,x_0) \right\} = V(x_0), \end{aligned}$$

where the strict inequality follows from the strict monotonicity of function k, i.e. $k(t_1, \cdot) < k(t_2, \cdot)$ for $t_1 < t_2$. The upper Dini derivative of $V(\chi(t, x_0))$ along a trajectory $\chi(t, x_0)$ at the point x_0 is given by

$$D^+V(x_0)F(x_0) = \limsup_{h \to 0^+} \frac{1}{h} \left[V(\chi(h, x_0)) - V(x_0)\right] ,$$

almost everywhere. Since the inequality $V(\chi(\tau, x_0)) < V(x_0)$ have been proven for any (small) $\tau > 0$, then $D^+V(x_0)F(x_0) < 0$ is deduced for almost all $x_0 \in \mathbb{R}^n \setminus \{0\}$. This concludes the proof of Theorem 3.2.

Appendix B

Analysis of stability of homogeneous systems in presence of parasitic dynamics: proofs

B.1 Proof of Theorem 4.3

Recall the system (4.10)-(4.11) given by

$$\dot{x} = f(x, y), \tag{B.1}$$

$$\epsilon\dot{y} = g(x, y), \tag{B.2}$$

where $x \in \mathbb{R}^n$ and $y \in \mathbb{R}^m$ are the state variables, $\epsilon > 0$ is a small parameter, and $f : \mathbb{R}^{n+m} \to \mathbb{R}^n$ and $g : \mathbb{R}^{n+m} \to \mathbb{R}^m$ are continuous vector fields ensuring forward existence and uniqueness of system trajectories. Moreover, for some vector of weights r and $\tilde{r}$ the vector fields f and g are $(r, \tilde{r})$-homogeneous of degree ν and μ, respectively.

Under a hypothesis like Assumption 4.1, the concepts of the singular perturbation theory aims to show that the behavior of the singularly perturbed system (B.1)-(B.2) is pretty similar to the behavior of the ROD

$$\dot{\bar{x}} = f(\bar{x}, h(\bar{x})), \tag{B.3}$$

such that, the presence of the PD (B.2) in the control loop can be neglected (see [Kokotovic et al., 1999] and references therein). Thus, the stability of the system (B.1)-(B.2) is warrantied by proving that the trajectories y of the PD converge to the equilibrium manifold $h(x)$. However, since the initial condition y_0 differs from the initial value $h(x_0)$, there exists a transitory response of the system (B.2) before the trajectories y can reach the desired behavior. Let's represent such a transitory by the variable z, such that, $y = z + h(x)$ and the system (B.1) is rewritten as

$$\dot{x} = f(x, z + h(x)). \tag{B.4}$$

It can be readily seen that if $z = 0$, the system (B.4) collapse to the ROD. Therefore, (global, local or practical) asymptotic stability of the origin of the system (B.4) can be concluded from ISS stability of the system (B.4) w.r.t. z, plus (global, local or practical) vanishing of z to zero.

First, let's investigate the ISS properties of the system (B.4) by using $V(x)$ as an ISS-LF candidate, which satisfies the inequalities:

$$V(x) = \lambda^{-\kappa} V(\Lambda_r(\lambda)x), \tag{B.5}$$

$$\underline{a}_x \|x\|_r^\kappa \leq V(x) \leq \bar{a}_x \|x\|_r^\kappa, \tag{B.6}$$

$$\tfrac{\partial V(x)}{\partial x} f(x, h(x)) \leq -b_x \|x\|_r^{\nu+\kappa}, \tag{B.7}$$

$$\sup_{\|x\|_r \leq 1} \| \tfrac{\partial V(x)}{\partial x} \| \leq c_x, \tag{B.8}$$

for all $x \in \mathbb{R}^n$ and for some $\underline{a}_x, \bar{a}_x, b_x, c_x > 0$, where $\kappa > \max\{0, -\nu\}$ is its HD.

So, the derivative of V along the trajectories of the system (B.4) is given by

$$\begin{aligned}\dot{V} =& \tfrac{\partial V(x)}{\partial x} f(x, z + h(x)) \\ =& \tfrac{\partial V(x)}{\partial x} f(x, h(x)) + \tfrac{\partial V(x)}{\partial x} \left(f(x, z + h(x)) - f(x, h(x)) \right).\end{aligned}$$

Since V is r homogeneous of degree κ and f is $r, \tilde{r}$-homogeneous of degree ν, by means of the dilations $\Lambda_r(\lambda)$ and $\Lambda_{\tilde{r}}(\lambda)$ where $\lambda = \|x\|_r^{-1}$, it is obtained

$$\begin{aligned}\dot{V} =& \tfrac{\partial V(x)}{\partial x} f(x, h(x)) + \|x\|_r^{\nu+\kappa} \tfrac{\partial V(\xi)}{\partial \xi} \left(f(\xi, \Lambda_{\tilde{r}}(\|x\|_r^{-1})z + h(\xi)) - f(\xi, h(\xi)) \right) \\ \leq& \tfrac{\partial V(x)}{\partial x} f(x, h(x)) + \|x\|_r^{\nu+\kappa} \left\| \tfrac{\partial V(\xi)}{\partial \xi} \right\| \left\| f(\xi, \Lambda_{\tilde{r}}(\|x\|_r^{-1})z + h(\xi)) - f(\xi, h(\xi)) \right\|,\end{aligned} \tag{B.9}$$

where $\xi = \Lambda_r(\|x\|_r^{-1})x$ and $\xi \in S_r(1)$.

Recall that by the continuity of $f(x, y)$ on the unit sphere, for any b_x, c_x and $0 < \theta < 1$, there exists δ, such that, if $\|\Lambda_{\tilde{r}}(\|x\|_r^{-1})z\|_{\tilde{r}} \leq \delta$, then

$$\|f(\xi, h(\xi) + \Lambda_{\tilde{r}}(\|x\|_r^{-1})z) - f(\xi, h(\xi))\| \leq \frac{\theta b_x}{c_x}, \tag{B.10}$$

for all $\xi \in S_r(1)$.

Therefore, substituting (B.7), (B.8) and (B.10) in (B.9), it can be concluded that

$$\begin{aligned}\dot{V} \leq& -b_x \|x\|_r^{\nu+\kappa} + \theta b_x \|x\|_r^{\nu+\kappa} \\ \leq& -(1-\theta) b_x \|x\|_r^{\nu+\kappa}, \quad \text{if} \quad \|x\|_r \geq \delta^{-1} \|z\|_{\tilde{r}},\end{aligned} \tag{B.11}$$

where $0 < \theta < 1$. According to Definition 4.2, $V(x)$ is an ISS-LF for the system (B.4) hence it is ISS w.r.t. input z. Moreover, from Definition 4.1, the solution $x(t)$ of the system (B.4) is bounded by

$$\|x(t)\|_r \leq \max\{\beta_1(\|x_0\|_r, t), \gamma_1(\sup_{\tau \in [0,t)} \|z(\tau)\|_{\tilde{r}})\}, \tag{B.12}$$

for all $t \geq 0$, where β_1 is a $\mathcal{KL}$ function and, from Definition 4.2, Remark 2.1 and inequalities (B.6) and (B.11), γ_1 is a $\mathcal{K}$ function given by

$$\gamma_1(s) = \delta^{-1}\frac{\bar{a}_x}{\underline{a}_x}s. \tag{B.13}$$

Now, let's investigate the scenarios where the transitory z vanishes to zero, such that, the convergence of the trajectories y to the desired behavior $h(x)$ can be concluded. The dynamics of the variable z is given by

$$\dot{z} = \tfrac{1}{\epsilon}g(x, z + h(x)) - \tfrac{\partial h(x)}{\partial x}f(x, z + h(x)), \tag{B.14}$$

where x can be seen as an input.

The stability of the system (B.14) can be proven by using $W(z, x)$ as an ISS-LF candidate, which satisfies the inequalities:

$$W(\Lambda_{\tilde{r}}(\lambda)z, \Lambda_r(\lambda)x) = \lambda^{\iota}W(z, x), \tag{B.15}$$

$$\underline{a}_z\|z\|_{\tilde{r}}^{\iota} \leq W(z, x) \leq \bar{a}_z\|z\|_{\tilde{r}}^{\iota}, \tag{B.16}$$

$$\tfrac{\partial W(z,x)}{\partial z}g(x, z + h(x)) \leq -b_z\|z\|_{\tilde{r}}^{\mu+\iota}, \tag{B.17}$$

$$\sup_{\substack{\|\zeta\|_{\tilde{r}}\leq 1\\ \|\xi\|_r\leq 1}} \left\| \tfrac{\partial W(\zeta,\xi)}{\partial \zeta} \right\| \leq c_z, \tag{B.18}$$

$$\sup_{\substack{\|\zeta\|_{\tilde{r}}\leq 1\\ \|\xi\|_r\leq 1}} \left\| \tfrac{\partial W(\zeta,\xi)}{\partial \xi} \right\| \leq d_z, \tag{B.19}$$

for all $z \in \mathbb{R}^m$, $x \in \mathbb{R}^n$ and for some $\underline{a}_z, \bar{a}_z, b_z, c_z, d_z > 0$, where $\iota > \max\{0, -\mu\}$ is its HD. So, the derivative of W along the trajectories of the system (B.14) is given by

$$\begin{aligned}\dot{W} =& \tfrac{\partial W(z,x)}{\partial z}\left(\tfrac{1}{\epsilon}g(x, z + h(x)) - \tfrac{\partial h(x)}{\partial x}f(x, z + h(x))\right) + \tfrac{\partial W(z,x)}{\partial x}f(x, z + h(x))\\ =& \tfrac{1}{\epsilon}\tfrac{\partial W(z,x)}{\partial z}g(x, z + h(x)) + \left(\tfrac{\partial W(z,x)}{\partial x} - \tfrac{\partial W(z,x)}{\partial z}\tfrac{\partial h(x)}{\partial x}\right)f(x, z + h(x)).\end{aligned} \tag{B.20}$$

By homogeneity of each component in (B.20), applying the dilations $\Lambda_r(\lambda^{-1})$ and $\Lambda_{\tilde{r}}(\lambda^{-1})$ where $\lambda = \max\{\|z\|_{\tilde{r}}, \|x\|_r\}$,

$$\begin{aligned}\dot{W} =& \tfrac{1}{\epsilon}\tfrac{\partial W(z,x)}{\partial z}g(x, z + h(x)) + \lambda^{\nu+\iota}\left(\tfrac{\partial W(\zeta,\xi)}{\partial \xi} - \tfrac{\partial W(\zeta,\xi)}{\partial \zeta}\tfrac{\partial h(\xi)}{\partial \xi}\right)f(\xi, \zeta + h(\xi))\\ \leq& \tfrac{1}{\epsilon}\tfrac{\partial W(z,x)}{\partial z}g(x, z + h(x)) + \lambda^{\nu+\iota}\left(\left\|\tfrac{\partial W(\zeta,\xi)}{\partial \xi}\right\| + \left\|\tfrac{\partial W(\zeta,\xi)}{\partial \zeta}\right\|\left\|\tfrac{\partial h(\xi)}{\partial \xi}\right\|\right)\|f(\xi, \zeta + h(\xi))\|,\end{aligned} \tag{B.21}$$

where $\xi = \Lambda_r^{-1}(\lambda)x$ and $\zeta = \Lambda_{\tilde{r}}^{-1}(\lambda)z$ (*i.e.*, $\xi \in B_r(1)$ and $\zeta \in B_{\tilde{r}}(1)$). Now, substituting (B.17), (B.18) and (B.19) in (B.21), we obtain

$$\dot{W} \leq -\tfrac{b_z}{\epsilon}\|z\|_{\tilde{r}}^{\mu+\iota} + b_z\eta\lambda^{\nu+\iota},$$

where

$$\eta = \frac{1}{b_z} \sup_{\substack{\xi \in B_r(1) \\ \zeta \in B_{\tilde{r}}(1)}} \left\{ \left(d_z + c_z \left\| \frac{\partial h(\xi)}{\partial \xi} \right\| \right) \| f(\xi, \zeta + h(\xi)) \| \right\}. \tag{B.22}$$

Then, for any $0 < \tilde{\theta} < 1$, we have

$$\dot{W} \leq -(1-\tilde{\theta}) \tfrac{b_z}{\epsilon} \|z\|_{\tilde{r}}^{\mu+\iota} - \tilde{\theta} \tfrac{b_z}{\epsilon} \|z\|_{\tilde{r}}^{\mu+\iota} + b_z \eta \max\{\|z\|_{\tilde{r}}^{\nu+\iota}, \|x\|_r^{\nu+\iota}\}.$$

Since $\max\{a, b\} \leq a + b$ for any $a, b \in \mathbb{R}_+$, the last expression can be rewritten as

$$\dot{W} \leq -(1-\tilde{\theta}) \tfrac{b_z}{\epsilon} \|z\|_{\tilde{r}}^{\mu+\iota} - \tfrac{(\tilde{\theta}_1+\tilde{\theta}_2) b_z}{\epsilon} \|z\|_{\tilde{r}}^{\mu+\iota} + b_z \eta \|z\|_{\tilde{r}}^{\nu+\iota} + b_z \eta \|x\|_r^{\nu+\iota},$$

where $\tilde{\theta}_1, \tilde{\theta}_2 > 0$ are such that $\tilde{\theta}_1 + \tilde{\theta}_2 = \tilde{\theta}$. Hence, if

$$\|z\|_{\tilde{r}}^{\mu+\iota} \geq \tfrac{\eta\epsilon}{\tilde{\theta}_2} \|x\|_r^{\nu+\iota}, \tag{B.23}$$

then

$$\dot{W} \leq -(1-\tilde{\theta}) \tfrac{b_z}{\epsilon} \|z\|_{\tilde{r}}^{\mu+\iota} - \tfrac{\tilde{\theta}_1 b_z}{\epsilon} \|z\|_{\tilde{r}}^{\mu+\iota} + b_z \eta \|z\|_{\tilde{r}}^{\nu+\iota},$$

and therefore the system (B.14) is

- ISS w.r.t. x, if $\mu = \nu$ and
$$\epsilon \leq \tfrac{\tilde{\theta}_1}{\eta}. \tag{B.24}$$
- locally ISS w.r.t. x, if $\mu < \nu$ and
$$\|z\|_{\tilde{r}} \leq \left(\tfrac{\tilde{\theta}_1}{\epsilon\eta} \right)^{\frac{1}{\nu-\mu}}. \tag{B.25}$$
- ISpS w.r.t. x, if $\mu > \nu$ and
$$\|z\|_{\tilde{r}} \geq \left(\tfrac{\epsilon\eta}{\tilde{\theta}_1} \right)^{\frac{1}{\mu-\nu}}. \tag{B.26}$$

Accordingly, from Definition 4.1, the trajectories of the system (B.14) are bounded by

$$\|z(t)\|_{\tilde{r}} \leq \max\{\beta_2(\|z_0\|_{\tilde{r}}, t), \gamma_2(\sup_{\tau \in [0,t)} \|x(\tau)\|_r), \rho\},$$

for all $t \geq 0$, where β_2 is a $\mathcal{KL}$ function, ρ is a constant given by $\rho = 0$ for $\mu \leq \nu$, and $\rho = \frac{\bar{a}_z}{\underline{a}_z} \left(\frac{\epsilon\eta}{\tilde{\theta}_1} \right)^{\frac{1}{\mu-\nu}}$ for $\mu > \nu$, also considering Definition 4.2, Remark 2.1 and inequalities (B.16) and (B.23), γ_2 is a class $\mathcal{K}$ function given by

$$\gamma_2(s) = \tfrac{\bar{a}_z}{\underline{a}_z} \left(\tfrac{\eta\epsilon}{\tilde{\theta}_2} s^{\nu+\iota} \right)^{\frac{1}{\mu+\iota}}. \tag{B.27}$$

Now, the systems (B.4) and (B.14) are interconnected. So, the internal stability of the interconnection can be investigated by using Theorem 4.2 (considering (4.9) for local behaviors). Likely, the functions

(B.13) and (B.27) are the nonlinear asymptotic gains for the systems (B.4) and (B.14), respectively. According to the small-gain condition (4.8) or (4.9), the stability of the interconnected system (B.4)-(B.14) is insured if the composition

$$\gamma_1(\gamma_2(s)) = \delta^{-1}\frac{\bar{a}_x\bar{a}_z}{\underline{a}_x\underline{a}_z}\left(\frac{\eta\epsilon}{\tilde{\theta}_2}s^{\nu+\iota}\right)^{\frac{1}{\mu+\iota}},$$

is a contraction, i.e., $\gamma_1(\gamma_2(s)) < s$, that is,

$$\delta^{-1}\frac{\bar{a}_x\bar{a}_z}{\underline{a}_x\underline{a}_z}\left(\frac{\eta\epsilon}{\tilde{\theta}_2}s^{\nu+\iota}\right)^{\frac{1}{\mu+\iota}} < s,$$

and

$$\frac{\epsilon\eta}{\tilde{\theta}_2\left(\delta\frac{\underline{a}_x\underline{a}_z}{\bar{a}_x\bar{a}_z}\right)^{\mu+\iota}} < s^{\mu-\nu}. \tag{B.28}$$

According to the HD's of the systems (B.1) and (B.2), from inequality (B.28) there are three different cases:

- For $\mu = \nu$, the system (B.4)-(B.14) is GAS if

$$\epsilon < \frac{\tilde{\theta}_2\left(\delta\frac{\underline{a}_x\underline{a}_z}{\bar{a}_x\bar{a}_z}\right)^{\mu+\iota}}{\eta}, \tag{B.29}$$

  which can be always guaranteed for a sufficiently small value of ϵ.

- For $\mu < \nu$, the system (B.4)-(B.14) is locally asymptotically stable if

$$\|x\|_r < \left(\frac{\tilde{\theta}_2\left(\delta\frac{\underline{a}_x\underline{a}_z}{\bar{a}_x\bar{a}_z}\right)^{\mu+\iota}}{\epsilon\eta}\right)^{\frac{1}{\nu-\mu}}, \tag{B.30}$$

- For $\mu > \nu$, the system (B.4)-(B.14) is practically GAS if

$$\|x\|_r > \left(\frac{\epsilon\eta}{\tilde{\theta}_2\left(\delta\frac{\underline{a}_x\underline{a}_z}{\bar{a}_x\bar{a}_z}\right)^{\mu+\iota}}\right)^{\frac{1}{\mu-\nu}}. \tag{B.31}$$

Finally, for the cases where $\nu \geq \mu$, vanishing of the transitory z can be concluded (at east locally), which warranties GAS (or local asymptotic stability) of the interconnected system (B.1)-(B.2) at the origin. However, for the case $\nu < \mu$ only practical stability can be proven, but since the system (B.4) is ISS w.r.t. z then the same property can be concluded for the MD (B.1) in presence of the PD (B.2).

The estimations (4.27), (4.28) and (4.30) are derived from inequalities (B.29)-(B.31), where (B.24) is also considered. Similarly, since $z = y - h(x)$ and $h(0) = 0$, the estimations (4.29) and (4.31) can be readily obtained from the composition $\gamma_2(\gamma_1(s)) < s$, where (B.25) and (B.26) are considered, too. Thus, Theorem 4.3 is proven.

Appendix C

Third-order Continuous Twisting Algorithm: proofs

C.1 Proof of Theorem 5.1

Consider the system (5.6), where the disturbance $\phi(t)$ satisfies $|\frac{d}{dt}\phi(t)| \leq \rho$, and the 3-CTA (5.7), where η is the integral term. Define $x_4 = \eta + \phi(t)$ as a virtual state, thus the closed-loop system (5.6)-(5.7) can be written as

$$\begin{array}{rcl} \dot{x}_1 & = & x_2 \\ \dot{x}_2 & = & x_3 \\ \dot{x}_3 & = & -k_1 L^{\frac{3}{4}} \lceil x_1 \rfloor^{\frac{1}{4}} - k_2 L^{\frac{2}{3}} \lceil x_2 \rfloor^{\frac{1}{3}} - k_3 L^{\frac{1}{2}} \lceil x_3 \rfloor^{\frac{1}{2}} + x_4 \\ \dot{x}_4 & \in & -k_4 L \lceil x_1 \rfloor^0 - k_5 L \lceil x_2 \rfloor^0 - k_6 L \lceil x_3 \rfloor^0 + [-\rho, \rho] \,, \end{array} \tag{C.1}$$

where $\lceil x_i \rfloor^0$ represents the set-valued sign function.

The system (C.1) has a r-homogeneous vector-set field of degree $p = -1$ and wights $r = [4, 3, 2, 1]$ for variables x_1, x_2, x_3 and x_4, respectively. Furthermore, the system (C.1) is multivalued, hence, its solutions are understood in the Filippov's sense (see [Filippov, 1988]).

Note that the origin is an equilibrium point for (C.1) if $x_2 = 0, x_3 = 0, -k_1 L^{\frac{3}{4}} \lceil x_1 \rfloor^{\frac{1}{4}} = x_4$ and

$$0 \in k_4 \lceil x_1 \rfloor^0 + [-k_5, k_5] + [-k_6, k_6] + [-\rho, \rho] \,. \tag{C.2}$$

Hence, $x_1 = 0$ is the unique solution of (C.2) iff $k_4 > |k_5| + |k_6| + \rho$. Otherwise, x_1 can take any value and the system (C.1) may have multiple equilibrium points. Therefore, the existence and uniqueness of an equilibrium point in the origin requires that $k_4 > |k_5| + |k_6| + \rho$ holds, as it is mentioned in Remark 5.1.

Let us scale the variables

$$x_1 = L z_1, \qquad x_2 = L z_2, \qquad x_3 = L z_3, \qquad x_4 = L z_4 \,, \tag{C.3}$$

where $L \in \mathbb{R}_+$. The system (C.1) in the new coordinates z can be rewritten as

$$\begin{array}{rcl} \dot{z}_1 & = & z_2 \\ \dot{z}_2 & = & z_3 \\ \dot{z}_3 & = & -k_1\lceil z_1\rfloor^{\frac{1}{4}} - k_2\lceil z_2\rfloor^{\frac{1}{3}} - k_3\lceil z_3\rfloor^{\frac{1}{2}} + z_4 \\ \dot{z}_4 & \in & -k_4\lceil x_1\rfloor^0 - k_5\lceil x_2\rfloor^0 - k_6\lceil x_3\rfloor^0 + \left[-\frac{\rho}{L}, \frac{\rho}{L}\right]. \end{array} \tag{C.4}$$

In [Mendoza-Avila et al., 2017] a LF candidate for the system (C.4) is proposed as

$$\begin{aligned} V_1(z) = \alpha_1|z_1|^{\frac{7}{4}} + \alpha_2|z_2|^{\frac{7}{3}} + \alpha_3|z_3|^{\frac{7}{2}} + \alpha_4|z_4|^7 + \alpha_5\lceil z_1\rfloor^{\frac{5}{4}} z_3 \\ + \alpha_6 z_1 z_2 + \alpha_7\lceil z_2\rfloor^{\frac{5}{3}} z_3 - \alpha_8 z_2\lceil z_4\rfloor^4 - \alpha_9 z_3 z_4^5 - \alpha_{10} z_1 z_4^3, \end{aligned} \tag{C.5}$$

where $\alpha_i;\ i = 1, ..., 10$ are the coefficients. The derivative of function (C.5) along the trajectories of the system (C.4) is given by

$$\begin{array}{rcl} \dot{V}_1(z) & \in & -W_1(z) + U_1(z)\left[-\frac{\rho}{L}, \frac{\rho}{L}\right], \\ & \leq & -\left(1 - \dfrac{U_1(z)}{W_1(z)}\dfrac{\rho}{L}\right) W_1(z), \end{array} \tag{C.6}$$

where $U_1(z)$ is a continuous function given by

$$U_1(z) = 3\alpha_{10} z_1 z_4^2 + 4\alpha_8 z_2|z_4|^3 + 5\alpha_9 z_3 z_4^4 - 7\alpha_4\lceil z_4\rfloor^6, \tag{C.7}$$

and $W_1(z)$ is the derivative of function (C.5) along the trajectories of the nominal system (C.4) (with $\phi(t) = 0$) given by

$$\begin{aligned} W_1(z) = \ & \alpha_5 k_1|z_1|^{\frac{3}{2}} + \alpha_5 k_2\lceil z_1\rfloor^{\frac{5}{4}} z_2^{\frac{1}{3}} - \alpha_5\lceil z_1\rfloor^{\frac{5}{4}} z_4 + \alpha_5 k_3\lceil z_1\rfloor^{\frac{5}{4}}\lceil z_3\rfloor^{\frac{1}{2}} - \alpha_6 z_1 z_3 \\ & -\tfrac{7}{4}\alpha_1\lceil z_1\rfloor^{\frac{3}{4}} z_2 - \beta_1 z_1 z_4^2 + \alpha_7 k_1\lceil z_1\rfloor^{\frac{1}{4}} z_2^{\frac{5}{3}} - \alpha_9 k_1\lceil z_1\rfloor^{\frac{1}{4}} z_4^5 + \tfrac{7}{2}\alpha_3 k_1\lceil z_1\rfloor^{\frac{1}{4}}\lceil z_3\rfloor^{\frac{5}{2}} \\ & -\tfrac{5}{4}\alpha_5|z_1|^{\frac{1}{4}} z_2 z_3 + \beta_2 z_2^2 + \alpha_7 k_3 z_2^{\frac{5}{3}}\lceil z_3\rfloor^{\frac{1}{2}} - \alpha_7 z_2^{\frac{5}{3}} z_4 - \tfrac{7}{3}\alpha_2\lceil z_2\rfloor^{\frac{4}{3}} z_3 - \beta_3 z_2 z_4^3 \\ & -\tfrac{5}{3}\alpha_7 z_2^{\frac{2}{3}} z_3^2 + \tfrac{7}{2}\alpha_3 k_2 z_2^{\frac{1}{3}}\lceil z_3\rfloor^{\frac{5}{2}} - \alpha_9 k_2 z_2^{\frac{1}{3}} z_4^5 + \tfrac{7}{2}\alpha_3 k_3|z_3|^3 - \tfrac{7}{2}\alpha_3\lceil z_3\rfloor^{\frac{5}{2}} z_4 \\ & -\beta_4 z_3 z_4^4 - \alpha_9 k_3\lceil z_3\rfloor^{\frac{1}{2}} z_4^5 + \beta_5 z_4^6, \end{aligned} \tag{C.8}$$

where $\beta_i;\ \ i = 1, \ldots, 5$ are

$$\begin{array}{rcl} \beta_1 & \triangleq & 3\alpha_{10}\left(k_4\lceil z_1\rfloor^0 + k_5\lceil z_2\rfloor^0 + k_6\lceil z_3\rfloor^0\right), \\ \beta_2 & \triangleq & \alpha_7 k_2 - \alpha_6, \\ \beta_3 & \triangleq & 4\alpha_8\left(k_4\lceil z_1\rfloor^0 + k_5\lceil z_2\rfloor^0 + k_6\lceil z_3\rfloor^0\right)\lceil z_4\rfloor^0 - \alpha_{10}, \\ \beta_4 & \triangleq & 5\alpha_9\left(k_4\lceil z_1\rfloor^0 + k_5\lceil z_2\rfloor^0 + k_6\lceil z_3\rfloor^0\right) - \alpha_8\lceil z_4\rfloor^0, \\ \beta_5 & \triangleq & 7\alpha_4\left(k_4\lceil z_1\rfloor^0 + k_5\lceil z_2\rfloor^0 + k_6\lceil z_3\rfloor^0\right)\lceil z_4\rfloor^0 + \alpha_9. \end{array}$$

Note that both functions (C.5) and (C.8) are GF's. Thus, following [Sánchez and Moreno, 2016, Sanchez and Moreno, 2019], the analysis of positive definiteness of (C.5) and (C.8) can be done through the analysis of positive definiteness of their associated forms $\{V_{1i}\}$ and $\{W_{1j}\}$, respectively, which can be studied by using the SOS representation [Parrilo, 2000] (see Section 5.1 for details). So, if every form in the sets $\{V_{1i}\}$ and $\{W_{1j}\}$ is positive definite, then the GF's (C.5) and (C.8) are positive definite, as needed.

From (5.1), the associated forms $\{V_{1i}\}$ and $\{W_{1j}\}$ of GF's (C.5) and (C.8) are obtained through the change of variables

$$|z_1| = y_1^8, \qquad |z_2| = y_2^6, \qquad |z_3| = y_3^4, \qquad |z_4| = y_4^2.$$

Usually, a SOS polynomial is only positive semi-definite. Then, consider the forms $\bar{V}_{1i}(y) = V_{1i}(y) - \epsilon_1(y_1^{14} + y_2^{14} + y_3^{14} + y_4^{14})$ and $\bar{W}_{1j}(y) = W_{1j}(y) - \epsilon_1(y_1^{12} + y_2^{12} + y_3^{12} + y_4^{12})$, such that, if they are SOS for some $\epsilon_1 > 0$ then the strict positive definiteness of every associated form in $\{V_{1i}\}$ and $\{W_{1j}\}$ is ensured.

Using SOSTOOLS [Prajna et al., 2002] we can find the coefficients of the associated form $\{V_{1i}\}$ by solving an LMI. However, in $\{W_{1j}\}$ gains k_i and coefficients α_i appear as products, making the problem bilinear. To overcome this problem we select *a priori* the gains k_i by simulation, and we only use SOSTOOLS to get the coefficients for both sets of the polynomials $\{V_{1i}\}$ and $\{W_{1j}\}$, simultaneously.

So, considering $\frac{\rho}{L} < \mu_c$; $\mu_c = 0.001$, $\epsilon_1 = 0.1$ and selecting the gains k_i of controller (5.7) as

$$\begin{array}{lll} k_1 = 1.3, & k_2 = 2.2, & k_3 = 3, \\ k_4 = 0.009, & k_5 = 0.004, & k_6 = 0.002, \end{array} \tag{C.9}$$

the coefficients α_i; $i = 0, \ldots, 10$ of function (C.5) are

$$\begin{array}{lllll} \alpha_1 = 202100 & \alpha_2 = 1225000 & \alpha_3 = 214400 & \alpha_4 = 213600 & \alpha_5 = 21077 \\ \alpha_6 = 268300 & \alpha_7 = 502400 & \alpha_8 = 254500 & \alpha_9 = 23933 & \alpha_{10} = 234100 \end{array} \tag{C.10}$$

such that all elements of $\{V_{1i}\}$ and $\{W_{1j}\}$ are positive definite. In consequence, by the continuity of functions (C.5) and (C.8) on the boundary between each hyper-octant, it is possible to conclude that this functions are also positive definite on every point of the state space.

Since $W_1(z)$ in (C.8) is positive definite, the fraction $\frac{U_1(z)}{W_1(z)}$ is well defined on $\mathbb{R}^n$. Besides, $W_1(z)$ in (C.8) and $U_1(z)$ in (C.7) are r-homogeneous of degree 6 then the fraction $\frac{U_1(z)}{W_1(z)}$ is r-homogeneous of degree 0, i.e.,

$$\frac{U_1(\Lambda_\lambda^r z)}{W_1(\Lambda_\lambda^r z)} = \lambda^0 \frac{U_1(z)}{W_1(z)} = \frac{U_1(z)}{W_1(z)}; \quad \forall z \in S_r(1),$$

Since the function $\frac{U_1(z)}{W_1(z)}$ is continuous on the sphere $S_r(1)$, which is a compact set, it follows from the Bolzano–Weierstrass theorem that there exists a maximum value $0 < \delta_c = \max_{S_r(1)} \frac{U_1(z)}{W_1(z)}$. Note that for homogeneous functions it is enough to obtain its values on the unit sphere $S_r(1)$ and the remaining values on $\mathbb{R}^n$ are recovered by applying the dilatation $\Lambda^r(\lambda)$. Finally, from (C.6) we have that if

Sample	V_{min}	$\dot{V}_{min}$
M_1	4402.3	1.2794
M_2	4402.7	0.761
M_3	4402.3	2.2962
M_4	4401.4	0.7306
M_5	4400.9	0.5196

Table C.1: Minimums of functions (C.5) and (C.8) taking 10^8 random points in the unit sphere.

$\mu_c < \frac{1}{\delta_c}$ and $W_1(z)$ is positive definite, then the inequality $\dot{V}_1(z) < 0$ holds. Thus, the following lemma is derived.

Lemma C.1. *Consider the system* (C.4) *with* $L_{min} > \frac{\rho}{\mu_c}$, *and the GF's* (C.5) *and* (C.8). *Then there exist gains* $k_1, k_2, k_3 \in \mathbb{R}_{>0}$, $k_4 > |k_5| + |k_6| + \rho > 0$, $k_5, k_6 \in \mathbb{R}$ *and coefficients* $\alpha_j \in \mathbb{R}$; $j = 1, ..., 10$ *such that* (C.5) *and* (C.8) *are positive definite functions for certain value of* μ_c. *Accordingly, the GF* (C.5) *is a LF for the system* (C.4). △

From Lemma C.1 and the direct Lyapunov theorem (see [Khalil, 2002]), we can concluded that the origin of the system (C.4) is a globally uniformly asymptotically stable equilibrium point. Moreover, the closed-loop system (C.4) has a negative homogeneity degree $p = -1$, hence, its origin is finite-time stable.

Taking into account that the diffeomorphism (C.3) is linear, the behavior of the trajectories of the system (C.4) is preserved in the original coordinates x for any value of L. It can be easily seen that the stability of the system (C.1) is ensured for an arbitrary bound of perturbation $\dot{\phi}(t)$ by selecting the scale factor as $L > \frac{\rho}{\mu_c}$; $\mu_c = 1 \times 10^{-3}$. Finally, Theorem 5.1 has been proved.

Numerical verification

An alternative and independent way to verify if homogeneous functions (C.5) and (C.8) with coefficients (C.10) and gains (C.9) are positive definite, is the evaluation of such functions within the unit sphere $\mathbb{S}$. If the minimum values of functions (C.5) and (C.8) in the unit sphere are positive then by homogeneous properties functions (C.5) and (C.8) are positive definite as well. Consider the change of coordinates

$$\begin{aligned} z_1 &= \Gamma \sin\varphi \sin\omega \cos\theta \\ z_2 &= \Gamma \sin\varphi \sin\omega \sin\theta \\ z_3 &= \Gamma \sin\varphi \cos\omega \\ z_4 &= \Gamma \cos\varphi. \end{aligned} \tag{C.11}$$

The ratio $\Gamma = 1$ is fixed and a sample of 10^8 points are randomly taken between the limits $0 \leq \omega \leq 2\pi$, $0 \leq \theta \leq 2\pi$ and $0 \leq \varphi \leq \pi$ for variables ω, θ and φ, respectively. After 5 iterations, the minimums V_{min} and $\dot{V}_{min}$ of functions (C.5) and (C.8), respectively, are shown in Table C.1.

C.2 Proof of Theorem 5.2

Consider the system (5.6), where the perturbation $\phi(t)$ satisfies $|\dot{\phi}(t)| < \rho$ for a unknown $\rho > 0$, and the 3-ACTA (5.9) where η is the integral term and the adaptive gain $L(t)$ is given by (5.10). Define the variable $x_4 = \eta + \phi(t)$, then the closed-loop system (5.6)-(5.9) is given by

$$\begin{array}{rcl} \dot{x}_1 & = & x_2 \\ \dot{x}_2 & = & x_3 \\ \dot{x}_3 & = & -k_1 L^{\frac{3}{4}}(t)\lceil x_1 \rfloor^{\frac{1}{4}} - k_2 L^{\frac{2}{3}}(t)\lceil x_2 \rfloor^{\frac{1}{3}} - k_3 L^{\frac{1}{2}}(t)\lceil x_3 \rfloor^{\frac{1}{2}} + x_4 \\ \dot{x}_4 & \in & -k_4 L(t)\lceil x_1 \rfloor^0 - k_5 L(t)\lceil x_2 \rfloor^0 - k_6 L(t)\lceil x_3 \rfloor^0 + [-\rho, \rho]\,. \end{array} \tag{C.12}$$

Taking some ideas presented in [Negrete and Moreno, 2014], finite-time stability of the origin of the closed-loop system (C.12) is proven as follows. Consider the change of variables

$$z_1 = \frac{x_1}{L(t)^{4q+1}}, \qquad z_2 = \frac{x_2}{L(t)^{3q+1}}, \qquad z_3 = \frac{x_3}{L(t)^{2q+1}}, \qquad z_4 = \frac{x_4}{L(t)^{q+1}}, \tag{C.13}$$

where $L(t) > 0 \forall t \geq 0$ and $q > 0$ to be selected. The system (C.12) in the new coordinates ζ is given by

$$\begin{array}{rcl} \dot{z}_1 & = & -(4q+1)\frac{\dot{L}(t)}{L(t)} z_1 + \frac{1}{L^q(t)} z_2 \\ \dot{z}_2 & = & -(3q+1)\frac{\dot{L}(t)}{L(t)} z_2 + \frac{1}{L^q(t)} z_3 \\ \dot{z}_3 & = & -(2q+1)\frac{\dot{L}(t)}{L(t)} z_3 - \frac{k_1}{L^q(t)}\lceil z_1 \rfloor^{\frac{1}{4}} - \frac{k_2}{L^q(t)}\lceil z_2 \rfloor^{\frac{1}{3}} - \frac{k_3}{L^q(t)}\lceil z_3 \rfloor^{\frac{1}{2}} + \frac{1}{L^q(t)} z_4 \\ \dot{z}_4 & \in & -(q+1)\frac{\dot{L}(t)}{L(t)} z_4 - \frac{k_4}{L^q(t)}\lceil z_1 \rfloor^0 - \frac{k_5}{L^q(t)}\lceil z_2 \rfloor^0 - \frac{k_6}{L^q(t)}\lceil z_3 \rfloor^0 + \left[-\frac{\rho}{L^{q+1}(t)}, \frac{\rho}{L^{q+1}(t)}\right]. \end{array} \tag{C.14}$$

Since the change of coordinates (C.13) is linear w.r.t. the state variables, if the states z_1, z_2, z_3, z_4 of system (C.14) converge to zero in finite-time, the states x_1, x_2, x_3, x_4 of system (C.12) will also converge to zero in finite-time.

Let us take the function (C.5) as a LF candidate for the system (C.14). The derivative of the function (C.5) along the trajectories of the system (C.14) is given by

$$\dot{V}(z) \leq -\left(1 - \frac{U(z)}{W(z)}\frac{\rho}{L(t)}\right)\frac{W(z)}{L^q(t)} - 7q\frac{\dot{L}(t)}{L(t)}H(z), \tag{C.15}$$

where $W(z)$ is given by (C.8), $U(z)$ is given by (C.7), and

$$\begin{array}{rcl} H(z) & = & (1+\frac{1}{4q})\alpha_1|z_1|^{\frac{7}{4}} + (1+\frac{1}{3q})\alpha_2|z_2|^{\frac{7}{3}} + (1+\frac{1}{2q})\alpha_3|z_3|^{\frac{7}{2}} + (1+\frac{1}{q})\alpha_4|z_4|^7 \\ & & +(1+\frac{9}{28q})\alpha_5\lceil z_1 \rfloor^{\frac{5}{4}} z_3 + (1+\frac{2}{7q})\alpha_6 z_1 z_2 + (1+\frac{8}{21q})\alpha_7\lceil z_2 \rfloor^{\frac{5}{3}} z_3 \\ & & -(1+\frac{6}{7q})\alpha_9 z_3 z_4^5 - \alpha_{10} z_1 z_4^3 - (1+\frac{5}{7q})\alpha_8 z_2\lceil z_4 \rfloor^4. \end{array} \tag{C.16}$$

For sufficiently large values of q, the coefficients of (C.16) are similar to the coefficients of (C.5), accordingly, by continuity of (C.5) w.r.t. its coefficients, if (C.5) is positive definite then function (C.16) is positive definite, as well.

Selecting the parameters $\alpha_j;\ \ j = 1,\dots,10$ and the gains $k_i;\ \ i = 1,\dots,6$, such that, they satisfy Lemma C.2, then $V(z)$ in (C.5) and $W(z)$ in (C.8) are positive definite functions. Then, by homogeneity arguments the inequality $W(z) \leq \epsilon_{max} V^{\frac{6}{7}}(z)$ holds. Therefore, inequality (C.15) becomes

$$\dot{V}(z) \leq -\epsilon_{max}\left(1 - \frac{U(z)}{W(z)}\frac{\rho}{L(t)}\right)\frac{V^{\frac{6}{7}}(z)}{L^q(t)} - 7q\frac{\dot{L}(t)}{L(t)}V(z), \tag{C.17}$$

By its definition $L(t) > 0$ and $\dot{L}(t) \geq 0$ for all $t > 0$, and $L(0) > 0$ and $\dot{L}(0) > 0$ (see equation (5.10)), hence the second term on the right-hand side of the latter expression is negative definite. Furthermore, since $V(z)$ is r-homogeneous of degree 7 (see equation (C.5)), the second term dominates the first one for all z outside of the unit ball, i.e., for all $z \notin B_r(1)$. On the other hand, due to $L(t)$ is an increasing function in time then there exist a finite time $T \geq 0$ from which $L(t) > \delta_c\rho$, where $0 < \delta_c = \max_{\mathbb{S}} \frac{U(z)}{W(z)}$, making the first term on the right-hand side of inequality (C.17) negative definite, and the inequality $\dot{V}(z) < 0$ holds for all $t \geq T$ and $z \in \mathbb{R}^n$. If $t < T$ and $z \in B_r(1)$, then inequality (C.17) can be positive but the solutions of closed-loop system (C.14) cannot escape to infinity in finite-time because the negative definiteness of (C.17) is warrantied outside of the unit ball for all $t \geq 0$.

Finally, we conclude that function (C.5) is positive definite and function (C.15) is negative definite, hence the states of the system (C.14) converge to zero and it means that the states of system (C.12) converge to zero too. Therefore, Theorem 5.2 is proven.

C.3 Proof of Theorem 5.3

Consider the system (5.6), where the perturbation term $\phi(t)$ satisfies $|\dot{\phi}(t)| \leq \rho$ and $\sigma = x_1$ is a measurable output. Moreover, consider the observer (5.17), where ζ is a discontinuous term. Now, define the observation errors:

$$e_1 = \hat{x}_1 - x_1, \quad e_2 = \hat{x}_2 - x_2, \quad e_1 = \hat{x}_3 - x_3, \quad e_4 = \epsilon - \phi(t), \tag{C.18}$$

such that, the error dynamics is given by

$$\begin{array}{rcl} \dot{e}_1 & = & -\lambda_1 H^{\frac{1}{4}}\lceil e_1 \rfloor^{\frac{3}{4}} + e_2 \\ \dot{e}_2 & = & -\lambda_2 H^{\frac{2}{4}}\lceil e_1 \rfloor^{\frac{2}{4}} + e_3 \\ \dot{e}_3 & = & -\lambda_3 H^{\frac{3}{4}}\lceil e_1 \rfloor^{\frac{1}{4}} + e_4 \\ \dot{e}_4 & \in & -\lambda_4 H\lceil e_1 \rfloor^0 - [-\rho, \rho]. \end{array} \tag{C.19}$$

where $\lceil x_i \rfloor^0$ represents the set-valued sign function. Moreover, the solutions of the system (C.19) are understood in the Filippov's sense (see [Filippov, 1988]).

Applying the change of variables

$$e_1 = H\xi_1, \qquad e_2 = H\xi_2, \qquad e_3 = H\xi_3, \qquad e_4 = H\xi_4, \tag{C.20}$$

to the system (C.19) we obtain

$$\begin{array}{rcl} \dot{\xi}_1 & = & -\lambda_1 \lceil \xi_1 \rfloor^{\frac{3}{4}} + \xi_2 \\ \dot{\xi}_2 & = & -\lambda_2 \lceil \xi_1 \rfloor^{\frac{2}{4}} + \xi_3 \\ \dot{\xi}_3 & = & -\lambda_3 \lceil \xi_1 \rfloor^{\frac{1}{4}} + \xi_4 \\ \dot{\xi}_4 & \in & -\lambda_4 \lceil \xi_1 \rfloor^{0} - [-\frac{\rho}{H}, \frac{\rho}{H}]. \end{array} \tag{C.21}$$

The system (C.19) has an homogeneous vector-set field of degree $p = -1$ and weights $r = [4, 3, 2, 1]$ for variables ξ_1, ξ_2, ξ_3 and ξ_4, respectively.

Following [Cruz-Zavala and Moreno, 2018] (see also [Sanchez et al., 2017a]), a LF for the arbitrary order Levant's differentiator is given by

$$V_{RED}(\xi) = \sum_{j=1}^{n-1} a_j \Xi_j(\xi_j, \xi_{j+1}) + a_n \tfrac{1}{p} |\xi_n|^p, \tag{C.22}$$

with coefficients $a_i > 0, \quad i = 1, \ldots, n$, and

$$\Xi_i(\xi_i, \xi_{i+1}) = \tfrac{r_i}{p} |\xi_i|^{\frac{p}{r_i}} - \xi_i \lceil \xi_{i+1} \rfloor^{\frac{p-r_i}{r_{i+1}}} + \tfrac{p-r_i}{p} |\xi_{i+1}|^{\frac{p}{r_{i+1}}}$$

where $p \geq r_1 + r_2$ is the homogeneity degree of function (C.22) and r_i are the weights of variables ξ_i.

According to equation (C.22), a stability analysis and gains design for the system (C.21) can be performed by using the LF

$$\begin{aligned} V_2(\xi) = \tfrac{4}{7} a_1 |\xi_1|^{\frac{7}{4}} - a_1 \xi_1 \xi_2 + \tfrac{3}{7}(a_1 + a_2) |\xi_2|^{\frac{7}{3}} - a_2 \xi_2 \lceil \xi_3 \rfloor^2 \\ + \tfrac{2}{7}(2a_2 + a_3) |\xi_3|^{\frac{7}{2}} - a_3 \xi_3 \xi_4^5 + \tfrac{1}{7}(5a_3 + a_4) |\xi_4|^7, \end{aligned} \tag{C.23}$$

where $a_i > 0, \quad i = 1, \ldots, 4$; are positive constants. The derivative of function (C.23) along the trajectories of system (C.21) is given by

$$\begin{array}{rcl} \dot{V}_2(z) & \in & -W_2(z) + U_2(z) \left[-\frac{\rho}{H}, \frac{\rho}{H}\right] \\ & \leq & -\left(1 - \dfrac{U_2(z)}{W_2(z)} \dfrac{\rho}{H}\right) W_2(z), \end{array}$$

where $U_2(z)$ is a continuous function given by

$$U_2(z) = -5a_3 \xi_3 \xi_4^4 + (5a_3 + a_4) \xi_4^6, \tag{C.24}$$

and $W_2(z)$ is the derivative of function (C.23) along the trajectories of nominal system (C.21) (with $\phi(t) = 0$) given by

$$\begin{array}{rcl} W_2(\xi) & = & a_1(\lambda_1 - \lambda_2) |\xi_1|^{\frac{3}{2}} - a_1(1 + \lambda_1) \lceil \xi_1 \rfloor^{\frac{3}{4}} \xi_2 + a_1 \xi_1 \xi_3 + (a_1 + a_2) \lambda_2 \lceil \xi_1 \rfloor^{\frac{1}{2}} \lceil \xi_2 \rfloor^{\frac{4}{3}} \\ & & + (2a_2 + a_3) \lambda_3 \lceil \xi_1 \rfloor^{\frac{1}{4}} \lceil \xi_3 \rfloor^{\frac{5}{2}} - a_3 \lambda_3 \lceil \xi_1 \rfloor^{\frac{1}{4}} \xi_4^5 - a_2 \lambda_2 \lceil \xi_1 \rfloor^{\frac{1}{2}} \lceil \xi_3 \rfloor^2 + a_1 \xi_2^2 \\ & & - (a_1 + a_2) \lceil \xi_2 \rfloor^{\frac{4}{3}} \xi_3 + 2a_2 \xi_2 |\xi_3| \xi_4 + a_2 |\xi_3|^3 - (2a_2 + a_3) \lceil \xi_3 \rfloor^{\frac{5}{2}} \xi_4 \\ & & - 2a_2 \lambda_3 \lceil \xi_1 \rfloor^{\frac{1}{4}} \xi_2 |\xi_3| - 5a_3 (\lambda_4 \lceil \xi_1 \rfloor^0) \xi_3 \xi_4^4 + (a_3 + \lambda_4 (5a_3 + a_4) \lceil \xi_1 \rfloor^0 \lceil \xi_4 \rfloor^0) \xi_4^6. \end{array} \tag{C.25}$$

From results presented in [Cruz-Zavala and Moreno, 2018], for any positive coefficients $a_j > 0;\ \ j = 1,\dots,4$ there exist gains $\lambda_i;\ \ i = 1,\dots,4$ such that functions (C.23) and (C.25) are positive definite.

Suitable values of $\lambda_i;\ \ i = 1,\dots,4$ can be computed by using SOSTOOLS [Prajna et al., 2002]. For this, consider the functions $\bar{V}_2(\zeta) = V_2(\zeta) - \epsilon_3(\zeta_1^{14} + \zeta_2^{14} + \zeta_3^{14} + \zeta_4^{14}) \geq 0$ and $\bar{W}_2(\zeta) = W_2(\zeta) - \epsilon_3(\zeta_1^{12} + \zeta_2^{12} + \zeta_3^{12} + \zeta_4^{12}) \geq 0$, with $\epsilon_3 = 1$. Now, recall the change of variables (5.1) in Section 5.1. By applying the change of variables

$$|\xi_1| = \zeta_1^8, \qquad |\xi_2| = \zeta_2^6, \qquad |\xi_3| = \zeta_3^4, \qquad |\xi_4| = \zeta_4^2.$$

to functions $\bar{V}_2(\zeta)$ and $\bar{W}_2(\zeta)$, we obtain the sets of associated forms $\{\bar{V}_{2i}\}$ and $\{\bar{W}_{2j}\}$ $i,j = 1,\dots,16$, respectively. Thus, by means of SOSTOOLS we evaluate the sets of associated forms $\{\bar{V}_{2i}\}$ and $\{\bar{W}_{2j}\}$ $i,j = 1,\dots,16$ with the coefficients a_i as

$$a_1 = 134.5, \quad a_2 = 232.2, \quad a_3 = 220.2, \quad a_4 = 231.3, \tag{C.26}$$

and $\mu_o = 0.01$, and we obtain the gains λ_i as

$$\lambda_1 = 4.5, \qquad \lambda_2 = 2.4, \qquad \lambda_3 = 0.8, \qquad \lambda_4 = 0.1, \tag{C.27}$$

such that, every form in the sets $\{\bar{V}_{2i}\}$ and $\{\bar{W}_{2j}\}$ is a SOS. Hence, functions (C.23) and (C.25) are strictly positive definite.

Since $W_2(z)$ and $U_2(z)$ are r-homogeneous of degree 6, the fraction $\frac{U_2(z)}{W_2(z)}$ is r-homogeneous of degree 0, hence all its values are contained on the unit sphere $S_r(1)$ which is a compact set. So, there exists a maximum value $0 < \delta_o = \max_{S_r(1)} \frac{U_1(z)}{W_1(z)}$. Accordingly, if $\mu_o < \frac{1}{\delta_o}$ and $W_2(z)$ is positive definite, then the inequality $\dot{V}_2(z) < 0$ holds.

Lemma C.2. *Let system* (C.21) *with* $H_{min} > \frac{|\dot{\phi}(t)|}{\mu_o}$, *and* $V_3(\xi) : \mathbb{R}^4 \to \mathbb{R}$ *a homogeneous function of degree* $p = 7$ *given by* (C.23). *For any coefficients* $a_j > 0;\ \ j = 1,\dots,4$ *and certain value* μ_o, *there exist gains* $\lambda_i;\ \ i = 1,\dots,4$ *(e.g.* (C.27)*) such that* (C.23) *is a LF for the 3-RED in* (C.21). △

Since function (C.23) is a LF for the system (C.21), its origin $\xi = 0$ is asymptotically stable. Furthermore, the change of variables (C.20) is linear, therefore, for any value of H the asymptotic stability of the origin $e = 0$ of the system (C.19) is ensured, as well. Moreover, the system (C.19) has a negative homogeneity degree, hence, its trajectories exhibit finite-time convergence to zero. Finally, the proof of Theorem 5.3 is completed.

C.4 Proof of Theorem 5.4

Consider the system (5.6), where the perturbation term $\phi(t)$ satisfies $|\dot{\phi}(t)| \leq \rho$ and $\sigma = x_1$ is a measurable output. Also, consider the controller (5.18). The closed-loop system (5.6)-(5.18) can be

written as

$$\begin{aligned}
\dot{x}_1 &= x_2\\
\dot{x}_2 &= x_3\\
\dot{x}_3 &= -k_1 L^{\frac{3}{4}} \lceil x_1 \rfloor^{\frac{1}{4}} - k_2 L^{\frac{2}{3}} \lceil x_2 + e_2 \rfloor^{\frac{1}{3}} - k_3 L^{\frac{1}{2}} \lceil x_3 + e_3 \rfloor^{\frac{1}{2}} + x_4\\
\dot{x}_4 &= -k_4 L \lceil x_1 \rfloor^0 - k_5 L \lceil x_2 + e_2 \rfloor^0 - k_6 L \lceil x_3 + e_3 \rfloor^0 + \dot{\phi}(t)\\
\dot{e}_1 &= -\lambda_1 H^{\frac{1}{4}} \lceil e_1 \rfloor^{\frac{3}{4}} + e_2\\
\dot{e}_2 &= -\lambda_2 H^{\frac{2}{4}} \lceil e_1 \rfloor^{\frac{2}{4}} + e_3\\
\dot{e}_3 &= -\lambda_3 H^{\frac{3}{4}} \lceil e_1 \rfloor^{\frac{1}{4}} + e_4\\
\dot{e}_4 &= -\lambda_4 H \lceil e_1 \rfloor^0.
\end{aligned} \tag{C.28}$$

where $x_4 = \eta + \phi(t)$ and $e_i;\ i = 1, 2, 3, 4$ are given by (C.18). The solutions of the system (C.28) are defined in the Filippov's sense [Filippov, 1988]. Now, define the new variables

$$z_1 = x_1, \qquad z_2 = x_2 + e_2, \qquad z_3 = x_3 + e_3, \qquad z_4 = x_4,$$

such that, the closed-loop system (C.28) in the new coordinates z is given by

$$\begin{aligned}
\dot{z}_1 &= z_2 - e_2\\
\dot{z}_2 &= z_3 - \lambda_2 H^{\frac{2}{4}} \lceil e_1 \rfloor^{\frac{2}{4}}\\
\dot{z}_3 &= -k_1 L^{\frac{3}{4}} \lceil z_1 \rfloor^{\frac{1}{4}} - k_2 L^{\frac{2}{3}} \lceil z_2 \rfloor^{\frac{1}{3}} - k_3 L^{\frac{1}{2}} \lceil z_3 \rfloor^{\frac{1}{2}} + z_4 - \lambda_3 H^{\frac{3}{4}} \lceil e_1 \rfloor^{\frac{1}{4}} + e_4\\
\dot{z}_4 &= -k_4 L \lceil z_1 \rfloor^0 - k_5 L \lceil z_2 \rfloor^0 - k_6 L \lceil z_3 \rfloor^0 + \dot{\phi}(t)\\
\dot{e}_1 &= -\lambda_1 H^{\frac{1}{4}} \lceil e_1 \rfloor^{\frac{3}{4}} + e_2\\
\dot{e}_2 &= -\lambda_2 H^{\frac{2}{4}} \lceil e_1 \rfloor^{\frac{2}{4}} + e_3\\
\dot{e}_3 &= -\lambda_3 H^{\frac{3}{4}} \lceil e_1 \rfloor^{\frac{1}{4}} + e_4\\
\dot{e}_4 &= -\lambda_4 H \lceil e_1 \rfloor^0.
\end{aligned} \tag{C.29}$$

The system (C.29) has a homogeneous vector-set field of degree $k = -1$ and weights $\mathbf{r} = [4, 3, 2, 1, 4, 3, 2, 1]^T$ for the extended state $\psi = [z^T, e^T]$. Moreover, the system (C.29) is a cascade connection of the system (C.1) and the system (C.19).

From Lemmas C.1 and C.2, LF's for the systems (C.1) and (C.19) are given by (C.5) and (C.23), respectively. Thus, a LF candidate for (C.29) can be proposed as

$$V(\psi) = V_1(z) + \gamma V_2(e), \qquad \gamma \in \mathbb{R}_{>0}, \tag{C.30}$$

where V_1 and V_2 are given by (C.5) and (C.23), respectively. Note that V is positive definite for any $\gamma > 0$. The derivative of V along the trajectories of the system (C.29) satisfies the following inequality

$$\dot{V} \leq \dot{V}_1(z) + |S(\psi)| + \gamma \dot{V}_2(e), \tag{C.31}$$

where $\dot{V}_1(z)$ is the derivative of V_1 along the trajectories of the system (C.1), $\dot{V}_2(e)$ is the derivative of V_2 along the trajectories of the system (C.19) and $S(\psi)$ is given by

$$\begin{aligned}
S(\psi) = \ & (\tfrac{7}{4}\alpha_1 \lceil x_1 \rfloor^{\frac{3}{4}} + \tfrac{5}{4}\alpha_5 |x_1|^{\frac{1}{4}} x_3 + \alpha_6 x_2 - \alpha_{10} x_4^3) e_2 + (\tfrac{7}{3}\alpha_2 \lceil x_2 \rfloor^{\frac{4}{3}}\\
& + \alpha_6 x_1 + \tfrac{5}{3}\alpha_7 |x_2|^{\frac{2}{3}} x_3 - \alpha_8 \lceil x_4 \rfloor^4) \lambda_2 H^{\frac{2}{4}} \lceil e_1 \rfloor^{\frac{1}{2}} + (\tfrac{7}{2}\alpha_3 \lceil x_3 \rfloor^{\frac{5}{2}}\\
& + \alpha_5 \lceil x_1 \rfloor^{\frac{5}{4}} + \alpha_7 \lceil x_2 \rfloor^{\frac{5}{3}} x_3 - \alpha_9 x_4^5)(\lambda_3 H^{\frac{3}{4}} \lceil e_1 \rfloor^{\frac{1}{4}} - e_4).
\end{aligned} \tag{C.32}$$

Now, define $W_1(z) = -\dot{V}_1(z)$ and $W_2(e) = -\dot{V}_2(e)$, which are positive definite and $\mathbf{r}$-homogeneous functions of degree 6. Then, from [Bhat and Bernstein, 2005] (see Lemma 4.2) there exist the constants $\mu_1, \mu_2 \in \mathbb{R}_{>0}$ such that the inequalities $\mu_1 V_1^{\frac{6}{7}}(z) < W_1(z)$, and $\mu_2 V_2^{\frac{6}{7}}(z) < W_2(z)$ hold.

Moreover,

$$|S(\psi)| \leq g_1(z)h_1(e) + g_2(z)h_2(e) + g_3(z)h_3(e)$$

, where

$$\begin{aligned}
g_1(z) &= |\tfrac{7}{4}\alpha_1 \lceil x_1 \rfloor^{\frac{3}{4}} + \tfrac{5}{4}\alpha_5 |x_1|^{\frac{1}{4}} x_3 + \alpha_6 x_2 - \alpha_{10} x_4^3|,\\
g_2(z) &= |\tfrac{7}{3}\alpha_2 \lceil x_2 \rfloor^{\frac{4}{3}} + \alpha_6 x_1 + \tfrac{5}{3}\alpha_7 |x_2|^{\frac{2}{3}} x_3 - \alpha_8 \lceil x_4 \rfloor^4|,\\
g_3(z) &= |\tfrac{7}{2}\alpha_3 \lceil x_3 \rfloor^{\frac{5}{2}} + \alpha_5 \lceil x_1 \rfloor^{\frac{5}{4}} + \alpha_7 \lceil x_2 \rfloor^{\frac{5}{3}} x_3 - \alpha_9 x_4^5|,\\
h_1(e) &= |e_2|,\\
h_2(e) &= |\lambda_2 H^{\frac{1}{2}} \lceil x_1 \rfloor^{\frac{1}{2}}|,\\
h_3(e) &= |\lambda_3 H^{\frac{3}{4}} \lceil x_1 \rfloor^{\frac{1}{4}} - e_4|,
\end{aligned}$$

Since g_1, g_2 and g_3 are continuous, positive semi-definite and $\mathbf{r}$-homogeneous functions of degree 3, 4 and 5, respectively, and h_1, h_2 and h_3 are also continuous, positive semi-definite and $\mathbf{r}$-homogeneous functions of degree 3, 2 and 1, respectively.

From Lemma 4.2 in [Bhat and Bernstein, 2005], it follows $g_1(z) \leq \epsilon_1 V_1^{\frac{3}{7}}(z)$, $g_2(z) \leq \epsilon_2 V_1^{\frac{4}{7}}(z)$, $g_3(z) \leq \epsilon_3 V_1^{\frac{5}{7}}(z)$, $h_1(e) \leq \epsilon_4 V_2^{\frac{3}{7}}(z)$, $h_2(e) \leq \epsilon_5 V_2^{\frac{2}{7}}(z)$ and $h_3(e) \leq \epsilon_6 V_2^{\frac{1}{7}}(z)$, for some $\epsilon_1, \ldots, \epsilon_6 \in \mathbb{R}_{>0}$. Therefore,

$$|S(\psi)| \leq \mu_3 V_1^{\frac{3}{7}} V_2^{\frac{3}{7}} + \mu_4 V_1^{\frac{4}{7}} V_2^{\frac{2}{7}} + \mu_5 V_1^{\frac{5}{7}} V_2^{\frac{1}{7}},$$

where $\mu_3 = \epsilon_1\epsilon_4$, $\mu_4 = \epsilon_2\epsilon_5$ and $\mu_5 = \epsilon_3\epsilon_6$. Then, inequality (C.31) can be rewritten as

$$\dot{V} \leq -\mu_1 V_1^{\frac{6}{7}}(z) + \mu_3 V_1^{\frac{3}{7}} V_2^{\frac{3}{7}} + \mu_4 V_1^{\frac{4}{7}} V_2^{\frac{2}{7}} + \mu_5 V_1^{\frac{5}{7}} V_2^{\frac{1}{7}} - \gamma\mu_2 V_2^{\frac{6}{7}}(e). \tag{C.33}$$

Recall the Young's inequality, where for any $a, b, c \in \mathbb{R}_{>0}$ and $p, q > 1$ satisfying $\frac{1}{p} + \frac{1}{q} = 1$, we have $ab \leq \frac{c^p}{p} a^p + \frac{c^{-q}}{q} b^q$.

Thus, for any $c_1, c_2, c_3 > 0$, the inequalities

$$\begin{aligned}
V_1^{\frac{3}{7}} V_2^{\frac{3}{7}} &\leq \tfrac{c_1^2}{2} V_1^{\frac{6}{7}} + \tfrac{1}{2c_1^2} V_2^{\frac{6}{7}},\\
V_1^{\frac{4}{7}} V_2^{\frac{2}{7}} &\leq \tfrac{2c_2^{3/2}}{3} V_1^{\frac{6}{7}} + \tfrac{1}{3c_2^3} V_2^{\frac{6}{7}},\\
V_1^{\frac{5}{7}} V_2^{\frac{1}{7}} &\leq \tfrac{5c_3^{6/5}}{6} V_1^{\frac{6}{7}} + \tfrac{1}{6c_3^6} V_2^{\frac{6}{7}},
\end{aligned}$$

hold. Hence, $\dot{V} \leq \kappa_1 V_1^{\frac{6}{7}} + \kappa_2 V_2^{\frac{6}{7}}$ where

$$\begin{aligned}
\kappa_1 &= -\mu_1 + \tfrac{\mu_3 c_1^2}{2} + \tfrac{2\mu_4 c_2^{3/2}}{3} + \tfrac{5\mu_5 c_3^{6/5}}{6}\\
\kappa_2 &= -\gamma\mu_2 + \tfrac{\mu_3}{2c_1^2} + \tfrac{\mu_4}{3c_2^3} + \tfrac{\mu_5}{6c_3^6}.
\end{aligned}$$

Now, selecting $c_2 = c_1^{4/3}$ and $c_3 = c_1^{5/3}$ then

$$\begin{array}{rcl} \kappa_1 & = & -\mu_1 + \frac{c_1^2}{6}\left(3\mu_3 + 4\mu_4 + 5\mu_5\right) \\ \kappa_2 & = & -\gamma\mu_2 + \frac{1}{6c_1^{10}}\left(3\mu_3 c_1^8 + 2\mu_4 c_1^6 + \mu_5\right). \end{array}$$

Note that $\kappa_1 < 0$ if

$$c_1 < \sqrt{\frac{6\mu_1}{3\mu_3+4\mu_4+5\mu_5}}$$

and $\kappa_2 < 0$ if

$$\gamma > \frac{1}{6\mu_2 c_1^{10}}\left(3\mu_3 c_1^8 + 2\mu_4 c_1^6 + \mu_5\right).$$

Therefore, $\dot{V}$ is negative definite, so that, $\psi = 0$ is an asymptotically stable equilibrium point of the system (C.29). Due to the negative homogeneity degree of the system (C.29), finite-time stability is concluded. Thus, Theorem 5.4 is proven.

Appendix D

Design of a PID-like controller based on Discontinuous Integral Control: proofs

D.1 Proof of Lemma 6.1

GAS of the ideal model (6.8), with the set of gains proposed by Propositions 6.3 and 6.4, can be studied by means of the design of a LF. With this aim let's follow the GF approach presented by [Sanchez and Moreno, 2019]. See Section 5.1 in Chapter 5 for some details about this methodology.

Let us recall the system (6.8):

$$\begin{aligned} \dot{x}_1 &= x_2\,, \\ \dot{x}_2 &= -k_1\lceil x_1\rfloor^{1/3} - k_2\lceil x_2\rfloor^{1/2} + x_3\,, \\ \dot{x}_3 &= -k_3\lceil x_1\rfloor^{0} + \dot{f}\,. \end{aligned} \tag{D.1}$$

Note that the system (D.1) has a r-homogeneous vector-set field of degree $p = -1$ and wights $r = [3, 2, 1]$ for variables x_1, x_2 and x_3, respectively (see Chapter 2 for detail about homogeneity). Furthermore, the system (D.1) is discontinuous, hence, its solutions are understood in the Filippov's sense (see [Filippov, 1988]).

A LF candidate for the system (D.1) is given by Lemma 6.1 as

$$\begin{aligned} V(x) = \alpha_1|x_1|^{\frac{7}{3}} + \alpha_2|x_2|^{\frac{7}{2}} + \alpha_3|x_3|^{7} + \alpha_4\lceil x_1\rfloor^{\frac{5}{3}}x_2 + \alpha_5|x_1|x_2^2 \\ + \alpha_6 x_1\lceil x_3\rfloor^{4} + \alpha_7|x_1|^{\frac{5}{3}}x_3^2 + \alpha_8 x_2 x_3^5 + \alpha_9|x_2|^{\frac{3}{2}}x_3^4. \end{aligned} \tag{D.2}$$

So, the derivative of function (D.2) along the trajectories of the system (D.1) (where $|\dot{f}| < L$) is given by

$$\dot{V}(x) \in -\sigma(x) + \psi(x)\,[-L, L] \tag{D.3}$$

$$\leq -\left(1 - \frac{\psi(x)}{\sigma(x)}L\right)\sigma(x), \tag{D.4}$$

where $\psi(x)$ is a continuous function given by

$$\psi(x) \;=\; 7\alpha_3\lceil x_3\rfloor^6 + 4\alpha_6 x_1|x_3|^3 + 5\alpha_8 x_2 x_3^4 + 2\alpha_7|x_1|^{\frac{5}{3}}x_3 + 4\alpha_9|x_2|^{\frac{3}{2}}x_3^3, \tag{D.5}$$

and $\sigma(x)$ is the derivative of function (D.2) along the trajectories of the unperturbed system (D.1), i.e., considering $f = 0$, which is given by

$$\begin{aligned}\sigma(x) = \;& \alpha_4 k_1 x_1^2 + \alpha_4 k_2\lceil x_1\rfloor^{\frac{5}{3}}\lceil x_2\rfloor^{\frac{1}{2}} + (2\alpha_7 k_3 - \alpha_4)\lceil x_1\rfloor^{\frac{5}{3}}x_3 + (2\alpha_5 k_1 \\ & -\tfrac{7}{3}\alpha_1)\lceil x_1\rfloor^{\frac{4}{3}}x_2 + 2\alpha_5 k_2|x_1||x_2|^{\frac{3}{2}} + 4\alpha_6 k_3|x_1||x_3|^3 - 2\alpha_5|x_1|x_2x_3 \\ & -\tfrac{5}{3}\alpha_7\lceil x_1\rfloor^{\frac{2}{3}}x_2x_3^2 + \tfrac{7}{2}\alpha_2 k_1\lceil x_1\rfloor^{\frac{1}{3}}\lceil x_2\rfloor^{\frac{5}{2}} + \tfrac{3}{2}\alpha_9 k_1\lceil x_1\rfloor^{\frac{1}{3}}\lceil x_2\rfloor^{\frac{1}{2}}x_3^4 \\ & -\tfrac{5}{3}\alpha_4|x_1|^{\frac{2}{3}}x_2^2 + \alpha_8 k_1\lceil x_1\rfloor^{\frac{1}{3}}x_3^5 + (\tfrac{7}{2}\alpha_2 k_2 - \alpha_5\lceil x_1\rfloor^0\lceil x_2\rfloor^0)|x_2|^3 \\ & -\tfrac{7}{2}\alpha_2\lceil x_2\rfloor^{\frac{5}{2}}x_3 + 4\alpha_9 k_3\lceil x_1\rfloor^0|x_2|^{\frac{3}{2}}x_3^3 + (5\alpha_8 k_3\lceil x_1\rfloor^0\lceil x_2\rfloor^0 \\ & -\alpha_6\lceil x_2\rfloor^0\lceil x_3\rfloor^0 + \tfrac{3}{2}\alpha_9 k_2)|x_2|x_3^4 + (\alpha_8 k_2 - \tfrac{3}{2}\alpha_9)\lceil x_2\rfloor^{\frac{1}{2}}x_3^5 \\ & +(7\alpha_3 k_3\lceil x_1\rfloor^0\lceil x_3\rfloor^0 - \alpha_8)x_3^6.\end{aligned} \tag{D.6}$$

Note that both functions (D.2) and (D.6) are GF's. Thus, following [Sanchez and Moreno, 2019], the analysis of positive definiteness of these functions can be done through the analysis of positive definiteness of their associated forms $\{V_i\}$ and $\{W_j\}$, respectively, which can be studied by using the SOS representation [Parrilo, 2000] (see Section 5.1 in Chapter 5 for details). So, if every form in the sets $\{V_i\}$ and $\{W_j\}$ is positive definite, then the GF's (D.2) and (D.6) are positive definite, as needed.

The associated forms $\{V_i\}$ and $\{\sigma_j\}$ $(i, j = 1, 2, 3)$ of GF's (D.2) and (D.6), respectively, are obtained by the change of variables

$$|x_1| = y_1^8, \qquad |x_2| = y_2^6, \qquad |x_3| = y_3^4. \tag{D.7}$$

This change of variables is obtained from 5.1 in Section 5.1 of Chapter 5.

Usually, a SOS polynomial is only positive semi-definite. Then, consider the forms $\bar{V}_i(y) = V_i(y) - \epsilon_1(y_1^{14} + y_2^{14} + y_3^{14})$ and $\bar{W}_j(y) = W_j(y) - \epsilon_1(y_1^{12} + y_2^{12} + y_3^{12})$, such that, if they are SOS for some $\epsilon_1 > 0$ then the strict positive definiteness of every associated form in $\{V_i\}$ and $\{W_j\}$ is ensured.

Using SOSTOOLS [Prajna et al., 2002] we can find the coefficients of the associated form $\{V_i\}$ by solving an LMI. However, in $\{W_j\}$ gains k_i and coefficients α_i appear as products, making the problem bilinear. Fortunately, we have selected the gains k_i *a priori* from Propositions 6.3 or 6.4, and we only use SOSTOOLS to get the coefficients for both sets of the polynomials $\{V_i\}$ and $\{W_j\}$, simultaneously.

Then, consider $\epsilon = 1$ and the gains given by Table 6.1. By means of SOSTOOLS, the coefficients $\alpha_i;\quad i = 0, \ldots, 9$ of function (D.2) are computed as Table D.1 shows. So, all elements of $\{V_i\}$ and $\{W_j\}$ are positive definite. In consequence, by the continuity of functions (D.2) and (D.6) on the boundary between each hyper-octant, it is possible to conclude that this functions are also positive definite on every point of the state space.

Since (D.6) is positive definite, then the quotient $\frac{\psi(x)}{\sigma(x)}$ is well defined on $\mathbb{R}^n$. Moreover, both functions (D.5) and (D.6) are r-homogeneous of degree 6, hence $\frac{\psi(x)}{\sigma(x)}$ is r-homogeneous of degree 0,

Set	Gains λ_i	Coefficients α_i		
D_1	$\lambda_1 = 2.7$	$\alpha_1 = 18477$	$\alpha_2 = 1351$	$\alpha_3 = 53.55$
	$\lambda_2 = 5.345$	$\alpha_4 = 10222$	$\alpha_5 = 4775$	$\alpha_6 = -932.3$
	$\lambda_3 = 1.1$	$\alpha_7 = 6026$	$\alpha_8 = -1025$	$\alpha_9 = 3118$
D_2	$\lambda_1 = 2.7$	$\alpha_1 = 4810$	$\alpha_2 = 433.7$	$\alpha_3 = 30.3$
	$\lambda_2 = 4.281$	$\alpha_4 = 2717$	$\alpha_5 = 1560$	$\alpha_6 = -320.2$
	$\lambda_3 = 1.1$	$\alpha_7 = 1720$	$\alpha_8 = -479.8$	$\alpha_9 = 1139$

Table D.1: Sets of gains for the PID-CSMC and coefficients of LF (D.2).

i.e.,

$$\frac{\psi(\Lambda_r(\lambda)x)}{\sigma(\Lambda_r(\lambda)x)} = \lambda^0 \frac{\psi(x)}{\sigma(x)} = \frac{\psi(x)}{\sigma(x)}; \quad \forall z \in S_r(1)$$

Also, the fraction $\frac{\psi(x)}{\sigma(x)}$ is continuous on $S_r(1)$, which is a compact set, hence it follows from the Bolzano–Weierstrass theorem that there exists a maximum value $0 < \delta_c = \max_{S_r(1)} \frac{\psi(x)}{\sigma(x)}$. Note that for homogeneous functions it is enough to obtain its values on the unit sphere $S_r(1)$ and the remaining values on $\mathbb{R}^n$ are recovered by applying the dilatation $\Lambda^r(\lambda)$. Then, from (D.4) if $L < \frac{1}{\delta_c}$ and $\sigma(x)$ is positive definite, the inequality $\dot{V}(z) < 0$ holds.

Finally, LF (D.2) proves the stability of the closed-loop system D.1 with the proposed gains. Since the scaling $k_1 = \lambda_1 \Delta^{2/3}$, $k_2 = \lambda_2 \Delta^{1/2}$ and $k_3 = \lambda_3 \Delta$ is homogeneous, the stability analysis is also valid for any size of the perturbation derivative $|f(t)| \leq \bar{L}$ provided that $\Delta > \frac{\bar{L}}{L}$. Finally, Lemma 6.1 is proven.

D.2 Proof of Lemma 6.2

GAS of the ideal model (6.32), with the set of gains proposed by Propositions 6.7 and 6.8, can be studied by means of the design of a LF. Again, we are going to use the GF approach, again (see [Sanchez and Moreno, 2019]).

Let us recall the system (6.32):

$$\begin{aligned} \dot{x}_1 &= x_2\,, \\ \dot{x}_2 &= -k_1 \lceil x_1 \rfloor^{1/3} - k_2 \lceil x_2 \rfloor^{1/2}\,. \end{aligned} \tag{D.8}$$

Note that the system (D.8) has a r-homogeneous vector-set field of degree $p = -1$ and wights $r = [\frac{3}{2}, 1]$ for variables x_1 and x_2, respectively (see Chapter 2 for details about homogeneity).

A LF candidate for the system (D.8) is given by Lemma 6.2 as

$$V(x) = \alpha_1 |x_1|^{5/3} + \alpha_2 |x_2|^{5/2} + \alpha_3 x_1 x_2. \tag{D.9}$$

Set	Gains λ_i	Coefficients α_i
D_1	$\lambda_1 = 1 \quad \lambda_2 = 2.375$	$\alpha_1 = 18477 \quad \alpha_2 = 1351 \quad \alpha_3 = 53.55$
D_2	$\lambda_1 = 1 \quad \lambda_2 = 2$	$\alpha_1 = 4810 \quad \alpha_2 = 433.7 \quad \alpha_3 = 30.3$

Table D.2: Sets of gains for the PID-CSMC and coefficients of LF (D.9).

So, the derivative of function (D.9) along the trajectories of the system (D.8) is given by $\dot{V}(x) = -W(x)$, where

$$W(x) = \alpha_3 k_1 |x_1|^{4/3} + \alpha_3 k_2 x_1 \lceil x_2 \rfloor^{1/2} - \tfrac{5}{3}\alpha_1 \lceil x_1 \rfloor^{2/3} x_2 + \tfrac{5}{2}\alpha_2 k_1 \lceil x_1 \rfloor^{1/3} \lceil x_2 \rfloor^{3/2} + (\tfrac{5}{2}\alpha_2 k_2 - \alpha_3) x_2^2 \quad \text{(D.10)}$$

Note that both functions (D.9) and (D.10) are GF's. Thus, following [Sanchez and Moreno, 2019], the analysis of positive definiteness of those functions can be done through the analysis of positive definiteness of their associated forms $\{V_i\}$ and $\{W_j\}$, respectively. For this, we can use the SOS representation [Parrilo, 2000] (see Section 5.1 in Chapter 5 for details). So, if every form in the sets $\{V_i\}$ and $\{W_j\}$ is positive definite, then the GF's (D.2) and (D.6) are positive definite, as needed.

The associated forms $\{V_i\}$ and $\{\sigma_j\}$ $(i, j = 1, 2, 3)$ of GF's (D.2) and (D.6), respectively, are obtained by the change of variables

$$|x_1| = y_1^8, \qquad |x_2| = y_2^6, \qquad |x_3| = y_3^4. \quad \text{(D.11)}$$

This change of variables is obtained from 5.1 in Section 5.1 of Chapter 5.

Moreover, consider the forms $\bar{V}_i(y) = V_i(y) - \epsilon_1(y_1^{14} + y_2^{14} + y_3^{14})$ and $\bar{W}_j(y) = W_j(y) - \epsilon_1(y_1^{12} + y_2^{12} + y_3^{12})$, such that, if they are SOS for some $\epsilon_1 > 0$ then the strict positive definiteness of every associated form in $\{V_i\}$ and $\{W_j\}$ is ensured.

Using SOSTOOLS [Prajna et al., 2002] we can find the coefficients of the associated form $\{V_i\}$ by solving an LMI. However, in $\{W_j\}$ gains k_i and coefficients α_i appear as products, making the problem bilinear. Fortunately, we have selected the gains k_i *a priori* from Propositions 6.7 or 6.8, and we only use SOSTOOLS to get the coefficients for both sets of the polynomials $\{V_i\}$ and $\{W_j\}$, simultaneously.

Then, consider $\epsilon = 1$ and the gains given by Table 6.2. By means of SOSTOOLS, the coefficients $\alpha_i; \quad i = 0, \ldots, 9$ of function (D.9) are computed as Table D.2 shows. So, all elements of $\{V_i\}$ and $\{W_j\}$ are positive definite. In consequence, by the continuity of functions (D.9) and (D.10) on the boundary between each hyper-octant, it is possible to conclude that this functions are also positive definite on every point of the state space.

Therefore, LF (D.9) proves the stability of the closed-loop system D.1 with the proposed gains. Since the scaling $k_1 = \lambda_1 \Delta^{2/3}$, $k_2 = \lambda_2 \Delta^{1/2}$ and $k_3 = \lambda_3 \Delta$ is homogeneous, the stability analysis is also valid for any $\Delta > 0$. Finally, Lemma 6.2 is proven.

Bibliography

[Andrieu et al., 2008] Andrieu, V., Praly, L., and Astolfi, A. (2008). Homogeneous approximation, recursive observer design, and output feedback. *SIAM Journal on Control and Optimization*, 47(4):1814–1850. 16

[Aström and Hägglund, 2005] Aström, K. J. and Hägglund, T. (2005). *Advanced PID Control*. ISA-The Instrumentation, Systems, and Automation Society. 17, 90, 91

[Atherton, 1975] Atherton, D. P. (1975). *Nonlinear control engineering*. Van Nostrand Reinhold, London. 17, 92, 96, 104

[Bacciotti and Rosier, 2005] Bacciotti, A. and Rosier, L. (2005). *Lyapunov functions and stability in control theory*. Springer-Verlag, Berlin, second edition. 15, 19, 21, 22, 27, 34, 51

[Banza et al., 2020] Banza, A. T., Tan, Y., and Mareels, I. M. Y. (2020). Integral sliding mode control design for systems with fast sensor dynamics. *Automatica*, 119:109093. 49

[Bernuau et al., 2013a] Bernuau, E., Efimov, D., Perruquetti, W., and Polyakov, A. (2013a). On an extension of homogeneity notion for differential inclusions. In *Proceedings of the 2013 European Control Conference (ECC)*, pages 2204–2209, Zürich, Switzerland. IEEE. 15, 19, 26, 27, 28, 37

[Bernuau et al., 2014] Bernuau, E., Efimov, D., Perruquetti, W., and Polyakov, A. (2014). On homogeneity and its application in sliding mode control. *Journal of the Franklin Institute*, 351(4):1866–1901. 16, 19, 26

[Bernuau et al., 2013b] Bernuau, E., Polyakov, A., Efimov, D., and Perruquetti, W. (2013b). Verification of ISS, iISS and IOSS properties applying weighted homogeneity. *Systems & Control Letters*, 62(12):1159–1167. 16, 50, 103

[Bhat and Bernstein, 1997] Bhat, S. P. and Bernstein, D. S. (1997). Finite-time stability of homogeneous systems. In *Proceedings of the 1997 American Control Conference*, volume 4, pages 2513–2514. IEEE. 28, 29, 49, 61

[Bhat and Bernstein, 2005] Bhat, S. P. and Bernstein, D. S. (2005). Geometric homogeneity with applications to finite-time stability. *Mathematics of Control, Signals, and Systems (MCSS)*, 17(2):101–127. 16, 28, 139

[Boiko, 2009] Boiko, I. (2009). *Discontinuous control systems: frequency-domain analysis and design*. Birkhäuser, Boston. 17, 50, 66, 92, 94, 95, 102

[Boiko, 2018] Boiko, I. (2018). On inherent gain margins of sliding-mode control systems. In *Advances in variable structure systems and sliding mode control—theory and applications*, pages 133–147. Springer. 17, 92

[Boiko, 2020] Boiko, I. (2020). On phase deficit of homogeneous sliding mode control. *International Journal of Robust and Nonlinear Control*, 31(9):3767–3778. 49

[Boiko and Fridman, 2005] Boiko, I. and Fridman, L. (2005). Analysis of chattering in continuous sliding mode controllers. *IEEE Transactions on Automatic Control*, 50(9):1442–1446. 17, 31, 90, 95

[Boiko et al., 2006] Boiko, I., Fridman, L., Iriarte, R., Pisano, A., and Usai, E. (2006). Parameter tuning of second-order sliding mode controllers for linear plants with dynamic actuators. *Automatica*, 42(5):833–839. 17, 91

[Boiko et al., 2007] Boiko, I., Fridman, L., Pisano, A., and Usai, E. (2007). Analysis of chattering in systems with second-order sliding modes. *IEEE transactions on Automatic control*, 52(11):2085–2102. 31

[Boiko, 2014a] Boiko, I. M. (2014a). Application of second-order sliding-mode control algorithms in continuous cycling tests for pid tuning. In *Proceedings of the 2014 European Control Conference (ECC)*, pages 2284–2290, Strasbourg, France. IEEE. 17

[Boiko, 2014b] Boiko, I. M. (2014b). On relative degree, chattering and fractal nature of parasitic dynamics in sliding mode control. *Journal of the Franklin Institute*, 351(4):1939–1952. 49, 91

[Butcher, 2003] Butcher, J. C. (2003). *Numerical methods for ordinary differential equations*. John Wiley & Sons, New York, NY, USA. 40, 42, 46

[Cheney, 1995] Cheney, E. W. (1995). Approximation and interpolation on spheres. In Singh, S., editor, *Approximation Theory, Wavelets and Applications*, chapter 3, pages 47–53. Springer, Berlin, Germany. 42

[Choi et al., 1995] Choi, M.-D., Lam, T. Y., and Reznick, B. (1995). Sums of squares of real polynomials. In *Proceedings of Symposia in Pure mathematics*, volume 58, pages 103–126. American Mathematical Society. 71

[Christofides and Teel, 1996] Christofides, P. D. and Teel, A. R. (1996). Singular perturbations and input-to-state stability. *IEEE Transactions on Automatic Control*, 41(11):1645–1650. 49

[Clarke et al., 1998] Clarke, F. H., Ledyaev, Y. S., and Stern, R. J. (1998). Asymptotic stability and smooth lyapunov functions. *Journal of differential Equations*, 149(1):69–114. 34

[Cortes, 2008] Cortes, J. (2008). Discontinuous dynamical systems. *IEEE Control Systems Magazine*, 28(3):36–73. 35, 36

[Cruz-Zavala and Moreno, 2018] Cruz-Zavala, E. and Moreno, J. A. (2018). Levant's arbitrary-order exact differentiator: a lyapunov approach. *IEEE Transactions on Automatic Control*, 64(7):3034–3039. 136, 137

[Dashkovskiy and Kosmykov, 2013] Dashkovskiy, S. and Kosmykov, M. (2013). Input-to-state stability of interconnected hybrid systems. *Automatica*, 49(4):1068–1074. 50

[Dashkovskiy et al., 2010] Dashkovskiy, S. N., Kosmykov, M., and Wirth, F. R. (2010). A small-gain condition for interconnections of ISS systems with mixed ISS characterizations. *IEEE Transactions on Automatic Control*, 56(6):1247–1258. 52

[Dashkovskiy and Rüffer, 2010] Dashkovskiy, S. N. and Rüffer, B. S. (2010). Local ISS of large-scale interconnections and estimates for stability regions. *Systems & Control Letters*, 59(3-4):241–247. 52

[Efimov et al., 2018] Efimov, D., Ushirobira, R., Moreno, J. A., and Perruquetti, W. (2018). Homogeneous Lyapunov functions: From converse design to numerical implementation. *SIAM Journal on Control and Optimization*, 56(5):3454–3477. 15, 25, 26, 28, 34, 35, 38, 40, 41, 42, 43

[Emel'Yanov et al., 1986] Emel'Yanov, S., Korovin, S., and Levantovskii, L. (1986). Higher-order sliding modes in binary control systems. In *Soviet Physics Doklady*, volume 31, pages 291–293. 31

[Feng et al., 2002] Feng, Y., Yu, X., and Man, Z. (2002). Non-singular terminal sliding mode control of rigid manipulators. *Automatica*, 38(12):2159–2167. 31

[Filippov, 1988] Filippov, A. F. (1988). *Differential equations with discontinuous right-hand side*. Kluwer, The Netherlands, Dordrecht. 15, 19, 27, 35, 36, 130, 135, 138, 141

[Franco et al., 2021] Franco, R., de Loza, A. F., Ríos, H., Cassany, L., Gucik-Derigny, D., Cieslak, J., Henry, D., and Olçomendy, L. (2021). Output-feedback sliding-mode controller for blood glucose regulation in critically ill patients affected by type 1 diabetes. *IEEE Transactions on Control Systems Technology*. 69

[Fridman, 1999] Fridman, L. (1999). The problem of chattering: an averaging approach. In Young, K. D. and Ozguner, U., editors, *Variable structure systems, sliding mode and nonlinear control*, pages 363–386. Springer-Verlag, London, UK. 49, 95

[Fridman and Levant., 2002] Fridman, L. and Levant., A. (2002). *Higher order sliding modes in Sliding Mode Control in Engineering*. J.P. Barbot, W. Perriguetti (Eds.), Marcel Dekker. 30

[Fridman et al., 2015] Fridman, L., Moreno, J. A., Bandyopadhyay, B., Kamal, S., and Chalanga, A. (2015). *Continuous Nested Algorithms : The Fifth Generation of Sliding Mode Controllers*, pages 5–35. Springer International Publishing, Cham. 16, 30, 33, 90

[Fridman, 2002] Fridman, L. M. (2002). Singularly perturbed analysis of chattering in relay control systems. *IEEE Transactions on Automatic Control*, 47(12):2079–2084. 49

[Gelb and Vander Velde, 1968] Gelb, A. and Vander Velde, W. E. (1968). *Multiple-input describing functions and nonlinear system design*. McGraw-Hill, New York. 17, 92, 93, 96, 102, 104

[Golkani et al., 2020] Golkani, M. A., Seeber, R., Reichhartinger, M., and Horn, M. (2020). Lyapunov-based saturated continuous twisting algorithm. *International Journal of Robust and Nonlinear Control*. 68

[Gutiérrez-Oribio et al., 2020] Gutiérrez-Oribio, D., Mercado-Uribe, J. A., Moreno, J. A., and Fridman, L. (2020). Robust global stabilization of a class of underactuated mechanical systems of two degrees of freedom. *International Journal of Robust and Nonlinear Control*. 69

[Hahn, 1967] Hahn, W. (1967). *Stability of motion*, volume 138. Springer. 22, 27

[Haimovich and De Battista, 2019] Haimovich, H. and De Battista, H. (2019). Disturbance-tailored super-twisting algorithms: Properties and design framework. *Automatica*, 101:318–329. 49

[Hardy et al., 1988] Hardy, G. H., Littlewood, J. E., and Polya, G. (1988). *Inequalities*. Cambridge Mathematical Library, second edition. 70

[Hermes, 1986] Hermes, H. (1986). Nilpotent approximations of control systems and distributions. *SIAM journal on control and optimization*, 24(4):731–736. 15

[Hermes, 1991] Hermes, H. (1991). Nilpotent and high-order approximations of vector field systems. *SIAM review*, 33(2):238–264. 15, 16

[Hong, 2001] Hong, Y. (2001). H∞ control, stabilization, and input–output stability of nonlinear systems with homogeneous properties. *Automatica*, 37(6):819–829. 16

[Hong et al., 1999] Hong, Y., Huang, J., and Xu, Y. (1999). On an output feedback finite-time stabilisation problem. In *Proceedings of the 38th IEEE Conference on Decision and Control (CDC)*, volume 2, pages 1302–1307. IEEE. 28

[Hubbert, 2002] Hubbert, S. (2002). *Radial basis function interpolation on the sphere*. PhD thesis, Imperial College London, London, UK. 42

[Jiang et al., 1996] Jiang, Z.-P., Mareels, I. M., and Wang, Y. (1996). A Lyapunov formulation of the nonlinear small-gain theorem for interconnected ISS systems. *Automatica*, 32(8):1211–1215. 50

[Jin et al., 2019] Jin, X., Du, W., He, W., Kocarev, L., Tang, Y., and Kurths, J. (2019). Twisting-based finite-time consensus for euler–lagrange systems with an event-triggered strategy. *IEEE Transactions on Network Science and Engineering*, 7(3):1007–1018. 69

[Kamal et al., 2016] Kamal, S., Moreno, J. A., Chalanga, A., Bandyopadhyay, B., and Fridman, L. M. (2016). Continuous terminal sliding-mode controller. *Automatica*, 69:308–314. 16, 33, 90

[Kellett and Teel, 2004] Kellett, C. M. and Teel, A. R. (2004). Smooth lyapunov functions and robustness of stability for difference inclusions. *Systems & Control Letters*, 52(5):395–405. 34

[Keshtkar et al., 2018] Keshtkar, S., Moreno, J. A., Kojima, H., and Hernández, E. (2018). Design concept and development of a new spherical attitude stabilizer for small satellites. *IEEE Access*, 6:57353–57365. 69

[Khalil, 2002] Khalil, H. (2002). *Nonlinear Systems*. Prentice Hall, Upper Saddle River, New Jersey, 3rd edition. 15, 21, 81, 133

[Klimushchev and Krasovskii, 1961] Klimushchev, A. I. and Krasovskii, N. N. (1961). Uniform asymptotic stability of systems of differential equations with a small parameter in the derivative terms. *Journal of Applied Mathematics and Mechanics*, 25(4):1011–1025. 49

[Kokotovic et al., 1999] Kokotovic, P., Khali, H. K., and O'Reilly, J. (1999). *Singular perturbation methods in control: analysis and design*, volume 25. Society for Industrial and Applied Mathematics. 49, 55, 125

[Kurzweil, 1963] Kurzweil, J. (1963). On the inversion of Lyapunov's second theorem on stability of motion. *AMS Translations Series 2*, 24:19–77. 16, 34, 35, 38

[Laghrouche et al., 2017] Laghrouche, S., Harmouche, M., and Chitour, Y. (2017). Higher order super-twisting for perturbed chains of integrators. *IEEE Transactions on Automatic Control*, 60(7):3588–3593. 16, 33, 90

[Levant, 1993] Levant, A. (1993). Sliding order and sliding accuracy in sliding mode control. *International journal of control*, 58(6):1247–1263. 16, 30, 31, 32, 68, 69, 72, 90

[Levant, 1998] Levant, A. (1998). Robust exact differentiation via sliding mode technique. *automatica*, 34(3):379–384. 31

[Levant, 2001] Levant, A. (2001). Universal single-input-single-output (siso) sliding-mode controllers with finite-time convergence. *IEEE transactions on Automatic Control*, 46(9):1447–1451. 16, 32

[Levant, 2003a] Levant, A. (2003a). Higher-order sliding modes, differentiation and output-feedback control. *International journal of Control*, 76(9-10):924–941. 16, 32, 79

[Levant, 2003b] Levant, A. (2003b). Higher-order sliding modes, differentiation and output-feedback control. *International Journal of Control*, 76:924–941. 30

[Levant, 2005a] Levant, A. (2005a). Homogeneity approach to high-order sliding mode design. *Automatica*, 41(5):823–830. 16, 19, 26, 28, 32, 49

[Levant, 2005b] Levant, A. (2005b). Quasi-continuous high-order sliding-mode controllers. *Automatic Control, IEEE Transactions on*, 50(11):1812–1816. 16, 32

[Levant, 2010] Levant, A. (2010). Chattering analysis. *IEEE Transactions on Automatic Control*, 55(6):1380–1389. 49, 95

[Levant, 2018] Levant, A. (2018). Filtering differentiators and observers. In *Proceedings of the 15th International Workshop on Variable Structure Systems (VSS)*, pages 174–179. 81

[Levant et al., 2016] Levant, A., Efimov, D., Polyakov, A., and Perruquetti, W. (2016). Stability and robustness of homogeneous differential inclusions. In *Proceedings of the 55th IEEE Conference on Decision and Control (CDC)*, pages 7288–7293. IEEE. 15, 19

[Levant and Fridman, 2010] Levant, A. and Fridman, L. M. (2010). Accuracy of homogeneous sliding modes in the presence of fast actuators. *IEEE Transactions on Automatic Control*, 55(3):810. 31, 32, 69, 72, 95, 97

[Levant and Livne, 2016] Levant, A. and Livne, M. (2016). Weighted homogeneity and robustness of sliding mode control. *Automatica*, 72:186 – 193. 16

[Loeb, 1956] Loeb, J. (1956). Recent advances in nonlinear servo theory. pages 260–268. Oldenburger R. (ed.), Frequency response. Macmillan, New York. 93

[Lopez-Ramirez et al., 2020] Lopez-Ramirez, F., Efimov, D., Polyakov, A., and Perruquetti, W. (2020). Finite-time and fixed-time input-to-state stability: Explicit and implicit approaches. *Systems & Control Letters*, 144:104775. 51

[Massera, 1949] Massera, J. L. (1949). On Lyapounov's conditions of stability. *Annals of Mathematics*, pages 705–721. 16, 34, 35, 38, 39

[Mendoza-Avila et al., 2020a] Mendoza-Avila, J., Efimov, D., Moreno, J. A., and Fridman, L. (2020a). Analysis of singular perturbations for a class of interconnected homogeneous systems: Input-to-state stability approach. Proceedings of the 21st IFAC World Congress. IFAC. 16

[Mendoza-Avila et al., 2021] Mendoza-Avila, J., Efimov, D., Ushirobira, R., and Moreno, J. A. (2021). Numerical design of lyapunov functions for a class of homogeneous discontinuous systems. *International Journal of Robust and Nonlinear Control*, 31(9):3708–3729. 15, 35, 37

[Mendoza-Avila et al., 2017] Mendoza-Avila, J., Fridman, L. M., and Moreno, J. A. (2017). An idea for lyapunov function design for arbitrary order continuous twisting algorithms. In *Proceedings of the 56th IEEE Conference on Decision and Control (CDC)*, pages 5426–5431. IEEE. 16, 69, 72, 131

[Mendoza-Avila et al., 2018] Mendoza-Avila, J., Moreno, J. A., and Fridman, L. (2018). Adaptive continuous twisting algorithm of third order. In *Proceedings of the 15th International Workshop on Variable Structure Systems (VSS)*, pages 144–149. 16

[Mendoza-Avila et al., 2020b] Mendoza-Avila, J., Moreno, J. A., and Fridman, L. (2020b). Continuous twisting algorithm for third order systems. *IEEE Transactions on Automatic Control*, 65(7):2814 – 2825. 16, 33, 90

[Mercado-Uribe and Moreno, 2020] Mercado-Uribe, J. Á. and Moreno, J. A. (2020). Discontinuous integral action for arbitrary relative degree in sliding-mode control. *Automatica*, 118:109018. 16, 33, 90

[Moreno, 2016] Moreno, J. A. (2016). Discontinuous integral control for mechanical systems. In *Proceedings of the 14th International Workshop on Variable Structure Systems (VSS)*, pages 142–147. 16, 33, 90, 91, 94

[Moreno, 2018] Moreno, J. A. (2018). *Discontinuous Integral Control for Systems with Relative Degree Two*, pages 187–218. Springer International Publishing, Cham. 16, 33, 90, 91, 94

[Moreno et al., 2016] Moreno, J. A., Negrete, D. Y., Torres-González, V., and Fridman, L. (2016). Adaptive continuous twisting algorithm. *International Journal of Control*, 89(9):1798–1806. 68, 74

[Moreno and Osorio, 2012] Moreno, J. A. and Osorio, M. (2012). Strict lyapunov functions for the super-twisting algorithm. *IEEE transactions on automatic control*, 57(4):1035–1040. 35

[Nakamura et al., 2002] Nakamura, H., Yamashita, Y., and Nishitani, H. (2002). Smooth Lyapunov functions for homogeneous differential inclusions. In *Proceedings of the 41st SICE Annual Conference (SICE 2002)*, volume 3, pages 1974–1979. IEEE. 15, 28, 29, 34

[Negrete and Moreno, 2014] Negrete, D. Y. and Moreno, J. A. (2014). Adaptive output feedback second order sliding mode control with unknown bound of perturbation. *IFAC Proceedings Volumes*, 47(3):10832–10837. 134

[Parrilo, 2000] Parrilo, P. A. (2000). *Structured semidefinite programs and semialgebraic geometry methods in robustness and optimization*. PhD thesis, California Institute of Technology. 68, 70, 71, 132, 142, 144

[Pérez-Ventura et al., 2020] Pérez-Ventura, U., Fridman, L., Capello, E., and Punta, E. (2020). Fault tolerant control based on continuous twisting algorithms of a 3-dof helicopter prototype. *Control Engineering Practice*, 101:104486. 69

[Persidskii, 1937] Persidskii, K. (1937). On a theorem of Lyapunov. In *Dokl. Akad. Nauk SSSR*, volume 14, pages 541–544. 16, 34, 35, 38, 40

[Pilloni et al., 2012a] Pilloni, A., Pisano, A., and Usai, E. (2012a). Oscillation shaping in uncertain linear plants with nonlinear pi control: analysis and experimental results. *IFAC Proceedings Volumes*, 45(3):116–121. 17, 90, 91, 95

[Pilloni et al., 2012b] Pilloni, A., Pisano, A., and Usai, E. (2012b). Parameter tuning and chattering adjustment of super-twisting sliding mode control system for linear plants. pages 479–484. Proceedings of the 12th International Workshop on Variable Structure Systems (VSS). 17, 90, 91, 95

[Pólya, 1928] Pólya, G. (1928). Über positive darstellung von polynomen. *Vierteljschr. Naturforsch. Ges. Zürich*, 73:141–145. 68, 70

[Polyakov, 2012] Polyakov, A. (2012). Nonlinear feedback design for fixed-time stabilization of linear control systems. *IEEE Transactions on Automatic Control*, 57(8):2106–2110. 19

[Polyakov, 2020] Polyakov, A. (2020). *Generalized Homogeneity in Systems and Control*. Springer. 15, 19, 21, 22, 27

[Polyakov et al., 2016] Polyakov, A., Coron, J., and Rosier, L. (2016). On finite-time stabilization of evolution equations: A homogeneous approach. In *Procedings of the 55th IEEE Conference on Decision and Control (CDC)*, pages 3143–3148, Las Vegas, NV, USA. IEEE. 42

[Polyakov and Poznyak, 2009] Polyakov, A. and Poznyak, A. (2009). Lyapunov function design for finite-time convergence analysis:"twisting" controller for second-order sliding mode realization. *Automatica*, 45(2):444–448. 35

[Polyakov and Poznyak, 2012] Polyakov, A. and Poznyak, A. (2012). Unified lyapunov function for a finite-time stability analysis of relay second-order sliding mode control systems. *IMA Journal of Mathematical Control and Information*, 29(4):529–550. 35

[Prajna et al., 2002] Prajna, S., Papachristodoulou, A., and Parrilo, P. A. (2002). Introducing sostools: A general purpose sum of squares programming solver. In *Proceedings of the 41st IEEE Conference on Decision and Control (CDC)*, volume 1, pages 741–746. IEEE. 71, 132, 137, 142, 144

[Pérez-Ventura and Fridman, 2019] Pérez-Ventura, U. and Fridman, L. (2019). When is it reasonable to implement the discontinuous sliding-mode controllers instead of the continuous ones? frequency domain criteria. *International Journal of Robust and Nonlinear Control*, 29(3):810–828. 17, 73, 90, 91, 95, 96, 104

[Pérez-Ventura et al., 2021] Pérez-Ventura, U., Mendoza-Avila, J., and Fridman, L. (2021). Design of a proportional integral derivative-like continuous sliding mode controller. *International Journal of Robust and Nonlinear Control*, pages 1–16. 17

[Rojas-Contreras et al., 2017] Rojas-Contreras, F.-G., Castillo-Lopez, A.-I., Fridman, L., and Gonzalez-Villela, V.-J. (2017). Trajectory tracking using continuous sliding mode algorithms for differential drive robots. In *Proceedings of the 56th IEEE Conference on Decision and Control (CDC)*, pages 6027–6032. IEEE. 69

[Rosales et al., 2018] Rosales, A., Shtessel, Y., and Fridman, L. (2018). Analysis and design of systems driven by finite-time convergent controllers: practical stability approach. *International Journal of Control*, 91(11):2563–2572. 49, 104

[Rosier, 1992] Rosier, L. (1992). Homogeneous Lyapunov function for homogeneous continuous vector field. *Systems & Control Letters*, 19(6):467–473. 15, 27, 28, 34

[Rosier, 1999] Rosier, L. (1999). Smooth Lyapunov functions for discontinuous stable systems. *Set-Valued Analysis*, 7(4):375–405. 34

[Ryan, 1995] Ryan, E. (1995). Universal stabilization of a class of nonlinear systems with homogeneous vector fields. *Systems & Control Letters*, 26(3):177–184. 16

[Saberi and Khalil, 1984] Saberi, A. and Khalil, H. (1984). Quadratic-type Lyapunov functions for singularly perturbed systems. *IEEE Transactions on Automatic Control*, 29(6):542–550. 49

[Sanchez et al., 2017a] Sanchez, T., Cruz-Zavala, E., and Moreno, J. A. (2017a). An sos method for the design of continuous and discontinuous differentiators. *International Journal of Control*, (just-accepted):1–38. 136

[Sánchez and Moreno, 2012] Sánchez, T. and Moreno, J. A. (2012). Construction of lyapunov functions for a class of higher order sliding modes algorithms. In *Proceedings of the 51st IEEE Conference on Decision and Control (CDC)*, pages 6454–6459, Maui, HI, USA. IEEE. 35

[Sánchez and Moreno, 2014] Sánchez, T. and Moreno, J. A. (2014). A constructive Lyapunov function design method for a class of homogeneous systems. In *Proceedings of the 53rd IEEE Conference on Decision and Control (CDC)*, volume 1, pages 5500–5505. IEEE. 68, 69, 71

[Sánchez and Moreno, 2014] Sánchez, T. and Moreno, J. A. (2014). Lyapunov functions for twisting and terminal controllers. In *Proceedings of the 13th International Workshop on Variable Structure Systems (VSS)*, pages 1–6, Nantes, France. IEEE. 35

[Sánchez and Moreno, 2016] Sánchez, T. and Moreno, J. A. (2016). Construction of Lyapunov functions for high order sliding modes. In Fridman, L., Barbot, J.-P., and Plestan, F., editors, *Recent Trends in Sliding Mode Control*, pages 77–99. The Institution of Engineering and Technology (IET), London. 15, 34, 35, 68, 71, 132

[Sanchez and Moreno, 2019] Sanchez, T. and Moreno, J. A. (2019). Design of Lyapunov functions for a class of homogeneous systems: Generalized forms approach. *International Journal of Robust and Nonlinear Control*, 29(3):661–681. 15, 34, 35, 68, 71, 132, 141, 142, 143, 144

[Sanchez et al., 2017b] Sanchez, T., Torres, V., Fridman, L., and Moreno, J. A. (2017b). Output feedback continuous twisting algorithm. *Automatica*. 68

[Seeber and Horn, 2017] Seeber, R. and Horn, M. (2017). Stability proof for a well-established super-twisting parameter setting. *Automatica*, 84:241–243. 49

[Shtessel et al., 2014] Shtessel, Y., Edwards, C., Fridman, L., and Levant., A. (2014). *Sliding Mode Control and Observation*. Brikhauser: Basel, New York, NY, USA. 16, 29, 30, 35, 37, 44

[Torres-González et al., 2015] Torres-González, V., Fridman, L. M., and Moreno, J. A. (2015). Continuous twisting algorithm. In *Proceedings of the 54th IEEE Conference on Decision and Control (CDC)*, pages 5397–5401. IEEE. 68

[Torres-González et al., 2017] Torres-González, V., Sanchez, T., Fridman, L., and Moreno, J. A. (2017). Design of continuous twisting algorithm. *Automatica*, 80:119–126. 16, 33, 68, 90, 91, 94

[Tuna and Teel, 2006] Tuna, S. E. and Teel, A. R. (2006). Homogeneous hybrid systems and a converse lyapunov theorem. In *Proceedings of the 45th IEEE Conference on Decision and Control (CDC)*, pages 6235–6240, San Diego, CA, USA. IEEE. 15, 35

[Utkin, 2016] Utkin, V. (2016). Discussion aspects of high-order sliding mode control. *IEEE Transactions on Automatic Control*, 61(3):829–833. 17, 92, 94, 95

[Utkin, 1992] Utkin, V. I. (1992). *Sliding modes in control and optimization*, volume 116. Springer-Verlag Berlin. 16, 29, 31

[West et al., 1956] West, J. C., Douce, J. L., and Livesley, R. K. (1956). The dual-input describing function and its use in the analysis of non-linear feedback systems. *Proceedings of the IEE - Part B: Radio and Electronic Engineering*, 103(10):463–473. 102

[Wu et al., 1998] Wu, Y., Yu, X., and Man, Z. (1998). Terminal sliding mode control design for uncertain dynamic systems. *Systems & Control Letters*, 34(5):281–287. 31, 32

[Yoshizawa et al., 1955] Yoshizawa, T. et al. (1955). On the stability of solutions of a system of differential equations. *Memoirs of the College of Science, University of Kyoto. Series A: Mathematics*, 29(1):27–33. 16, 34, 35, 38

[Zamora et al., 2013] Zamora, C. A., Moreno, J. A., and Kamal, S. (2013). Control integral discontinuo para sistemas mecánicos. In *Proceedings of the Congreso Nacional de Control Automático (CNCA AMCA) 2013*, pages 11–16, Ensenada, Baja California, Mexico. Asociación de México de Control Automático (AMCA). 16, 17, 33, 91, 94

[Ziegler and Nichols, 1942] Ziegler, J. G. and Nichols, N. B. (1942). Optimum settings for automatic controllers. *ASME Transactions*, 64:759–768. 17, 90, 91

[Zubov, 1964] Zubov, V. I. (1964). *Methods of A.M. Lyapunov and their application*. Popko Noordhoff, Groningen, Netherlands. 15, 19, 24, 26, 27, 28, 34, 37